

Bioconversion of Glycerol by Immobilized *Clostridium pasteurianum*: Process Development, Optimization and Intensification

A Thesis
Submitted in Partial
Fulfillment of the Requirements for the Degree of

DOCTOR OF PHILOSOPHY

By

Swati Khanna



**Center for Energy
Indian Institute of Technology Guwahati
Guwahati – 781039, Assam, India
December 2012**

Dedicated
to
My Parents who Mean
the
World to me

CERTIFICATE

It is certified that the work contained in the thesis entitled “**BIOCONVERSION OF GLYCEROL BY IMMOBILIZED *Clostridium pasteurianum*: PROCESS DEVELOPMENT, OPTIMIZATION AND INTENSIFICATION**”, by **Swati Khanna** (Roll No. 08615105), has been carried out under our supervision and that this work has not been submitted elsewhere for a degree.

Dr. V.S. Moholkar

Associate Professor

Department of Chemical Engineering

Indian Institute of Technology Guwahati

Professor A. Goyal

Professor

Department of Biotechnology

Indian Institute of Technology Guwahati

CONTENTS

LIST OF TABLES	i
LIST OF FIGURES	v
ABBREVIATIONS	xi
CHAPTER 1: GENERAL INTRODUCTION AND MOTIVATION FOR THE THESIS	1
1.1 Biodiesel policy and program of India	2
1.2 Hurdles in biodiesel program: problems and solutions	5
1.3 Forward integration of biodiesel plant: conversion of glycerol to value added products	6
1.4 Aim and scope of present thesis	10
CHAPTER 2: GLYCEROL BIOCONVERSION: REVIEW AND ANALYSIS	13
2.1 Introduction	13
2.2 Generalized metabolic pathway of glycerol bioconversion	19
2.3 Economically significant products of glycerol bioconversion	24
2.3.1 1,3-Propanediol	24
2.3.2 Butanol	27
2.3.3 Dihydroxyacetone	33
2.3.4 Citric acid	36
2.3.5 Glyceric acid	38
2.3.6 3-Hydroxypropionaldehyde	42
2.3.7 Biosurfactants	44
2.3.8 Propionic acid	46
2.3.9 Polyhydroxyalkanoates	49
2.3.10 Single cell oils	52
2.3.11 Extracellular polysaccharides	54
2.4 Miscellaneous products	56
2.4.1 Succinic acid	56

2.4.2	Erythritol	57
2.4.3	Mannitol	58
2.4.4	Ethanol	58
2.4.5	Lactic acid	59
2.4.6	Methane	60
2.4.7	3-Hydroxypropionic acid	61
2.4.8	Oxalic acid	61
2.4.9	2,3-Butanediol	62
2.4.10	Pigments	62
2.4.11	Hydrogen	62
2.4.12	Glycerol as a supplementary carbon source	64
2.5	Economic feasibility of glycerol bioconversion	67
2.6	Inference and justification of the present thesis	69

CHAPTER 3: GLYCEROL FERMENTATION BY IMMOBILIZED CELLS:

	PRELIMINARY OPTIMIZATION	73
3.1	Introduction	73
3.2	Materials and methods	75
3.2.1	Materials	75
3.2.2	Growth and maintenance of <i>C. pasteurianum</i>	76
3.2.3	Pure and crude glycerol fermentation by free cells	76
3.2.4	Determination of cell morphology in presence of glycerol	77
3.2.5	Immobilization and cross linking of cells	77
3.2.6	Initial media selection for immobilized cells	78
3.2.7	Shake flask experiments for support selection	78
3.2.8	Preliminary optimization studies with silica gel as a support	78
3.2.9	Enzymes extraction and kinetics	79
3.2.10	Analytical methods	80
3.3	Results	80
3.3.1	Comparison of growth of cells on CMM and RCM and immobilization on supports	80
3.3.2	Study of cell morphology of <i>C. pasteurianum</i>	81
3.3.3	Batch fermentation by free cells	83

3.3.4	Initial media selection for glycerol fermentation by immobilized cells	85
3.3.5	Glycerol fermentation by immobilized cells on Amberlite	86
3.3.6	Glycerol fermentation by cells immobilized on silica gel	89
3.3.7	Glycerol fermentation by cells immobilized on reticulated polyurethane foam	91
3.3.8	Comparison of immobilization supports	91
3.3.9	Preliminary optimization studies with silica gel as an immobilization support	93
3.3.10	Enzyme kinetics study	94
3.3.11	Comparison of pure and crude glycerol as substrate for free and immobilized cells	96
3.4	Discussion	97
3.5	Conclusions	99
CHAPTER 4: KINETICS STUDIES FOR GLYCEROL BIOCONVERSION:		101
4.1	Introduction	101
4.2	Materials and methods	102
4.2.1	Materials	102
4.2.2	Immobilization of cells	102
4.2.3	Batch fermentation	103
4.2.4	Analysis and calculations	103
4.3	Results	104
4.3.1	Trends in butanol production	104
4.3.2	Trends in 1,3-PDO production	104
4.3.3	Trends in ethanol production	107
4.3.4	Rate constants and activation energy	107
4.3.5	Utilization of crude glycerol	110
4.4	Discussion	110
4.5	Conclusions	112
CHAPTER 5: MEDIUM OPTIMIZATION FOR GLYCEROL BIOCONVERSION		113
5.1	Introduction	113

5.2	Materials and methods	114
5.2.1	Micro-organism, culture revival and maintenance	114
5.2.2	Immobilization and cross linking of <i>C. pasteurianum</i> cells	115
5.2.3	Fermentation conditions	115
5.2.4	Taguchi's orthogonal array	116
5.2.5	Confirmatory experiments	117
5.2.6	Experiments with media optimized for free cells	117
5.2.7	Method of analysis	118
5.3	Results and discussion	119
5.3.1	Taguchi analysis and ANOVA	119
5.3.2	Result prediction and confirmatory experiments in shake flasks and scale-up to bioreactor level	122
5.3.3	Comparative evaluation with optimized media for free cells	126
5.4	Conclusions	126
CHAPTER 6: PROCESS OPTIMIZATION FOR GLYCEROL BIOCONVERSION		129
6.1	Introduction	129
6.2	Materials and methods	130
6.2.1	Materials	130
6.2.2	Micro-organism, culture revival and maintenance	130
6.2.3	Fermentation conditions	130
6.2.4	Taguchi's orthogonal array	131
6.2.5	Confirmatory experiments	133
6.2.6	Analysis	133
6.3	Results and discussion	134
6.3.1	Taguchi analysis	135
6.3.2	ANOVA results	136
6.3.3	Selection of optimum levels of factors for enhancing bio-alcohols production	137
6.3.4	Confirmatory experiments	139
6.3.5	Analysis of results and comparison with previous literature	145
6.4	Conclusions	148

CHAPTER 7: ULTRASOUND ENHANCED BIOCONVERSION OF GLYCEROL**BY FREE CELLS: MECHANISTIC ISSUES 149**

7.1	Introduction	149
7.2	Materials, methods and simulations	152
7.2.1	Micro-organism, growth and maintenance	152
7.2.2	Apparatus and reaction setup	153
7.2.3	Analytical methods	154
7.2.4	Simulations of cavitation bubble dynamics	155
7.2.5	Enzyme extraction and kinetic study	159
7.3	Results and discussion	163
7.3.1	Determination of cell morphology and growth	168
7.3.2	Analysis of variance	171
7.3.3	Analysis of results	171
7.4	Conclusions	174

CHAPTER 8: ULTRASOUND ENHANCED BIOCONVERSION OF GLYCEROL BY**IMMOBILIZED CELLS 175**

8.1	Introduction	175
8.2	Materials, methods and simulations	176
8.2.1	Materials	176
8.2.2	Micro-organism growth and maintenance	176
8.2.3	Immobilization of <i>C. pasteurianum</i> and glycerol fermentation	176
8.2.4	Apparatus and reaction setup	177
8.2.5	Analysis	178
8.2.6	Simulations of cavitation bubble dynamics	179
8.2.7	Enzymes extraction and kinetic parameters determination	179
8.3	Results and discussion	181
8.3.1	Analysis	188
8.4	Conclusions	189

CHAPTER 9: OVERVIEW AND SCOPE FOR FUTURE WORK 191

9.1	Overview	191
-----	----------	-----

CONTENTS

9.2	Scope for future work	195
REFERENCES		197
ACKNOWLEDGEMENTS		223
RESEARCH OUTPUT OF THE THESIS		225
CORRECTION APPENDIX		229



LIST OF TABLES

Chapter 1

Table 1.1	Statistics of crude oil production and import in India	3
Table 1.2A	Projected waste land requirement to meet 20% blending of petro–diesel targets by 2017	3
Table 1.2B	Categorization of waste land in India suitable for <i>Jatropha curcas</i> plantations (Planning Commission, 2003)	3
Table 1.3	Cost estimation for biodiesel production	7
Table 1.4	Trends in production of refined and crude glycerol in Europe	7
Table 1.5	Trends in the international prices of refined glycerin in past two decades	8
Table 1.6	Applications of glycerin (distribution in terms of end use in wt%)	9

Chapter 2

Table 2.1	Biodiesel and glycerin production scenario	14
Table 2.2	Representative summary of catalytic or chemical transformation of glycerol	17
Table 2.3	Summary of literature on bioconversion of glycerol to 1,3–PDO	28
Table 2.4	Summary of literature on biochemical conversion of glycerol to butanol	32
Table 2.5	Summary of literature on biochemical conversion of glycerol to citric acid	38
Table 2.6	Summary of literature on biochemical conversion of glycerol to glyceric acid	40
Table 2.7	Summary of literature on glycerol bioconversion to 3–hydroxypropionaldehyde	43
Table 2.8	Summary of literature on biochemical conversion of glycerol to biosurfactants	45
Table 2.9	Summary of literature on biochemical conversion of glycerol to propionic acid	48

LIST OF TABLES

Table 2.10	Summary of literature on bioconversion of glycerol to polyhydroxyalkanoates	50
Table 2.11	Summary of literature on biochemical conversion of glycerol to SCOEs	55
Chapter 3		
Table 3.1	Comparison of yields of the three fermentation products formed by free and immobilized cells with pure glycerol as a substrate	96
Table 3.2	Comparison of yields of the three fermentation products formed by free and immobilized cells with crude glycerol as a substrate	96
Table 3.3	Comparison of the maximum yields of all the three products obtained in the current work with published literature on free cells of <i>C. pasteurianum</i> . All yields are in gram of product formed per gram substrate (g/g)	98
Chapter 5		
Table 5.1	The factors and their corresponding levels used in Taguchi statistical design for optimal mixed alcohols production by immobilized <i>C. pasteurianum</i>	117
Table 5.2	Taguchi design matrix and corresponding average concentrations (g/L) of the products formed and substrate left in shake flask at the end of the fermentation by immobilized <i>C. pasteurianum</i>	120
Table 5.3	Taguchi analysis of factors affecting total alcohols production by immobilized <i>C. pasteurianum</i>	120
Table 5.4	ANOVA table for the significant factors obtained from Taguchi analysis	122
Chapter 6		
Table 6.1	The factors and their corresponding levels used in Taguchi statistical design for optimal mixed alcohols production by immobilized <i>C. pasteurianum</i>	132
Table 6.2	Taguchi design matrix and corresponding total mixed alcohols production (g/L) by immobilized <i>C. pasteurianum</i> (MTCC 6013) with pure and crude glycerol as substrates in shake flask	132
Table 6.3A	Taguchi analysis of factors affecting total alcohols production by immobilized <i>C. pasteurianum</i> with pure glycerol as a carbon source	135

Table 6.3B	Taguchi analysis of factors affecting total alcohols production by immobilized <i>C. pasteurianum</i> with crude glycerol as a carbon source	135
Table 6.4A	ANOVA table for all four significant factors and interaction of factor A and B for pure glycerol fermentation by immobilized <i>C. pasteurianum</i> cells	137
Table 6.4B	ANOVA table for the significant factors for crude glycerol fermentation by immobilized <i>C. pasteurianum</i> cells	137
Table 6.5	Comparison of the maximum yields and selectivity of products obtained in the current work with published literature	147
Chapter 7		
Table 7.1	Material balance for glycerol bioconversion	165
Table 7.2	Yields for products of glycerol bioconversion and enhancement effect of ultrasound	166
Table 7.3	Selectivity for products of glycerol bioconversion	166
Table 7.4	Enzyme kinetics parameters	166
Table 7.5A	ANOVA of ethanol concentrations formed in absence and in presence of ultrasound at different concentrations of glycerol	170
Table 7.5B	ANOVA of 1,3-PDO concentrations formed in absence and in presence of ultrasound at different concentrations of glycerol	170
Chapter 8		
Table 8.1	Material balance for glycerol bioconversion by immobilized <i>C. pasteurianum</i> in presence and in absence of ultrasound	183
Table 8.2A	Yields for products of glycerol bioconversion and percentage enhancement by ultrasonic treatment	184
Table 8.2B	Selectivity for ethanol and 1,3-PDO production from bioconversion of glycerol	184
Table 8.3	Enzyme kinetics parameters for ethanol dehydrogenase and 1,3-PDO dehydrogenase	184
Table 8.4	Analysis of Variance (ANOVA) of 1,3-PDO concentrations formed in test and in control experiments at different concentrations of glycerol	185



LIST OF FIGURES

Chapter 2

- Figure 2.1 Metabolic pathway of glycerol bioconversion: Oxidative and reductive wings of glycerol assimilation (E₁–Glycerol dehydratase; E₂–1,3–PDO dehydrogenase; E₃–Aldehyde dehydrogenase; E₄–Glycerol dehydrogenase type 1; E₅–Dihydroxy acetone kinase; E₆–Triose phosphate isomerase; E₇–Lactate dehydrogenase; E₈–Pyruvate decarboxylase; E₂₆–Pyruvate kinase; E₂₇– α –Acetolactate decarboxylase; E₂₈–Acetoin reductase; E₂₉–Diacetyl reductase; E₃₁–Glycerol–3–phosphate dehydrogenase) 19
- Figure 2.2 Metabolic pathway of glycerol bioconversion: Pathway depicting alternate metabolic fate of an intermediate of glycerol assimilation, Glyceraldehyde–3–phosphate, which finally converts into various sugars, eventually forming biosurfactants (E₉–Aldolase; E₁₀–Fructose 1,6 biphosphatase; E₁₁–Hexose phosphate isomerase) 21
- Figure 2.3 Metabolic pathway of glycerol bioconversion: Pathways depicting different metabolic fate of pyruvate, an intermediate of glycerol bioassimilation (E₁₂–Phospho–transacetylase; E₁₃–Acetaldehyde dehydrogenase; E₁₄–Alcohol dehydrogenase; E₁₅–Pyruvate dehydrogenase complex; E₁₆–Pyruvate formate lyase; E₁₇–Pyruvate carboxylase; E₁₈–Malate dehydrogenase; E₁₉–Fumarase; E₂₀–Thiolase; E₂₁– β –Hydroxybutyryl CoA dehydrogenase; E₂₂–Crotonase; E₂₃–Butyryl CoA dehydrogenase; E₂₄–Butyraldehyde dehydrogenase; E₂₅–Butanol dehydrogenase; E₃₂–Butyrate kinase; E₃₃–Phosphobutyryl transferase; E₃₄–Acetate kinase; E₃₅–Formate hydrogen lyase; E₃₆–Fumarate reductase) 23
- Figure 2.4 Effect of acetate on yield of different products formed in chemostat by *Clostridium butyricum* LMG1212t₂, utilizing glycerol (Heyndrickx et al., 1991). The figure legend indicates concentration of glycerol (G) and acetate (Ac) in mmol/L 26
- Figure 2.5 Comparison of yield of citric acid formed in batch and fed batch process on bioconversion of glycerol by various strains of *Yarrowia lipolytica* 37
- Figure 2.6 A comparative assessment of concentration of glyceric acid and dihydroxyacetone formed by various strains of *Gluconobacter* utilizing glycerol as a carbon source 39

Chapter 3

- Figure 3.1 Growth curve of *C. pasteurianum* on (A) CMM, and (B) RCM 81
- Figure 3.2 SEM image of (A) Amberlite without cells, (B) *C. pasteurianum* cells immobilized on Amberlite and cross-linked by glutaraldehyde, (C) silica gel without cells, (D) Glutaraldehyde treated cells immobilized on silica gel, (E) reticulated polyurethane foam without cells, (F) *C. pasteurianum* cells immobilized and cross-linked on PU foam 82
- Figure 3.3 Flow cytometric analyses for estimation of morphological changes of *C. pasteurianum*. Acquisition dot plots (FSC vs SSC) of *C. pasteurianum* cells in (A) control, (B) pure glycerol and (C) crude glycerol. (A1), (B1), and (C1) Histogram plots (Counts vs FSC) of *C. pasteurianum* in control, pure glycerol and crude glycerol, respectively. As there is no significant change in FSC and M2 in absence and in presence of both pure and crude glycerol therefore, morphology of cells remains same 83
- Figure 3.4 Trends in production of (A) 1,3-PDO with pure glycerol, (B) 1,3-PDO with crude glycerol, (C) butanol with pure glycerol, (D) butanol with crude glycerol, (E) ethanol with pure glycerol and, (F) ethanol with crude glycerol by free cells of *C. pasteurianum* 84
- Figure 3.5 Plot of total products concentration vs different fermentation media. Medium A performed the best and thus, was used for all preliminary immobilization experiments 86
- Figure 3.6 Trends in (A) 1,3-PDO yield with varying concentration of glycerol at definite time intervals. The optimum substrate concentration for maximal 1,3-PDO production was 10 g/L, (B) butanol yield with varying concentration of glycerol at definite time intervals. 25 g/L crude glycerol concentration yielded maximum butanol, (C) ethanol yield with varying concentration of glycerol at definite time intervals. 5 g/L crude glycerol gave highest ethanol yield while no ethanol was observed with 150 g/L substrate concentration 87
- Figure 3.7 Trends in production of (A) 1,3-PDO from pure glycerol, (B) 1,3-PDO from crude glycerol, (C) butanol from pure glycerol, (D) butanol from crude glycerol, (E) ethanol from pure glycerol and (F) ethanol from crude glycerol 90
- Figure 3.8 (A) Trends in production of the three fermentation products by *C. pasteurianum* cells immobilized on reticulated polyurethane foam at different concentrations of crude glycerol, (B) Comparison of three immobilization supports in terms of total yield of products at varied crude glycerol concentrations. Silica gel was found to be the most suitable support for *C. pasteurianum* immobilization and was chosen for all further studies 92

Figure 3.9	(A) Comparison of glutaraldehyde treated and untreated cells for production of total solvent, and (B) effect of variation of amount of support with immobilized cells on formation of products	93
Figure 3.10	Lineweaver Burk plots. Pure glycerol as substrate for determination of kinetic parameters of: (A) 1,3-PDO dehydrogenase, (C) butanol dehydrogenase, (E) ethanol dehydrogenase. Crude glycerol as substrate for determination of kinetic parameters of: (B) 1,3-PDO dehydrogenase, (D) butanol dehydrogenase, and (F) ethanol dehydrogenase	95
Chapter 4		
Figure 4.1	Trends in production of butanol with initial crude glycerol concentration of (A) 5 g/L, (B) 10 g/L, and (C) 25 g/L at varied temperatures. 10 g/L crude glycerol formed minimum amount of butanol at all temperatures as compared to other concentrations studied	105
Figure 4.2	Trends in production of 1,3-PDO with initial crude glycerol concentration of (A) 5 g/L, (B) 10 g/L, and (C) 25 g/L at three different fermentation temperatures	106
Figure 4.3	Trends in ethanol production with (A) 5 g/L, (B) 10 g/L, and (C) 25 g/L initial crude glycerol concentration at three fermentation temperatures	108
Figure 4.4	Calculation of first order rate constants for glycerol bioconversion by immobilized <i>C. pasteurianum</i> at fermentation temperature of (A) 30°C, (B) 37°C, and (C) 45°C. The highest value for first order rate constant for glycerol bioconversion was obtained at 37°C	109
Figure 4.5	In k vs $1/T$ (Kelvin ⁻¹) curve for calculating activation energy (E_a) of glycerol bioconversion by immobilized <i>C. pasteurianum</i>	110
Chapter 5		
Figure 5.1	The mean of main effects plot for each medium component at two levels (1 and 2)	121
Figure 5.2	(A) Production of ethanol, butanol and 1,3-PDO in shake flasks containing optimized medium. The total product concentration after completion of fermentation was 14.17 g/L, and (B) product formation profiles in stirred tank bioreactor with optimized medium components. The final concentration of products achieved was 17.67 g/L which was higher than the predicted value	124
Figure 5.3	Trends in concentration of glycerol left unutilized in the fermentation broth during the course of fermentation. The final concentration of glycerol utilized by <i>C. pasteurianum</i> was higher in bioreactor than in	125

shake flask

Chapter 6

- Figure 6.1 Main effect mean plots of process variables with: (A) pure glycerol, and (B) crude glycerol 138
- Figure 6.2 Trends in production of ethanol, butanol, and 1,3-PDO under optimized fermentation conditions with pure glycerol as substrate in (A) anaerobic shake flask, and (B) bioreactor. The total product concentration after completion of fermentation in shake flask and in bioreactor was 18.9 g/L and 19.7 g/L, respectively 140
- Figure 6.3 Trends in production of ethanol, butanol and 1,3-PDO under optimized fermentation conditions with crude glycerol as substrate in (A) anaerobic shake flask, and (B) bioreactor. The final total product concentration in shake flask and in bioreactor was 16.54 g/L and 16.75 g/L, respectively 141
- Figure 6.4 Comparison of uptake of glycerol in shake flask and in a bioreactor under optimized fermentation conditions with (A) pure glycerol as a substrate, and (B) crude glycerol as a substrate 142
- Figure 6.5 Recyclability study of immobilized biocatalyst in presence of (A) pure glycerol, and (B) crude glycerol. Immobilized biocatalyst retained its catalytic potential for more number of fermentation cycles in pure glycerol containing medium than crude glycerol containing medium 144

Chapter 7

- Figure 7.1 Schematic diagram of the experimental setup (Legends: (1) Ultrasound bath; (2) Test tube containing glycerol fermentation mixture; (3) Rotameter for control of gas flow; (4) Burette stand and test tube holder; (5) Nitrogen cylinder; (6) Connection of the gas to the rubber cork covering test tube) 154
- Figure 7.2A Metabolic pathway for glycerol bioconversion to ethanol (Enzymes: E_3 = Glycerol dehydrogenase Type I; E_4 = Dihydroxyacetone kinase; E_5 = Triose phosphate isomerase; E_6 = Pyruvate dehydrogenase complex; E_7 = Acetaldehyde dehydrogenase; E_8 = Alcohol dehydrogenase) 161
- Figure 7.2B Michaelis–Menten reaction scheme 161
- Figure 7.3A Metabolic pathway for glycerol bioconversion to 1,3-PDO (Enzymes: E_1 = Glycerol dehydratase; E_2 = 1,3-PDO dehydrogenase) 162
- Figure 7.3B Haldane reaction scheme for substrate inhibited conversion 162
- Figure 7.4 Trends in bioconversion of glycerol at different initial concentrations 164

	(5, 10 and 25 g/L) with mechanical shaking (control experiments), (A) Time variation of ethanol production, (B) time variation of 1,3-PDO production, (C) time variation of glycerol concentration in fermentation broth. Trends in bioconversion of glycerol at different initial concentrations (5, 10 and 25 g/L) with ultrasound irradiation (test experiments), (D) time variation of ethanol production, (E) time variation of 1,3-PDO production, (F) time variation of glycerol concentration in fermentation broth	
Figure 7.5	Simulation results for the radial dynamics of 5 micron air bubble and the convection generated thereby in the fermentation medium with 10 g/L glycerol concentration. (Positive velocity indicates liquid motion away from bubble center, while negative velocity indicates motion towards bubble center)	167
Figure 7.6	Flow cytometric analyses for estimation of morphological changes. (A) and (B) Acquisition dot plots (FSC vs SSC) of <i>C. pasteurianum</i> cells in control and test samples, respectively. (C) and (D) Histogram plots (Counts vs FSC) of <i>C. pasteurianum</i> in control and test samples cells, respectively. As there is no significant change in FSC after sonication as shown by both plots, therefore morphology of cells remains same	169
Figure 7.7	Morphology of cells of <i>C. pasteurianum</i> (A) before sonication, and (B) after sonication	170
Chapter 8		
Figure 8.1	Schematic of experimental set-up. Legends: 1 – ultrasound bath, 2 – test tube containing fermentation broth and immobilized cells, 3 – pressure gauze and gas flow control valve, 4 – burette stand for holding test tube, 5 – gas cylinder, 6 – silicon tubing	177
Figure 8.2	(A) Trends in bioconversion of glycerol to 1,3-PDO by immobilized <i>C. pasteurianum</i> with mechanical shaking at different initial glycerol concentrations, (B) time variation of different initial glycerol concentrations with mechanical shaking. Trends in bioconversion of different initial glycerol concentrations to (C) ethanol (D) 1,3-PDO in presence of ultrasound at elevated pressure. (E) Time variation of different initial glycerol concentrations in the fermentation broth subjected to ultrasound treatment at elevated pressure	186
Figure 8.3	Simulation results for the radial dynamics of 5 micron air bubble and the convection generated thereby in the fermentation medium with 25 g/L glycerol concentration	187
Correction Appendix		
Figure A1	Picture of a custom fabricated Erlenmeyer flask for anaerobic	

fermentation

Figure A2 Trends in consumption of glycerol during the course of fermentation at three different fermentation temperatures



ABBREVIATIONS

1,3-PDO	1,3-Propanediol
2,3-BDO	2,3-Butanediol
ANOVA	Analysis Of Variance
BDPS	Biodiesel Product Stream
CG	Crude Glycerol
CMM	Cooked Meat Media
CNG	Compressed Natural Gas
COD	Chemical Oxygen Demand
DF	Degree of Freedom
DHA	Dihydroxyacetone
DOE	Design of Experiments
EMP	Emden Meyerhof Parnas
EPA	Eicosapentenoic acid
EPS	Extracellular Polysaccharides
FAD	Flavin Adenine Dinucleotide
FAME	Fatty Acid Methyl Ester
FFA	Free Fatty Acid
FSC	Forward Scatter
GA	Glyceric Acid

ABBREVIATIONS

GC	Gas Chromatography
GLA	Gamma Linolenic Acid
HPLC	High Performance Liquid Chromatography
kgoe	Kilograms Of Oil Equivalent
MEL	Mannosylerythritol lipid
MMT	Million Metric Ton
MS	Mean of Squares
MTCC	Microbial Type Culture Collection
PA	Propionic Acid
PG	Pure Glycerol
PHA	Polyhydroxyalkanoate
PHB	Polyhydroxybutyrate
PPP	Pentose Phosphate Pathway
PPP	Pentose Phosphate Pathway
PQQ	Pyrroloquinoline quinone
PUFA	Poly-Unsaturated Fatty Acids
RCM	Reinforced Clostridial Media
RL	Rhamnolipid
SCOs	Single Cell Oils
SEM	Scanning Electron Microscope
SL	Sophorolipid
SS	Sum of Squares
SSC	Side Scatter
γ -PGA	Poly Gamma Glutamic Acid

GENERAL INTRODUCTION AND MOTIVATION FOR THE THESIS

With the global energy demand increasing by ~ 40% by 2030, and as the global population crosses the 6 billion mark, energy security has become a prime global policy issue, and is likely to remain so for decades to come. The global energy need is primarily supplied by fossil fuels like oil, natural gas and coal, which meet approx. 80% of world's primary energy needs. Extensive use of these fossil fuels have not only raised the global prices of the fuels, causing serious threat to energy security, but have also resulted in serious and adverse impact on global environment due to green house gas emissions, and global warming. Thus, the key challenge facing the developing world is to seek judicious solutions to the growing energy need, and at the same time avoid adverse climate changes. Obviously, the only possible solution to the problem of global energy and environmental crisis is use of cleaner renewable sources of energy, in terms of biofuels.

India, with a population of over 1.2 billion, is one of the most energy-deficit nations

of the world. As per the Integrated Energy Policy Report, the per capita energy consumption in India was meager 439 kgoe (kilograms of oil equivalent, typically 41868 kJ/kg) in 2003, against the global average of 1688 kgoe. The per capita electricity consumption in India stands at 778 kW–h in 2012, against the global average of over 2000 kW–h. For achieving sustained growth rate of 8–9% through next 25 years till 2030, and to meet the life line energy needs of population over 1.2 billion, India needs to increase the primary energy resources by at least 3 to 4 times, and the electricity generation by minimum 6 times. India has proven oil reserves of about 775 million tons; however, the production is quite small (for example, only 37.71 million tons in the year 2010–11). The net consumption of petroleum products in India during 2010–11 was estimated at 142 million tons. These figures clearly indicate India's inability to meet country's growing energy demand from indigenous sources, and as a consequence, India is increasingly relying on the import of crude oil creating heavy burden on national economy. The import of crude oil in India has increased from 57.8 million tons (worth \$9.21 billion) in 1999–2000 to approx 163.4 million tons (worth \$91.8 billion) in 2009–10 (see the details given in Table 1.1). With a targeted GDP growth of 8%, the energy demands in various sectors like industry, agriculture, domestic are going to rise very fast, and the demand for transportation fuel and electricity will dramatically rise in future. It could be inferred from above discussion that there is an urgent need for large-scale production and promotion of biofuels in India, not only to meet the energy needs with a cleaner climate, but also to reduce the burden of oil import.

1.1 BIODIESEL POLICY AND PROGRAM OF INDIA

India's biofuels policy has undergone several developments since its inception in 2009. The current National Biofuels Policy has set an ambitious target of achieving 20% blending of both gasoline and diesel with ethanol and biodiesel, respectively.

Table 1.1 Statistics of crude oil production and import in India

Year	Crude oil production (MMT)	Crude oil import (MMT)	Average crude oil price (US \$/bbl.)
2002–03	33.04	81.99	26.59
2003–04	33.37	90.43	27.98
2004–05	33.98	95.86	39.21
2005–06	32.19	99.41	55.72
2006–07	33.99	111.50	62.46
2007–08	34.12	121.67	79.25
2008–09	33.51	132.78	83.57
2009–10	33.69	159.26	69.76
2010–11	37.71	163.59	85.09

Imports of Crude Oil during 2010–11 valued at Rs. 4559 billion (for 163.59 MMT crude oil), which is an increase of 21.45% from year 2009–10 where the total value of import was Rs. 3753.78 billion (for 159.259 MMT crude oil). Source: Indian Petroleum and Natural Gas statistics (2010–11)

Table 1.2A Projected waste land requirement to meet 20% blending of petro–diesel targets by 2017

Year	Diesel demand (MMT)	20% biodiesel quantity (MMT)	Area for 20% biodiesel quantity (Mha)
2011–2012	66.90	13.38	13.38
2017–2018	92.12	18.40	18.40

Adopted from Kumar et al. (2012)

Table 1.2B Categorization of waste land in India suitable for *Jatropha curcas* plantations (Planning Commission, 2003)

Type of land	Area in Mha
Forest area	3
Boundary plantations	3
Agro forestry	2
Cultivable fallow lands	2.4
Waste lands under integrated watershed development	2
Strip land like: railway, road and canal	1
Total	13.4

The target of biodiesel blending is to be achieved by 2011–12, while the target of ethanol blending is to be achieved by 2017. In view of shortage of edible oil in India for food,

the non-edible oil seeds of *Jatropha* and *Karanja* were targeted as the primary feedstock for oil. *Jatropha* is a small plant that grows on the degraded land, producing seeds within 3 years that have moderate to high content of oil (~ 40% w/w). In order to meet the 10% blending target, it was required to cultivate *Jatropha* on 11.2 million ha of under-utilized and degraded land, while for 20% blend the required plantation area was 13.4 million ha (see Table 1.2A, Kumar et al., 2012). The “waste-land” was categorized in several types as mentioned in Table 1.2B. The implementation of biodiesel program of India was envisaged in two stages: (1) Research and demonstration phase I from 2003–2007, and (2) Implementation phase II from 2007–2012. The first phase had three goals: (1) cultivate 4,00,000 ha of land with *Jatropha* plantation; (2) establish a research network of universities and research institutions, and (3) achieve 5 wt% blending target. Ministry of Petroleum and Natural Gas also enacted a National Biodiesel Purchase Policy to support the program, and the guarantee price of biodiesel was set at Rs. 25 per liter (as of Nov 2006, which was revised to Rs 26.5 in Oct 2008). This program received good response, and more than 9,00,000 ha of land was cultivated with *Jatropha* by 2009. Despite this initial progress, India’s biodiesel program suffered several setbacks later due to reasons such as fluctuating international oil prices, fluctuations in agronomic performance of crop, varying seed yield, input and maintenance requirement of crops, concerns regarding land tenure, and rural livelihood benefits. In view of above, 11th five-year plan recommended revised blending of 5 wt% biodiesel by 2012, which was significant reduction from 20 wt% blend proposed under National Mission on Biodiesel.

The revised National Biofuels Policy adopted by Government of India in Dec 2009 aims at achieving 20% blends by 2017 for both ethanol and biodiesel; however, these targets will be phased in over time, and will be periodically reviewed and adjusted as per needs. The policy proposed establishment of a National Registry for feedstock availability that would help set a realistic blending target. The oil marketing companies will be responsible for

purchasing, storing, distributing and marketing of biofuels, and Ministry of New and Renewable Energy will be the co-coordinator for the policy. The policy also identified several mechanisms to promote biofuels production such as subsidies, preferential financing, fiscal incentives, research, development, and demonstration and international collaboration.

1.2 HURDLES IN BIODIESEL PROGRAM: PROBLEMS AND SOLUTIONS

Despite its potential and promise, the biodiesel program of India has not achieved its goals and targets. There are several hurdles that have contributed to this effect. We give below a brief description of these problems (Kumar et al., 2012; Biswas and Pohit, 2013).

(1) Technological problems such as oxidation during storage, poor lubrication properties, and problems in cold starting. Moreover, increase in viscosity of the blended fuel at low temperatures, filter blockage, injector failure and clogging of fuel lines are also major operational problems.

(2) No institutional support was sought for development of high oil yielding *Jatropha* seeds. No insurance cover mechanism for plantation of biofuels crops was given in the first phase of National Biodiesel Mission. A suitable crop insurance scheme needs to be formulated.

(3) Suitable fiscal policy measures should be devised to be an integral part of biodiesel mission. One of the major reasons leading to failure of National Biodiesel Mission was absence of budgetary support. Budgetary support should be an integral part of any biofuels policy. The support should be in various forms like support livelihood for the cultivator, subsidy in sales tax and VAT, minimum support price and increase in import duty on biodiesel.

(4) There is a major discrepancy between the purchase price of biodiesel decided by oil marketing companies, and the actual manufacturing price of *Jatropha*-based biodiesel. The Biodiesel Association of India has requested a hike of purchase price to Rs 32 (from Rs 25

per liter decided by Ministry of Petroleum and Natural Gas earlier). However, even with most conservative estimates of cost of seeds, oil extraction, trans-esterification etc., the manufacturing cost of Jatropha based biodiesel comes out to be Rs. 46 per liter (refer to Table 1.3 for greater details). To reduce this cost, subsidies are required to ensure viable pricing for selling the biodiesel. Subsidies can also be given on biofuel crops with tax credits on the energy crops.

1.3 FORWARD INTEGRATION OF BIODIESEL PLANT: CONVERSION OF GLYCEROL TO VALUE ADDED PRODUCTS

Transesterification of oil to produce biodiesel yields crude glycerol as a byproduct (in quantities of 10% w/w of biodiesel produced). This glycerol is contaminated with water, salt, methanol and free fatty acids. The global demand for biodiesel is projected to be 8 billion gallons by 2020. This will bring in approximately 5.8 billion pounds of crude glycerol into the market from biodiesel industry alone. The current market for refined glycerin is approx. 2 billion pounds with market value of \$1 billion. Due to rapid growth of biodiesel industry, the current production of glycerin will be tripled by biodiesel industry alone. Biodiesel industry in Europe is growing fast and the trends in production of crude and refined glycerol in Europe since 1995 are given in Table 1.4. Due to very large supply of glycerol, the prices of refined glycerin have reduced sharply in past few years. As per the data reported by US Soybean Export Council, the prices of refined glycerin in US have reduced from 80 cents per pound in 2002 to 37 cents per pound in 2006. Table 1.5 gives the trends in the prices of refined glycerin in Europe and USA in past two decades. The market for refined glycerin in US fluctuates every year, but remains typically in the range of 450–500 million pounds. The prices of glycerin have fallen significantly in last few years, leading to closure of the Dow Chemicals plant producing 140 million tons of natural glycerin.

Table 1.3 Cost estimation for biodiesel production[#]

Cost component	Rate (Rs/ kg)	Quantity (kg)	Cost (Rs)
Seed	16	3.28	52.48
Cost of collection and oil extraction	2.36	1.05	2.478
Less cake produced	1	2.23	-2.73
Trans-esterification cost	6.67	1	6.67
Less cost of glycerol produced	50	0.095	-4.75
Cost of biodiesel per kg			54.65
Cost of biodiesel/liter (specific gravity of 0.85 at 15°C)			46.45

adopted from Kumar et al. (2012)

Table 1.4 Trends in production of refined and crude glycerol in Europe

Year	Europe Refined Glycerin Production (Million lbs)	Europe Crude Glycerin Production (Million lbs)
1995	382	102
1996	396	142
1997	459	170
1998	477	204
1999	537	227
2000	438	319
2001	333	308
2002	378	284
2003	460	337
2004	366	338
2005	533	350
2006	606	445

Source: Glycerin Market Analysis (2012)

However, some biodiesel manufacturers have added glycerin refineries on their plant site to process and purify the biodiesel derived glycerin. Although, US have imported ~55 million tons of refined glycerin in past two years, it has been an exporter of crude glycerin since 2007.

Refining of glycerol: The current installed capacity of glycerin refinery is not large enough to handle all crude glycerin originating from biodiesel industry.

Table 1.5 Trends in the international prices of refined glycerin in past two decades

Year	99.5% Refined Glycerin Price – US (cent/lb)	Europe Kosher 99.7% Refined Glycerin – Price (€/ MT)
1990	58	1023
1991	49	946
1992	61	1074
1993	74	1636
1994	93	1841
1995	98	1508
1996	75	1048
1997	53	844
1998	50	946
1999	50	1023
2000	75	1457
2001	74	997
2002	80	1180
2003	77	630
2004	92	570
2005	47	450
2006	37	450

MT – metric ton. Source: Glycerin Market Analysis (2012)

This is due to the fact that there was a very sharp rise in the crude glycerin supply from biodiesel industry that did not go hand-in-hand with the growth of refinery. For example, in the US, the installed capacity of glycerol refinery is only 500 million pounds, and is designed to refine natural glycerin (and not biodiesel derived glycerin). Very low prices of crude glycerin are prohibitive for expansion of the refining capacity. High transportation cost of glycerin restricts the market access. Germany and Malaysia are the largest suppliers of glycerin in the world. The import of glycerol in the US is mainly from Malaysia, as the market price of crude glycerin doesn't meet the cost of shipping of crude glycerin from Europe to the US. For example, the cost of shipping of glycerin from European parts to American market is \$0.04 to 0.05 per pound, and quite often the transportation is higher than the domestic market cost.

Table 1.6 Applications of glycerin (distribution in terms of end use in wt%)

Applications	End Use (in %)
Food products	24
Personal care products	23
Oral care products	17
Tobacco Humectant	11
Polyether polyols for urethanes	8
Pharmaceuticals	7
Miscellaneous	10

Source: Glycerin Market Analysis (2012)

The end uses of refined glycerin are mainly in three sectors: food products, personal care products and oral care products. Table 1.6 shows the complete distribution of outlets of glycerin. Biodiesel derived glycerin, being crude, is useless for these applications. The common use of crude glycerin is for incineration, i.e. as a fuel in industrial boilers. Currently, this is the major outlet for crude glycerin, which does not require refining. However, this outlet for glycerin has the least value, as crude glycerin does not fetch much price, and doesn't add to the revenue of biodiesel industry. The demand for glycerin in conventional applications is increasing, but it is not enough to keep up with supply of crude glycerin from biodiesel industry. For example, large consumers of glycerin like Japan and US have growth rate of only 2% in the glycerin market. The demand of glycerol in Asian markets is also on rise, as the market for personal care products like soaps, cosmetics and other hygiene products is fast expanding. China has a rapidly growing market for glycerin. Even with this, the rise in international glycerin market is not large enough to accommodate all crude glycerin that is entering the market.

For value addition to crude glycerol from biodiesel industry, new processes need to be explored. The supply of crude glycerol is likely to reach a crisis level. The international prices of glycerol are the lowest. Glycerol can form feedstock for several processes for

production of value-added chemicals. These processes could be forward integration of the biodiesel industry, and will provide simultaneous solutions to two problems, viz. (1) effective utilization of crude glycerol and, (2) increasing the revenues of biodiesel industry, making the economy of the biodiesel attractive. It is in this spirit that the present research work was undertaken with aim of development, optimization and intensification of a bioprocess for conversion of glycerol to value-added products. Given below are the scope of the research work carried out and also a broad outline of the thesis.

1.4 AIM AND SCOPE OF PRESENT THESIS

This research work was aimed at developing the biochemical process of converting glycerol into two main products, viz. 1,3-propanediol and butanol. Ethanol was also a side product of the process. We have taken a step-by-step approach for development, optimization and intensification of the bioprocess for glycerol fermentation using immobilized cells. The micro-organism used is a glycerol fermenting anaerobe called *Clostridium pasteurianum*. The thesis comprises of 9 chapters (including the present one) that describe our results in each step of process development. The contents of these chapters are briefly outlined below:

In Chapter 2, we have given a comprehensive review of the bioconversion of glycerol to numerous value-added products. We have presented review of literature for conversion of glycerol to as many as 23 products.

In Chapter 3, we have presented the preliminary optimization studies of glycerol bioconversion. These include selection of micro-organism, support for immobilization and initial studies on glycerol fermentation by free and immobilized cells.

In Chapter 4, we have assessed the kinetics of glycerol bioconversion. We have determined the optimum temperature of the process, and have also determined the activation

energy of the process.

In Chapter 5, we have presented results of selection and optimization of the fermentation medium using Taguchi design of experiment. We have assessed the scale up of glycerol bioconversion at bioreactor level using optimized fermentation medium.

In Chapter 6, we have addressed the issue of optimization of the physical parameters of glycerol fermentation process using Taguchi statistical design. We have also assessed scale up of the process at optimized conditions of physical parameters and have ascertained the recyclability potential of the immobilized biocatalyst.

One of the major drawbacks of the biochemical process is its kinetics. In Chapter 7, we have presented our results on intensification of the glycerol bioconversion process with free *Clostridium pasteurianum* cells using ultrasound irradiation as means of enhancing kinetics of the process. Moreover, we have analyzed the results by fitting the enzyme kinetic model (Michaelis–Menten and Haldane kinetics), and its concurrent analysis with simulations of cavitation bubble dynamics. This analysis has revealed interesting mechanistic features of the process.

In Chapter 8, we have extended the theme and approach of Chapter 7 for immobilized *C. pasteurianum*. Again, the concurrent analysis of experimental and simulation result has shed interesting light on the glycerol bioconversion process.

In Chapter 9, we have summarized the results of all chapters, and have presented a coherent and unified picture of process development, optimization and intensification for glycerol bioconversion. We have also given several suggestions for future work in this area.



GLYCEROL BIOCONVERSION: LITERATURE REVIEW AND ANALYSIS

2.1 INTRODUCTION

Glycerol (1,2,3-Propanetriol) is one of the most versatile molecules in organic chemistry that can form primary building feedstock for manufacture of numerous commodity chemicals of day-to-day applications. The principal conventional routes to production of glycerol are: (1) yeast fermentation, where glycerol is a by-product of sugar-ethanol in redox neutral process; (2) by-product of the hydrolysis of soap manufacture from fats; (3) oxidation or chlorination of propylene. However, in the current scenario, glycerol production through all three routes is becoming less popular due to various reasons. The rising cost of propylene and limited availability of propylene feedstock has made oxidation/chlorination route uneconomical. The current international price of glycerol stands at US \$ 0.21–0.23/lb with an estimated global production of 1.78 million tons per annum.

Table 2.1 Biodiesel and glycerin production scenario (Biodiesel 2020)

Year	Biodiesel production capacity (in ^a MMT)	Actual biodiesel production (in ^a MMT)	Glycerin production (in ^a MMT)
USA			
2004	0.26	0.26	0.029
2006	1.99	0.85	0.094
2008	11.27	2.21	0.246
2010	–	6.96	0.773
Europe			
2004	2.8	2	0.222
2006	5	4	0.444
2008	12.2	7.1	0.789
2010	32.6	11.1	1.233

^aMMT indicates Million Metric Tons

The projected global demand for glycerol that finds application in manufacture of variety of products such as drugs, tobacco, glycerin triacetate, food, paints, cellophane, toothpaste and cosmetics, stands at 1.81 million tons per annum. More recently, another major source through which very large quantities of crude glycerol are available is the biodiesel industry. Biodiesel is essentially methyl/ ethyl ester of fatty acid and is produced through transesterification of vegetable oils or animal fats. Glycerol is the principal by-product of the process. Stoichiometrically, 1 mole of triglyceride gives 3 moles of esters or biodiesel and 1 mole of glycerol. Although the molecular weight of the fatty acid methyl ester or biodiesel varies in a wide range depending on the type of alkyl group, typically on weight basis, per 9 kg of biodiesel, 1 kg of glycerol is produced. The annual production of biodiesel in Europe was 11.2 million tons and in USA was 6.96 million tons in 2010 (Biodiesel 2020: A global market survey, 2nd edition). These productions are expected to rise significantly over next decade (Table 2.1 gives the trends). Even in Asian and Latin American countries, the biodiesel production and consumption is rising fast. The amount of glycerol annually available through biodiesel industry in Asian and Latin American countries is estimated at

130,000 tons. Effective and economic utilization of these enormous quantities of glycerol is a daunting challenge facing biodiesel industry. Another driving force for the utilization of glycerol is the low economic viability of the current biodiesel processes. Tran et al. (2011) have given an economic analysis of biodiesel derived from different sources such as vegetable (edible and non-edible) oils, waste oils, waste grease and animal fats in Hawaii's agricultural sector. Even with best possible estimates (inclusive of pretreatment and on spot availability of feedstock) of capital and operating costs, the breakeven price of biodiesel with palm oil as feedstock is \$2.98 per liter, and with *Jatropha* as feedstock is \$4.96 per liter. These prices may vary from region to region and figures given above are only representative (Tran et al., 2011). Comparing these costs with the costs of petroleum derived fuels, which stand at \$2.03 per liter in Europe and \$1.08 per liter in USA, one can realize that biodiesel does not stand competition. Therefore, the biodiesel industry has to seek alternate sources of revenue. Obviously, the best option is upgradation of the glycerol, which is the main by-product, to value-added products through chemical and biochemical processes.

Direct utilization of the glycerol generated from biodiesel industry for conventional applications is not possible due to significant amounts of contaminants in it. These contaminants are mainly catalysts (usually NaOH) and unreacted alcohol. Purification of glycerol through different means such as extraction/distillation is prohibitively expensive. Use of this glycerol through conventional catalytic chemistry route is an option (Zheng et al., 2008). Principal products from chemical (or catalytic) transformation of glycerol are: dihydroxyacetone, glyceraldehyde and acids such as glyceric acid, mesoxalic acid, tarconic acid, hydroxypyruvic acid and oxalic acid through oxidation route; 1,3-Propanediol (PDO) and 1,2-PDO through reduction route; glycerol carbonate and diacylglycerol through esterification; polyglycerols through etherification; acrolein by dehydration; acrylic acid by oxidation and dichloropropanol and epichlorohydrin by chlorination.

Conversion of glycerol to value-added products can also be achieved through biochemical route. Due to its greater degree of reduction than conventional sugars, glycerol forms a versatile substrate (or carbon source) for synthesis of a variety of chemicals such as 1,3-PDO, dihydroxyacetone, citric acid, glyceric acid, 3-hydroxypropionaldehyde, succinic acid, erythritol, polyhydroxyalkanoates etc. The main bacteria that have the capability of utilizing glycerol are the members of Enterobacteriaceae family belonging to genus *Citrobacter*, *Klebsiella*, *Clostridium*, *Enterobacter* and *Lactobacillus*. There are several arguments as why biochemical route is preferable over the catalytic chemistry route for a particular product. Most of the routes through catalytic chemistry involve harsh operating conditions, in terms of high temperature and pressure. The catalyst is also an expensive component of the process. Table 2.2 gives a summary of reaction conditions, catalyst, yield and selectivity for catalytic conversion of glycerol to some major products. The biochemical processes, on the other hand, operate at ambient conditions with selectivity of almost 100%. However, the principal demerit of biochemical route is that the kinetics of conversion is significantly slower. To overcome this and other demerits, significant research has been dedicated in recent years to optimize the reaction conditions and configuration.

In this chapter, we have attempted to present an overview of the research activity in the area of bioconversion of glycerol to numerous value-added products. We have also given analysis and interpretation of the published literature from engineering and economic viewpoint, i.e. the potential of these processes for scale-up and large-scale implementation. Several previous reviews have addressed the matter of production as well as conversion of glycerol through microbial routes. The major contributions are by da Silva et al. (2009), Amaral et al. (2009), Saxena et al. (2009), Wang et al. (2001), Deckwer (1995). In this chapter, we have spanned as many as 23 products through biochemical conversion of glycerol.

Table 2.2 Representative summary of catalytic or chemical transformation of glycerol

Reaction Type	Catalyst	Product	Reaction Conditions	Yield (% g/g)	Selectivity	Reference
Oxidation	Bi promoted Pt	Dihydroxyacetone	–	–	50%	Garcia et al., 1995
	Pd/C	Glyceric acid	pH 11.0	–	70%	
	Pt/C	Glyceric acid	–	–	55%	
Electrocatalytic oxidation	15 mol% 2,2,6,6-Tetramethylpiperidine-1-oxyl	Dihydroxyacetone	pH 9.1 buffered with 0.2 M bicarbonate, 1.1 V vs Ag/AgCl	–	–	Ciriminna et al., 2006
Oxidation	Au nanoparticles supported on graphite in NaOH	Sodium glycerate	–	–	100%	Carrettin et al., 2002
Oxidation	1% Au/Carbon	Glyceric acid	0.3 MPa O ₂ , 30°C, 0.3M NaOH, NaOH/Gl _{ol} = 4, Gl _{ol} /Au = 500, 20 h	–	92%	Porta, 2004
Reduction (Hydrogenolysis)	Rh(CO) ₂ (acac) and tungstenic acid	1,3-PDO	300 bar syngas, 200°C	20%	–	Che, 1987
Reduction Hydrogenolysis	Ni/Re	1,3-PDO	8.2 MPa H ₂ , 230°C, 4 h	5%	–	Werpy et al., 2002
Reduction Hydrogenolysis	Rh, tungstenic acid	1,3-PDO	8MPa H ₂ , 180°C, sulfolane solvent	–	67%	Chaminand et al., 2004
Dehydration	5mM H ₂ SO ₄ in water	Acrolein	34.5 MPa, 350°C	–	84%	Ramayya et al., 1987
Dehydration	ZnSO ₄	Acrolein	25–34 MPa, 300–390°C, 10–60 s	–	75%	Ott et al., 2006
Dehydration	Silicotungstic acid supported on silica	Acrolein	0.1 MPa, 275°C	–	85%	Tsukuda et al., 2007

Table 2.2 (.....Continued)

Reaction Type	Catalyst	Product	Reaction Conditions	Yield (% g/g)	Selectivity	Reference
Oxidation	Nanosized carbon supported on 3.7 nm Au particle	Glyceric acid	–	–	75%	Demirel et al., 2007
Etherification	Amberlyst 35	<i>tert</i> -butyl ethers	60°C, <i>tert</i> butanol	–	–	Klepacova et al., 2005
Carboxylation	Ethylene carbonate in presence of NaHCO ₃	Glycerol carbonate	125°C	81%	–	Bell et al., 1959
Pyrolysis	CeO ₂ supported Ir	Hydrogen	400°C	–	85%	Zhang et al., 2007a
Steam reforming	MgO supported Ni	Hydrogen	650°C	4 mol out of max 7 mol	–	Adhikari et al., 2008
Supercritical water reforming	Ru/Al ₂ O ₃	Hydrogen	800°C	7 mol	–	Byrd et al., 2008

2.2 GENERALIZED METABOLIC PATHWAY OF GLYCEROL BIOCONVERSION

Glycerol contains highly reduced carbon, which facilitates its direct utilization by the cells as a sole carbon source for their growth and maintenance of cellular processes. Apart from increasing the cell biomass, glycerol as a carbon source can also be utilized in the production of various enzymes, recombinant proteins, amino acids, vitamins, etc. The metabolism of glycerol in micro-organisms mainly occurs by two distinct and parallel pathways, oxidative and reductive (Yazdani and Gonzalez, 2007). The members of Enterobacteriaceae family such as *Klebsiella*, *Citrobacter* and *Clostridia* are the primary producers of 1,3-PDO, and exhibit both oxidative and reductive pathway. Both oxidative and reductive pathways are shown in Fig. 2.1.

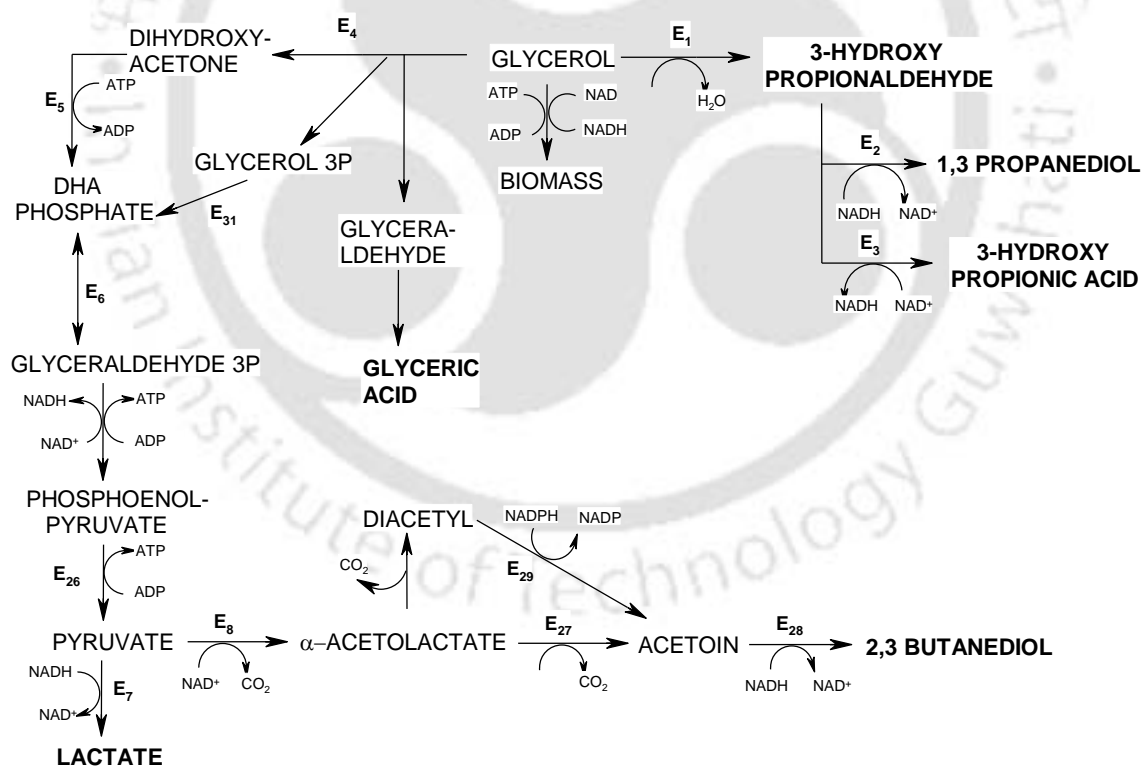


Figure 2.1 Metabolic pathway of glycerol bioconversion: Oxidative and reductive wings of glycerol assimilation (E₁–Glycerol dehydratase; E₂–1,3-PDO dehydrogenase; E₃–Aldehyde dehydrogenase; E₄–Glycerol dehydrogenase type 1; E₅–Dihydroxy acetone kinase; E₆–Triose phosphate isomerase; E₇–Lactate dehydrogenase; E₈–Pyruvate decarboxylase; E₂₆–Pyruvate kinase; E₂₇–α-Acetolactate decarboxylase; E₂₈–Acetoin reductase; E₂₉–Diacetyl reductase; E₃₁–Glycerol-3-phosphate dehydrogenase)

The reductive pathway proceeds by the dehydration of glycerol to 3-hydroxypropionaldehyde, also called as *Reuterin*, in presence of vitamin B₁₂ dependant glycerol dehydratase. It can also spontaneously undergo dehydration to form acrolein. The 3-HPA so formed is then reduced to 1,3-PDO by a NADH dependant 1,3-PDO dehydrogenase, regenerating NAD⁺ for oxidative branch. 3-HPA can be further oxidized to 3-hydroxypropionic acid by NAD⁺ linked aldehyde dehydrogenase. A parallel oxidative branch produces dihydroxyacetone, and ultimately channels glycerol to Embden–Meyerhof–Parnas (EMP) pathway for production of number of important metabolites such as ethanol, citric acid, succinic acid, lactate, 2,3-butanediol, etc. The Enterobacteriaceae members contain both type 1 glycerol dehydrogenase and 1,3-PDO dehydrogenase.

The oxidative wing progresses by the oxidation of glycerol to dihydroxyacetone (DHA) by NAD⁺ linked type 1 glycerol dehydrogenase. This is further phosphorylated by ATP dependant DHA kinase to a glycolytic intermediate, DHA phosphate, which enters EMP pathway. The production of DHA from glycerol oxidation is primarily observed in acetic acid bacteria, *Acetobacter* and *Gluconobacter*. These microorganisms carry out glycerol oxidation in a similar fashion to the Enterobacteriaceae members, but the reaction is catalyzed by a membrane bound glycerol dehydrogenase (Gupta et al., 2001). These micro-organisms are anaerobes, and hence, they lack glycolytic and Kreb's cycle enzymes. As a consequence, further metabolism of DHA is not carried out by them.

The phosphorylated DHA isomerizes to glyceraldehyde-3-phosphate by triose phosphate isomerase. The phosphorylated DHA can be derived from 3 different routes: (1) From glycerol via type 1 glycerol dehydrogenase; (2) From glycerol via membrane bound glycerol dehydrogenase; (3) From phosphorylated glycerol, formed by ATP dependant glycerol kinase, catalyzed by glycerol-3-phosphate dehydrogenase.

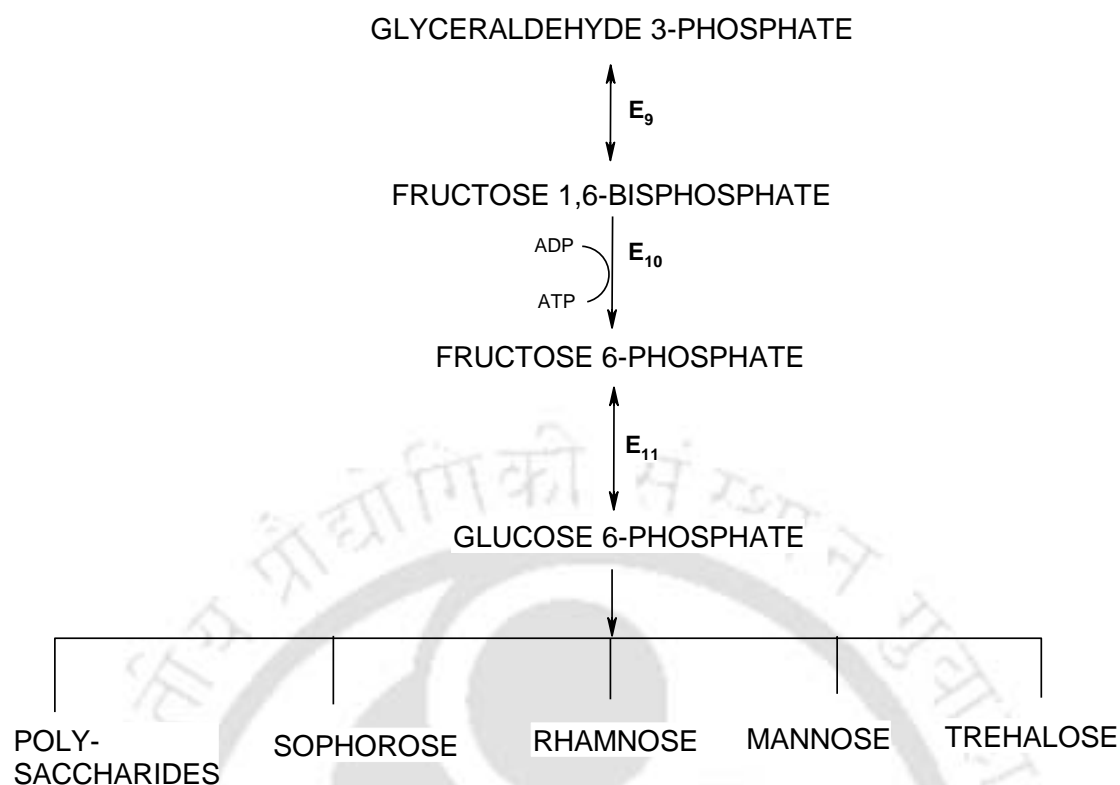


Figure 2.2 Metabolic pathway of glycerol bioconversion: Pathway depicting alternate metabolic fate of an intermediate of glycerol assimilation, Glyceraldehyde-3-phosphate, which finally converts into various sugars, eventually forming biosurfactants (E_9 -Aldolase; E_{10} - Fructose 1,6-bisphosphatase; E_{11} -Hexose phosphate isomerase)

Glyceraldehyde-3-phosphate converts to phosphoenolpyruvate through a series of steps, and finally undergoes substrate level phosphorylation to form pyruvate by pyruvate kinase, generating an ATP in the process. Glyceraldehyde-3-phosphate can undergo gluconeogenesis to reversibly form fructose 1,6-bisphosphate by aldolase enzyme. Fructose 1,6-bisphosphatase further converts fructose 1,6-bisphosphate to fructose-6-phosphate regenerating an ATP. Fructose-6-phosphate isomerizes to glucose-6-phosphate, which is a building block for several polysaccharides and various di and trisaccharides such as sophorose, rhamnose, mannose and trehalose. This metabolic pathway is depicted in Fig. 2.2. These sugars are acetylated and get attached to lipid moiety to form various glycolipids which work as biosurfactants. The sugars may also get associated with nucleic acids or lipids

to constitute microbial extracellular polysaccharides.

As shown in Fig. 2.3, pyruvate formed in the earlier step can have various metabolic fates:

1. It can be reduced to lactate by NADH dependant lactate dehydrogenase.
2. It may undergo decarboxylation by pyruvate decarboxylase to form α -acetolactate, which is further decarboxylated to acetoin. α -Acetolactate may also decarboxylate to diacetyl, which in turn is reduced to acetoin by NADPH dependant diacetyl reductase. The acetoin so formed, through any of the two routes, is reversibly reduced to 2,3-butanediol by NADH dependant acetoin reductase (Syu, 2001).
3. Pyruvate may also convert into formate in presence of pyruvate formate lyase, which is further cleaved to gaseous products H_2 and CO_2 by formate hydrogen lyase.
4. Pyruvate can be carboxylated by pyruvate carboxylase to oxaloacetate, which is further reduced by NADH dependant malate dehydrogenase to malate. Malate then gradually forms fumarate by fumarase, and fumarate in turn converts into succinate by fumarate reductase.
5. It can form acetyl-CoA in presence of pyruvate dehydrogenase complex, which can anaerobically form ethanol via acetaldehyde by alcohol dehydrogenase.

Acetyl CoA is the precursor for the formation of acetate, butyrate, butanol, and ethanol. Acetyl CoA can also form acetate, or alternatively, can combine with another molecule of acetyl CoA to generate a molecule of acetoacetyl CoA. Acetoacetyl CoA undergoes a NADPH dependant reduction to β -hydroxybutyryl CoA. This further undergoes dehydration by crotonase to crotonyl CoA, which is reduced to butyryl CoA by NADH dependant butyryl CoA dehydrogenase. Butyryl CoA can then finally form either butyrate or butanol, via butyraldehyde formation. The final step in butanol production pathway is catalyzed by butanol dehydrogenase. Acetyl CoA can also enter in lipid biosynthesis pathway to produce triacylglycerols also known as single cell oil (SCO).

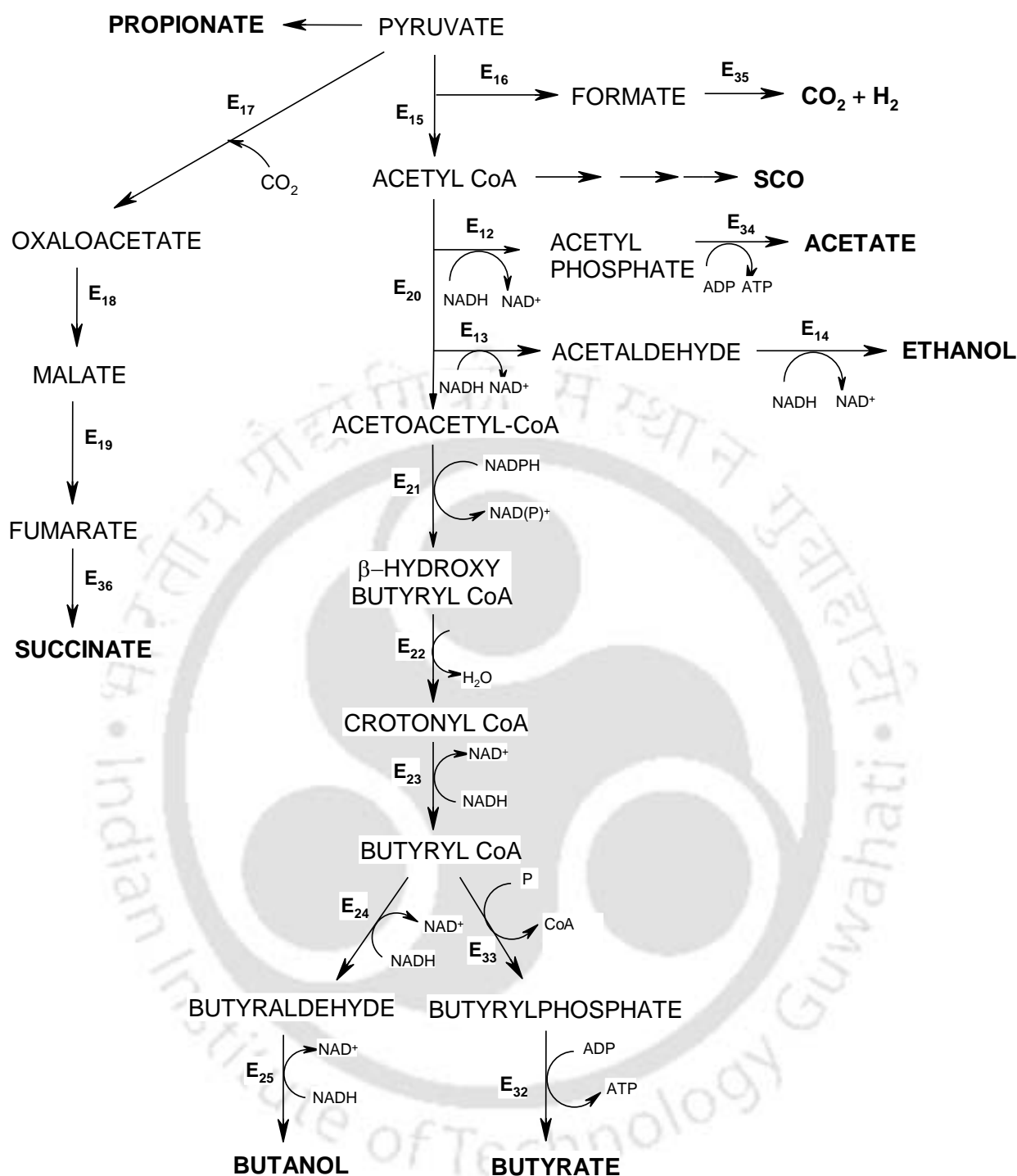


Figure 2.3 Metabolic pathway of glycerol bioconversion: Pathways depicting different metabolic fate of pyruvate, an intermediate of glycerol bioassimilation (E₁₂–Phospho-transacetylase; E₁₃–Acetaldehyde dehydrogenase; E₁₄–Alcohol dehydrogenase; E₁₅–Pyruvate dehydrogenase complex; E₁₆–Pyruvate formate lyase; E₁₇–Pyruvate carboxylase; E₁₈–Malate dehydrogenase; E₁₉–Fumarase; E₂₀–Thiolase; E₂₁–β–Hydroxybutyryl CoA dehydrogenase; E₂₂–Crotonase; E₂₃–Butyryl CoA dehydrogenase; E₂₄–Butyraldehyde dehydrogenase; E₂₅–Butanol dehydrogenase; E₃₂–Butyrate kinase; E₃₃–Phosphobutyryl transferase; E₃₄–Acetate kinase; E₃₅–Formate hydrogen lyase; E₃₆–Fumarate reductase)

Apart from these major pathways, a minor and independent pathway also operates in few micro-organisms that comprises of conversion of glycerol to glyceric acid with glyceraldehyde as the intermediate. The enzymes responsible for the two steps of this pathway are yet to be identified. Although the complete assimilation pathway of glycerol is rather complex, every step in it yields a particular product. The gamut of metabolites or products formed varies from one micro-organism to another, depending on the presence of a particular enzyme or a group of enzymes.

2.3 ECONOMICALLY SIGNIFICANT PRODUCTS OF GLYCEROL BIOCONVERSION

2.3.1 1,3-Propanediol

1,3-Propanediol (1,3-PDO) serves as a monomer for synthesis of many photo-stable polymers such as polyesters and polyurethanes, and also finds application in food, cosmetic and pharmaceutical industries. It is also an important starting material for the synthesis of biodegradable plastic, polytrimethylene terephthalate. It is chemically produced from acrolein or propylene or ethylene derived from petroleum. The process suffers from low selectivity and requires stringent reaction conditions (high pressure, high temperature). Moreover, it produces toxic intermediates with very low yield of product. The microbial production of 1,3-PDO is carried out mainly by anaerobic bacteria belonging to family Enterobacteriaceae, namely, *Clostridia*, *Klebsiella*, *Citrobacter*, *Enterobacter* and *Lactobacillus*, on dehydration of a part of glycerol to 3-hydropropionaldehyde (3-HPA), which in turn is reduced to 1,3-PDO. The formation of reduced 1,3-PDO regenerates reducing equivalent NAD^+ from NADH, which is continuously formed from the oxidation of glycerol to dihydroxyacetone (DHA).

The members of Enterobacteriaceae convert glycerol mainly to 1,3-PDO and acetate

along with the formation of by-products, succinate, lactate and formate. The two most extensively studied strains for 1,3-PDO production are *Klebsiella pneumoniae* and *Clostridium butyricum*. The production of 1,3-PDO by *C. butyricum* occurs by a vitamin B₁₂ dependant enzyme, glycerol dehydratase. These two strains show the highest substrate tolerance, least inhibition, the highest yield and productivity. The typical product profile of *C. butyricum* consists of 1,3-PDO, butyric acid, acetic acid, CO₂ and H₂. The production of 1,3-PDO is inhibited by the accumulation of an intermediary metabolite, 3-HPA, at a critical inhibitory concentration of 10 mmol/L. 3-HPA exerts its inhibitory effect by inhibiting 1,3-PDO synthesizing enzymes, namely, 1,3-PDO oxidoreductase and 3-HPA dehydratase. Glycerol plays a key role in regulating the concentration of 3-HPA in the media. A low glycerol concentration of less than 7–8 g/L in the media limits the concentration of 3-HPA, and thereby, enhances the productivity of 1,3-PDO. 1,3-PDO also exerts a feedback inhibition on its own production.

The un-dissociated acetic acid and butyric acid do not exert any inhibitory effect on 1,3-PDO production from glycerol, while the dissociated form of acetic acid, i.e. acetate, increases the biomass yield and butyrate production along with a decrease in 1,3-PDO yield. On the other hand, dissociated form of butyric acid i.e. butyrate increases 1,3-PDO well as butyrate production (Colin et al., 2001). The effect of addition of acetate to a glycerol containing media, on yield of products formed by *C. butyricum* LMG1212₂ in a chemostat is shown in Fig. 2.4 (Heyndrickx et al., 1991).

The most efficient production of 1,3-PDO by *K. pneumoniae* occurs in anaerobic or microaerobic condition. It is already established that the cells form comparable amount of 1,3-PDO (65.26 g/L) even in aerobic fed-batch fermentation (Ma et al., 2009). In presence of oxygen, *K. pneumoniae* cells form more lactic acid than ethanol.

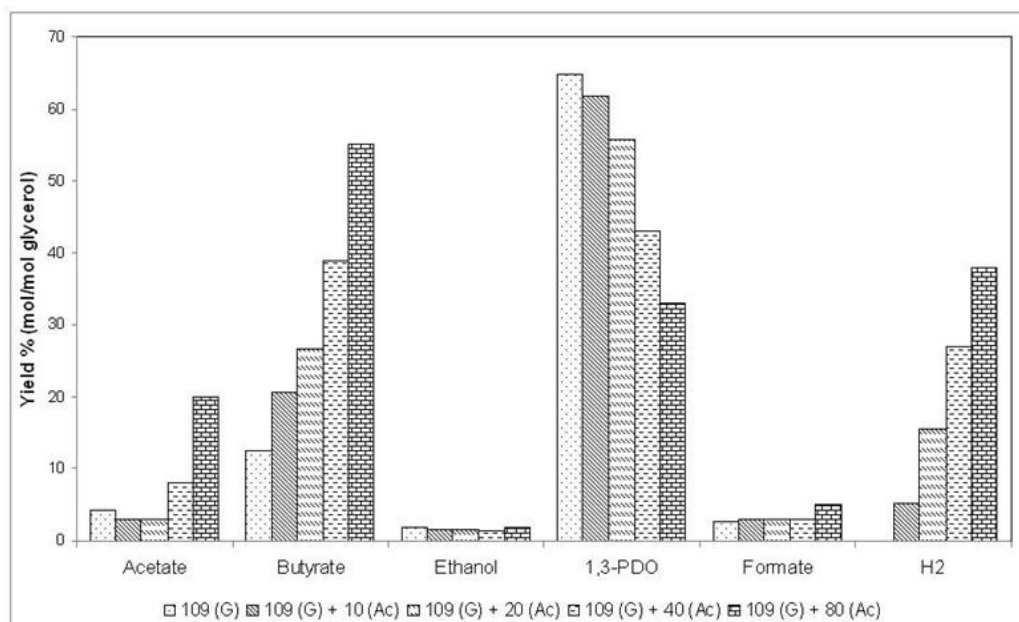


Figure 2.4 Effect of acetate on yield of different products formed in chemostat by *Clostridium butyricum* LMG1212t₂, utilizing glycerol (Heyndrickx et al., 1991). The figure legend indicates concentration of glycerol (G) and acetate (Ac) in mmol/L

At 110 and 133 g/L glycerol concentration, there is a complete inhibition of cell growth under aerobic and anaerobic condition respectively (Cheng et al., 2005). The cells form 61.9 g/L 1,3-PDO with pure glycerol, which is more than that formed with crude glycerol (51.3 g/L). This is due to the presence of methanol, soaps and other impurities in glycerol (Mu et al., 2006). The production of 1,3-PDO from crude glycerol by *C. butyricum* cells requires optimum temperature of 35°C and pH 7.0. This process is independent of aeration rate and stirring speed (Günzel et al., 1991). The fed-batch fermentation (to avoid inhibition caused by glycerol) produces maximum 1,3-PDO (65 g/L) (Saint-Amans et al., 1994). In batch experiments, 50 g/L glycerol exerts almost 50% inhibition as compared to 35 g/L glycerol. The growth of *C. butyricum* cells is inhibited at 50 g/L concentration of 1,3-PDO and 85 g/L concentration of glycerol. However, the production of 1,3-PDO by *C. butyricum* can tolerate a higher concentration of 83.7 g/L of 1,3-PDO. The inhibition by 1,3-

PDO is manifested by inhibition of membrane-bound ATPases, or by an enhancement in the membrane fluidity leading to a complete change in membrane structure, and thus, change in transport mechanism of alcohols (Colin et al., 2000). The strain shows same tolerance to both raw and commercial glycerol with similar grade of 87% w/v. The mode of fermentation also influences the nature of intermediates formed in the metabolic pathway. For example, butyric acid formation is not observed in batch cultures but in continuous cultures. Similarly, lactate formation is observed in batch cultures but not in continuous cultures (González-Pajuelo et al., 2004). The summary of literature for 1,3-PDO production by bioconversion of glycerol is given in Table 2.3.

2.3.2 Butanol

Butanol is being looked at as a promising alternate fuel due to its comparable properties with gasoline. It is used as a solvent for production of hormones, vitamins and brake fluid formulation. It is also used as a feedstock for production of methacrylate and butylacrylate. The chemical synthesis of butanol occurs through the petrochemical route. Traditionally, butanol or biobutanol was derived from ligno-cellulosic biomass through ABE fermentation process. The conventional process suffers from various drawbacks such as butanol toxicity of cells, low yield of butanol, difficulty in separation of butanol from acetone and ethanol and gradual degeneration of cultures with time. These shortcomings impair industrial level of biobutanol production. Apart from biomass, the other substrate that can be looked into for biobutanol production is glycerol. The only known organism that can grow on and utilize glycerol for biobutanol production belongs to genus *Clostridium* named as *Clostridium pasteurianum*. ABE producing enzyme *C. acetobutylicum* is also shown to utilize glycerol only in the presence of glucose (Andrade and Vasconcelos, 2003).

Table 2.3 Summary of literature on bioconversion of glycerol to 1,3-PDO

Micro organisms	Reactor design/mode of operation	Productivity g/L-h	Molar yield mol/mol	Byproducts	Reference
<i>Clostridium butyricum</i> DSM 5431	Fed Batch	2.76	0.66	ethanol, acetate, butyrate	Gunzel et al., 1991
<i>Clostridium butyricum</i> LMG 1212t ₂	Batch (Chemostat)	–	0.65	formate, acetate, butyrate	Heyndrickx et al., 1991
<i>Citrobacter freundii</i> DSM 30040	Batch	5.5	0.60	ethanol, pyruvate, acetate, lactate	Boenigk et al., 1993
	Continuous	11.0 (at 0.3 h ⁻¹ dilution)	0.67		
	Two stage chemostat	1.38	0.62		
<i>Clostridium butyricum</i> VPI 3266	Batch	0.722	0.54	butyrate	Saint Amans et al., 1994
	Fed Batch	1.21	0.56		
<i>Citrobacter freundii</i> DSM 30040 immobilized on PU foam	Fixed bed, continuous	8.2	0.57	ethanol, acetate, lactate	Pflugmacher and Gottschalk, 1994
<i>Clostridium butyricum</i> DSM 5431 mutant 2/2	Fed Batch	0.657	0.66	butyrate, acetate	Abbad-Andalousi et al., 1995
<i>Clostridium butyricum</i> E5	Batch	1.4	–	butyrate, acetate	Petitdemange et al., 1995
	Fed Batch	2.8 (with industrial glycerol)			
<i>Clostridium butyricum</i> DSM 5431	Fed batch with continuous feeding	2.4	0.62	butyrate, acetate	Reimann and Biebl, 1996

Table 2.3 (.....Continued)

Micro organisms	Reactor design/mode of operation	Productivity g/L-h	Molar yield mol/mol	Byproducts	Reference
<i>Klebsiella pneumoniae</i> DSM 2026	Continuous	4.9	0.61	acetate, lactate, ethanol, butanediol, formic acid	Menzel et al., 1997
<i>Enterobacter agglomerans</i> CNCM 1210	Continuous	–	0.51	acetate, lactate, succinate, formate, ethanol	Barbirato and Bories, 1997
<i>Citrobacter freundii</i> ATCC 8090	Batch	–	0.65	acetate, lactate, succinate, formate, ethanol	Barbirato et al., 1998
<i>K. pneumoniae</i> ATCC 25955	Batch	–	0.65	acetate, lactate, succinate, formate, ethanol	
<i>Enterobacter agglomerans</i> CNCM 1210	Batch	–	0.51	acetate, lactate, succinate, formate, ethanol	
<i>Clostridium butyricum</i> CNCM 1211	Batch	–	0.62	acetate, butyrate	
<i>Clostridium butyricum</i> F2b	Batch	1.74	0.63	acetate, butyrate, lactate	Himmi et al., 1999
<i>Clostridium butyricum</i> F2b	Two stage continuous fermentation	3.4	0.55 g/g with 90 g/L glycerol	butyrate, acetate	Papanikolaou et al., 2000
	Single stage continuous fermentation	5.5	0.67 g/g with 30 g/L glucose	butyrate, acetate	

Table 2.3 (.....Continued)

Micro organisms	Reactor design/mode of operation	Productivity g/L-h	Molar yield mol/mol	Byproducts	Reference
Strain AT1	Batch	0.17	0.39	ethanol, butyrate	Wittlich et al., 2001
<i>Caloramator viterbensis</i> JW/MS-VS5	Batch	–	0.69	acetate, H ₂	Seyfried et al., 2002
<i>Clostridium butyricum</i> VPI 3266	Batch	–	0.51	acetate, lactate, butyrate	González-Pajuelo et al., 2004
	Continuous	3.02	0.60		
<i>Clostridium butyricum</i> VPI 3266	Continuous chemostat	10.3	0.65	butyrate, acetate	González-Pajuelo et al., 2005a
rDG1(pSPD5) <i>Clostridium acetobutylicum</i>	Fed batch	1.8	0.65	butyrate, acetate, lactate	González-Pajuelo et al., 2005b
	Continuous	3.0	0.65		
<i>K. pneumoniae</i> ZJU 5205 encapsulated in NaCS/PDMDAAC	Batch	5.74	0.65	acetic acid, ethanol	Zhao et al., 2006
	Fed Batch	1.08	0.39		
	Continuous (All fixed bed)	4.49(at 0.33/h)	0.43		
<i>K. pneumoniae</i> DSM 2026	Shake flask	–	0.62	ethanol, acetic acid, 2,3-butanediol	Mu et al., 2006
	Fed Batch	1.7	0.46		
<i>K. pneumoniae</i> M5a1	Batch	0.89	–	acetate, ethanol, lactate 2,3-butanediol	Cheng et al., 2006
	Fed Batch	0.94	–		
<i>K. pneumoniae</i> XJ-Li	Batch	1.53	0.75	Acetate	Zhang et al., 2007b
	Fed Batch	0.79	0.70		

Table 2.3 (.....Continued)

Micro organisms	Reactor design/mode of operation	Productivity g/L-h	Molar yield mol/mol	Byproducts	Reference
<i>K. pneumoniae</i> DSM 2026	Microaerobic fed batch (1m ³ reactor)	2.1	0.57	ethanol, acetic acid, 2,3 butanediol	Liu et al., 2007
<i>K. pneumoniae</i> M5a1	Pilot scale fed batch (5000l fermentor)	0.92	0.53	acetic acid, lactic acid, 2,3 butanediol, ethanol	Cheng et al., 2007
<i>Clostridium butyricum</i> F2b	Two stage continuous	3.58-1 st stage 1.74-2 nd stage	- -	acetate, butyrate	Papanikolaou et al., 2008
<i>K. pneumoniae</i> ME-308	pH fluctuating Fed Batch	0.97	0.70	2,3 butanediol, lactate, ethanol	Ji et al., 2009
	pH stat Fed Batch	0.83	0.62		

Table 2.4 Summary of literature on biochemical conversion of glycerol to butanol

Micro organism	Yield	Mode of operation	Reference
<i>Clostridium pasteurianum</i> LMG 3285	0.11 g/g (without acetate) 0.098 g/g (with acetate)	Batch Chemostat	Heyndrickx et al., 1991
<i>C. pasteurianum</i> DSM 525	0.30 g/g (Fe limitation) 0.18 g/g (PO ₄ ³⁻ limitation)	Continuous	Dabrock et al., 1992
<i>C. pasteurianum</i> ATCC 6013	0.388 mol/mol 0.318 mol/mol	Batch Fed Batch	Biebl, 2001
<i>C. acetobutylicum</i> ATCC 824	0.32 g/g	Continuous Chemostat	Andrade and Vasconcelos, 2003
<i>C. acetobutylicum</i> ATCC 4259	0.41 g/g (glucose, glycerol mixture)		
<i>C. pasteurianum</i> ATCC 6013	0.36 g/g (pure glycerol) 0.30 g/g (crude glycerol)	Batch	Taconi et al., 2009

Glycerol is channeled to glycolytic cycle to form pyruvate, which is finally converted to butanol. The typical product profile of *C. pasteurianum* consists of *n*-butanol, ethanol, 1,3-PDO, lactate, CO₂ and traces of acetate and butyrate. Like *C. acetobutylicum*, *C. pasteurianum* also shows a typical biphasic fermentation pattern, whereby acetic acid and butyric acid are produced in acidogenic stage, which is the first stage and the solvents butanol and ethanol are produced during second stage of solventogenesis. This strain forms a bulk amount of 1,3 PDO prior to acidogenic phase (0.141 g/g from 5 g/L glycerol) (Taconi et al., 2009). *C. pasteurianum* produces 0.36 g/g butanol when grown on pure glycerol, while growth on crude glycerol slightly decreases the yield to 0.30 g/g due to presence of methanol, salts and soaps in crude glycerol. The cells tolerated glycerol concentration as high as 25 g/L, but higher glycerol concentration increases the lag phase of the cultures. Lower concentration of 5 or 10 g/L crude glycerol takes almost 10–15 days for complete consumption. But a

higher concentration of 25 g/L required 14–24 days for complete metabolization.

However, exact information on extension of the lag phase has not been reported by Taconi et al. (2009). An increase in glycerol concentration from 8% to 17% favors 1,3-PDO production while lower substrate concentration favors solvent production (Taconi et al., 2009). Under iron limiting conditions, *n*-butanol is formed due to inactivation of Fe dependent dehydrogenases (Dabrock et al., 1992). *n*-Butanol production by *C. pasteurianum* is unaffected by addition of acetate as a co-substrate. Also, chemostat cultures formed 94% *n* butanol and only 6% 1,3-PDO (Heyndrickx et al., 1991). The production of *n*-butanol is independent of pH range 4.5–7.5, but cells show inclination to slightly acidic pH. In continuous chemostat cultures at high dilution rates, butanol and ethanol are formed, while low dilution rate favors 1,3-PDO production. Also, in batch cultures butanol was the major product with production of 1,3-PDO, butyrate, acetate and ethanol (Biebl, 2001). A summary of results obtained by different research groups is given in Table 2.4.

2.3.3 Dihydroxyacetone

Dihydroxyacetone (DHA) is used as an artificial tanning agent without harmful effects of UV rays, thus, preventing skin cancer. Therefore, it finds use in the treatment of number of skin diseases such as Vitiligo (Fesq et al., 2001) and Variegata porphyria (Asawanonda et al., 1999). It is also an important feedstock for production of industrially important chemicals such as 1,2-propylene glycol, lactic acid, methotrexate, surfactants etc (Deppenmeier et al., 2002; Hekmat et al., 2003). The production of DHA through chemical route uses two substrates viz. glycerol and formaldehyde.

The microbial route for DHA production from glycerol is mediated by a number of strains belonging to acetic acid bacteria family such as *Gluconobacter oxydans*, *Acetobacter xylinum* and *Acetomonas*. The first report of DHA production from glycerol employed *Sorbose bacillus* (Bertrand, 1898). The most potent and widely studied strain for DHA

production is gram-positive *Gluconobacter oxydans*. Apart from being used as a DHA producer, it also finds application in production of d-gluconic acid, l-sorbose, 2-ketogluconic acid, ascorbic acid, etc (Gupta et al., 2001). The biochemical pathway of DHA synthesis is mediated by two different kinds of glycerol dehydrogenase enzyme. First is a membrane-bound FAD (Flavin Adenine Dinucleotide) and PQQ (Pyrroloquinoline quinone)-dependant glycerol dehydrogenase, which incompletely oxidizes glycerol to DHA and in turn accumulates it outside the cell. Another is cytoplasmic NAD(P) and NAD-dependant glycerol dehydrogenase. The cytoplasmic formation of DHA starts with the phosphorylation of glycerol, and its oxidation to DHA phosphate. This DHA phosphate is further channeled to Pentose Phosphate Pathway (PPP) for growth of cells (Adachi, 2008).

The *Gluconobacter* cells exhibit biphasic fermentation (Batzing and Claus, 1971). The differentiated cells in the stationary phase produce around twice more DHA than undifferentiated exponential phase cells (Claus et al., 1975). At high glycerol concentration, *Gluconobacter* cells acquire the shape of long filaments instead of short rods. This proves that glycerol mainly inhibits the cellular growth by interfering in cell division, but it does not in any way effect either its own oxidation or the metabolism of DHA. It does in fact slightly decrease the oxygen uptake rate and CO₂ evolution rate (Ohrem and Voß, 1995). Glycerol manifests its inhibitory effect only during the initial growth phase, and not during the termination of growth.

Apart from studies using free/intact cells of DHA producing strains, some studies have also dealt with immobilized cells to increase the viability of the process, counteract substrate and product inhibition, and decrease the downstream processing costs. In one such study, *A. xylinum* cells were immobilized on polyacrylamide gel. The cells exhibited maximum activity of 7.7 µmol/min/g of gel at 35°C, pH 4.0–5.5 and glycerol concentration of 0.3–0.5 M (Nabe et al., 1979). *G. oxydans* was also immobilized in calcium alginate beads.

The cells showed maximum activity at 40°C and pH 5.0, but the immobilized system did not present a clear advantage over free cells, as their activities were similar (Adlercreutz et al., 1985). Microbial DHA production also suffers from substrate and product inhibition. It has been found that high DHA concentration inhibits PPP as well as membrane bound glycerol dehydrogenase, and hence, irreversibly damages the cells (Deppenmeier et al., 2002). An increase in glycerol concentration from 31–129 g/L was found to increase the time required for conversion of glycerol to DHA, but the yield of DHA remained the same (Claret et al., 1992). In view of inhibition caused by DHA itself in batch mode, the DHA production from glycerol was carried out in a fed–batch mode. The fed–batch process was modified and optimized as a repeated fed batch process. The cells tolerated a high DHA concentration of 60 g/L (Hekmat et al., 2003).

The modulation of *G. oxydans* genome for DHA production has also been carried out. Recombinant *G. oxydans* over–expressing gene encoding for glycerol dehydrogenase showed enhanced tolerance towards high concentration of DHA up to 30 g/L than the wild type strain. The enhanced glycerol dehydrogenase production increased the net DHA production as well as the viability of the cells (Gätgens et al., 2007). The future of large–scale microbial DHA production from glycerol containing feedstock depends on counteracting the problems of substrate (glycerol) and DHA inhibition. Timely removal of DHA from the fermentation broth (essentially in–situ recovery) is vital for an efficient fermentation process, and possible solution for product inhibition. A possible solution to substrate inhibition is the fed–batch process. However, no research has been reported on a suitable fed–batch process for DHA production. Although these problems may be solved by using immobilized systems, but these themselves present a problem of oxygen diffusion limitation to the obligatory aerobic *G. oxydans* cells. New recombinants need to be tested to overcome the inhibition along with increasing DHA yield.

2.3.4 Citric acid

Citric acid is an important commodity chemical and finds use in food, beverage, chemical, agricultural and pharmaceutical industries. It is an effective preservative, acidifier, antioxidant, and readily used in carbonated beverages, cosmetics and washing detergents (Soccol et al., 2006). The annual production of citric acid in the world is around 800 tons, far above the production rate of any organic acid produced through fermentation route. Citric acid is industrially produced through submerged type fermentation using filamentous fungi *Aspergillus niger*. Apart from *A. niger*, some of the yeasts belonging to the species *Yarrowia lipolytica*, *Candida oleophila* (Anastassiadis and Rehm 2006) and *Candida quillermondii* are also found to be efficient citric acid producers (Rymowicz et al., 2006). Among all these *Y. lipolytica* is the only known organism that gives maximal yield of citric acid, when grown on glycerol and similar substrates. High affinity of *Y. lipolytica* for hydrophobic compounds such as oil, fats and n-alkanes is mainly attributed to the hydrophobic surface active compounds present on its cell surface, with their interaction being mediated by glycoprotein or proteins of the cell wall. Glycerol, being hydrophilic, is transported inside the cell through facilitated diffusion.

Glucose, ethanol, methanol, n-hydrocarbons, oils and glycerol have been extensively studied as a carbon source for citric acid production. Recently, the focus has shifted towards utilizing raw glycerol discharged from biodiesel industries as an alternative. The only disadvantage of using *Y. lipolytica* as a citric acid producer is the simultaneous production of the by-product isocitric acid. The extent of its production depends on the substrate and the particular strain of *Y. lipolytica* used (Levinson et al., 2007, Fickers et al., 2005, Roehr et al., 1996). The production of citric acid starts after the exponential growth phase ends (Levinson et al., 2007), and requires nitrogen limiting conditions in the media (Rymowicz et al., 2006, Papanikolaou et al., 2008).

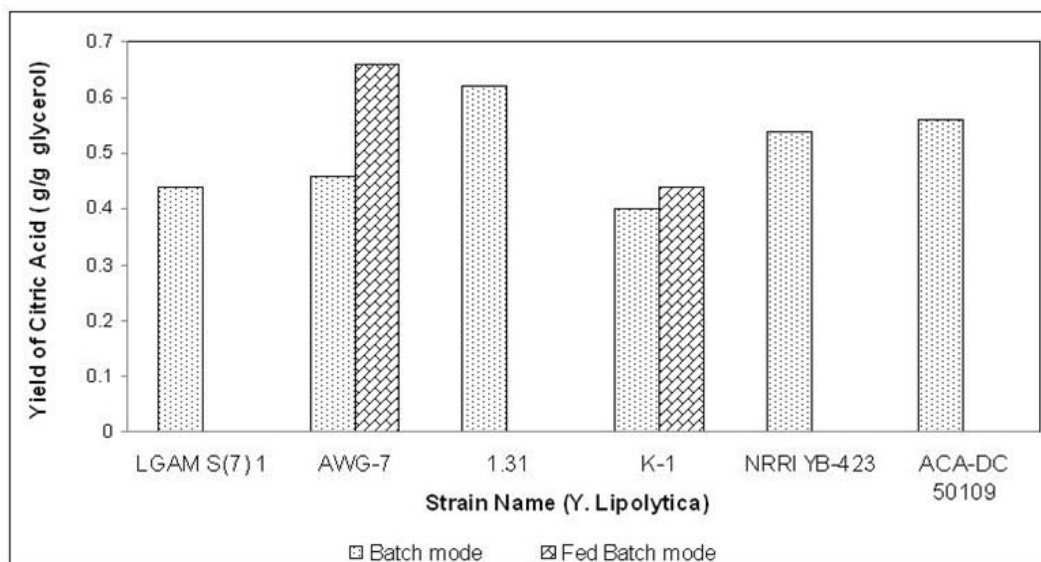


Figure 2.5 Comparison of yield of citric acid formed in batch and fed batch process on bioconversion of glycerol by various strains of *Yarrowia lipolytica*

A comparison of yield of citric acid formed by different strains of *Y. lipolytica* in batch and fed-batch process is depicted in Fig. 2.5. The selectivity of this organism towards isocitrate decreases when acetate negative strains are used (Rymowicz et al., 2006). Citric acid production is also accompanied with the production of erythritol (Rymowicz et al., 2008) and mannitol, which work as osmoregulators to counteract the high concentration of glycerol in the media. The final concentration of mannitol was higher (8–9 g/L) in the cultures grown on pure glycerol as compared to the cultures grown on crude glycerol (3 g/L) (Rywinska et al., 2009). A summary of results obtained from different strains of *Y. lipolytica* is mentioned in Table 2.5.

Table 2.5 Summary of literature on biochemical conversion of glycerol to citric acid

Micro organism	Productivity (g/L-h)	Yield (g/g)	Reactor configuration	Reference
<i>Yarrowia lipolytica</i> LGAM S(7)1	0.11 CG	0.43	Single stage continuous fermentation	Papanikolaou and Aggelis, 2002
<i>Yarrowia lipolytica</i> LGAM S(7)1	0.15 CG	0.42–0.44	Flask cultures, Batch mode	Papanikolaou et al., 2002b
<i>Yarrowia lipolytica</i> 1.31 (acetate mutant)	0.88	0.62	Stirred tank	Rymowicz et al., 2006
<i>Yarrowia lipolytica</i> K-1 (acetate mutant)	0.81	0.40		
<i>Yarrowia lipolytica</i> AWG-7 (acetate mutant)	0.91	0.46		
<i>Yarrowia lipolytica</i> NRRL YB-423	0.13 PG 0.09 CG	0.54	Flask culture	Levinson et al., 2007
<i>Yarrowia lipolytica</i> ACA-DC 50109	0.13 CG	0.56	Flask culture	Papanikolaou et al., 2008
<i>Yarrowia lipolytica</i> Wratistavia K1 (acetate mutant)	0.73 1.50 ± 0.02	0.44 ± 0.02 0.38–0.43	Flask culture, Batch mode Fed batch	Rymowicz et al., 2008
<i>Yarrowia lipolytica</i> Wratistavia AWG7 (acetate mutant)	1.16 PG 1.05 CG	0.69 PG 0.66 CG	Fed batch, stirred tank reactor	Rywinska et al., 2009
<i>Yarrowia lipolytica</i> Wratistavia K1 (acetate mutant)	1.0 PG 0.99 CG	0.45 PG 0.43 CG		

PG = Pure glycerol, CG = Crude glycerol

2.3.5 Glyceric acid

Glyceric acid (GA) is another important chemical derived from glycerol. It is a major phytochemical constituent in majority of plants, viz. peanut, tomato, apple, banana, etc.

Phosphate derivatives of GA such as 1,3-bisphosphoglycerate, 3-phosphoglycerate, and

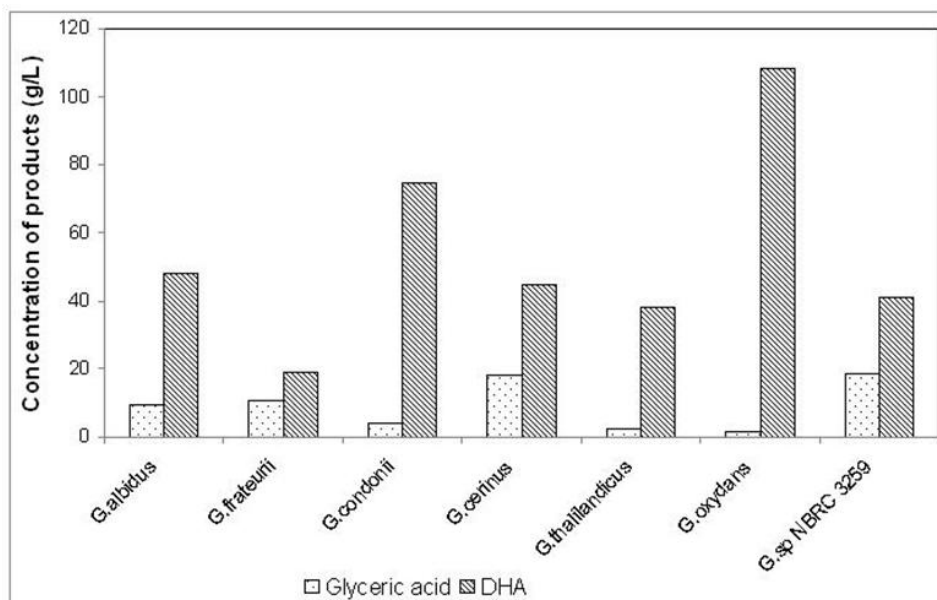


Figure 2.6 A comparative assessment of concentration of glyceric acid and dihydroxyacetone formed by various strains of *Gluconobacter* utilizing glycerol as a carbon source

2-phosphoglycerate are important intermediates of glycolytic pathway. Although, there are limited applications of GA, it is rather atypical that several patents have been awarded for use of GA in pharmaceutical, cosmetic and chemical industries (Rosseto et al., 2008). Chemically, GA is synthesized by selective oxidation of primary alcoholic group of glycerol by heterogeneous catalysts of Pd/Pt/Au supported over carbon. The chemo-selectivity of the catalysts is important in the sense that oxidation of primary alcohol group produces GA, while oxidation of secondary alcohol group forms dihydroxyacetone. The best chemo-selectivity is achieved under basic conditions and in the presence of Au or Pd catalysts (Garcia et al., 1995, Carretin et al., 2002). The biosynthesis of GA occurs by aerobic oxidation of glycerol by bacteria belonging to acetic acid family.

Table 2.6 Summary of literature on biochemical conversion of glycerol to glyceric acid

Micro organism	Glycerol concentration g/L	GA concentration (g/L)	DHA concentration (g/L)	Reference
<i>G. thailandicus</i> NBRC3172	100	27.2	–	Patent JP0751069,
<i>G. oxydans</i> NBRC3292		36.0		Daicel
<i>G. oxydans</i> NBRC3294		32.6		chemical
<i>G. frateurii</i> NBRC3262		57.2		industries,
				1987
<i>Gluconobacter sp.</i> NBRC3259	170	18.2 PG 45.9 CG	41.0 PG 28.2 CG	Habe et al., 2009a
<i>G. albidus</i> NBRC3250		9.1	48.2	
<i>G. frateurii</i> NBRC3262		10.4	18.9	
<i>G. condonii</i> NBRC3266		4.1	74.4	
<i>G. cerinus</i> NBRC3267		18.0	44.6	
<i>G. thailandicus</i> NBRC100600		2.3	37.9	
<i>G. oxydans</i> NBRC14819		1.4	108.2	
<i>Acetobacter tropicalis</i> NBRC16470	200	22.7	–	Habe et al., 2009c
<i>G. frateurii</i> NBRC 103465	220	127.6	–	Habe et al., 2009d

PG = Pure glycerol, CG = Crude glycerol

These are *Gluconobacter*, *Acetobacter*, and *Gluconacetobacter*. *Gluconobacter* catalyzes oxidation of sugars and sugar alcohols, whereas acetobacter preferentially oxidizes ethanol to acetic acid. These bacteria are major producers of DHA, and therefore, GA is formed to a concentration of 5–12 g/L simultaneously during DHA production by *Gluconobacter* cells (Švitel and Sturdik, 1994). A comparison of concentrations of GA and DHA formed by different strains of *Gluconobacter* is shown in Fig. 2.6. The biochemistry of GA production has not been studied in detail as yet. Also the genes and the corresponding enzymes involved in GA production pathway have not been reported till date. An important difference between the chemical and biological synthesis of GA is evident from the products

seen in the two pathways. The chemical synthesis of GA always yields a racemic mixture of d and l form of GA, while biological synthesis preferentially produces d form in enantiomeric excess over l form. Habe et al. (2009a) tested *Gluconobacter* sp. NBRC 3259 for GA production from raw glycerol. They found that the production of GA was tightly regulated with the pH of the medium and the degree of aeration. When the cells were in the stationary phase, the pH of the medium became around 3.2 leading to complete cessation of GA and DHA production. On controlling the pH to 5.0, GA productivity was found to increase two fold. Also higher GA production was observed at 500 rpm agitation speed than at 700 rpm. The DHA production was found to follow just the reverse trend with the degree of aeration in the medium. The organism produced 45.9 g/L GA and 28.2 g/L DHA from 174 g/L raw glycerol in a period of 4 days. d-GA (88.4%) was formed in enantiomeric excess over l form (11.6%).

Habe et al. (2009c) screened *Acetobacter* and *Gluconacetobacter* cells for GA production. Out of these two strains, *Acetobacter tropicalis* NBRC 16470 was found to be the best GA producer, as it tolerated twice higher concentration of glycerol (10% v/v) than *Gluconacetobacter* (5% v/v). The addition of 10 g/L of a nutrient source such as yeast extract or polypeptone was found to be mandatory for the synthesis of GA. A recent study (Habe et al., 2009d) has proven that *Gluconobacter frateurii* is the best strain for d-GA production with a concentration of 127.6 g/L. The results obtained in each set of study are given in greater detail in Table 2.6. All these studies reveal that the major reaction parameters, which need to be optimized for bulk GA production, are initial glycerol concentration in the medium, agitation speed, pH and the amount and type of nitrogen source. Recovery of the products from the reaction mixture is the last phase of all the production processes. d-GA recovery can be done by using any traditional separation technique such as distillation, solvent extraction, adsorption etc., but these techniques may not be economically feasible due

to high capital and operating costs.

Habe et al. (2009b) applied desalting electro dialysis for recovering highly concentrated d-GA. This technique is fast, separates non-ionic substances effectively and prevents use of solvents for separation. In this process, 14.6 g/L of glycerate used as a feed solution was recovered to a final concentration of 41.6 g/L during 80 min operation. 99.4% of the product was recovered, while 99% of the glycerol added was excluded. As already mentioned, addition of nutrient source is essential for d-GA production. When yeast extract or polypeptone was added to the culture media, operating time was prolonged and current efficiency was lowered. The biocatalytic production of GA is still in its nascent stage, and detailed study taking into account the different reactor configurations, and their different modes of operation needs to be done. Although, new microorganisms for GA production are looked for and the optimization of GA production process is being tried, there are no new avenues for utilization of excess d-GA that will be produced through biological route. The future applications of d-GA at industrial level needs to be looked into soon, otherwise the surplus product produced will lower down the economy of the process.

2.3.6 3-Hydroxypropionaldehyde

3-Hydroxypropionaldehyde (3-HPA), also known as *Reuterin*, is a potent antimicrobial agent. It is a precursor for large number of compounds such as acrolein, 1,3-PDO, 3-Hydroxypropionic acid, etc. It is chemically synthesized from petrochemical feedstock. It is biologically synthesized by metabolism of glycerol by *Lactobacillus* species. 3-HPA as such is very rarely accumulated in cells, and is rather spontaneously converted into 1,3-PDO by 1,3 PDO oxidoreductase. The extracellular production of 3-HPA is observed in very few species of *Lactobacillus* (Bauer et al., 2010, Tanaka et al., 2009, Sauvegeot et al., 2000). The most widely studied organisms for production of 3-HPA belongs to *Lactobacillus* species, viz. *L. brevis*, *L. pentosus* (Bauer et al., 2010), *L. collinoides*, *L. reuteri*.

Table 2.7 Summary of literature on glycerol bioconversion to 3-hydroxypropionaldehyde

Micro organism	Yield (mM)	Reference
<i>Enterobacter agglomerans</i>	–	Barbirato et al., 1996
<i>Desulfovibrio fructosovorans</i> + <i>Methanospirillum hungatei</i>	4.36	Qatibi et al., 1998
<i>Desulfovibrio carbinolicus</i> + <i>Methanospirillum hungatei</i>	3.55	
<i>Lactobacillus collinoides</i>	–	Sauvageot et al., 2000
<i>Lactobacillus coryniformis</i> 394	–	Tanaka et al., 2009
<i>Lactobacillus reuteri</i> DSMZ 20016	~30	Bauer et al., 2010

Some species of *Enterobacter*, *Desulphovibrio* and *Methanospirillum* have also been studied for their HPA production potential (Barbirato et al., 1996; Qatibi et al., 1998). 3-HPA is found to inhibit the production of 1,3-PDO by *Enterobacter agglomerans* by inhibiting the enzyme glycerol dehydrogenase (Barbirato et al., 1996). The production of 3-HPA is a function of pH, and so lower pH facilitates the accumulation of this inhibitor. NAD/NADH ratio of 1.7 is an indication of the starting of 3-HPA accumulation (Bauer et al., 2010). A study on *Desulphovibrio* revealed that it degraded glycerol to 3-HPA with concomitant production of sulphide in pure culture and methane in co-culture. *D. fructosovorans* and *Desulphovibrio carbinolicus* grown in syntrophic association with *Methanospirillum hungatei*, yielded 3.55 mM and 4.36 mM of 3-HPA respectively. *D. carbinolicus* always forms 3-HPA from glycerol, while *D. fructosovorans* degrades glycerol to acetate in presence of sulphate and 3-HPA in co-culture with *M. hungatei* (Qatibi et al., 1998). *Lactobacillus collinoides* consumes glycerol supplemented with glucose to form 3-HPA (Sauvageot et al., 2000), while optimal production of 3-HPA occurs at pH 6 and in presence of 300 mM glycerol (Bauer et al., 2010). *L. collinoides* and *L. reuteri* start 3-HPA production in stationary phase in batch fermentation. 3-HPA accumulated to a concentration of 38

arbitrary unit (AU)/ml in batch culture and 94 AU/ml in chemostat cultures. A summary of literature on bioconversion of glycerol to 3-HPA is given in Table 2.7.

2.3.7 Biosurfactants

Biosurfactants are extracellular products of microorganisms growing mainly on hydrocarbons or on water insoluble substrates. These include a variety of compounds with diverse structures such as glycolipid, phospholipid, lipopeptide, lipoproteins, etc. They act by lowering interfacial or surface tension and so find applications in variety of fields such as pulp and paper industries, textile, detergent, petrochemical industries etc. They are better than highly recalcitrant petrochemically derived surfactants due to their biodegradability, renewability, low toxicity, and the advantage of being used at extreme conditions of high temperature and pressure. The most widely studied biosurfactants possess glycolipid structure. Mannosylerythritol lipid (MEL) is one of them and is synthesized from glycerol by yeast *Pseudozyma antarctica*. The maximum MEL yield of 16.3 g/L has been obtained by adding 2% mannose and by intermittent (discontinuous) addition of 10% glycerol (Morita et al., 2007).

Sphorolipids (SL) are another member of extracellular glycolipids, produced by yeast *Candida bombicola* grown on glycerol as a carbon source. SLs are basically composed of a disaccharide sophorose, linked by a glycosidic bond to a hydroxyfattyacyl moiety (Asmer et al., 1998, Nuñez et al., 2001). Biodiesel coproduct stream containing glycerol, free fatty acids (FFAs) and fatty acid methyl ester (FAME) gave a higher yield of SL (60 g/L), as compared to pure glycerol (9 g/L). This exceptionally high yield with crude glycerol can be explained by the high osmotic stress on the cells exerted by pure glycerol and the absence of FFAs in it (Ashby et al., 2005a). The production of SLs was further studied by supplementing substrate glycerol with soy fatty acid esters of propanol, ethanol and methanol.

Table 2.8 Summary of literature on biochemical conversion of glycerol to biosurfactants

Micro organism	Type of lipid	Concentration (g/L)	Reference
<i>Pseudomonas aeruginosa</i> PA1	Rhamnolipid	1.7 with 1% glycerol	Santa Anna et al., 2001
<i>Pseudomonas aeruginosa</i> PA1	Rhamnolipid	3.34	Santos et al., 2002
<i>Candida bombicola</i> ATCC 22214	Sophorolipid	~ 9 with PG 60 with CG containing FFA	Ashby et al, 2005a
<i>Pseudomonas aeruginosa</i> J4	Rhamnolipid	1.4–1.5	Wei et al., 2005
<i>Pseudomonas aeruginosa</i>	Rhamnolipid	15.4	Guo–liang et al., 2005
<i>Pseudomonas aeruginosa</i>	Rhamnolipid	2.8 with 5% glycerol 4.2 with glycerol and NaNO ₃ (C/N =55:1)	Rashedi et al., 2005
<i>Candida bombicola</i> ATCC 22214	Sophorolipid	46 ± 4 Me–Soy 42 ± 7 Et–Soy 18 ± 6 Pro–Soy	Ashby et al., 2006
<i>Rhodococcus erythropolis</i> ATCC 4277	Glycolipid and polysaccharides	1.7	Ciapina et al., 2006
<i>Pseudozyma antarctica</i> JCM 10317	Mannosyl erythritol lipids	4.0	Morita et al., 2007
<i>Pseudomonas aeruginosa</i> EM1	Rhamnolipid	4.93 with 40 g/L glycerol	Wu et al., 2008a
<i>Pseudomonas aeruginosa</i> J16	di–Rhamnolipid (RL ₂)	2.121	Wei et al., 2008

PG = Pure glycerol, CG = Crude glycerol, Me = Methyl, Et = Ethyl, Pro = Propyl

The maximum SL yield of 46 ± 4 g/L was obtained with methyl soy fatty acid esters (Ashby et al., 2006). Another strain, which produces glycolipid surfactant from glycerol, is *Rhodococcus erythropolis*. This strain, when grown on glycerol produced 1.7 g/L surfactant. The substrate glycerol was also found to enhance the release of biosurfactant from the cell wall (Ciapina et al., 2006). Another type of biosurfactant, which has been widely studied, is Rhamnolipid (RL). It is of two kinds, mono RL and di RL, which in turn are composed of either one or two rhamnose molecule connected with β–hydroxydecanoyl–β–

hydroxydecanoate (Soberon–Chavez et al., 2005).

The best RL producer is *Pseudomonas aeruginosa*. It produces 1.7 g/L RL with 1% glycerol (Santa Anna et al., 2001). The variation of carbon and nitrogen source on RL production by *P. aeruginosa* revealed that nitrates as nitrogen source and glycerol, as carbon source gives the highest RL yield of 3.34 g/L (Santos et al., 2002). Similar study done with this organism revealed that the use of sodium nitrate as nitrogen source gave higher RL concentration of 4.2 g/L with C/N ratio of 55/1 (Rashedi et al., 2005).

The effect of nitrogen and carbon source on newly isolated *P. aeruginosa* EM1 strains from oil contaminated sites for RL production has been studied by Wu et al. (2008a). Glycerol as a carbon source produced 4.9 g/L RL, and addition of sodium nitrate as a preferable nitrogen source increased this concentration to 8.6 g/L. Both RL₁ and RL₂ were formed in the ratio of 1:1. The production of RL₂ by *P. aeruginosa* was also studied with different carbon and nitrogen source. The highest RL₂ yield was obtained with glycerol and ammonium sulphate as carbon and nitrogen source, respectively. The ratio of RL₂/ RL₁ depends on carbon source, and reached a maximum value of 4.2 with glycerol (Wei et al., 2008). *P. aeruginosa* J4 strain, when tested for RL production, gave a concentration of 1.4–1.5 g/L at optimum conditions of 30°C and 200 rpm. RL concentration was inhibited at higher concentration of glycerol (over 2%) (Wei et al., 2005). The maximum concentration of RL (15.4 g/L) was obtained on growing *P. aeruginosa* on basal mineral media with glycerol as the carbon source (Guo–liang et al., 2005). The detailed results for different kinds of biosurfactants formed from bioconversion of glycerol are compiled in Table 2.8.

2.3.8 Propionic acid

Propionic acid (PA) serves as an intermediate for the synthesis of cellulosic fibers, herbicides, perfumes and some drugs. It is also used as a food preservative along with its Na⁺, K⁺ salts. PA, along with its salts, inhibits the growth of microorganisms. The inhibitory

action is probably manifested by the alteration of the pH gradient of the cells, which leads to the movement of excess protons inside the cell. These excess protons are expelled out by H⁺-ATPase at the cost of cell's ATP reserve. In fact, this depletion of ATP level within cell brings about the inhibition of microbial growth. Therefore, PA also finds application as an antifungal, antimold and antibacterial agent (Coral et al., 2008).

The most common route for synthesis of PA is the oxidation of propionaldehyde derived from petrochemical industries. Recently, biochemical routes for PA production are being looked into using glycerol as the substrate. The organism employed in PA production is well-known gram-positive, asporogenous *Propionibacteria*. These utilize carbohydrates (e.g. glucose, fructose, etc.) and polyols (such as glycerol) as substrates to yield mainly PA and acetic acid, while succinic acid, propanol and CO₂ are formed in minor quantities. Some of the potent PA producers are: *Propionibacterium acidipropionici* ATCC 4965, *P. thoenii* NCDO 1082, and *P. freudenreichii ssp. shermanii*. Apart from these strains, a novel strain named as *Propionispora vibroides* DSM 13305 also produces PA (Biebl et al., 2000). This strain is different from other strains, as it utilizes glycerol only in the presence of either acetate or pyruvate. The supplementation of glycerol with acetate and pyruvate gives experimental PA yield of 48% and 28%, respectively. This phenomenon can be explained by the acceptance of reducing equivalents (such as NADH, formed during biomass growth) by acetate and pyruvate. A summary of literature on bioconversion of glycerol to PA is given in Table 2.9. Himmi et al. (2000) studied the fermentation pattern of glycerol by *P. acidipropionici* and *P. freudenreichii*. The former strain gave higher PA yield of 0.64 g/g but both the strains exhibit different pattern of fermentation. While *P. acidipropionici* exhibits coupled substrate consumption product formation pattern, *P. freudenreichii* displayed unrelated substrate consumption-product formation pattern.

Table 2.9 Summary of literature on biochemical conversion of glycerol to propionic acid

Micro organism	Concentration (mmol/L)	Acetate concentration (mmol/L)	Reference
<i>Propionispora vibroides</i>	6.0 with glycerol 15.0 with glycerol + acetate 16.0 with glycerol + pyruvate	5.0 17.0 16.0	Biebl et al., 2000
<i>Propionibacterium acidipropionici</i> ATCC 4965	6.77 ± 0.11	–	Coral et al., 2008
<i>Propionibacterium acidipropionici</i> ACK–Tet (free cell fermentation)	19.3 ± 0.06 g/L	0.0	Zhang and Yang, 2009
Immobilized <i>P. acidipropionici</i> ACK–Tet (fibrous bed bioreactor)	19.7 ± 1.0 g/L	0.63±0.12	
Adapted <i>P. acidipropionici</i> ACK–Tet (free cell fermentation)	26.0 ± 0.6 g/L	1.1±0.6	
Adapted immobilized <i>P. acidipropionici</i> ACK–Tet (fibrous bed bioreactor)	23 ± 1.3	1.2±0.1	

Coral et al. (2008) tested the production of PA by *P. acidipropionici* grown on three different substrates, viz. sugarcane molasses, lactate and glycerol. Glycerol was found to be a favorable substrate, as it did not produce any acetic acid (a stronger acid inhibitor than PA), and absence of acetic acid in the product profile also simplifies the downstream processing of PA. The lower production of acetate from glycerol containing feedstock is explained by the regulation of intracellular redox balance of the cells. Glycerol as a substrate produces more reduced metabolites, while other carbohydrate substrates form more of oxidized compounds (Barbirato and Bories, 1997). Although PA productivity was lower with glycerol, but it gave the highest PA yield of 0.72 at a temperature of 30°C and pH 5.0. Glycerol concentration of over 60 g/L is inhibitory to the cell growth, but assists in PA production (Barbirato and

Bories, 1997). The cells stay between G2 phase and M phase of cell cycle, which in turn increases the production of PA as more glycerol is channeled for organic acid production over biomass production. A study has also dealt with genetically modified *P. acidipropionici* ATCC 4875 strain with acetate kinase knocked out gene (Zhang and Yang, 2009). This mutant exhibited extremely slow growth and took 700 h to produce ~19 g/L PA. As expected, acetate was not produced due to the absence of acetate kinase gene. The fermentation was carried out in a fibrous fed-batch bioreactor operated in a fed-batch mode. The reaction produced PA to a concentration of 106 g/L, almost 2.5 times higher than the highest concentration reported (42 g/L) (Barbirato et al., 1997). The fermentation on crude glycerol yielded 0.71 g/g PA, as compared to 0.54 g/g on pure glycerol. Although PA yield with crude glycerol was higher, but it showed lower PA productivity (0.085 g/L-h vs 0.1 g/L-h). This is explained by the presence of high concentration of salts and methanol in crude glycerol.

2.3.9 Polyhydroxyalkanoates

Polyhydroxyalkanoates (PHAs) are complex natural molecules synthesized by both bacteria and plants. These polyesters are known to be produced in bacteria under unbalanced growth conditions, and are accumulated intracellularly as both carbon and energy reserve (Solaiman et al., 2006, Koller et al., 2005). They are used as a substitute for non-biodegradable and highly recalcitrant petro-chemically derived plastics. This class consists of almost 150 different compounds. They are biodegradable thermoplastics, and are classified into two broad categories based on their chain length: (a) Short chain length PHA (scl-PHA), and (b) Medium chain length PHA (mcl-PHA). scl-PHAs exhibit the property of a semicrystalline thermoplastic. Some of its members are PHB (Polyhydroxybutyrate), PHB-Co-3-hydroxyvalerate. mcl-PHAs are amorphous, and can show both elastomeric and adhesive properties. They consist of 6-14 carbon length repeating monomeric units, composed of 3-hydroxy fatty acids.

Table 2.10 Summary of literature on bioconversion of glycerol to polyhydroxyalkanoates

Micro organism	Type	Concentration (g/L)	Reference
<i>Methylobacterium rhodesianum</i> MB 126-J (Capsule deficient)	PHB	13.5	Bormann and Roth, 1999
<i>Ralstonia eutropha</i> DSM 11348	PHB	17.0	
<i>Pseudomonas oleovorans</i> NRRL B-14682	PHB	0.4 at 5% BDPS C _{4:0} -100 mol%	Ashby et al., 2004
<i>Pseudomonas corrugata</i> 388	mcl-PHA	0.7 at 2-5% BDPS C _{8:0} -39 mol% C _{10:0} -26 mol% C _{14:2} -15 mol%	
<i>Pseudomonas oleovorans</i> NRRL B-14682	PHB	0.97 at 5% glycerol 0.67 at 2% glycerol	Ashby et al., 2005b
<i>Pseudomonas corrugata</i> 388	mcl-PHA	0.04 at 5% glycerol	
r <i>E. coli</i> containing Phasin producing gene of <i>Azotobacter</i> sp. strain FA8	PHB	7.9 ± 0.5	de Almeida et al., 2007
<i>Escherichia coli</i> arc A2 mutant	PHB	3.52 with batch culture 10.81 with fed batch micro aerobic culture	Nikel et al., 2008
<i>Cupriavidus necator</i> DSM 545	PHB	51.2 – PG 38.1 – CG	Cavalheiro et al., 2009
<i>Halomonas</i> sp KM-1	PHB	2.3 – 5% PG 1.6 – 3% CG	Kawata and Aiba, 2010

PG = Pure glycerol, CG = Crude glycerol

Their property depends on both the chain length and the degree of unsaturation. The mass production of PHA is limited due to its high production cost and the process being energy intensive due to its aerobic nature. The initial study regarding bioconversion of glycerol to PHA was carried out using a facultative methylotrophic bacterium, *Methylomonas extroquens*. The reaction was carried out in a batch mode with biodiesel derived glycerol and

20% methanol as a substrate (Braunegg et al., 1999). The strain was found to be a poor PHA producer and a slow grower.

A member of the class scl-PHA, PHB was synthesized using *Methylobacterium rhodesium*, and *Ralstonia eutropha* strains, grown on glycerol with casein hydrolysates as nitrogen supplement (Bormann and Roth, 1999). *M. rhodesium* produced 39% PHB in 92 h when cultivated in flasks, while the experiments in fermentor yielded 50% PHB in 45 h. The fermentor cultures of latter strain with casein peptone as a nitrogen source produced 47% PHB in 67 h, while supplementation with casamino acids as nitrogen source yielded 65% PHB in 45 h. It was concluded that the complete cleavage of nitrogen source enhanced the production of PHB. Another strain employed for PHA production is *Pseudomonas oleovorans* and *P. corrugata*. The two strains when grown on 5% biodiesel product stream (BDPS) gave different products. *P. oleovorans* synthesized principally PHB, while *P. corrugata* produced mcl-PHA mainly consisting of 3-hydroxyoctanoic acid, 3-hydroxydecanoic acid and 3-hydroxytetradecadienoic acid (Ashby et al., 2004). *P. oleovorans* preferred glycerol as a substrate over FFA and FAME present in BDPS, and gave higher polymeric yield on increasing BDPS concentration, while *P. corrugata* utilized both glycerol and FFA/FAME at the same rate but depicted a decrease in cell growth with increasing BDPS concentration. When the same reaction was carried out only on glycerol as a substrate, higher glycerol concentration produced PHB, while lower glycerol concentration gave mcl-PHA as the major product (Ashby et al., 2005b). *Cupriavidus necator* (formerly *Ralstonia eutropha*), when grown on crude glycerol in a fed-batch reactor, gave PHB yield of 0.36 g/g (Cavalheiro et al., 2009). It was concluded that PHB formation required high C/N ratio. When nitrogen is in sufficient amount in the media, glycerol is channeled for cell production and maintenance, whereas when nitrogen source becomes limiting, glycerol is diverted for PHB production. When PHB accumulation was tested on both pure and crude

glycerol, the total period of accumulation on crude glycerol was half of that on pure glycerol. The study for production of PHB using *Halomonas sp.* gave higher PHB yield with pure glycerol (4.6%) than with waste glycerol (Kawata and Aiba, 2010). The concentration of different polyalkanoates obtained in each study is summarized in Table 2.10.

2.3.10 Single cell oils

Single cell oils (SCOs) are edible oils produced by oleigogenous microorganisms, and have similar properties as oils or fats produced by plants and animals. However, SCOs mainly contain polyunsaturated fatty acids (PUFAs) that are rarely found in any other plant or animal. A large variety of PUFAs such as γ -linolenic acid, arachidonic acid, docosahexaenoic acid are found in SCOs. Apart from being used as a nutrient supplement, SCOs are also looked as a potential feedstock for biodiesel production. A variety of microorganisms have been tested for production of different PUFAs. An important PUFA, docosahexaenoic acid belongs to omega-3-PUFA class, and finds use as a dietary supplement, and as a therapeutic agent for the treatment of cardiovascular diseases, cancer, Alzheimer's disease, etc. (Simopolous, 1999). Most of the PUFAs studied belong to the family of n-3 unsaturated fatty acids. They are important components of phospholipids, and are involved in production of signaling molecules such as leukotrienes, prostaglandins and thromboxanes. These signaling molecules regulate important processes in cell signaling pathway, such as immune response, blood pressure, wake sleep cycle, etc. The production of docosahexaenoic from crude glycerol was studied by using a microalga *Schizochytrium limacinum* (Chi et al., 2007, Pyle et al., 2008). This alga also produced a significant amount of palmitic acid (C16:0) (54.7%) along with docosahexaenoic acid production (33.62%). Maximal docosahexaenoic acid production of 4.91 g/L with *S. limacinum* requires optimum conditions of 75–100 g/L glycerol and 1.0 g/L $\text{CH}_3\text{COONH}_4$ in the medium, and a temperature of 19.2°C (Chi et al., 2007). The production of fatty acids is inhibited by

methanol and soaps present in biodiesel derived crude glycerol (Pyle et al., 2008).

Another n-3 fatty acid, γ -linolenic acid (GLA) production was studied using a fungus *Mortierella isabellina*. The organism gave a maximal lipid production of 4.4 g/L, whereas maximal GLA concentration achieved was 0.12 g/L (Papanikolaou et al., 2008). Other strains of *Mortierella* (*M. alpina* and *M. zychae*) were also tested for GLA and arachidonic acid production. The fatty acid composition was found to be independent of glycerol concentration; however, higher amount of glycerol inhibited cell growth. The optimum production of arachidonic acid with *M. zychae* occurred at pH 6.0, agitation rate of 120 rpm and temperature of 20°C (Tou, 2008). *M. alpina* grew poorly on glycerol, whereas *M. zychae* showed better Arachidonic acid production. *Cunninghamella echinulata* produces 7.8 g/L biomass with 25.6% oil content, while *M. isabellina* produces 6.5 g/L of biomass with oil content of 53.8%. The concentration of n-3 fatty acid, GLA and linolenic acid increases at the beginning of growth and at lower oil content of 10%. Oleic acid is the major fatty acid found in microbial oil. GLA yield with raw glycerol as a substrate by *Cunninghamella echinulata* was 0.190 g/L, while *M. isabellina* yielded 0.065 g/L GLA. It is noteworthy that the impurities present in industrial feedstock do not have any impact on the metabolism of the strains (Fakas et al., 2008). *Mortierella elongata* 1S-5 also forms Arachidonic acid from glycerol at a concentration of ~ 0.15 g/L (Yamada et al., 1987).

The production of Eicosapentenoic acid (EPA) was tested using a fungus *Pythium irregulare* in presence of 30 g/L crude glycerol and 10 g/L yeast extract, serving as C and N source, respectively. EPA was obtained to a concentration of 0.090 g/L. The presence of soaps and methanol in crude glycerol inhibited EPA production as well as cell growth, while total fatty acid content increased in presence of soaps. The addition of pure vegetable oil to the culture increased the production of both EPA and biomass. This can be explained by the absorption of oil by the fungal cells and conversion of linolenic acid (shorter chain fatty

acids) to EPA (longer chain fatty acids) (Athalye et al., 2009). *L. edodes* exhibited maximal growth at pH 4.0, temperature 25°C and an agitation speed of 60 rpm (250 mL and 2 L Erlenmeyer flask) in rotary incubator–shaker. The cells produced lipid in the range of 0.08–0.11 g/g. Linoleic acid was the predominant fatty acid constituting 70% w/w of the total fatty acid content. As the fermentation time increased, the concentration of linoleic acid increased, while that of other fatty acids decreased (André et al., 2010). *Cryptococcus curvatus* cells, when grown on 16 g/L glycerol exhibited maximum specific growth rate of 0.43/h. The cells produced 0.5 g lipid/L–h with the cellular lipid content of 25% in a fed–batch process. The details of fatty acid composition of SCOs and concentration of SCOs produced by different microorganisms utilizing glycerol, is mentioned in Table 2.11.

2.3.11 Extracellular polysaccharides

Extracellular Polysaccharides (EPS) are polymers having a range of physical and chemical properties such as viscosity, solubility over wide pH range, power of chelation, etc. Due to these properties, they are used in variety of fields such as, textile, pharmaceuticals, emulsifiers and stabilizers. The use of *P. oleovorans* for EPS production from glycerol containing feedstock yielded 8.11 g/L EPS, with a productivity of 0.19 g/L. Galactose formed the bulk of EPS along with the monomeric sugars like mannose, glucose and rhamnose. It also contained acyl groups of pyruvate, succinate and acetate (Freitas et al., 2009b). Majority of the polysaccharide is formed when the cultures enter the stationary growth phase. Glycerol was found to increase the yield of poly–gamma glutamic acid (γ -PGA), and also modified its properties by decreasing its chain length. Glycerol also decreased the viscosity of fermentation medium facilitating the uptake of extracellular substrates, and increasing γ -PGA yield to approx. 31.7 g/L with 20 g/L glycerol (Wu et al., 2010). The emulsifying and rheological properties of EPS were tested, and the results revealed that the polymer exhibited pseudo–plastic behavior even at decreased apparent viscosity.

Table 2.11 Summary of literature on biochemical conversion of glycerol to SCOs

Micro organism	Type	FA composition (% Total FA)	Yield (g/L)	Reference
<i>Schizochytricum limacinum</i> SR21	Docosahexaenoic acid			Chi et al., 2007
	16:0	54.70±0.41	3.07±0.19	
<i>Schizochytricum limacinum</i> SR21	22:6	33.62±0.34		Pyle et al., 2008
	Docosahexaenoic acid			
<i>Mortierella alpina</i>	16:0	62.1±0.5	–	Hou, 2008
	22:6	27.3±0.6		
<i>Mortierella zychae</i>	Arachidonic acid(20:4)	24.83	–	Fakas et al., 2008
	Dihomo-γ-linolenic acid(20:3)	6.67		
	Arachidonic acid(20:4)	19.83		
<i>Cunninghamella echinulata</i>	Dihomo-γ-linolenic acid(20:3)	5.00		Papanikolaou et al., 2008
	SCO	25.6	2.0	
<i>Mortierella isabellina</i>	γ-Linolenic acid	16.2 (GLA/Oil%)	0.19	André et al., 2010
	SCO	53.2	3.3	
	γ-Linolenic acid	12.8 (GLA/Oil%)	0.116	
<i>Mortierella isabellina</i>	SCO	51.7	4.4	Papanikolaou et al., 2008
<i>Lentinula edodes</i> AMRL 121	Palmitic acid	15.1%w/w	–	André et al., 2010
	Stearic acid	10.9	–	
	Oleic acid	3.2	–	
	Linoleic acid	75.4	–	
<i>Aspergillus niger</i> LFMB1	Palmitic acid	13.1	3.1	Freitas et al., 2008
	Stearic acid	8.9		
	Oleic acid	38.6		
	Linoleic acid	37.1		
<i>A. niger</i> NRRL 364	Palmitic acid	17.1	3.4	Freitas et al., 2008
	Stearic acid	10.1		
	Oleic acid	37.7		
	Linoleic acid	32.3		

FA = Fatty acid

Also, the polymer showed emulsifying activity even at a broad range of temperature (30–50°C) and pH (2–12). In addition, the polymer is thermologically stable (Freitas et al.,

2009a; Alves et al., 2010).

2.4 MISCELLANEOUS PRODUCTS

2.4.1 Succinic acid

Succinic acid or butanedioic acid finds use in pharmaceutical, agriculture, food and beverage industries. It is a starting material for manufacture of many industrially important compounds, and biodegradable polymers such as Tetrahydrofuran (THF), polysuccinate esters, 1,4-butanediol, 4-aminobutanoic acid, γ -butyrolactone, etc. (Song and Lee, 2006). The most common chemical route for succinic acid production is through maleic anhydride from n-butane or other petrochemical sources. The current market price of succinic acid varies between \$5.0–9.0 per kg. The overall cost of succinic acid production is enhanced by the high cost of maleic anhydride feedstock. This contributes \$1.027 per kg of succinic acid. The biological route for succinic acid production basically consists of fermentation of carbon sources such as glucose, glycerol, xylose, galactose, etc. using a variety of microorganisms namely *Anaerobiospirillum succiniproducens*, *Actinobacillus succiniproducens*, *Manheimia succiniproducens*, *rE.coli*. Out of all these microorganisms, *Anaerobiospirillum succiniproducens* is the only studied strain that can utilize glycerol efficiently, and convert it into succinic acid (Lee et al., 2004). The biological production of succinic acid occurs under anaerobic condition, either through phosphoenolpyruvate carboxylase pathway or through pyruvate carboxylation pathway.

The use of glycerol over sugars for succinic acid production provides distinct advantage such as the demand for lower carbon source per gram of succinic acid, and also a lower production of by-products such as acetic acid, fumaric acid, lactic acid, which decrease the cost of downstream processing for succinic acid recovery (Scholten and Dägele, 2008). Additionally, *Anaerobiospirillum succiniproducens* can also utilize a variety of other carbon

sources such as glucose, sucrose, maltose, lactose, fructose etc. The use of glycerol as a carbon source gives an enhanced succinic acid yield of 1.71 g/g, and a higher ratio of succinic acid to acetic acid of 25.8:1 than that obtained from other sugars as carbon source (Lee et al., 2004). Another novel strain that can produce succinic acid using glycerol containing feedstock is *Basfia succiniproducens* DD1. This strain gave succinic acid yield of 1.02 g/g, and a productivity of 0.094 g/L-h at a dilution rate of 0.018 per hour (Scholten et al., 2009).

Succinic acid being an organic acid; numerous options exist for its recovery from fermentation broth. Electrodialysis is a well-known separation process employed in separation of ionized compounds. As succinic acid exists in ionized state in the fermentation broth, it can be easily separated from other non-ionized compounds such as carbohydrates, proteins, amino acids, etc (Glassner and Datta, 1992). Another process for succinic acid purification is precipitation of succinate salts as calcium succinate by a precipitant calcium hydroxide. Calcium succinate is in turn filtered, and converted into succinic acid by addition of H₂SO₄ (Datta et al., 1992). Other processes such as vacuum distillation, reactive extraction using tertiary amines as extractants can also be employed for efficient succinic acid recovery (Huh et al., 2004; Kim et al., 2004).

2.4.2 Erythritol

It is a sugar alcohol and used as an artificial sweetener. The industrial production of erythritol occurs by catalytic conversion of starch at high temperature. It is biologically synthesized by a number of microorganisms such as *Torula sp.*, *Candida magnoliae* (Ryu et al., 1999, Kim et al., 2000), and *Trichosporon* (Park et al., 1998), through fermentation of sugars. *Candida magnoliae* strain produces erythritol from glucose, but its production from glycerol containing feedstock needs to be studied (Koh et al., 2003). The production of erythritol from glycerol was tested using *Y. lipolytica* Wratislavia K1 acetate negative mutants. These strains showed the pH dependency of erythritol production. In a study

performed in a fed–batch mode, the cells gave erythritol yield of 81 g/L with 150 g/L glycerol at pH 5.5 but, there was simultaneous production of both erythritol and citric acid (Rymowicz et al., 2008). The fed–batch production of erythritol at pH 3 gave a yield of 170 g/L. Also, no citric acid was produced by the strain between pH 2.5 to 3.0, proving that this pH range is ideal for maximum erythritol production from glycerol, without channeling of glycerol to citric acid production pathway (Rymowicz et al., 2009).

2.4.3 Mannitol

Mannitol is a naturally occurring sugar alcohol found in a variety of vegetables and fruits. It has numerous medical applications such as a weak renal vasodilator, diuretic agent and as a laxative for children at higher doses. It is also used as an artificial sweetener for diabetic patients. It is industrially produced by hydrogenation of fructose, which also yields sorbitol as a by–product (Wikipedia, 2011a). The chemical process suffers from low yield and energy intensiveness of the process for separating sorbitol from mannitol. The production of mannitol from glycerol was tested using resting cells of *Candida magnoliae*. The cells completely consumed glycerol in 96 h, and exclusively produced mannitol at a concentration of 51 g/L as against a mixture of mannitol and erythritol produced by growing cells of *Candida magnoliae* on sole glycerol as a substrate. The supplementation of glycerol, with either yeast extract or KH_2PO_4 , decreased the production of mannitol (Khan et al., 2009). *Y. lipolytica* Wratislavia K1 acetate negative mutants also produce mannitol at a concentration of around 12–13.5 g/L, between pH 2.5–3.0. Here, erythritol is the major product (Rymowicz et al., 2009).

2.4.4 Ethanol

Ethanol is an alternative fuel and can be blended with gasoline typically in a ratio of 5–20% v/v. It is used as a solvent and also as a reactant in biodiesel production. The production of ethanol from biodiesel derived crude glycerol is carried out by *Enterobacter*

aerogenes. The cells immobilized on porous ceramics formed 0.43 g ethanol/g glycerol, while the self-immobilized cells produced slightly lower amount of ethanol (0.40 g/g glycerol). A higher concentration of glycerol inhibits the production of ethanol (Ito et al., 2005). Thin stillage containing high amounts of glycerol, glucose and other sugars can also be used for bioethanol production using *Escherichia coli* strains. The use of wild type *E. coli* strains for ethanol production from thin stillage suffers from carbon catabolite repression. Glycerol is metabolized only after complete utilization of glucose present in the medium. Hence, genetically engineered *E. coli* cells were used. The recombinant *E. coli* cells over-expressing glycerol dissimilation pathway produced 0.38 g ethanol/ g substrate consumed (Gonzalez et al., 2010). *Lactobacillus reuteri* cells also form appreciable amounts of ethanol as a by-product of glycerol-glucose co-fermentation. The batch cultures produce ~19.5 mM ethanol, while chemostat cultures accumulate glycerol to a concentration of ~ 22 mM.

2.4.5 Lactic acid

Lactic acid is used as a disinfectant and as a major component of intravenous fluids. The biological production of lactate occurs by fermentation of pyruvate by an NADH dependant enzyme Lactate dehydrogenase. Lactic acid production is mainly carried out by bacteria belonging to lactobacillus family, also known as Lactic acid bacteria. Apart from *Lactobacilli*, *Pediococcus pentosaceus* aerobically catabolizes glycerol to d-lactate and acetate. Lactate formation occurs in early growth phase. The concentration of by-products increases with an increase in initial concentration of glycerol. When glucose and glycerol are compared as carbon source, lactate production is lower with glycerol than with glucose, while the reverse holds true for acetate production. This strain accumulates d-lactate to a concentration of ~5.2 mM in presence of 42.6 mM glycerol along with the formation of 9.2 mM acetate (Pasteris & Strasser de Saad, 2005). Co-fermentation of glycerol and glucose by *L. reuteri* in a batch process produces 1,3-PDO and 3-HPA as the major product, along with

the formation of 27.5 mM lactate. The use of glucose as the sole carbon source in both batch and chemostat studies yield a higher amount of lactate, as compared to a mixture of glycerol and glucose. Chemostat cultures grown on glycerol–glucose mixture produced 6.8 mM lactate (El-Ziney et al., 1998).

Another bacteria belonging to Lactobacillus family *L. collinoides* also produces lactate by glycerol fermentation. This strain cannot grow on glycerol as a sole carbon source, due to the absence of oxidative pathway, but requires a sugar as a supplementary carbon source to enter into the glycerol dehydratase pathway. Maximum lactic acid production occurred at 15°C, pH 4.8. As the amount of sugar and glycerol decreased in the medium, there was a simultaneous decrease in the concentration of lactate. This is because the cells started utilizing lactate for the production of acetate (Garai–Ibabe et al., 2008).

2.4.6 Methane

Methane, also known as marsh gas, is a major constituent of natural gas. It is used as a motor fuel in the form of compressed natural gas (CNG), and also as a domestic fuel in many places. It is a feedstock for production of methanol, acetic acid, acetylene, hydrogen, etc. The production of methane from biodegradation of glycerol containing synthetic wastes is carried out mainly by two groups of Methanogens, viz. *Methanobacterium sp.* and *Methanosarcina sp.* Glycerol is an easily digestible and stored product. These properties make it an ideal feedstock for anaerobic digestion. The anaerobic fermentation of glycerol gives a methane yield of 0.45 NL per gram of dissolved organic carbon added. The process gives better methane yield under thermophilic conditions than in mesophilic conditions (Yang et al., 2008). The addition of glycerol increases the chemical oxygen demand (COD) of the medium, which in turn completely converts glycerol to methane. The addition of 1% v/v glycerol as a co–substrate to olive mill waste water and slaughter house water enhanced the production of methane from 479 ± 38 mL/ day to 1210 ± 205 mL/day. The co–digestion of

municipal solid waste with glycerol produced 1400 ± 305 mL methane/ day (Fountoulakis and Manios, 2009).

2.4.7 3-Hydroxypropionic acid

It is an industrially important chemical and is used as a feedstock for production of 1,3-PDO, methylacrylate, acrylonitrile, etc. It is also used as a lubricant and as a cross-linking agent in metallic coatings. It is biologically synthesized primarily by bacteria belonging to *Lactobacillus sp.* by oxidation of 3-Hydroxypropionaldehyde (Sobolov and Smiley, 1960). At pH 4.8, *Lactobacillus sp.* forms ~ 24 mM 3-hydroxypropionic acid from glycerol supplemented with glucose and fructose. The results show that the production of 3-hydroxypropionic acid is pH dependant, and decreases with a decrease in pH (Garai-Ibabe et al., 2008). The production of this compound using recombinant *Escherichia coli* cells in a pH regulated fed-batch process formed 31 g/L 3-hydroxypropionic acid in 3 days (Raj et al., 2009).

2.4.8 Oxalic acid

Oxalic acid is a dicarboxylic acid and exists naturally in plants and animals. It is used as a mordant in dyeing industry, and is also used as a cleaning agent (Wikipedia, 2011b). Its calcium salt, i.e. calcium oxalate, is a major component of kidney stones. Its conjugate base, i.e. oxalate, is used as a chelating agent. It is industrially manufactured by catalytic oxidation of carbohydrates. The biocatalytic production of oxalic acid from glycerol as a substrate is carried out by *Aspergillus sp. A. niger* NRRL 364 and LFMB1, when grown on glycerol extracellularly, produces oxalic acid. LFMB1 produced 2.5 g/L oxalic acid with 60 g/L glycerol, while NRRL 364 synthesized 20.5 g/L oxalic acid with the same concentration of glycerol. The concentration of oxalic acid increased with an increase in initial glycerol concentration. A higher concentration of oxalic acid was formed in a 2 L flask, as compared to 250 mL flask (André et al., 2010).

2.4.9 2,3-Butanediol

2,3-Butanediol is a feedstock for production of many industrially important compounds, such as 1,3-butadiene, methyl ethyl ketone (used as a fuel additive), diacetyl (used as a flavoring agent). Besides, it is also used as a solvent and an antifreeze agent. The microbial production of 2,3-BDO occurs using mixed cultures of *Klebsiella oxytoca* and *K. pneumoniae* (Wu et al., 2008b). 2,3-BDO exists in 3 stereoisomeric forms, viz. dextro, levo and meso. The production of 2,3-BDO from glycerol using solely *K. pneumoniae* cultures is pH dependant. The strain produced 49.2 g/L of 2,3-BDO at pH 8.0, with negligible production of 1,3-PDO, acetate and lactate. The production of 2,3-BDO and acetate were found to follow an inverse relationship. Also, more amount of 2,3-BDO was formed at a higher pH (Petrova and Petrova, 2009). The fed-batch process with pH control was found to considerably decrease the production of 2,3-BDO, as more and more glycerol was channeled towards the production of ethanol and lactic acid. 2,3-BDO is mainly produced as a self pH control mechanism due to the decrease in pH because of acetate accumulation.

2.4.10 Pigments

The production of β -carotene pigment by *Blakeslea trispora* from glycerol as a substrate has been studied (Mantzouridou et al., 2008). β -carotene production occurs after the growth phase, whereby all the lipid produced from the substrate in the early growth phase is consumed. Hence, the cells require supplementary carbon source such as glucose (in typical concentration of 50 g/L) or glycerol (in the concentration range of 10–180 g/L) to be used in the late growth phase. An initial glycerol concentration of 60 g/L produced 15 mg β -carotene/g of dry biomass.

2.4.11 Hydrogen

Hydrogen is an important alternative fuel due to its high calorific value of 142.3 kJ/g, and is a clean fuel as it only forms water on burning. It is used in hydrogenation of oils and in

synthesis of methanol, hydrochloric acid, etc. The industrial production of hydrogen occurs by steam reforming of natural gas. The photo-fermentation is the oldest known route for hydrogen production by purple non-sulfur photosynthetic bacteria using substrates such as carboxylic acids, sugars, etc. The anaerobic production of H₂ is catalyzed by Ni and Fe containing enzyme known as hydrogenases. These hydrogenases are membrane-bound in *Escherichia coli*, and are inhibited by sodium azide and N,N'-dicyclohexylcarbodiimide (Trchounian and Trchounian, 2009). Glycerol can also be used as a substrate for photo-fermentative hydrogen production by *Rhodospseudomonas palustris* with a yield of 0.13 g/g pure glycerol (Sabourin-Provost and Hallenbeck, 2009). The anaerobic production of hydrogen from olive mill water and slaughter house water supplemented with 1% glycerol yielded, 1.44 mg H₂/g glycerol. The use of municipal solid waste supplemented with glycerol as a substrate gave a higher yield of 5.8 mg H₂/g glycerol, due to higher amount of biomass in the reactor (Fountoulakis and Manios, 2009).

The self-immobilized *Enterobacter aerogenes* cells formed 0.017 g H₂/g glycerol in a packed bed reactor (a cylindrical glass vessel packed with diatomaceous clay). The cells of *E. aerogenes* show flocculation, and hence, are self-immobilized (an effect similar to dense clustering) (Ito et al., 2005). The dark fermentation of hydrogen from glycerol by digested sludge in a batch process produced 8.9 mg H₂/g glycerol. An increase in glycerol concentration from 5 to 30 g/L increased H₂ production; although, the initial concentration of glycerol did not affect the rate of H₂ production (Seifert et al., 2009).

Apart from these, many studies have also dealt with the use of microbial electrolysis cell for the production of H₂ from glycerol. Hydrogen was evolved in presence of both pure and crude glycerol with a yield of 0.08 and 0.04 g/g, respectively (Selembo et al., 2009). Another study mentioned a higher hydrogen yield of 0.12 g/g pure glycerol (Escapa et al., 2009). The experimental set up by Escapa et al. (2009) consisted of a continuous flow

microbial electrolytic cell, constructed of a series of polycarbonate plates (anodic chamber). The anodic chamber consisted of graphite felt filled with liquid. Gas diffusion electrode was used as a cathode, and was separated from the anode by a porous cellulosic fabric. The cathodic chamber consisted of a gas collection chamber with a volume of 250 mL.

2.4.12 Glycerol as a supplementary carbon source

Apart from synthesis of different kinds of value-added products discussed in previous sections, glycerol is also used as a major carbon source for the growth of microorganisms, production of enzymes, recombinant proteins, amino acids, etc. The photo-heterotrophic growth of microalga *Phaeodactylum tricorutum* is influenced by the use of glycerol as a carbon source. At 0.01 M glycerol concentration, maximum biomass concentration of 2.59 g/L was obtained. The supplementation of 0.1 M glycerol with 0.01 M urea in a fed-batch process gave a maximum productivity of 63.5 mg/L-h (Cerón Garcia et al., 2005). A lower glycerol concentration under uncontrolled pH conditions also promotes the growth of recombinant *Pichia pastoris*. For a constant media pH of 5.0, there was complete consumption of glycerol even at high concentration of 12% (Chiruvolu et al., 1998). The fixed feeding of glycerol and methanol to recombinant *P. pastoris* cells for production of heavy chain C of botulinum neurotoxin produces 3 mg protein/g wet cells (Zhang et al., 2003). *Streptovercillium ladakanum* produces transglutaminase protein in presence of glycerol, molasses and their mixture. The enhancement in agitation speed increased the growth of biomass. The use of glycerol as a sole carbon source denatured the protein to greater extent than molasses, due to higher viscosity and shear stress. On the other hand, a mixture of 30 g/L molasses and 30 g/L glycerol produced transglutaminase with a maximum activity of 0.46 U/mL at 400 rpm (Portilla-Rivera et al., 2009). Both glycerol and molasses exerted a synergistic action on production of trans-glutaminase protein.

Another industrially important enzyme phytase is also produced from glycerol with an

activity of 1125 U/mL on anaerobic fermentation of glycerol by *P. pastoris* in a fed–batch process (Tang et al., 2009). Clavulanic acid, a β –lactamase inhibitor, is produced by *Streptomyces clavuligerus* growing essentially on glycerol. The shake flask cultures fed with glycerol after every 12 h (for a total of 132 h) produced 270 mg/L of clavulanic acid. The glycerol feeding in fed–batch cultures produced 280 mg/L clavulanic acid, and showed more stability up to 130 h than shake flask cultures, although rate of production was almost the same in both cases (Chen et al., 2002). The same fed–batch process operated at low flow rate of 0.01 L/h and glycerol concentration of 120 g/L produced 719 mg/L of clavulanic acid, which is twice the value obtained in batch cultivation (Teodoro et al., 2006). Hence, maximum production of clavulanic acid occurs at low flow rates and high glycerol concentration.

Similarly, production of amino acid Phenylalanine was carried out by *Escherichia coli* BL21 cells using glycerol as a carbon source. The cells produced 0.58 g phenylalanine/g glycerol, under optimum conditions of 8 L/min aeration rate and agitation speed of 400 rpm. This is almost twice the value obtained on use of sucrose as a carbon source (Khamduang et al., 2009). These conditions were also optimum for the growth of biomass and highest biomass productivity. The process requires high aeration rate, but is inhibited at higher agitation speed due to enhanced shear stress. Recombinant *Pseudomonas putida* produces p–hydroxybenzoate via l–Tyrosine from glycerol or glucose. The production of p–hydroxybenzoate occurs during the growth phase and stops immediately after the cessation of growth. The use of glycerol as a substrate comparatively produces lesser amount of p–hydroxybenzoate (1.72 mM) than glucose (1.85 mM) in shake flask experiment. The reactions, when carried out in carbon limited fed–batch process using glycerol as a substrate, produced maximum concentration of p–hydroxybenzoate (12.9 mM) (Verhoef et al., 2007). Glycerol is also used as a carbon source for bioconversion of fumarate to succinate using

Enterococcus sp. The maximum amount of succinate produced was 65.9 g/L (82% molar yield) at pH 7.0. The supplementation of glycerol containing media with glycerol enhanced the bioconversion of fumarate to succinate with a molar yield of 103.8%. The production of succinate was found to be directly proportional to the initial concentration of fumarate (up to 100 g/L) (Ryu et al., 1999).

P. pastoris is the model organism for production of recombinant proteins, as it can be grown to a high cell density and is easy to handle. *P. pastoris* is used for the production of recombinant human erythropoietin hormone from biodiesel derived crude glycerol. Glycerol is utilized by the cells for growth and biomass production, while methanol present in crude glycerol induces the expression of recombinant protein. The protein is accumulated up to a concentration of 31 mg/L (Çelik et al., 2008). Recombinant *P. pastoris* also produces cystatin C, a human cysteine proteinase inhibitor which has numerous therapeutic applications. The cells formed maximum concentration of 0.6 $\mu\text{mol/L-h}$ cystatin C at pH 6.0 at methanol feeding rate of 1.8 g/L-h. The addition of 2.1 g/L-h glycerol to the same media increased the productivity to 0.96 $\mu\text{mol/L-h}$. The addition of methanol increases the concentration of cystatin C formed, while the addition of glycerol enhances volumetric productivity (Files et al., 2001).

The recombinant *P. pastoris* also produces human granulocyte colony stimulating factor, a protein which regulates the growth and differentiation of blood cells. This protein was formed under two phase glycerol feeding process. The carbon source glycerol was fed to the cells prior to induction so that the cells formed higher amount of biomass and exhibited high growth rate. The productivity of the protein under this condition was ~ 5.52 mg/L-h, which is 2.9 times of the productivity achieved in fed-batch process. This strategy also decreased the total induction time by ~ 30 h (Bahrami et al., 2008).

2.5 ECONOMIC FEASIBILITY OF GLYCEROL BIOCONVERSION

The preceding sections have outlined details of bioconversion of glycerol to numerous products. However, whether the technology of these bioconversions has any potential of commercialization remains a question. As noted in the introduction section, very large quantities of glycerol are going to be available worldwide, as a side product of the biodiesel industry. This glycerol is available at very cheap rates of about \$400–500/ton. A simple ratio of product cost to feedstock cost would reveal that value addition for most of the products derived from glycerol; bioconversion is > 100 , which is certainly a tremendous motive for the large-scale implementation of the process. Typically, in any fermentation based process, about 50–60% cost of the product is contributed by the feedstock, and hence, changeover of the process to cheaper feedstock is perhaps the most effective means of boosting the economics of the fermentation industry. However, there are several factors that need to be taken into account prior to drawing firm conclusions for the scale-up potential and economic feasibility of glycerol bioconversion.

In the first place, the current and projected demand for a particular product needs to be considered. The most widely studied bioconversion product from glycerol is 1,3-PDO, which is used in synthesis of biodegradable plastics. With greater quest for an eco-friendly plastic, which would also possess desirable properties like higher resistance and resilience, the market for 1,3-PDO is likely to grow fast. However, this may not be the case for all products. Secondly, the cost of transportation of glycerol also needs to be taken into account. This cost factor is of more relevance for grass-root plants. With rising cost of diesel and gasoline, the transportation costs are likely to raise the prices of glycerol significantly, which could adversely affect economics of a glycerol fermentation plant located away from the biodiesel plant. This factor would give an incentive for the forward integration of the biodiesel plants, which could simultaneously implement fermentation processes for

bioconversion of glycerol. Such an effort would give significant boost to the economy of biodiesel with reasonable fixed capital investments for expansion of existing facility of biodiesel production.

The third important factor is the difficulties involved in the fermentation process and the downstream processing. Most of the microorganisms for glycerol bioconversion are anaerobes, for which strict maintenance of sterility in the system is utmost essential. Although several new mutant strains have been developed, that have greater resistance towards substrate and product inhibition, these are yet to be tested even on pilot scale. Most of the studies involving these new strains are on lab scale, and cannot be directly used for designing industrial scale plants. Strict maintenance of sterility through automation and instrumentation is likely to raise the capital investment significantly. From sterility point of view, batch fermentation systems are easier to handle than continuous system. However, both yield and productivity of the batch system is smaller than continuous culture systems, and some compromise has to be made in this regard. Therefore, from investment point alone, although continuous systems are of advantage due to higher productivity, additional costs for maintenance of sterility need to be considered. Downstream processing of the fermentation broth is another challenge in the design of large-scale plant. For several products, in-situ removal is of advantage so as to tackle product inhibition. Several techniques are available for this such as adsorption, liquid-liquid extraction, membrane separation, gas stripping etc. The most economic technique depends on the spectrum of the products from fermentation. The best technique, which would give the highest selectivity for isolation of desired product, may change from product to product. Purification of the products is also an important component of the process. Usually, purification is done through distillation or membrane separation or chromatographic separation. However, a global viewpoint is needed for the choice of in-situ product removal and product purification for an optimum design. A cheaper

and simpler method for in-situ product removal may raise the cost of downstream processing, as it may remove undesired products as well from the broth, which are later difficult to separate from the main product.

Membrane separation is an attractive technique for in-situ product removal, as it is far less energy intensive than conventional liquid-liquid extraction. However, the membrane has to have high flux and selectivity. The investment costs for membrane are high, and hence, long-term stable operation with consistent results is crucial to economic viability of the membrane based downstream processing. Accumulation of impurities of the medium in the membrane pores, which would block them, could adversely affect the process. An optimization and trade off between fixed capital investment and operating costs is thus necessary to arrive at an economically feasible design.

Finally, the fluctuations in the demand and supply in the international market needs to be accounted for. The current market for some of the products may not be large enough to accommodate additional supply from glycerol fermentation industry. Given this uncertainty, the glycerol fermentation plant needs to be made “product flexible”, so as to change over production to different compounds, in concurrence with the changing market. For long-term viability of the process, it could be a wise idea to go for a product that has lesser value addition, but more stable market and more reliable prices.

2.6 INFERENCE AND JUSTIFICATION OF THE PRESENT THESIS

Fast depletion of fossil fuels has made quest for a sustainable, renewable and carbon neutral fuel. The most popular alternate liquid fuel that has met these expectations and has emerged as a potential diesel substitute is biodiesel, which is essentially alkyl (methyl or ethyl) ester of fatty acids manufactured by transesterification of vegetable oils. Even with the cheapest oil feedstock, the economy of biodiesel is not attractive, and the prices are

comparable or even higher than petro–diesel. An obvious option for boosting the economy of biodiesel is to find markets for the by–products of the process. The main by–product of transesterification process is glycerol. However, direct utilization of glycerol produced during transesterification for conventional products is not possible, as it is contaminated with alcohol and the (alkali or acid) catalyst used in transesterification. Therefore, conversion of this glycerol to other products is a feasible solution, and also a matter of intensive research in the past two decades. There are strong arguments as why bioconversion could be an alternative to usual catalytic processes. Bioconversion is not only quite specific (with high selectivity and very few by–products) but also takes place at ordinary (or room) temperature and pressure conditions, as against prohibitively harsh conditions used in catalytic processes. Moreover, catalyst is a highly expensive component of the process. The microbial cultures are not only cheaper but also renewable. Due to this, both fixed capital investments and operating costs of the bioconversion processes are likely to be smaller than the catalytic processes. However, these merits are offset by slower kinetics and rather dilute solutions of the products obtained in fermentation processes. Nonetheless, even with these limitations, glycerol conversion is a viable process and has potential of implementation on large–scale. The research done so far (albeit on laboratory scale) has shown good promise for the same. These processes, if implemented on large–scale, will provide a valuable outlet for over 1.8 million tons of crude glycerol generated from biodiesel industry. In addition to generating extra revenue for the biodiesel industry, it will also give an eco–friendly route for effective utilization of enormous quantities of glycerol generated from biodiesel industry. The research activity in the area has addressed several facets of the process, such as type of strain used, mode of fermentation, product recovery and purification technique, etc.

In this thesis, we have addressed the important issue of development, optimization and intensification of the glycerol bioconversion process using immobilized cells of

Clostridium pasteurianum. The beneficial effects of use of immobilized cells in fermentation processes are well-known. Immobilization offers greater control over the cell density in the fermentation broth, allows easy separation and recycle of the cells and also helps overcome substrate and product inhibition. We have taken a step-by-step approach for the development of glycerol bioconversion process. Initially, we selected the microbial strain for the process from the strains that were available in Indian culture banks. After selection of the strain *Clostridium pasteurianum*, which can utilize both pure and crude glycerol, we have screened different solid supports for immobilization of the cells. Next, we have tried to optimize other aspects such as the amount of support to be added, cross-linking of the cells, optimization of the glycerol concentration, comparison of free and immobilized cells and the kinetic analysis of the process. This is followed by selection and optimization of the medium components followed by optimization of the process. We have also attempted a possible solution to the slow kinetics of the bioconversion process in terms of application of ultrasound to the fermentation broth and have tried to get a mechanistic insight into the enhancement through analysis of the enzymatic kinetics and cavitation physics. Finally, we have also attempted a moderate scale-up of the process from flask level to bioreactor level, and have assessed the feasibility of the optimized parameters and protocols.

We believe that the results and analysis presented in this thesis addressing important issues of the glycerol bioconversion process will give important inputs for design, optimization and scale-up of the process.



GLYCEROL FERMENTATION BY IMMOBILIZED CELLS: PRELIMINARY OPTIMIZATION

3.1 INTRODUCTION

As noted in the previous chapter, the principal aim of the present thesis is to develop and optimize a bioprocess for conversion of glycerol into value added products using immobilized cells. In the last chapter, we outlined the plethora of diverse value-added products possible from glycerol bioconversion. Among these, 1,3-propanediol (PDO) and butanol are of special interest due to their large market potential. 1,3-PDO is a monomer used for synthesis of polymers such as polyesters, polyethers and polyurethanes. Butanol is an excellent solvent and in the present-day scenario, is also being looked upon as a potential alternate liquid transportation fuel, due to its very similar properties to gasoline. We have, therefore, focused the research work in this thesis on bioconversion of glycerol into the above two products.

The first step in development of the bioprocess is to decide the substrate and the targeted product. After zeroing on 1,3-PDO and butanol as the products of interest, we searched for the suitable microorganism for the process. Instead of isolation and characterization of a micro-organism from environment, we searched the literature for a suitable species for bioconversion of glycerol into the targeted products. Literature reports *Klebsiella*, *Citrobacter*, *Gluconobacter*, *Clostridium*, etc as some of the potent glycerol utilizing microbial strains (Yazdani and Gonzalez, 2007; Amaral et al., 2009; da Silva et al., 2009; Saxena et al., 2009). Out of these, only *Clostridium pasteurianum* can grow and utilize glycerol for production of both targeted compounds, butanol and 1,3-PDO. Moreover, ethanol is also produced as a side product. The most studied butanol producer *Clostridium acetobutylicum* is also known to utilize glycerol for biobutanol and ethanol production, but it requires some supplementary carbon source for utilizing glycerol as a substrate (Andrade and Vasconcelos, 2003).

The kinetics as well as yield of the bioconversion process is influenced by the cell density or population in the reaction system. Effective separation and recycle of the microbial cells (after completion of the process) is a possible solution to controlling the cell density in the medium. If free micro-organisms are used for bioconversion processes, it is rather difficult to separate and recycle them. Immobilization of cells on suitable supports simplifies the recovery and recycle of microorganisms in successive batches of bioconversion process. In addition, immobilization of cells is also reported to reduce substrate inhibition (giving higher productivity) in addition to lowering of foam formation (Van Ede, 1994). It also permits operation of the fermentation process in continuous mode in either fixed or fluidized bed mode of operation.

In view of the above contemplations, the current work aims to study the production of three value added products viz. 1,3-PDO, butanol and ethanol from glycerol as a feedstock

using a whole cell biocatalyst in the form of immobilized cells of *C. pasteurianum*. The immediate step in process development chain is to explore a suitable support for immobilization of the Clostridial cells, and this chapter addresses this important issue. The work presented in this chapter tries to evaluate three supports viz. silica gel, reticulated polyurethane foam and Amberlite for immobilization of *C. pasteurianum* cells and their corresponding solvent production capability on the three supports. The work also tries to determine the effect of cross linking of cells, the amount of support with immobilized cells and the amount and the kind of substrate (pure and crude glycerol) used for fermentation on the product profile, and also compares the free cells fermentation with immobilized fermentation system for mixed alcohols production.

3.2 MATERIALS AND METHODS

3.2.1 Materials

Clostridium pasteurianum MTCC 116 (ATCC 6013) was procured from Microbial Type Culture Collection, Chandigarh (India). Amberlite, a mixed bed ion exchange resin was procured from Sigma–Aldrich. 60–120 mesh size silica (column chromatography grade, Merck, Germany) was procured from Merck, Germany. Reticulated polyurethane foam was procured from local market. The analytical standards for gas chromatographic analysis were procured from Sigma Aldrich, USA and Merck, Germany. Crude glycerol was procured from alkali catalyzed methanolysis of soybean oil. The details of transesterification reaction are as follows: molar ratio 12:1, amount of oil (20 mL), amount of methanol (10 mL), catalyst amount (0.18 g, 1% w/v), temperature (65°C) and percentage conversion 98.6%. The composition of crude glycerol was as follows: 0.26 % methanol, 0.9 % sodium hydroxide (calculated by acid base titration) and rest was glycerol. Pure glycerol was procured from Merck, Germany. The glycerol assay kit was procured from Megazyme, Ireland. The

anaerobic assembly was procured from Himedia, India. All other chemicals used for media preparation were of analytical grade (Merck, Germany and Himedia, India). The anaerobic setup for maintenance of anaerobic environment was procured from Himedia. All other chemicals were purchased from either Himedia (India) or Merck (Germany).

3.2.2 Growth and maintenance of *C. pasteurianum*

The lyophilized *C. pasteurianum* cells were revived in Cooked Meat Media (CMM) agar slants, which were kept in an anaerobic tray system (Himedia, India) at 30°C for 24 h in an incubator. The revived cells on CMM agar slants were kept at 4°C and were sub-cultured every month. This stock culture was used throughout for inoculum preparation. Agar plates were prepared from CMM agar slants. The growth of the cells was carried out at 30°C, 120 rpm in Reinforced Clostridial Medium (RCM, Oxoid CM149) containing yeast extract (3 g/L), beef extract (10 g/L), peptone (10 g/L), NaCl (5 g/L), CH₃COONa (3 g/L), glucose (5 g/L), cysteine hydrochloride (0.5 g/L), soluble starch (1 g/L) and agar (0.5 g/L), and was inoculated with single colony from the agar plate. The initial pH of the media was adjusted to 6.8 ± 0.2. The broth was sparged with 99.98% pure nitrogen gas after every 24 h to ensure anaerobic conditions.

3.2.3 Pure and crude glycerol fermentation by free cells

Fermentation of glycerol was carried out in fermentation media containing KH₂PO₄ (0.5 g/L), K₂HPO₄ (0.5 g/L), CaCO₃ (2 g/L), MgSO₄·7H₂O (0.2 g/L), CaCl₂·2H₂O (0.02 g/L), FeSO₄·7H₂O (0.005 g/L), (NH₄)₂SO₄ (3 g/L), yeast extract (1 g/L), and SL₇ trace element solution (2 mL/L). The composition of SL₇ trace element solution is as follows: MnCl₂·4H₂O (0.1 g/L), ZnCl₂ (0.07 g/L), H₃BO₃ (0.06 g/L), NaMoO₄·2H₂O (0.04 g/L), CoCl₂·2H₂O (0.02 g/L), CuCl₂·2H₂O (0.02 g/L), NiCl₂·2H₂O (0.02 g/L), 25% HCl (1 mL/L). Glycerol was autoclaved separately. Pure/ crude glycerol in concentration of 5, 10 and 25 % w/v was added to the fermentation medium. 5% v/v of inoculum was used for fermentation of glycerol with

free cells. The fermentation was carried out in 250 mL custom fabricated Erlenmeyer flask (shown in correction appendix) at 37°C with agitation at 200 rpm. Nitrogen gas (99.98% pure) was sparged in the flask to maintain anaerobic conditions.

3.2.4 Determination of cell morphology in presence of glycerol

Morphological changes of *C. pasteurianum* cells in absence (control) and in presence of both pure and crude glycerol (25 g/L each) were investigated by Flow cytometry (BD FACS caliber). Flow cytometric analysis for all the samples was done using 488 nm laser and 530 nm emission filter. FSC (Forward Scatter) and SSC (Side Scatter) were used to evaluate the morphological changes in the cells.

3.2.5 Immobilization and cross linking of cells

The cells were immobilized on the three supports mentioned previously in RCM broth in custom fabricated Erlenmeyer flasks (vol. 250 mL). Amberlite and silica gel were dried overnight at 40 and 100°C prior to immobilization. The support was added to the broth at the onset of log phase of the culture. In case of Amberlite as a support, the pH of the solution had to be maintained at 6.8 (the initial value) with 1 N NaOH, as addition of Amberlite decreased the pH of the media to ~ 3. The support was incubated for 72 h in RCM broth at 30°C with shaking at 120 rpm. After incubation, the medium was centrifuged to separate immobilized and un-immobilized cells. The immobilized support was shaken with phosphate buffer (50 mM, pH 7.5) for 10 min. It was then washed twice with phosphate buffer and dried for 24 h at room temperature. The immobilized cells on support was incubated with 0.1% glutaraldehyde solution for 1 h, followed by washing with phosphate buffer and subsequently dried at room temperature for 24 h. The preliminary check for confirming immobilization was done by Bradford assay. The immobilized system was sonicated to release all the cell proteins. Bradford assay was carried out on this extract to determine the presence of protein. A positive test confirmed the presence of proteins, which were released from the cells

immobilized on the surface of the support.

3.2.6 Initial media selection for immobilized cells

As revealed by our studies with fermentation medium, the macro and micronutrient requirements of immobilized cells vary from that of free cells. Therefore, a different medium has to be selected for initial fermentation experiments with immobilized cells. Based on the literature reviews, following four different media were tested for fermentation with immobilized cells: (A) un-buffered + selected nutrients, (B) buffered + all nutrients, (C) un-buffered + all nutrients, (D) buffered + selected nutrients. Selected nutrients (common component in all studies) were yeast extract, $(\text{NH}_4)_2\text{SO}_4$, $\text{MgSO}_4 \cdot 7\text{H}_2\text{O}$, $\text{CaCl}_2 \cdot 2\text{H}_2\text{O}$, $\text{FeSO}_4 \cdot 7\text{H}_2\text{O}$. Buffered medium contained 50 mM phosphate buffer (pH 6.8). KH_2PO_4 and K_2HPO_4 were not added separately in buffered medium. Other nutrients apart from selected nutrients were $\text{CoCl}_2 \cdot 2\text{H}_2\text{O}$, PABA, NaCl and biotin. 25 g/L glycerol as a carbon source and cells immobilized on silica gel (2% w/v) were added in all four media studied.

3.2.7 Shake flask experiments for support selection

All batch fermentations were carried out in 250 mL custom fabricated anaerobic Erlenmeyer flasks containing 100 mL selected medium. The concentration of crude glycerol was varied as 5, 10, 25, 30 and 150 g/L in experiments with Amberlite as a support. The glycerol concentrations used for other two supports was restricted to only 5, 10 and 25 g/L, in view of the inhibitory effect of glycerol as indicated by our results with Amberlite. The assembly was kept at 30°C with shaking at 200 rpm. The samples were withdrawn at definite intervals for product analysis. Each experiment was carried out in triplicate so as to assess the reproducibility of results.

3.2.8 Preliminary optimization studies with silica gel as a support

The amount of support (with immobilized cells) required for optimum glycerol bioconversion was determined by studying five different quantities (in % w/v) of support

with cells immobilized on it, viz. 1, 2, 3, 5 and 10. In order to study the effect of cross-linking of cells by glutaraldehyde, immobilized but non cross-linked *C. pasteurianum* cells were added to the fermentation medium. 25 g/L glycerol was used in all set of experiments.

3.2.9 Enzymes extraction and kinetics

The enzymes butanol dehydrogenase, ethanol dehydrogenase and 1,3-PDO dehydrogenase were extracted from *C. pasteurianum* cells immobilized on silica gel. The protocol followed for this is as follows: The cells immobilized on silica support were centrifuged at 6000 rpm for 15 min. The immobilized cells were suspended in 50 mM phosphate buffer (pH 7.5) and sonicated in ice bath for 6 cycles (30 s on / 10 s off). The supernatant so obtained was separated from the support and cell lysate by centrifugation at 6000 rpm for 10 min. This supernatant was tested for determination of activities of all three dehydrogenases. The activity of dehydrogenases was tested with different concentrations of both pure and crude glycerol. The activity of 1,3-PDO dehydrogenase in the supernatant was determined by monitoring the increase in NADH concentration at 340 nm using a UV-Vis spectrophotometer (Make: Perkin Elmer, Model: Lambda 3). The assay mixture (1 mL final volume) for 1,3-PDO dehydrogenase had following constitution: glycerol (varying from 10 mM to 1 M), 2 mM NAD⁺, 30 mM ammonium sulfate and 10 mM potassium carbonate buffer (pH 9.7) (Malaoui and Marczak, 2000). Similar to 1,3-PDO dehydrogenase activity determination, the activity of ethanol dehydrogenase was also calculated by monitoring the absorbance at 340 nm, indicative of conversion of NAD⁺ to NADH. The assay was carried out according to the protocol given by Kato et al. (1984). The assay mixture consisted of 10 mM NAD⁺, glycerol (varying from 10 mM to 1 M) and 10 mM glycine-NaOH buffer (pH 9.0). For determination of activity of butanol dehydrogenase, the following assay system was used: glycerol (varying from 10 mM to 1 M), 0.23 mM NADPH, and 77 mM Tris-HCl (pH 7.8) (Dürre et al., 1987). The final volume of assay mixture was 0.86 ml. The change in

absorbance was monitored at 365 nm.

3.2.10 Analytical methods

The immobilization of cells on supports was confirmed by Scanning Electron Microscope (LEO, UK). The optical density of the cells was measured at 620 nm with a spectrophotometer (Thermo Fischer) after appropriate dilution in water. The fermentation products and their quantities were determined using Gas Chromatograph (Varian, CP 3800) with help of standard calibration plots. 1 μ L of supernatant from centrifuged fermentation broth was injected in a CP Wax 52 CB capillary column (250 mm \times 0.25 mm \times 0.39 mm, Varian). The oven temperature was programmed from 45 to 100°C with an increment of 3°C/min and after 100°C, an increment of 5°C/min upto 200°C. The injector and detector temperatures were 230 and 250°C, respectively. Nitrogen gas was used as a carrier at a flow rate of 2 mL/min.

3.3 RESULTS

3.3.1 Comparison of growth of cells on CMM and RCM and immobilization on supports

C. pasteurianum cells were found to grow equally well on both CMM and RCM. As depicted in Fig. 3.1A, the growth of cells on CMM showed an extended lag phase of 15–20 h, followed by a longer exponential growth phase of 30 h. The cells finally attained stationary phase after 50 h. Growth on RCM showed a much shorter lag phase of 5–10 h (Fig. 3.1B), log phase of 15 h and attainment of stationary phase after 25–30 h. The comparison of suitability of CMM and RCM for growth of *C. pasteurianum* showed that the growth cycle of the cell was comparatively shorter in RCM with a shorter lag phase, while growth in CMM exhibited longer lag as well as log phase. Thus, RCM was used in further experiments as a growth medium due to shorter lag phase, while CMM was used as a maintenance medium.

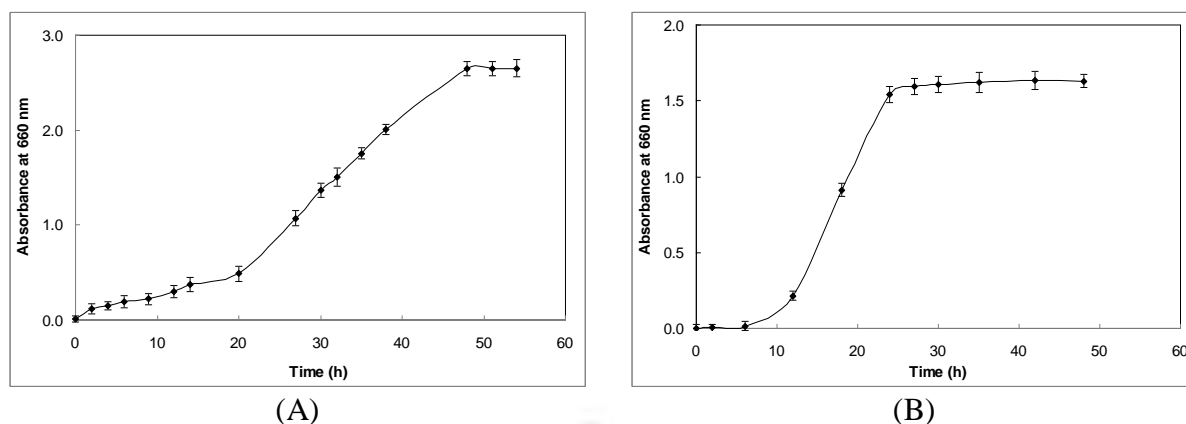


Figure 3.1 Growth curve of *C. pasteurianum* on (A) CMM and (B) RCM

Fig. 3.2A, C, and E depict the SEM image of the three supports prior to immobilization while, Fig. 3.2B, D, and F are the SEM images of cells immobilized on supports. The SEM micrographs revealed that the cells were properly adsorbed on the surface of supports and thus, confirm their immobilization.

3.3.2 Study of morphology of *C. pasteurianum* cells

SSC-H is a measure of cell surface topology i.e. when cell is under stress condition, its surface becomes rough and SSC-H increases. FSC parameter indicates the size of the cell i.e. greater the FSC, more will be the cell size. As per results shown in Fig. 3.3, we did not find any significant change in FSC and SSC of control cells and cells growing in presence of pure and crude glycerol. This is indicated by the presence of majority of cells in the lower left quadrant in control cells (91.8%), cells growing in presence of pure glycerol (88.21%) and crude glycerol (87.96%). Also, histogram plots showed similar pattern in all the three samples as M1 in all the cases is almost same (75.17%, 74.27% and 72.44% for control, pure and crude glycerol, respectively). Therefore, there is no morphological change in *C. pasteurianum* cells in presence of either type of glycerol.

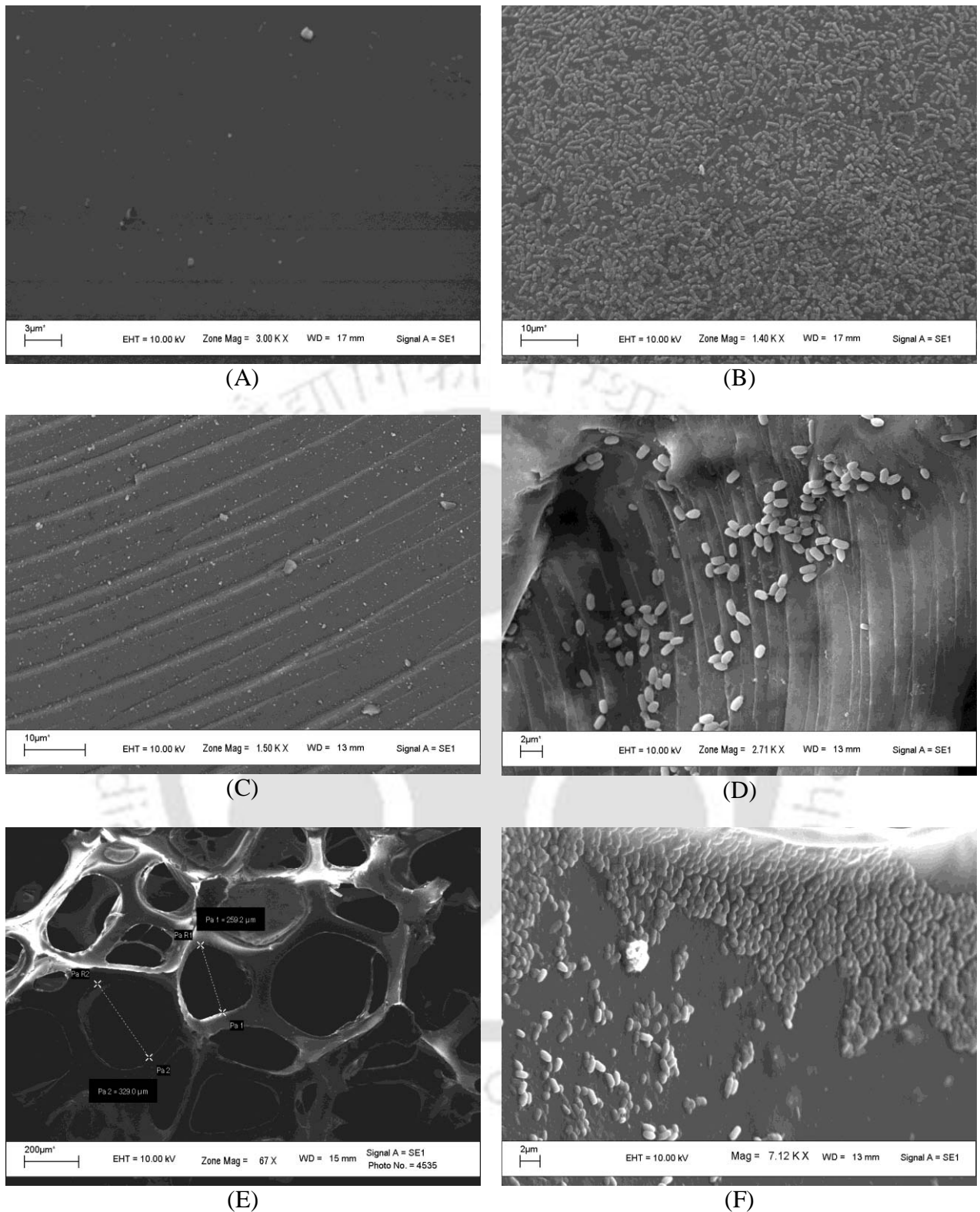


Figure 3.2 SEM image of (A) Amberlite without cells, (B) *C. pasteurianum* cells immobilized on Amberlite and cross-linked by glutaraldehyde, (C) silica gel without cells, (D) glutaraldehyde treated cells immobilized on silica gel, (E) reticulated polyurethane foam without cells, (F) *C. pasteurianum* cells immobilized and cross-linked on PU foam

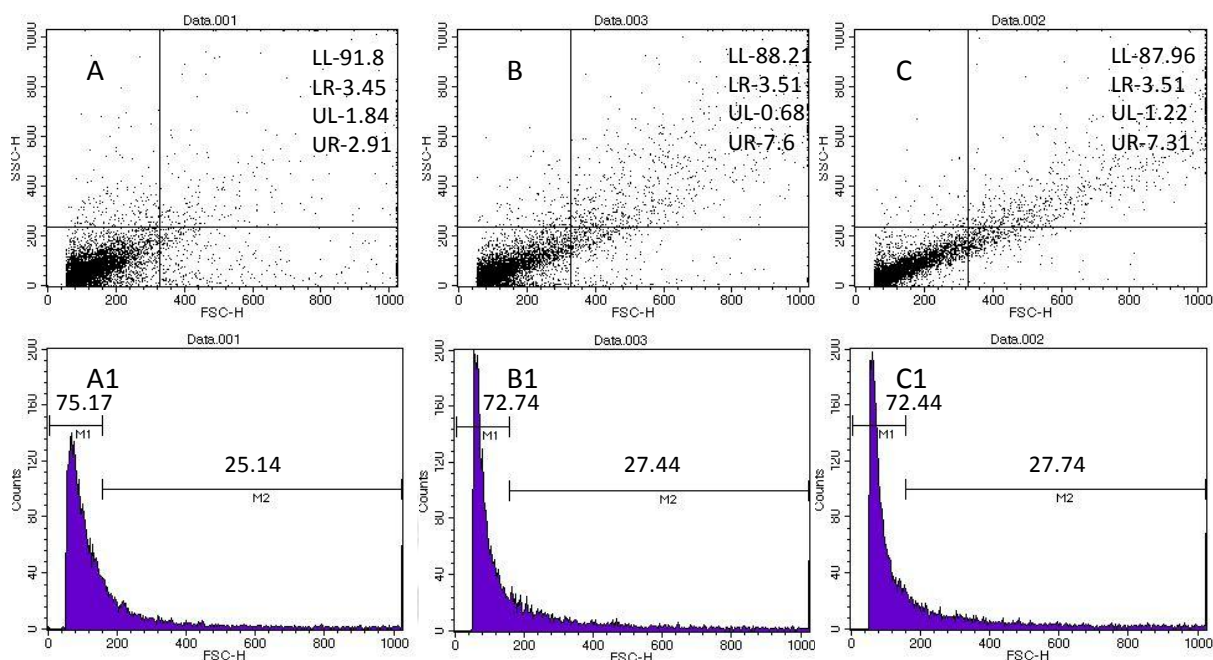


Figure 3.3 Flow Cytometric analysis for estimation of morphological changes of *C. pasteurianum*. Acquisition dot plots (FSC vs SSC) of *C. pasteurianum* cells in (A) control, (B) pure glycerol and (C) crude glycerol. (A1), (B1), and (C1) Histogram plots (Counts vs FSC) of *C. pasteurianum* in control, pure glycerol and crude glycerol, respectively. As there is no significant change in FSC and M2 in absence and in presence of both pure and crude glycerol therefore, morphology of cells remains same

Thus, alkali, unconverted alcohol and soap present in crude glycerol may have an inhibitory effect on product formation but they do not have any adverse effect on cellular morphology of *C. pasteurianum*.

3.3.3 Batch fermentation by free cells

Pure and crude glycerol fermentation was carried out by free cells of *C. pasteurianum*. Figs. 3.4A, C, and E depict the trends in production of the three fermentation products with pure glycerol as a substrate while, Figs. 3.4B, D, and F give the production profiles of the products with crude glycerol as a substrate. 5 g/L pure and crude glycerol as substrate gave highest butanol yield (0.31 and 0.21 g/g respectively). 10 g/L pure and crude glycerol was particularly inhibitory for butanol production by *C. pasteurianum* cells.

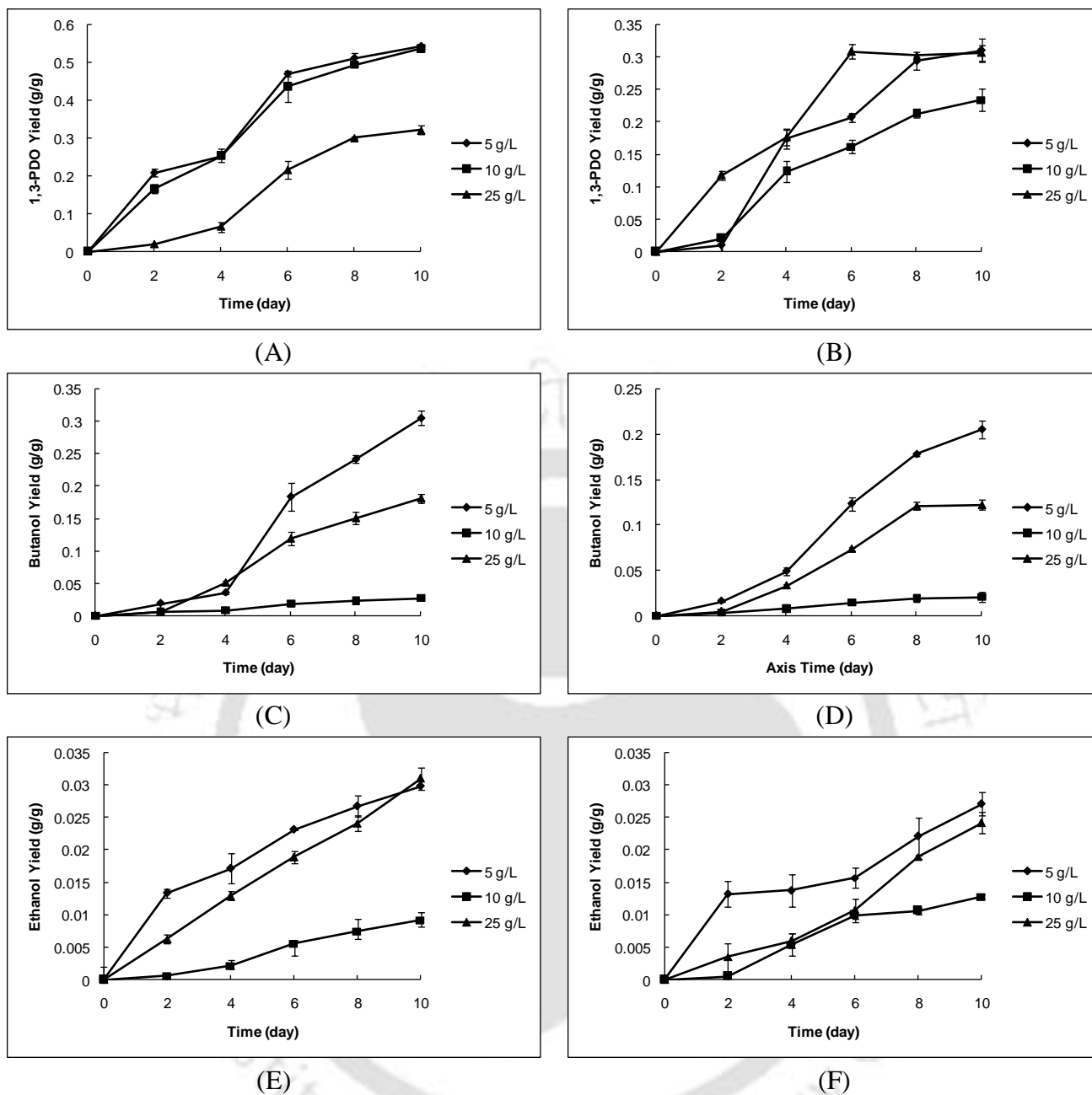


Figure 3.4 Trends in production of (A) 1,3-PDO with pure glycerol, (B) 1,3-PDO with crude glycerol, (C) butanol with pure glycerol, (D) butanol with crude glycerol, (E) ethanol with pure glycerol, and (F) ethanol with crude glycerol by free cells of *C. pasteurianum*

At all pure glycerol concentrations studied, 1,3-PDO was the major product. Maximum 1,3-PDO yield (0.54 g/g) was obtained with both 5 and 10 g/L pure glycerol. Further increase in pure glycerol concentration led to a decrease in 1,3-PDO production

probably due to substrate inhibition. Similarly with crude glycerol concentrations of 5 and 25 g/L highest yield of 1,3-PDO (0.31 g/g) was obtained. At all concentrations of pure and crude glycerol studied, only traces of ethanol were detected. The total yield of products decreased linearly with an increase in pure glycerol concentration and was highest at 5 g/L pure and crude glycerol. This may be attributed to the inhibition caused by increasing glycerol concentration. Comparing the results obtained with pure and crude glycerol, it can be perceived that total products yield was lower with crude glycerol than with pure glycerol at all glycerol concentrations studied. The same is true for individual products yields as well. This trend in results explains the inhibition caused due to the presence of unreacted methanol and alkali in crude glycerol.

3.3.4 Initial medium selection for glycerol fermentation by immobilized cells

Out of four different media compositions tested for glycerol fermentation by immobilized *C. pasteurianum* cells, highest total alcohols concentration of 9.5 g/L was observed in medium A, i.e. un-buffered medium containing selected nutrients (Fig. 3.5). The composition of medium A was 1 g/L yeast extract, 0.01 g/L $\text{CaCl}_2 \cdot 2\text{H}_2\text{O}$, 0.003 g/L $\text{FeSO}_4 \cdot 7\text{H}_2\text{O}$, 0.1 g/L $\text{MgSO}_4 \cdot 7\text{H}_2\text{O}$, 0.5 g/L KH_2PO_4 and 0.5 g/L K_2HPO_4 . Previous studies with free cells were conducted in fermentation medium with fixed pH (Heyndrickx et al., 1991; Biebl, 2001; Taconi et al., 2009). Thus, buffered media was tried in the present study. The buffered medium did not perform as expected, as buffering of the medium hindered the normal acidogenic shift of *C. pasteurianum* cells, which in turn is responsible for solvents production. The un-buffered medium allowed the immobilized cells to undergo normal growth cycle of acidogenesis followed by solventogenesis. Thus, medium A was used for all further studies with immobilized cells in this chapter.

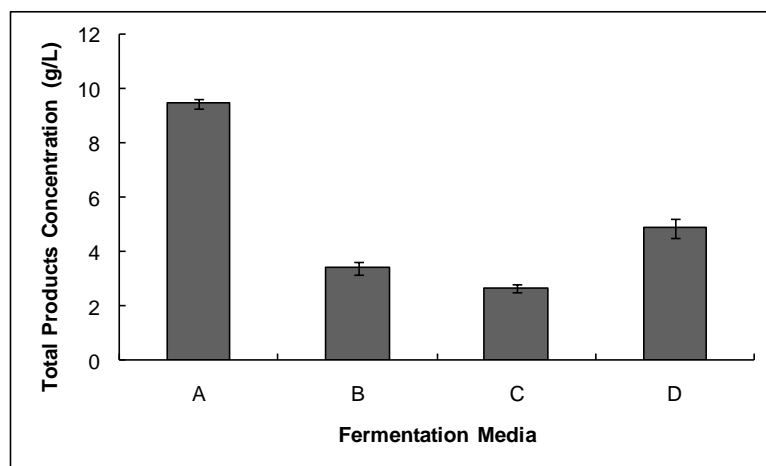
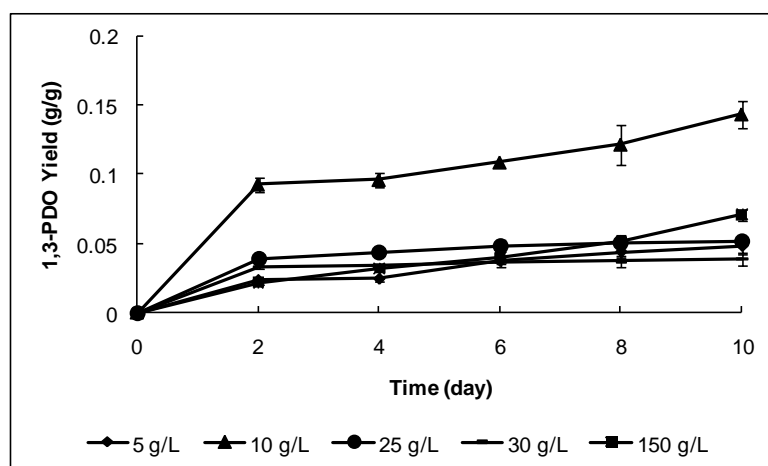


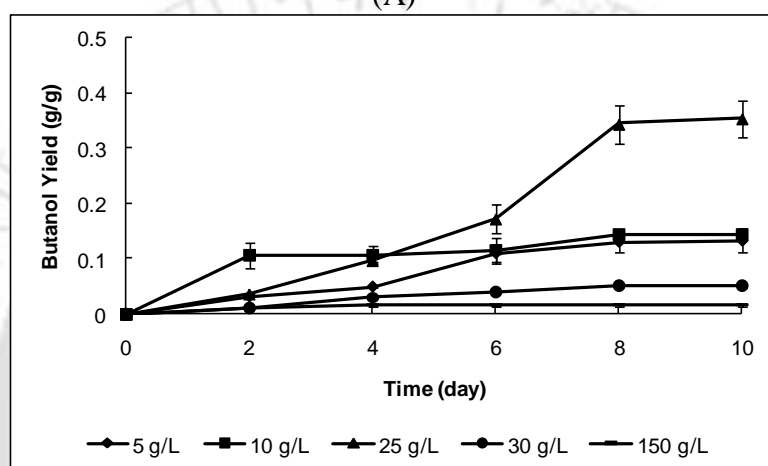
Figure 3.5 Plot of total products concentration vs different fermentation media. Medium A performed the best and thus, was used for all preliminary immobilization experiments

3.3.5 Glycerol fermentation by immobilized cells on Amberlite

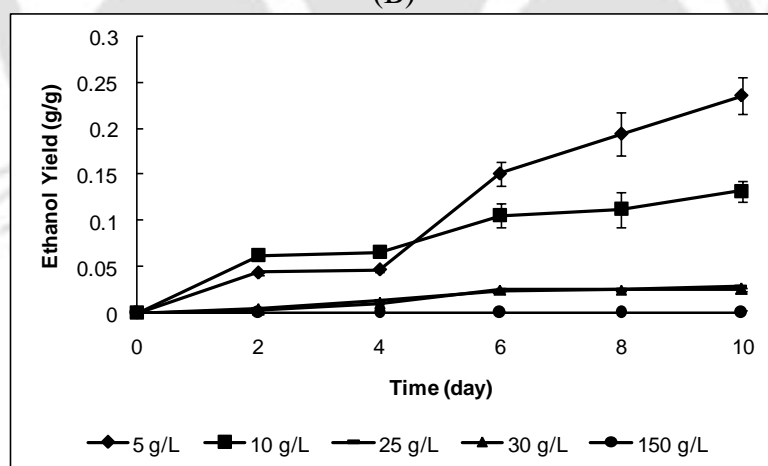
As already known, *C. pasteurianum* cells undergo acidogenesis during the lag phase of the growth cycle, while solventogenesis occurs during the log phase. The immobilization of cells after the end of lag phase prevented the accumulation of acids in the broth, and hence, simplified the analysis of the products. The use of immobilized cells also decreased the fermentation time, as the usual process with free cells takes almost 15–20 days to achieve maximum product yield (Taconi et al., 2009). The immobilized cells also took very less time to adjust to the high concentrations of crude glycerol. As shown in Fig. 3.6B, the batch fermentation of 5 g/L crude glycerol yielded 0.13 g of butanol/ g glycerol. The maximum amount of butanol formed increased further to 0.14 g/g with 10 g/L glycerol, and then reached a maximum amount of 0.35 g/g in presence of 25 g/L crude glycerol. Hence, the concentration of n-butanol was found to increase with increasing substrate concentration, and maximum concentration of n-butanol (8.84 g/L broth) was formed with 25 g/L substrate. Further increase in substrate concentration to 30 g/L unexpectedly produced very low amount of n-butanol (0.05 g/g), as compared to 25 g/L crude glycerol.



(A)



(B)



(C)

Figure 3.6 Trends in (A) 1,3-PDO yield with varying concentration of glycerol at definite time intervals. The optimum substrate concentration for maximal 1,3-PDO production was 10 g/L, (B) butanol yield with varying concentration of glycerol at definite time intervals. 25 g/L crude glycerol concentration yielded maximum n-butanol, (C) ethanol yield with varying concentration of glycerol at definite time intervals. 5 g/L crude glycerol gave highest ethanol yield while no ethanol was observed with 150 g/L substrate concentration

At 150 g/L substrate concentration, only traces of n-butanol were formed. This result was expected, as it is already known that very high glycerol concentration inhibits cell growth as well as butanol production. The maximum amount of 1,3-propanediol (0.14 g/g glycerol) was observed in presence of 10 g/L crude glycerol (Fig. 3.6A). As the concentration of substrate was increased from 10 to 25 g/L and further 30 g/L, 1,3-propanediol yield decreased to 0.05 and 0.04 g/g glycerol added. An interesting result was obtained with 10 g/L crude glycerol concentration for which 1,3-propanediol and n-butanol yield was found to be almost equal, with slightly lower ethanol yield. The concentration of n-butanol increased from 0.92 g/L (after 2 days) to 8.84 g/L broth at the end of fermentation. Similarly, 1,3-propanediol concentration increased from 0.93 g/L broth after 48 h to 1.44 g/L.

As depicted in Fig. 3.7C, maximum amount of ethanol was formed with 5 g/L crude glycerol with a maximum yield of 0.235 g/g glycerol added. The results for ethanol production showed that as the substrate concentration increased, there was a decrease in the production of ethanol, with more of glycerol getting channeled towards PDO production. As was the case with all substrate concentrations considered, the product formation was found to increase with time. Considering n-butanol, 1,3-propanediol and ethanol as only products formed, and ignoring any gaseous products or traces of acids formed, the maximum percentage conversion of glycerol was observed for 25 g/L crude glycerol. The percentage conversion of glycerol increased with an increase in glycerol concentration from 5 to 25 g/L, after which there was a sharp decrease at 30 g/L glycerol concentration.

An important point to note here is that percentage conversion is almost similar for 5 and 10 g/L crude glycerol concentration, with only a minor increase with 25 g/L substrate, but the yield of different products varied with substrate concentration. As we moved from 5 to 10 g/L glycerol, the yield of n-butanol varied slightly, but the yield of 1,3-propanediol increased significantly at the expense of ethanol leading to a decrease in ethanol yield in this

case. In case of 25 g/L crude glycerol as a substrate, yield of ethanol further decreased with concomitant increase in the production of n-butanol. These trends justify the phenomenon of substrate channeling, whereby at different concentrations, the substrate is channeled in different metabolic pathway that results in varied concentration of different products.

3.3.6 Glycerol fermentation by cells immobilized on silica gel

Experiments with pure glycerol: The results of previous section using Amberlite as an immobilization support revealed that crude glycerol concentrations beyond 25 g/L were inhibitory for solvents production by immobilized *C. pasteurianum* cells. Thus, all further immobilization studies were carried out with substrate concentrations limited to 25 g/L. As shown in Fig. 3.7, highest yield of butanol (0.36 g/g) was obtained with 25 g/L substrate. As was observed with free cells fermentation, the kinetics of butanol as well as ethanol production for 10 g/L glycerol concentration was quite slow, which can be perceived from the result that no butanol was detected in the broth even after 2 days of fermentation. Similarly, the yield of 1,3-PDO was the highest (0.54 g/g) for 10 g/L pure glycerol, which decreased further with an increase in substrate concentration. Thus, at 10 g/L pure glycerol concentration, the production of butanol followed an inverse variation with 1,3-PDO production, wherein less butanol and more 1,3-PDO was formed. This trend may be attributed to substrate mediated changes in cellular enzymatic activities for butanol and 1,3-PDO production. The highest ethanol yield (0.11 g/g) was observed with 10 g/L pure glycerol. Only traces of ethanol were observed at other two concentrations of pure glycerol studied. The yield of all three products increased with time for all concentrations of pure glycerol studied.

Experiments with crude glycerol: Butanol yield was maximum (0.23 g/g) with 25 g/L crude glycerol as a substrate (Fig. 3.7). Similar to pure glycerol, 10 g/L crude glycerol was also inhibitory to the cells for butanol production, as it yielded only 0.02 g butanol/g glycerol.

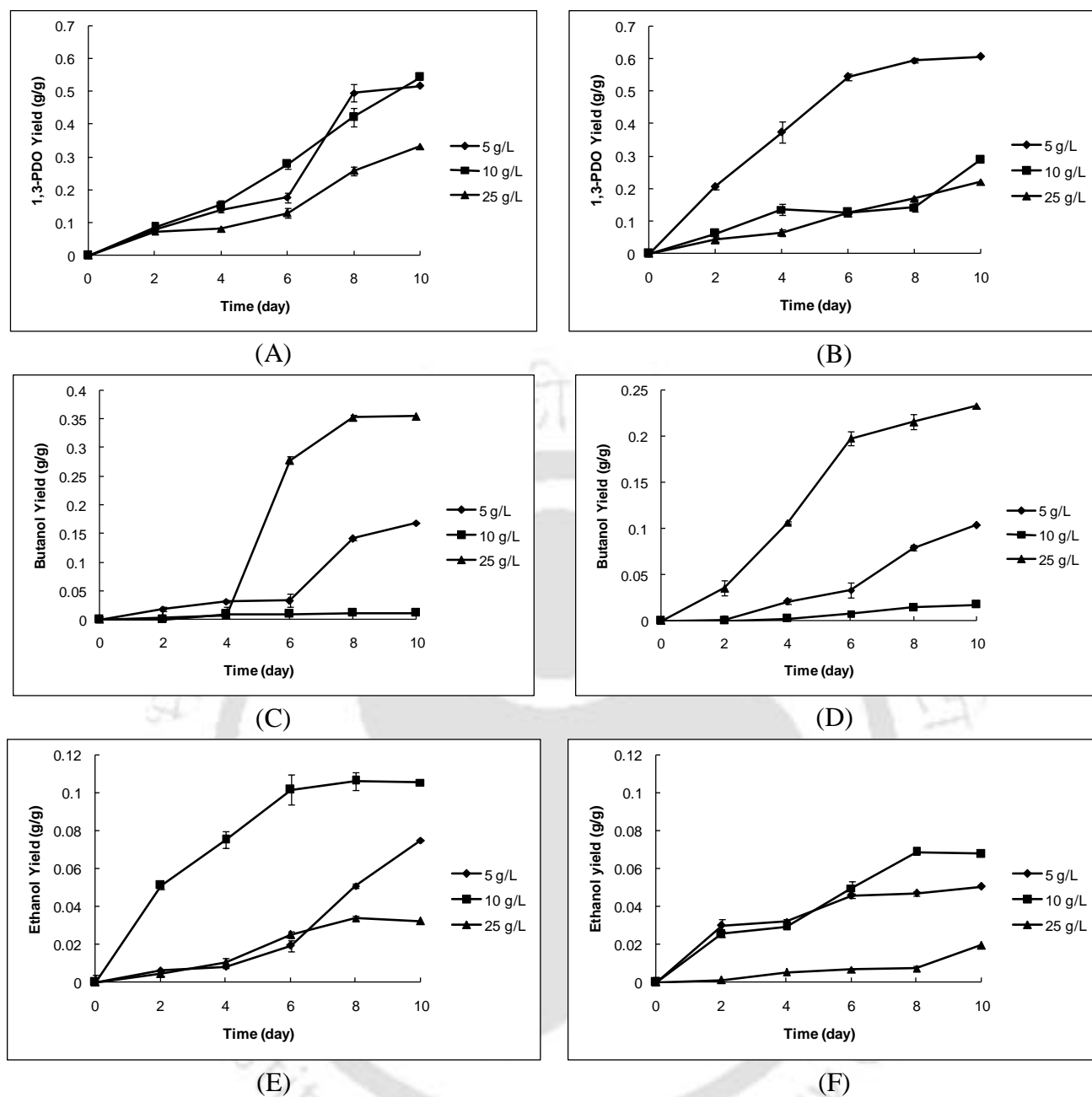


Figure 3.7 Trends in production of: (A) 1,3-PDO from pure glycerol, (B) 1,3-PDO from crude glycerol, (C) butanol from pure glycerol, (D) butanol from crude glycerol, (E) ethanol from pure glycerol, and (F) ethanol from crude glycerol

Similar trend in butanol production by free cells of *C. pasteurianum* were also observed by Taconi et al. (2009). 5 g/L crude glycerol gave lower yield (0.1 g/g) of butanol than 25 g/L substrate. An interesting result of this study is that, yield of 1,3-PDO decreases

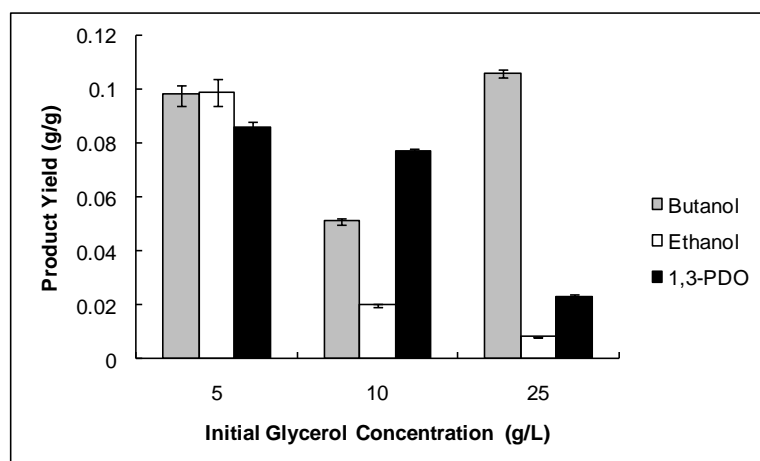
with increase in glycerol (both pure and crude) concentration. This is because, glycerol plays a key role in regulating the concentration of 1,3-PDO inhibitor, 3-hydroxypropionaldehyde (3-HPA) in the media. The production of 1,3-PDO proceeds by dehydration of glycerol to 3-Hydropropionaldehyde (3-HPA), which further undergoes reduction to form 1,3-PDO. Glycerol concentration lesser than 7–8 g/L in the medium, limits the concentration of 3-HPA, and thereby enhances the productivity of 1,3-PDO. Thus, lower glycerol concentrations favored higher production of 1,3-PDO. The presence of crude glycerol formed more of 1,3-PDO than rest of the two products. This result indicates that impurities present in biodiesel derived crude glycerol such as methanol, soaps and unconverted fatty acids do not adversely affect the metabolic pathway of 1,3-PDO for low glycerol concentration. Crude glycerol as a substrate yielded only traces of ethanol.

3.3.7 Glycerol fermentation by cells immobilized on reticulated polyurethane foam

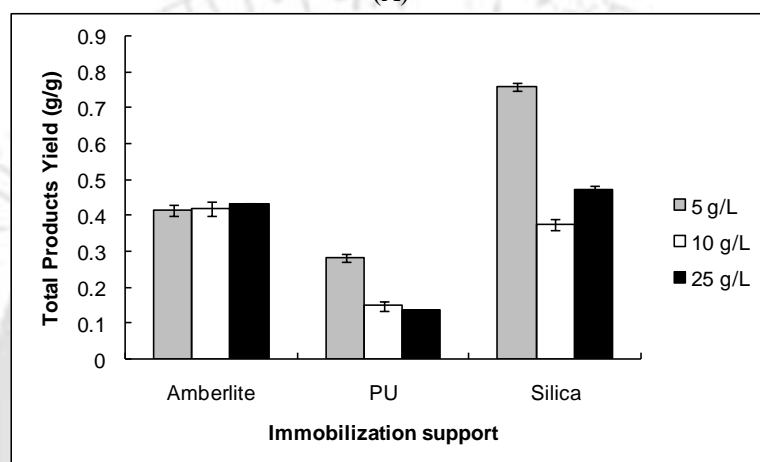
As shown in Fig. 3.8A, ethanol and 1,3-PDO yield decreased with an increase in glycerol concentration. Thus, the highest yield of both these products was obtained at the lowest glycerol concentration (5 g/L). 25 g/L crude glycerol gave a slightly higher yield of butanol than 5 g/L substrate. As was observed with Amberlite as a support, 10 g/L substrate formed 1,3-PDO as the major product. The yields of all three products were quite low. This may be attributed to the mass transfer resistance (due to diffusional limitation) rendered due to highly porous structure of polyurethane foam, which hinders transport of substrate as well as the products.

3.3.8 Comparison of immobilization supports

Among the three supports considered for immobilization of *C. pasteurianum*, silica gel was the best support at all crude glycerol concentrations studied (Fig. 3.8B). Total products yield was the lowest with polyurethane foam (with hydrophobic character) as a support, probably due to the mass transfer and diffusion limitation attributed to its porous structure.



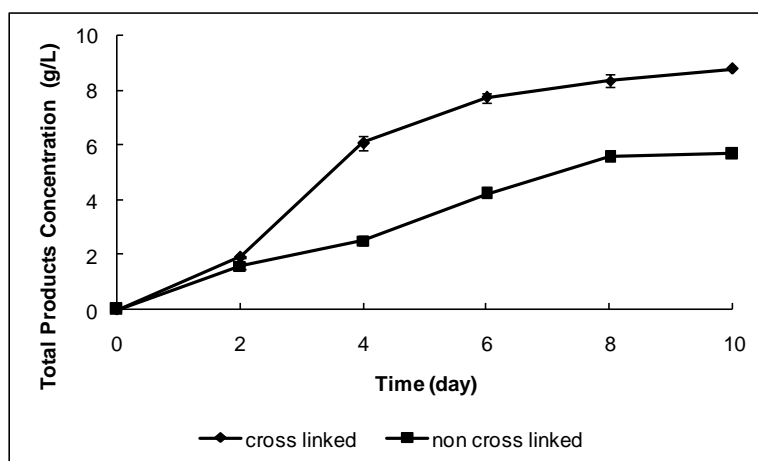
(A)



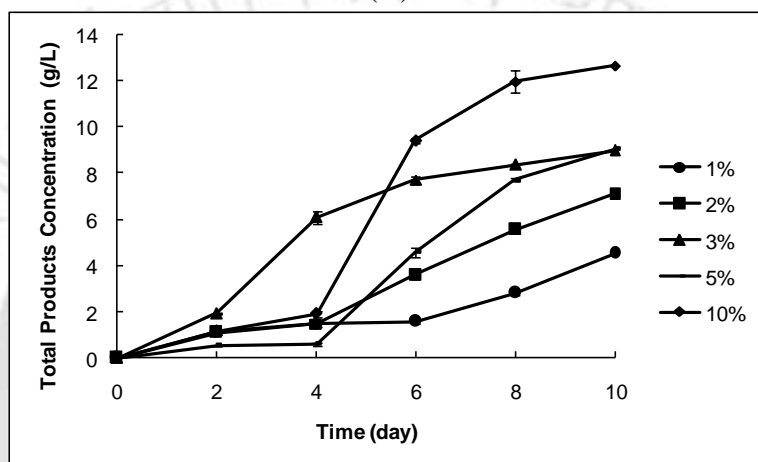
(B)

Figure 3.8 (A) Trends in production of the three fermentation products by *C. pasteurianum* cells immobilized on reticulated polyurethane foam at different concentrations of crude glycerol. (B) Comparison of three immobilization supports in terms of total yield of products at varied crude glycerol concentrations. Silica gel was found to be the most suitable support for *C. pasteurianum* immobilization and was chosen for all further studies

The same effect also led to a constant decrease in products yields with an increase in substrate concentration. The yield of fermentation products with Amberlite was either lower or comparable to silica. The net surface charge on Amberlite may have an adverse effect on activity of enzymes involved in glycerol metabolism, leading to lower yield of products. Also, high cost of Amberlite prohibits its use in industrial scale application. On the basis of these results, silica gel was the choice of immobilization support for the further steps of process development.



(A)



(B)

Figure 3.9 (A) Comparison of glutaraldehyde treated and untreated cells for production of total solvent, (B) Effect of variation of amount of support with immobilized cells on formation of products

3.3.9 Preliminary optimization studies with silica gel as an immobilization support

Effect of glutaraldehyde cross linking of cells and amount of cell immobilized

support: A comparison of total products concentration with both non cross-linked and cross-linked cells is shown in Fig. 3.9A. The total products concentration by glutaraldehyde cross-linked cells is higher than non cross-linked cells. This may be attributed to a higher number of cells on the surface of support due to glutaraldehyde treatment, as compared to untreated cells. The higher number of cells on glutaraldehyde treated support is probably due to the

retention of cells on the surface of support even after washing of the cells immobilized on support after immobilization. Although, total product yield became constant after 6 days of fermentation, but the individual products yield was found to vary even beyond 6 days, and became constant around 8–10 days. Thus, the individual product formation was studied for a period of 10 days. Fig. 3.9B depicts the effect of different amounts of support with immobilized cells on total solvents production. With all five concentrations (1, 2, 3, 5, 10% w/v) of cells– immobilized support considered, the total products concentration increased with an increase in the amount of immobilized biocatalyst. An increase in biocatalyst amount from 3 to 10% w/v (i.e. 3–fold increase) increased the total products concentration by less than 3 g/L. The total products concentration with 5% w/v biocatalyst was only slightly higher than 3% w/v catalyst. Thus, 3% w/v support with immobilized cells was the most suitable biocatalyst amount for formation of solvents.

3.3.10 Enzyme kinetics study

The kinetic parameters viz. V_{max} and K_m , for the 3 dehydrogenases, 1,3–PDO dehydrogenase, butanol dehydrogenase, and ethanol dehydrogenase, with both pure and crude glycerol as substrate, were determined using Lineweaver–Burk plots (Fig. 3.10). K_m for 1,3–PDO dehydrogenase, butanol dehydrogenase and ethanol dehydrogenase with pure glycerol as a substrate was calculated to be 73.83, 169.49 and 307.24 mM, respectively, while the same with crude glycerol was 28.87, 395.65 and 916.46 mM, respectively. The results revealed that except for 1,3–PDO dehydrogenase, K_m of other two dehydrogenases was higher with crude glycerol than with pure glycerol, which points towards the inhibitory nature of the substrate, crude glycerol. A decrease in K_m for 1,3–PDO dehydrogenase shows that the inhibition caused by methanol, alkali and unconverted fatty acids present in crude glycerol is less pronounced for 1,3–PDO dehydrogenase and more pronounced for other two dehydrogenases.

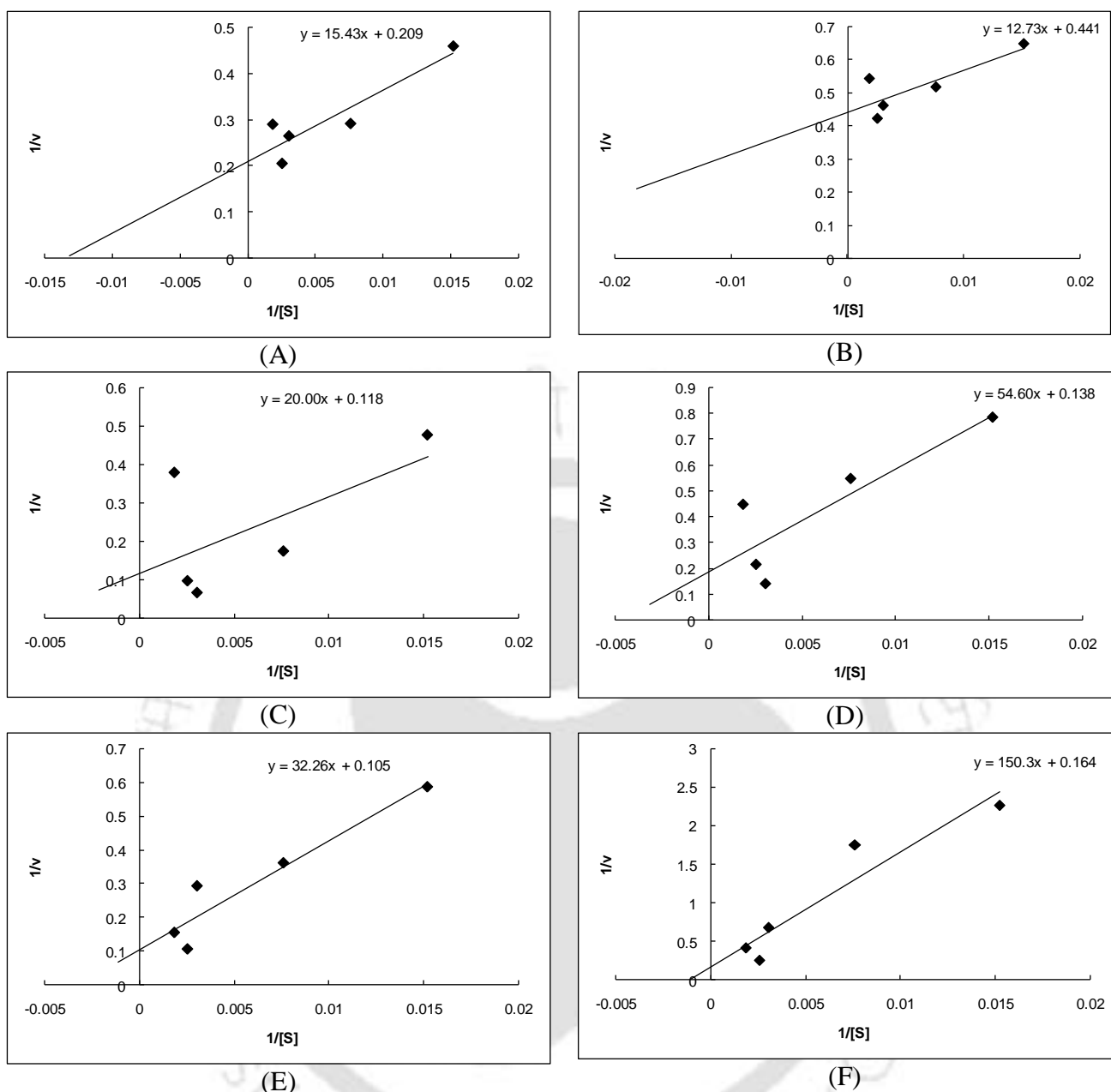


Figure 3.10 Lineweaver Burk plots. Pure glycerol as substrate for determination of kinetic parameters of: (A) 1,3-PDO dehydrogenase, (C) butanol dehydrogenase, (E) ethanol dehydrogenase. Crude glycerol as substrate for determination of kinetic parameters of: (B) 1,3-PDO dehydrogenase, (D) butanol dehydrogenase, and (F) ethanol dehydrogenase

V_{\max} of 1,3-PDO dehydrogenase, butanol dehydrogenase and ethanol dehydrogenase with pure glycerol as a substrate was calculated to be 3.32, 5.89 and 6.61 $\mu\text{M}/\text{min}$, respectively, while the same with crude glycerol was 1.58, 5.03 and 4.23 $\mu\text{M}/\text{min}$, respectively.

Table 3.1 Comparison of yields (mol/mol) of the three fermentation products formed by free and immobilized cells with pure glycerol as a substrate

Concentration (g/L)	Free Cells				Immobilized Cells			
	Butanol	1,3-PDO	Ethanol	Total	Butanol	1,3-PDO	Ethanol	Total
5	0.19	0.38	0.06	0.63	0.11	0.37	0.09	0.57
10	0.02	0.44	0.02	0.48	0.01	0.38	0.11	0.50
25	0.11	0.28	0.06	0.45	0.22	0.18	0.07	0.47

Table 3.2 Comparison of yields (mol/mol) of the three fermentation products formed by free and immobilized cells with crude glycerol as a substrate

Concentration (g/L)	Free Cell				Immobilized Cells			
	Butanol	1,3-PDO	Ethanol	Total	Butanol	1,3-PDO	Ethanol	Total
5	0.08	0.25	0.04	0.37	0.07	0.31	0.06	0.44
10	0.01	0.28	0.02	0.31	0.01	0.26	0.13	0.40
25	0.08	0.11	0.01	0.20	0.14	0.17	0.04	0.35

As can be seen from the values of V_{\max} , crude glycerol decreased V_{\max} of all three dehydrogenases. Thus, it may be inferred that crude glycerol manifests its inhibitory effect by increasing the K_m and decreasing V_{\max} of alcohol dehydrogenases.

3.3.11 Comparison of pure and crude glycerol as substrate for free and immobilized cells

Table 3.1 and 3.2 give a comparison of individual products yield with free and immobilized cells at different pure and crude glycerol concentrations. Highest concentration (25 g/L) of both pure and crude glycerol favored formation of butanol but, 25 g/L pure glycerol gave a higher butanol yield than the same concentration of crude glycerol studied. Similar trend was observed with other two products as well i.e. lower yield with crude glycerol than with pure glycerol. The presence of impurities such as methanol, salts and unconverted fatty acids present in biodiesel derived glycerol could be a possible cause leading to this effect. As far as total products yield is concerned, equal and the highest total

products yield was obtained with both 5 g/L pure and crude glycerol as a substrate. Comparing among pure and crude glycerol as substrates, the total products yield decreased with an increase in concentrations of substrates. Comparison of free and immobilized *C. pasteurianum* cells for glycerol bioconversion reveals that at high concentrations of pure glycerol immobilized cells performed better than free cells. At all crude glycerol concentrations studied immobilized cells gave a higher yield than free cells.

3.4 DISCUSSION

Previous researchers have addressed the matter of bioconversion of glycerol with different fermentation systems and *C. pasteurianum* cells obtained from different collection banks. A summary of the results of these studies is given in Table 3.3. Taconi et al. (2009) studied the solvent production efficiency of free cells of *C. pasteurianum* in presence of both pure and crude glycerol. This is the only published study with biodiesel derived crude glycerol using free cells of *C. pasteurianum*. In the study by Taconi et al. (2009), the free cells produced 0.36 g/g butanol when grown on pure glycerol, while growth on crude glycerol slightly decreased the yield to 0.30 g/g due to presence of impurities such as methanol, salts and soaps. The cells were reported to tolerate crude glycerol concentration as high as 25 g/L albeit with increase in the lag phase of the cells. The results of present study with free and immobilized *C. pasteurianum* differ from these results in several aspects as follows: 1. The time required for product formation (10 days) is same for both pure and crude glycerol, 2. The yield of 1,3-PDO is much higher with both pure and crude glycerol, 3. Except for 10 g/L, the total products yields with both free and immobilized cells are higher at other two crude glycerol concentrations.

Table 3.3 Comparison of the maximum yields of all the three products obtained in the current work with published literature on free cells of *C. pasteurianum*. All yields are in gram of product formed per gram substrate (g/g)

References	Pure Glycerol			Crude Glycerol		
	Ethanol	Butanol	1,3-PDO	Ethanol	Butanol	1,3-PDO
Heyndrickx et al. (1991)	0.01	0.098	0.33	–	–	–
Dabrock et al. (1992)	0.15	0.24	0.28	–	–	–
Biebl (2001)	0.13	0.31	0.22	–	–	–
Taconi et al. (2009)	0.36	0.36	0.41	0.23	0.30	0.28
Current work (free cells)	0.03	0.31	0.54	0.03	0.21	0.31
Current work (immobilized cells)	0.11	0.36	0.54	0.07	0.23	0.61

This comparison of results indicates that immobilized cells tolerated the inhibitory effects of crude glycerol better than the free cells. A comparative analysis of our results with some other studies is as follows: Heyndrickx et al. (1991) studied the fermentation of 10 g/L pure glycerol by free cells of *C. pasteurianum*. The batch study in absence of acetate formed 0.33 g/g 1,3-PDO as the major product. Similar trend is obtained in the present study as well. 10 g/L pure and crude glycerol as substrates formed 1,3-PDO as the major product of glycerol fermentation by both free and immobilized cells. Biebl (2001) studied the batch, chemostat and pH auxostat cultures of *C. pasteurianum* for solvent production. At pH 7.0, batch cultures formed almost equal amounts of butanol and 1,3-PDO. Our studies with batch cultures of free and immobilized cells formed 1,3-PDO as the major product, with butanol as the second major product. Dabrock et al. (1992) have mentioned that free cells of *C. pasteurianum* tolerated high glycerol concentrations of 17 g/L. In the current study, the immobilized cells formed high amounts of 1,3-PDO and n-butanol along with significant amounts of ethanol in presence of 25 g/L pure glycerol. Thus, immobilized cells can tolerate

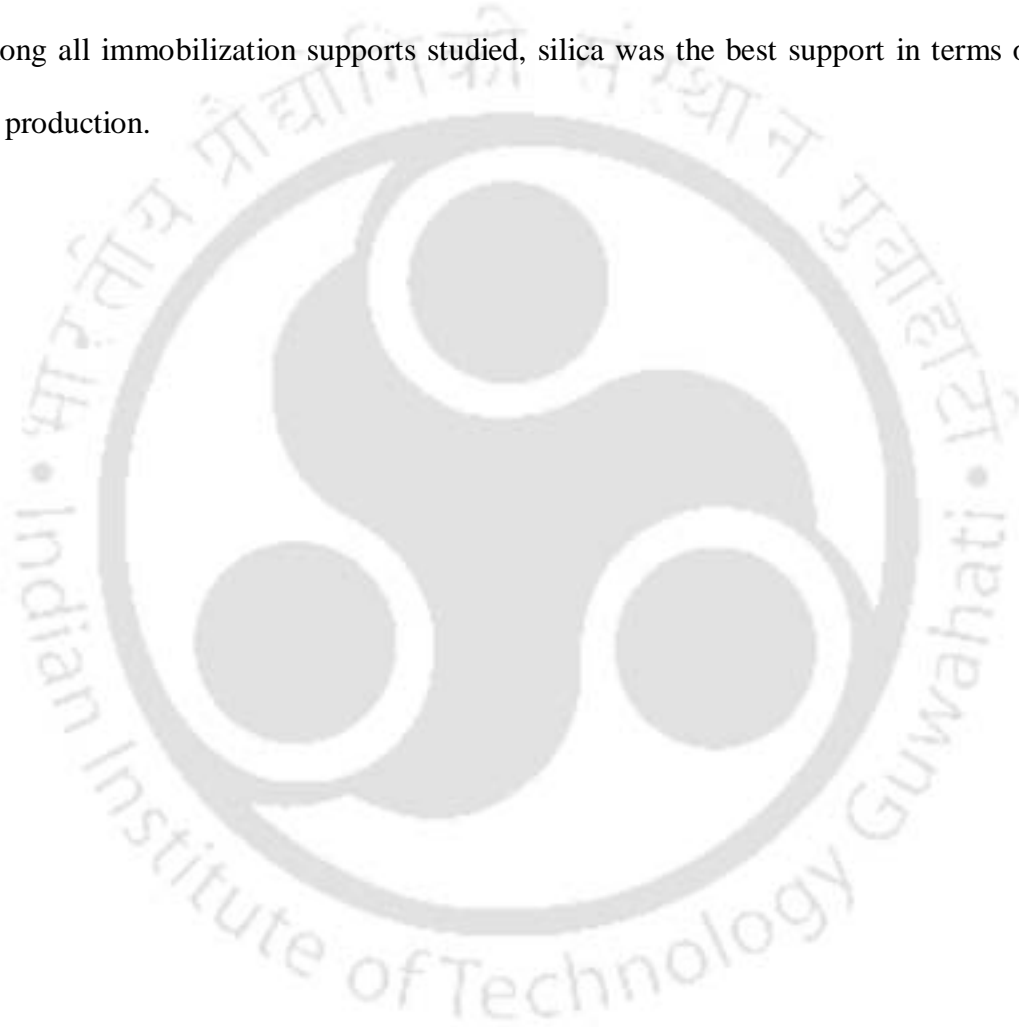
higher concentrations of substrate than free cells. Formation of high concentrations of 1,3-PDO in all set of experiments may also be attributed to the low levels of iron in the fermentation medium. It was proposed by Dabrock et al. (1992) that iron limitation inhibits the iron-dependant alcohol dehydrogenases involved in formation of ethanol and butanol. Zeng (1996) has suggested that under excess carbon source condition or under product inhibition, the cells tend to go for formation of 1,3-PDO, which is less inhibitory to the cells. Therefore, at high concentrations of both pure and crude glycerol, 1,3-PDO is the major fermentation product. We have observed that the variation of product profile with glycerol concentration and glycerol type is not tightly regulated, and only a slight variation of above factors changes the product profile considerably. Formation of 1,3-PDO is important, as it serves to regenerate NADH, a reducing equivalent required for formation of biomass. It could be perceived from the comparative analysis of results of previous studies with free cells and present study that immobilization of cells causes change in product distribution. It can also be seen that 1,3-PDO formation occurs from the beginning, while the formation of butanol starts after a lag of few hours.

3.5 CONCLUSIONS

This chapter reports our initial studies in development of process for bioconversion of glycerol to 1,3-propanediol and butanol. After selection of the microorganism for bioconversion, we have attempted to optimize the immobilization support for the microorganism, and study the bioconversion of both pure and crude glycerol with cells immobilize on these supports. The results of this study have revealed that immobilized *C. pasteurianum* cells are potent biocatalysts for production of value added products using both pure and crude glycerol as a substrate, and have distinct merits over free *C. pasteurianum*. Moreover, the results of this study have also highlighted interesting aspects of glycerol

assimilation by immobilized cells, which can be summarized as follows:

- (1) Sum of yield for all three products was higher at low substrate concentrations (5–10 g/L) due to substrate inhibition beyond 25 g/L substrate concentration.
- (2) The yield of the three products was found to be a function of substrate concentration and substrate type.
- (3) Immobilized cells showed high tolerance to glycerol inhibition.
- (4) Among all immobilization supports studied, silica was the best support in terms of total solvent production.



KINETICS STUDIES FOR GLYCEROL BIOCONVERSION

4.1 INTRODUCTION

In the previous chapter, we presented our studies on optimization of the immobilization support for cells of *Clostridium pasteurianum*, and also some initial optimization studies on bioconversion of glycerol using immobilized cells. In this chapter, we take ahead the task of process development by addressing the important issue of assessment of the kinetics of the glycerol bioconversion. Essentially, we have attempted to investigate the effect of variation of temperature on product profile of crude glycerol fermentation by immobilized *C. pasteurianum* cells. We have tried fitting first order rate equation for this immobilized system to obtain temperature specific rate constants. The rate constants so obtained were finally used for calculating the activation energy required for bioconversion of crude glycerol to butanol, 1,3-PDO and ethanol by immobilized cells.

4.2 MATERIALS AND METHODS

4.2.1 Materials

Clostridium pasteurianum MTCC 116 (ATCC 6013) was procured from Microbial Type Culture Collection, Chandigarh, India. 60–120 mesh size silica (column chromatography grade, Merck, Germany) was used as an immobilization support and was procured from Merck, Germany. Crude glycerol was generated in homogenous alkali catalysis of soybean oil with composition similar to that mentioned in Chapter 3. The anaerobic assembly for growth of *C. pasteurianum* on agar slants was procured from Himedia, India. The analytical standards for gas chromatographic (GC) and high performance liquid chromatographic (HPLC) analysis were procured from Sigma Aldrich, USA and Merck, Germany. All other chemicals used were of analytical grade (either from Merck, Germany or Himedia, India).

4.2.2 Immobilization of cells

The lyophilized cells were revived in Cooked Meat Media (CMM) and maintained on CMM agar slants under anaerobic condition. The cells were immobilized in Reinforced Clostridial Media (RCM) broth of following composition (g/L distilled water), beef extract (10), yeast extract (3), peptone (10), glucose (5), soluble starch (1), sodium chloride (5), sodium acetate (3), agar (0.5), cysteine hydrochloride (0.5). The initial pH of the media was adjusted to 6.8 ± 0.2 . The silica particles were dried at 120°C for 24 h in dry oven before use. The support was added to the media after approx. 24 h (at the end of lag phase of the culture). The support was kept for 72 h with the media at 30°C with shaking at 120 rpm. The broth was centrifuged and the support with immobilized cells was shaken with phosphate buffer (50 mM, pH 7.5) for 10 min. It was washed thoroughly with phosphate buffer (50 mM, pH 7.5) and dried for 24 h at room temperature. The cross linking of immobilized cells was done by incubating it with 0.1% glutaraldehyde solution for 1 h, followed by washing with phosphate

buffer (50 mM, pH 7.5), and drying at room temperature for 24 h.

4.2.3 Batch fermentation

Batch fermentation was carried out in 250 mL custom-built Erlenmeyer flasks containing 1 g/L yeast extract, 0.01 g/L $\text{CaCl}_2 \cdot 2\text{H}_2\text{O}$, 0.1 g/L $\text{MgSO}_4 \cdot 7\text{H}_2\text{O}$, 0.5 g/L KH_2PO_4 , 0.5 g/L K_2HPO_4 and 5 mg/L $\text{FeSO}_4 \cdot 7\text{H}_2\text{O}$ (pH = 6.8). Three different crude glycerol concentrations, 5, 10 and 25 g/L, were considered for the present study. Different concentrations of crude glycerol were added to each flask containing 3% w/v of immobilized support (optimized in previous chapter). Three fermentation temperatures, viz. 30, 37 and 45°C, were considered for the present study. The flasks were kept in an incubator shaker with shaking at 200 rpm. The flasks were sparged with nitrogen gas (99.98% pure) before incubation as well as after every 24 h to maintain anaerobic conditions. The samples of the fermentation broth were withdrawn after every 2 days upto a period of 10 days. All the batch fermentation experiments were carried out in triplicate, and the results presented are the mean of the three experimental runs.

4.2.4 Analysis and calculations

The fermentation products and their quantity were determined using Gas Chromatograph (Varian, CP 3800) using a CP Wax 52 CB capillary column (250 mm \times 0.25 mm \times 0.39 mm, Varian). The oven temperature was programmed from 45 to 100°C with an increment of 3°C/min and after 100°C, an increment of 5°C/min upto 200°C. The injector and detector temperatures were 230 and 250°C, respectively. Nitrogen gas was used as a carrier at a flow rate of 2 mL/min. The utilization of crude glycerol was determined by HPLC analysis using Hi-Plex-H column (8 μm \times 300 mm \times 7.7 mm, Varian) with 100% HPLC grade water as the mobile phase. The HPLC apparatus comprised of a pump (Series 200, Perkin Elmer) operated at a flow rate of 0.5 mL/min, a refractive index detector (Series 200, Perkin Elmer), a vacuum degasser (Series 200, Perkin Elmer). Standard calibration plots of substrate as well

as products were drawn for calculating their concentrations from GC and HPLC. The glycerol utilization results obtained with 25 g/L crude glycerol were fitted with first order rate equations to obtain rate constants (k) at three temperatures. These rate constants were then fitted to Arrhenius equation (plot of $\ln k$ vs $1/T$), from which the value of activation energy (E_a) for the bioconversion was calculated.

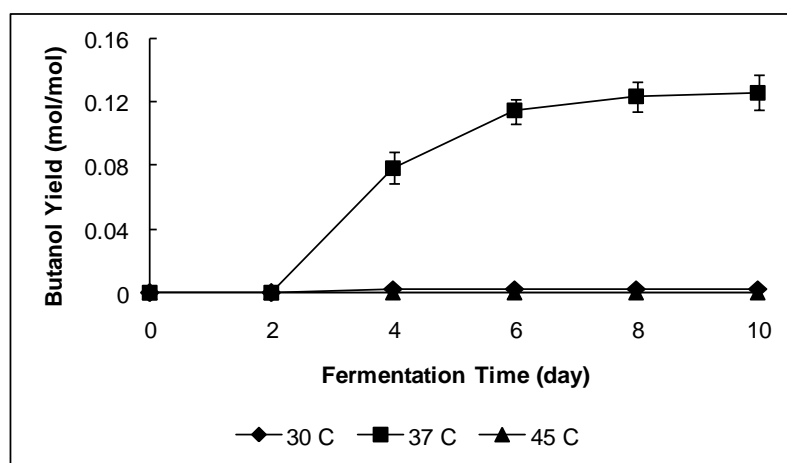
4.3 RESULTS

4.3.1 Trends in butanol production

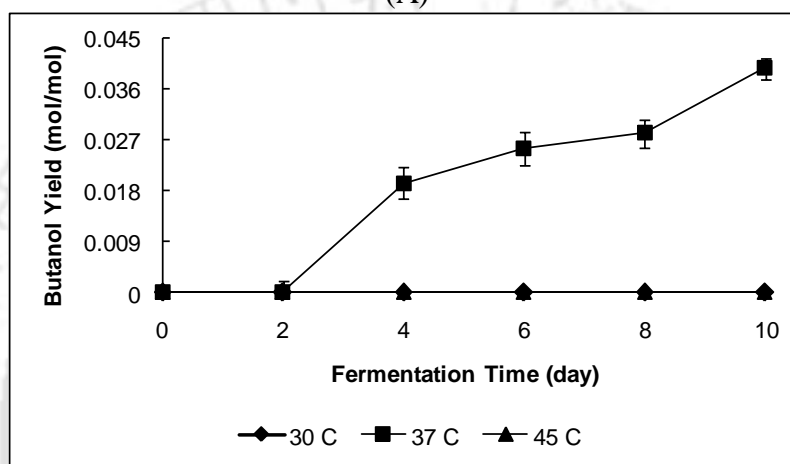
Maximum yield of butanol (0.28 mol/mol) was obtained with 25 g/L initial substrate concentration at 37°C (Fig. 4.1C). 5 g/L crude glycerol gave the next highest butanol yield of 0.13 mol/mol at 37°C. 10 g/L substrate concentration was particularly inhibitory for butanol production. Fermentation temperature of 30°C produced negligible amount of butanol from 25 g/L and 5 g/L substrate while, no butanol was detected with 10 g/L substrate at the same temperature (Fig. 4.1). Higher temperature of 45°C did not produce any butanol, with all three substrate concentrations studied, to be detected by gas chromatograph. Thus, 37°C is the most suitable fermentation temperature for production of butanol from crude glycerol by immobilized *C. pasteurianum* cells. For all three initial substrate concentrations considered, the yield of butanol was found to increase with time at both 30 and 37°C.

4.3.2 Trends in 1,3-propanediol production

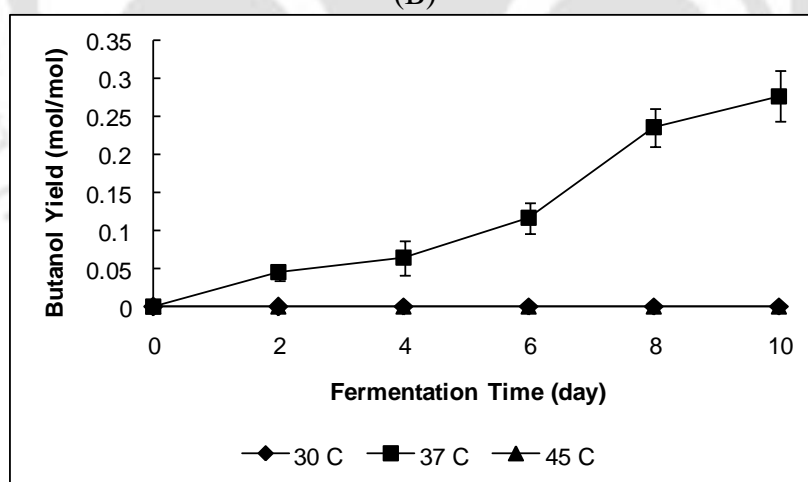
Fig. 4.2 depicts 1,3-PDO production profile for three different substrate concentrations at three temperatures. Maximum yield of 1,3-PDO (0.6 mol/mol) was obtained at 30°C with 10 g/L substrate. On further increasing the temperature to 37°C, 1,3-PDO yield decreased to 1/4th of that obtained at 30°C (0.15 mol/mol). An increase in substrate concentration from 10 g/L to 25 g/L led to a decrease in yield of 1,3-PDO at both 30 and 37°C.



(A)

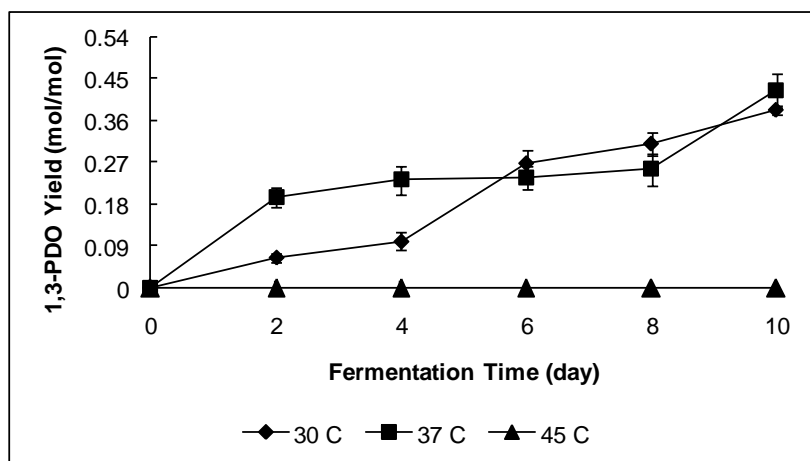


(B)

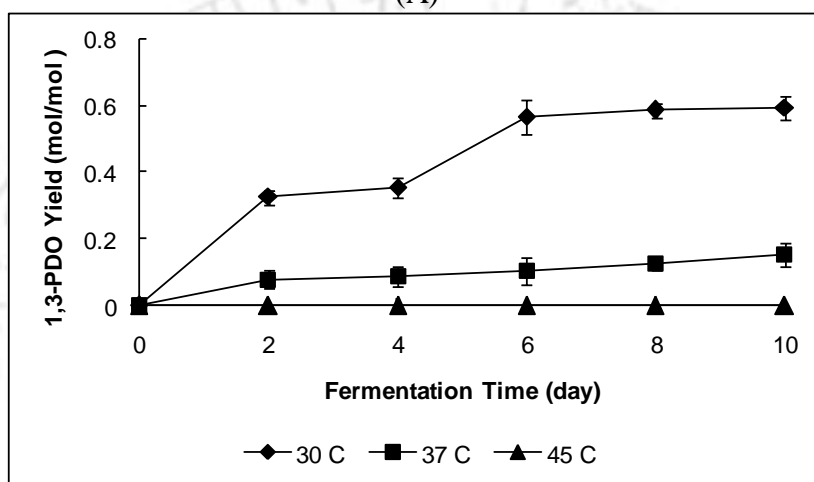


(C)

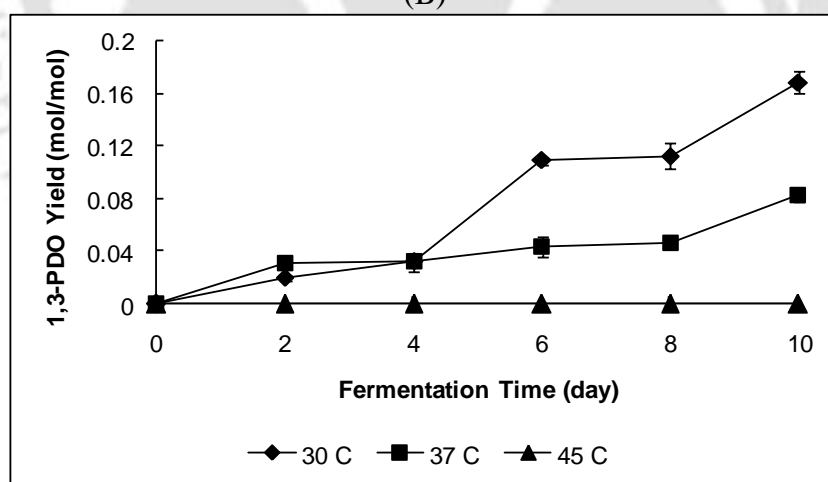
Figure 4.1 Trends in production of butanol with initial crude glycerol concentration of (A) 5 g/L, (B) 10 g/L, and (C) 25 g/L at varied temperatures. 10 g/L crude glycerol formed minimum amount of butanol at all temperatures as compared to other concentrations studied



(A)



(B)



(C)

Figure 4.2 Trends in production of 1,3-PDO with initial crude glycerol concentration of (A) 5 g/L, (B) 10 g/L, and (C) 25 g/L at three different fermentation temperatures

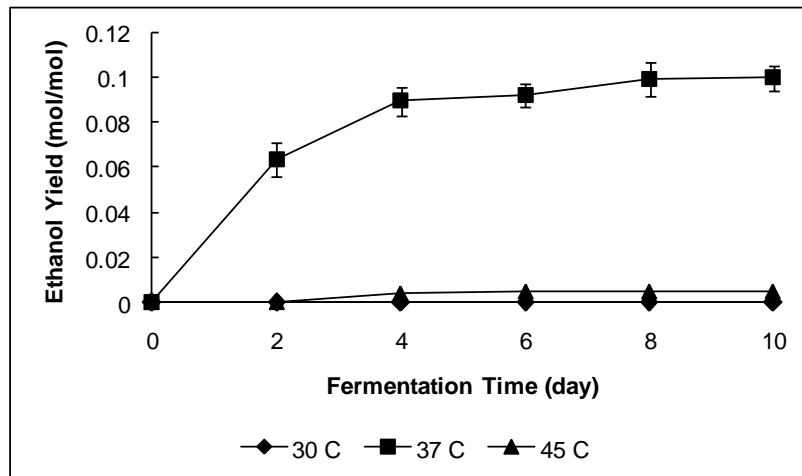
Both 10 and 25 g/L substrate yielded more product at the lowest fermentation temperature, except 5 g/L, which exhibited a higher production of 1,3-PDO at 37°C. No 1,3-PDO was detected at 45°C with all three substrate concentrations studied. As was observed in case of butanol production, the production of 1,3-PDO also increased with an increase in fermentation time.

4.3.3 Trends in ethanol production

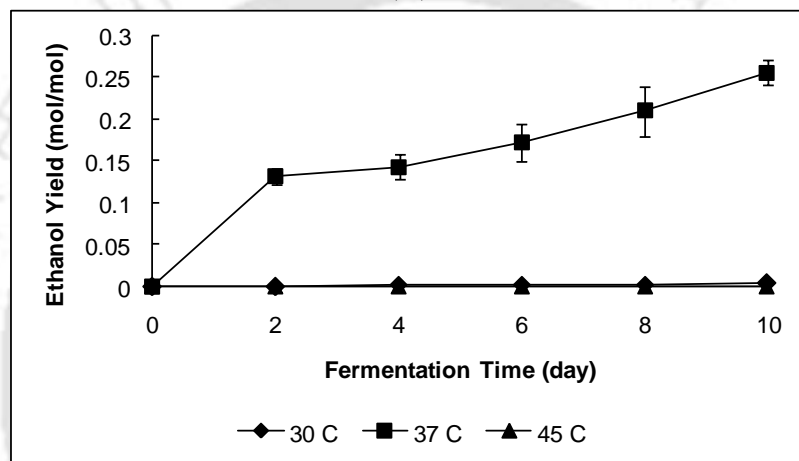
Fig. 4.3 depicts trends in ethanol production with change in temperature and initial substrate concentration. Maximum yield of ethanol (0.26 mol/mol) was obtained at 37°C with 10 g/L substrate. The next highest ethanol yield (0.10 mol/mol) was obtained at 37°C with 5 g/L crude glycerol. At 45°C, traces of ethanol were detected with 5 g/L substrate, but other two substrate concentrations did not yield any ethanol at the same temperature. Also, no ethanol was detected with 5 g/L substrate at fermentation temperature of 30°C, and only negligible amount of ethanol was formed with 10 g/L substrate at the same temperature. Consistent with the trend of production of other two products, the yield of ethanol increased with time, as temperature increased from 30 and 37°C.

4.3.4 Rate constants and activation energy

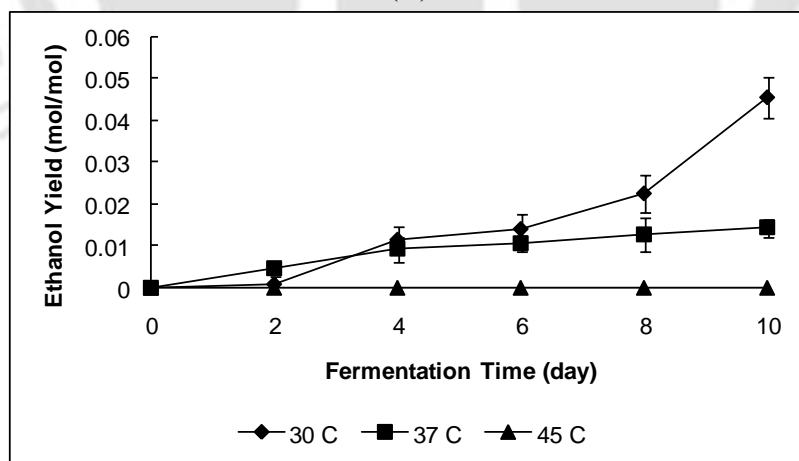
In order to understand the actual mechanism by which temperature exerts its effect on bioconversion of crude glycerol to solvents, one needs to look at the kinetic data as well as thermodynamic data. The substrate consumption data for 25 g/L initial substrate concentration was used further for calculating rate constants at three fermentation temperatures. The glycerol utilization data so obtained, fitted well into the first order kinetic equation with values of R^2 ranging from 0.85 to 0.95. The values of first order rate constant (k) at 30, 37 and 45°C were calculated to be 0.198, 0.294, 0.029 /day, respectively (Fig. 4.4). The k values depict clearly that for 25 g/L initial glycerol concentration, the rate of glycerol bioconversion is the highest at 37°C and the lowest at 45°C.



(A)

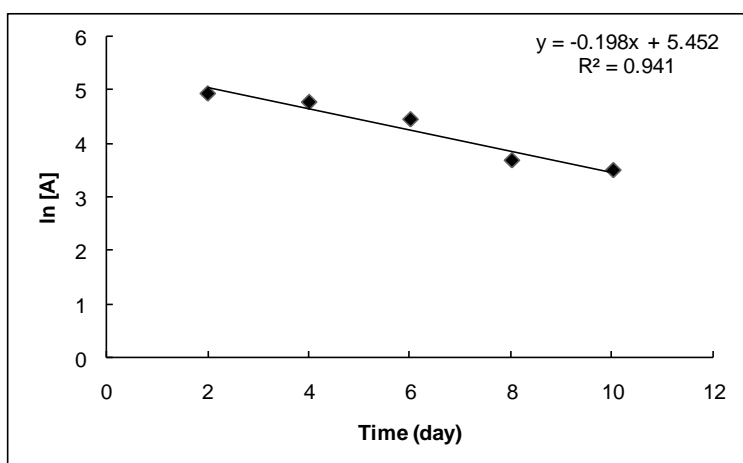


(B)

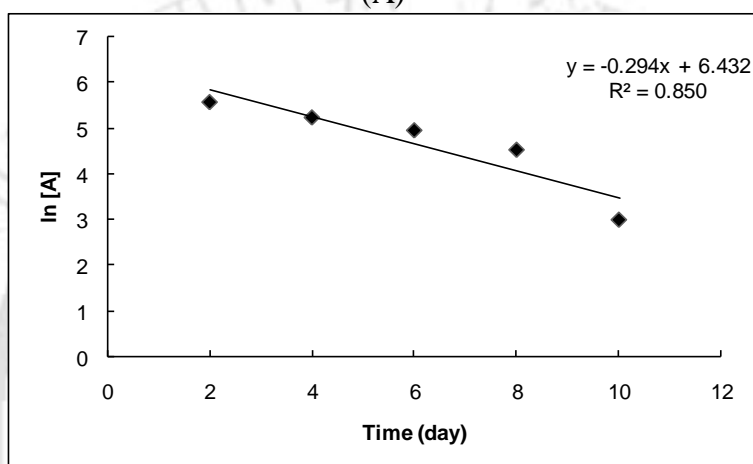


(C)

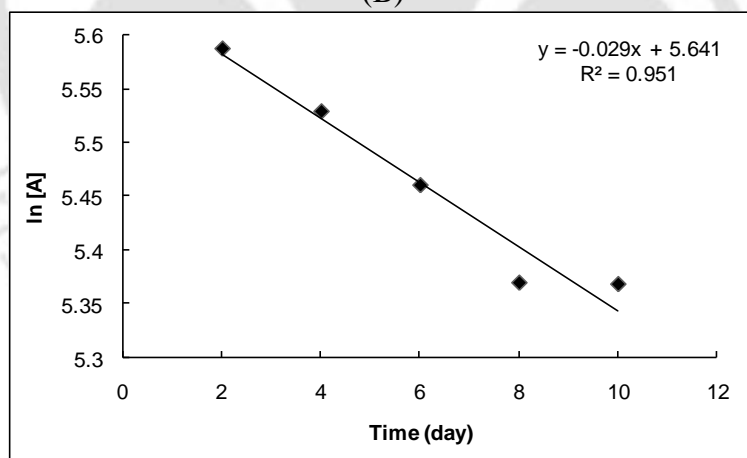
Figure 4.3 Trends in ethanol production with (A) 5 g/L, (B) 10 g/L, and (C) 25 g/L initial crude glycerol concentration at three fermentation temperatures



(A)



(B)



(C)

Figure 4.4 Calculation of first order rate constants for glycerol bioconversion by immobilized *C. pasteurianum* at fermentation temperature of (A) 30°C, (B) 37°C, and (C) 45°C. The highest value for first order rate constant for glycerol bioconversion was obtained at 37°C

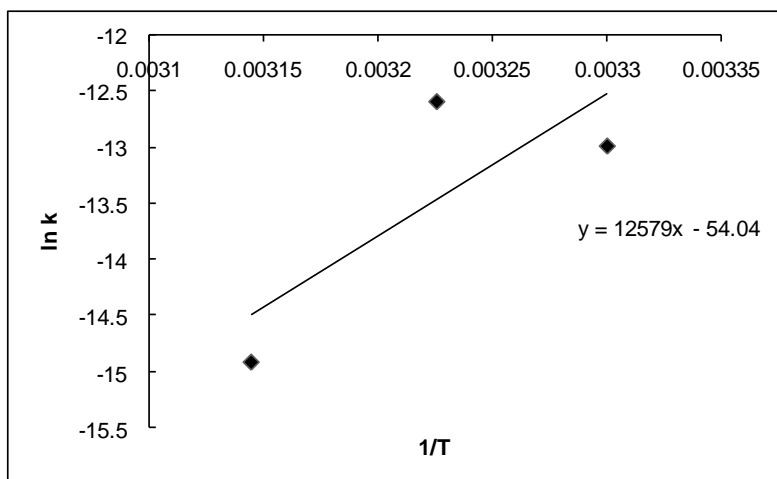


Figure 4.5 $\ln k$ vs $1/T$ (Kelvin⁻¹) curve for calculating activation energy (E_a) of glycerol bioconversion by immobilized *C. pasteurianum*

A higher k value at 37°C than at 30°C gave a higher total product yield at 37°C. Also, none of the desired products were detected at 45°C due to the lowest k value. Activation energy (E_a) for bioconversion of crude glycerol was found to be -57.62 kcal/mol using Arrhenius equation (Fig. 4.5).

4.3.5 Utilization of crude glycerol

The utilization of 25 g/L substrate after 2 days of fermentation was similar at both 37 and 45°C. The highest total product yield at 37°C may be attributed to the highest glycerol utilization at this temperature. Although approx. 6 g/L substrate was consumed at 45°C, but none of it was converted into detectable products. This may be due to conversion of glycerol to other undetectable compounds such as succinate, acetate, lactate, CO₂.

4.4 DISCUSSION

C. pasteurianum exhibits a biphasic fermentation pattern, wherein the cells first go for acids formation (acetate, butyrate) – known as acidogenic phase, and the lowering of pH due

to acids accumulation causes the production of solvents (ethanol, butanol) – known as solventogenic phase (Taconi et al., 2009). The production of 1,3-PDO occurs before accumulation of acids. A comparison of results obtained from present study with those reported in literature is rather difficult, as there is only limited literature on fermentation of crude glycerol by *C. pasteurianum* cells. Also, the effect of temperature on fermentation profile of crude glycerol by immobilized *C. pasteurianum* has not been studied as yet. Comparing among the product profiles obtained at three temperatures, it can be seen that total yield of products is higher at 37°C (0.66 and 0.37 mol/mol for 5 and 25 g/L, respectively) than at 30°C (0.38 and 0.22 mol/mol for 5 and 25 g/L, respectively) for both 5 and 25 g/L substrate, but the same is not true for 10 g/L substrate, which formed a higher amount of product at 30°C (0.60 mol/mol) than at 37°C (0.45 mol/mol). A higher temperature of 45°C is not at all suitable for production of solvents from crude glycerol. The trends observed in this study at 37°C matched well with earlier studies (Taconi et al., 2009) with free cells of *C. pasteurianum* (growing on crude glycerol) in many aspects:

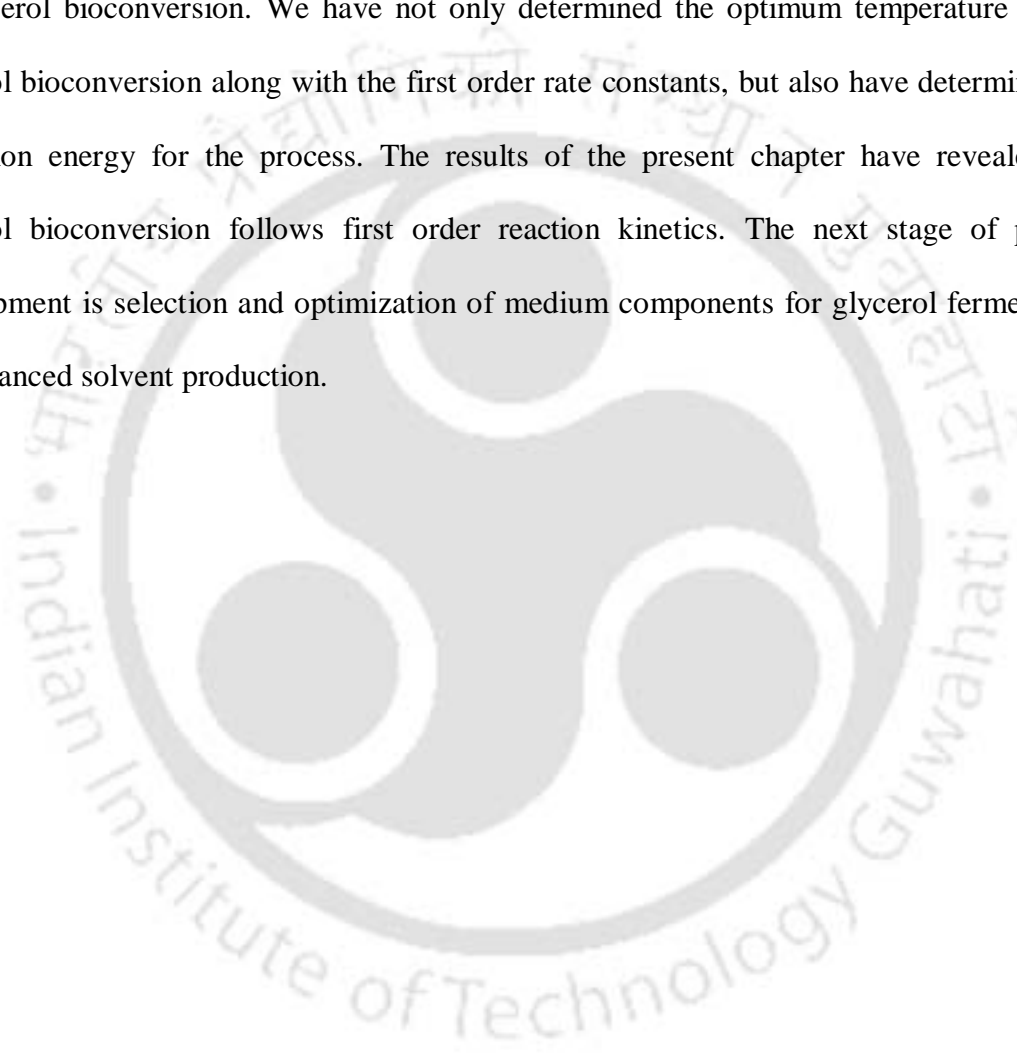
- 10 g/L substrate formed negligible amounts of butanol while, the highest amount of butanol was obtained with 25 g/L substrate.
- The highest ethanol yield obtained with free cells was for both 5 and 10 g/L substrate. The highest ethanol yield with immobilized cell was obtained with 10 g/L substrate.

It is known that high concentrations of glycerol are inhibitory to *C. pasteurianum* cells (Taconi et al., 2009) and our earlier study (reported in previous chapter and also in Khanna et al., 2011) had similar observations. The same effect is also observed in the present case, as there is a decrease in total solvent yield at 25 g/L crude glycerol concentration. 37°C was the most suitable temperature for obtaining maximum yield of butanol, while 30°C gave the highest yield of both 1,3-PDO and ethanol. It is thus clear from these results that production of the three products from fermentation of glycerol is temperature specific. This

may be due to different temperature optima for enzymes involved in ethanol, butanol and 1,3-PDO production pathways.

4.5 CONCLUSIONS

In the present chapter, we addressed the issue of kinetic and thermodynamic aspects of glycerol bioconversion. We have not only determined the optimum temperature for the glycerol bioconversion along with the first order rate constants, but also have determined the activation energy for the process. The results of the present chapter have revealed that glycerol bioconversion follows first order reaction kinetics. The next stage of process development is selection and optimization of medium components for glycerol fermentation for enhanced solvent production.



MEDIUM OPTIMIZATION FOR GLYCEROL BIOCONVERSION

5.1 INTRODUCTION

As noted in earlier chapters, high cell density of immobilized cells provides distinct merits over free cells, the most important being the ability to reuse immobilized cells for many cycles and ease in downstream processing. The yield and selectivity of products from fermentation of glycerol is greatly influenced by physical and chemical process parameters (Dabrock et al., 1992). In the previous chapter, we have optimized the important physical parameter of temperature from viewpoint of the kinetics of the process. However, in addition to the physical parameters (like pH, stirring speed, etc.), optimal production of targeted products from glycerol bioconversion in the present study (i.e. 1,3-PDO and butanol) is also dependent on the composition of the medium. Thus, development and optimization of the media is an important facet of process development for glycerol bioconversion.

Earlier authors have addressed this issue and optimization of media components for

enhanced butanol and 1,3-PDO by free cells of *Clostridium pasteurianum* has already been studied (Moon et al., 2011). However, no study has been carried out on optimizing the media components for bioconversion of glycerol by immobilized cells of *C. pasteurianum*. The glycerol metabolism of the cells is likely to change after immobilization, which would also affect the product profile. Hence, optimum composition of the media for free and immobilized cells is likely to be different. In this chapter, we present the results of our study on optimization of nutrient composition of the media for glycerol fermentation by immobilized cells of *C. pasteurianum*.

We have used the Taguchi statistical method for optimization of the media composition. This method has been widely used for optimization of other fermentation processes (Dasu et al., 2003; Chang et al., 2006; Sirisansaneeyakul et al., 2007). Taguchi method allows for the analysis of a large number of parameters in minimum number of experiments. This helps in identifying the key parameters that have the largest effect on process output. Optimization of media was done in shake flasks, and later, these results were reconfirmed at shake flask level, and later scale up in a bioreactor. Thus, the results of this chapter also provide an insight into the scale-up aspects of the glycerol bioconversion process.

5.2 MATERIALS AND METHODS

5.2.1 Micro-organism, culture revival and maintenance

Lyophilized cells of *Clostridium pasteurianum* (MTCC 116) were obtained from Institute of Microbial Technology (Chandigarh, India). The cells were revived on cooked meat media (CMM) agar plates, and in reinforced clostridial media (RCM) broth, as mentioned in earlier chapters. The revived cells were maintained on CMM agar slants at 4°C, and were used as a stock. The cells were sub-cultured every month. All chemicals and

reagents were purchased from Himedia, India or Merck, Germany. The chromatography grade standards were purchased either from Sigma, USA or Merck, Germany.

5.2.2 Immobilization and cross-linking of *C. pasteurianum* cells

C. pasteurianum cells were immobilized on column chromatography grade silica (Merck, India) in RCM broth. The silica particles were dried at 120°C for 24 h in a dry oven prior to use. The support was added to the media at the commencement of log phase of the growth (approx. after 24 h). The support was kept for 48 h with the media at 37°C with shaking at 120 rpm. The broth was centrifuged to separate silica immobilized cells and non-immobilized cells. The support with immobilized cells was shaken with 50 mM phosphate buffer (pH 7.5) for 10 min. It was then washed twice with 50 mM, pH 7.5 phosphate buffer, and dried for 24 h at room temperature. The cells immobilized on silica were incubated with 0.1% v/v glutaraldehyde solution for 1 h, followed by washing with phosphate buffer (50 mM, pH 7.5), and drying at room temperature for 24 h.

5.2.3 Fermentation conditions

The initial screening of the media constituents was done using one factor at a time approach. Total 10 media constituents, viz. NaCl, Biotin, $\text{CoCl}_2 \cdot 2\text{H}_2\text{O}$, $\text{KH}_2\text{PO}_4\text{--K}_2\text{HPO}_4$, PABA (p-aminobenzoic acid), $\text{MgSO}_4 \cdot 7\text{H}_2\text{O}$, $\text{CaCl}_2 \cdot 2\text{H}_2\text{O}$, $\text{FeSO}_4 \cdot 7\text{H}_2\text{O}$, yeast extract, $(\text{NH}_4)_2\text{SO}_4$ were screened. These media components and their concentrations were selected on the basis of *C. pasteurianum* media used in earlier studies (Heyndrickx et al., 1991; Dabrock et al., 1992; Biebl, 2001; Taconi et al., 2009). Out of these 10 components, 6 components ($\text{KH}_2\text{PO}_4\text{--K}_2\text{HPO}_4$, $\text{MgSO}_4 \cdot 7\text{H}_2\text{O}$, $\text{CaCl}_2 \cdot 2\text{H}_2\text{O}$, $\text{FeSO}_4 \cdot 7\text{H}_2\text{O}$, yeast extract, $(\text{NH}_4)_2\text{SO}_4$) showed significant effect on solvent production. These 6 components were shortlisted for Taguchi analysis, the details of which are described in next section. The optimization studies were carried out in custom fabricated 250 mL anaerobic Erlenmeyer flasks. Each flask contained solution of media components in desired proportions in 100 mL

distilled water. To this, 3 % w/v immobilized cells (as per results of optimization in Chapter 3) with support, and 25 % w/v pure glycerol as a sole carbon source were added. All flasks were sparged with nitrogen gas at the start and after every 24 h of fermentation to maintain anaerobic conditions. The flasks were kept in an incubator shaker at 200 rpm and 37°C. The samples of fermentation broth were withdrawn after every 2 days upto a period of 10 days. The initial pH of each set of medium was set at 6.8 ± 0.2 . All experiments were carried out in triplicate.

5.2.4 Taguchi's orthogonal array

In order to study the effect of each nutrient component on solvent production by immobilized *C. pasteurianum* and to optimize its concentration for maximum solvent production, a standard L8 Orthogonal array of experiments was used. 6 factors (media components) were examined at 2 levels denoted by 1 and 2 as depicted in Table 5.1. The value of level of each nutrient (indicating concentration) was set according to the Taguchi statistical design, wherein 8 sets of media composition were identified. All experimental runs were carried out in triplicate. The optimal conditions with respect to the factors tested have been determined on the basis of average of signal to noise ratio (S/N) for the factors at each factor level. Level 1 value of three factors or nutrients, viz. $\text{MgSO}_4 \cdot 7\text{H}_2\text{O}$, $\text{CaCl}_2 \cdot 2\text{H}_2\text{O}$, and $\text{FeSO}_4 \cdot 7\text{H}_2\text{O}$ was chosen to be zero, on the basis of initial screening experiments, which indicated the influence of zero concentration of certain factors on product pattern. The total solvent production by immobilized *C. pasteurianum* was considered as a desired variable, as a higher concentration of total solvents was required. The statistical significance of each factor was determined using ANOVA. Finally, the optimum conditions for solvent production by immobilized *C. pasteurianum* were determined. The Taguchi analysis and ANOVA were carried out using Minitab 15 software (trial version).

Table 5.1 The factors and their corresponding levels used in Taguchi statistical design for optimal mixed alcohols production by immobilized *C. pasteurianum*

Factors	Constituents	Level 1(g/L)	Level 2 (g/L)
A	$\text{KH}_2\text{PO}_4\text{--K}_2\text{HPO}_4$	1	2
B	Yeast Extract	1	5
C	$\text{MgSO}_4\cdot 7\text{H}_2\text{O}$	0	0.1
D	$\text{FeSO}_4\cdot 7\text{H}_2\text{O}$	0	0.005
E	$\text{CaCl}_2\cdot 2\text{H}_2\text{O}$	0	0.01
F	$(\text{NH}_4)_2\text{SO}_4$	0.1	5

5.2.5 Confirmatory experiments

Glycerol fermentation with optimized media components was rechecked in 250 mL custom fabricated Erlenmeyer flasks using the protocol as described previously. Further, the optimized fermentation media was tested in a 2 L microprocessor controlled bioreactor (Zenith, India) 1 L optimized medium, 3% w/v immobilized cells with support and 25% w/v glycerol were added to the bioreactor. The temperature was controlled at 37°C, 99.98% pure nitrogen was sparged at a rate of 0.1 vvm. The initial pH of the media and the agitation rate were set at 6.8±0.2 (using 0.1 M NaOH and 0.1 M HCl) and 200 rpm, respectively. The samples of fermentation broth were withdrawn after every 48 h upto a period of 10 days for analysis. The experiments in both shake flask and bioreactor were carried out in duplicate and the results presented as the means of two experimental runs. The standard deviations were shown in the form of error bars.

5.2.6 Experiments with media optimized for free cells

A similar study on media optimization for enhanced butanol and 1,3-PDO production by free cells of *C. pasteurianum* has been recently published by Moon et al. (2011). In this study, the optimum media composition for higher butanol production was determined to be 0.06 g/L $\text{FeSO}_4\cdot 7\text{H}_2\text{O}$, 7.35 g/L $(\text{NH}_4)_2\text{SO}_4$ and 5.08 g/L yeast extract, which happen to be

higher values for the first two factors, while lower value for the third factor. Similarly, the optimum media components for 1,3-PDO production were: 0 g/L $\text{FeSO}_4 \cdot 7\text{H}_2\text{O}$, 0 g/L $(\text{NH}_4)_2\text{SO}_4$ and 8 g/L yeast extract, which happen to be lower values for the first two factors, while higher value for the third factor. To assess whether the same media compositions were also optimum for immobilized cells, experiments were performed with compositions reported by Moon et al. (2011), and the results were compared with the present experiments. Except for the media composition, the other protocols were exactly same as mentioned in previous sections.

5.2.7 Method of analysis

Solvent production in the fermentation broth was monitored by gas chromatographic analysis using a CP Wax 52CB (250 mm \times 0.25 mm \times 0.39 mm) capillary column (Varian) and a flame ionization detector. The injector and detector temperatures were 230°C and 250°C, respectively. The oven temperature was programmed from 45°C to 100°C with an increment of 3°C/min and after 100°C, an increment of 5°C/min upto 200°C. The utilization of glycerol by immobilized *C. pasteurianum* cells in different media was determined by HPLC analysis using a HiPlex-H column (300 mm \times 5 μm \times 4.6 mm, Varian). The HPLC apparatus comprised of a pump (Series 200, Perkin Elmer), a refractive index detector (Series 200, Perkin Elmer) and a vacuum degasser (Series 200, Perkin Elmer). HPLC grade water (Milli Q) was used as the mobile phase at a flow rate of 0.5 mL/min. The analyses were carried out at 37 \pm 2°C. Samples were filtered through a 0.2 μm membrane filter, and diluted appropriately prior to analysis. Standard calibration plots were used for determination of concentrations of both substrate and products.

5.3 RESULTS AND DISCUSSION

Initial screening experiments helped in determining the media factors having relatively greater effect on products formation. The results obtained from one component at a time analysis indicated that components PABA, biotin, $\text{CoCl}_2 \cdot 2\text{H}_2\text{O}$, and NaCl had an insignificant impact on formation of products. The total products concentration obtained with PABA, biotin, $\text{CoCl}_2 \cdot 2\text{H}_2\text{O}$, and NaCl were 0.03, 0, 0 and 0 g/L, respectively. The results obtained with PABA and biotin, which are in agreement with earlier study by Sanchez (2009), indicated that *C. pasteurianum* is not an auxotroph for both of these nutrients. The components that exhibited influence on formation of solvents were $\text{CaCl}_2 \cdot 2\text{H}_2\text{O}$ (0.24 g/L), yeast extract (2.2 g/L), $(\text{NH}_4)_2\text{SO}_4$ (1.82 g/L), $\text{FeSO}_4 \cdot 7\text{H}_2\text{O}$ (0.38 g/L), $\text{MgSO}_4 \cdot 7\text{H}_2\text{O}$ (1.4 g/L), and $\text{KH}_2\text{PO}_4\text{-K}_2\text{HPO}_4$ (0.48). The values in parentheses are the total products concentration. Out of these, yeast extract had the highest effect on solvents production. Similarly, the study of Sanchez (2009) also showed that the cells can grow even in absence of micronutrients, viz. Co, Cu, Zn and Ni. This result is in concurrence to our study that the effect of $\text{CoCl}_2 \cdot 2\text{H}_2\text{O}$ on products formation was insignificant.

5.3.1 Taguchi analysis and ANOVA

Table 5.2 depicts the final total concentration of solvents formed with different media compositions. These results indicate that the solvent production is a major function of media composition. Among all 8 experimental runs, the highest total concentration of alcohols (9.9 g/L) was obtained in run 5. The percentage effect of each factor on alcohols production is depicted in Table 5.3. Out of 6 factors examined, factors A, B, C and F had major effect on mixed alcohols production, as indicated by their high delta S/N value. In Taguchi statistical design, S/N ratio is an important parameter for identifying optimal conditions for the process.

Table 5.2 Taguchi design matrix and corresponding average concentrations (g/L) of the products formed and substrate left in shake flask at the end of the fermentation by immobilized *C. pasteurianum*

Exp No	A	B	C	D	E	F	1,3-PDO	Butanol	Ethanol	Total	Glycerol
1	1	1	1	1	1	1	1.003	0.500	0.028	1.531	9.547
2	1	1	1	2	2	2	0.000	0.000	0.058	0.058	8.462
3	1	2	2	1	1	2	4.220	1.245	0.132	5.597	13.651
4	1	2	2	2	2	1	5.201	4.211	0.132	9.544	5.732
5	2	1	2	1	2	1	4.947	4.844	0.114	9.905	1.185
6	2	1	2	2	1	2	3.351	3.258	0.510	7.119	4.354
7	2	2	1	1	2	2	2.703	1.246	0.502	4.451	13.533
8	2	2	1	2	1	1	3.194	3.108	0.571	6.873	8.410

Table 5.3 Taguchi analysis of factors affecting total alcohols production by immobilized *C. pasteurianum*

Level	A	B	C	D	E	F
1	3.386	3.954	2.143	12.907	13.137	14.976
2	16.663	16.094	17.905	7.141	6.911	5.072
Delta S/N (main effect mean)	13.277	12.141	15.762	5.767	6.226	9.903
Percentage Contribution	21.05	19.25	24.99	9.14	9.87	15.70

A high S/N ratio indicates higher significance of the factor. Based on this logic, the order of effect of various factors on total alcohol production was $\text{MgSO}_4 \cdot 7\text{H}_2\text{O} > \text{KH}_2\text{PO}_4 - \text{K}_2\text{HPO}_4 > \text{Yeast extract} > (\text{NH}_4)_2\text{SO}_4 > \text{CaCl}_2 \cdot 2\text{H}_2\text{O} > \text{FeSO}_4 \cdot 7\text{H}_2\text{O}$. The concentration of $\text{MgSO}_4 \cdot 7\text{H}_2\text{O}$ was critical for mixed alcohols production, as it had the highest contribution of 24.99% to the main effect mean (or delta S/N). The insignificant effect of calcium on products formation may be explained in terms of immobilization of actively growing *C. pasteurianum* cells. Calcium is a component of endospore and is required for stabilizing endospore wall (de Gelder et al., 2007).

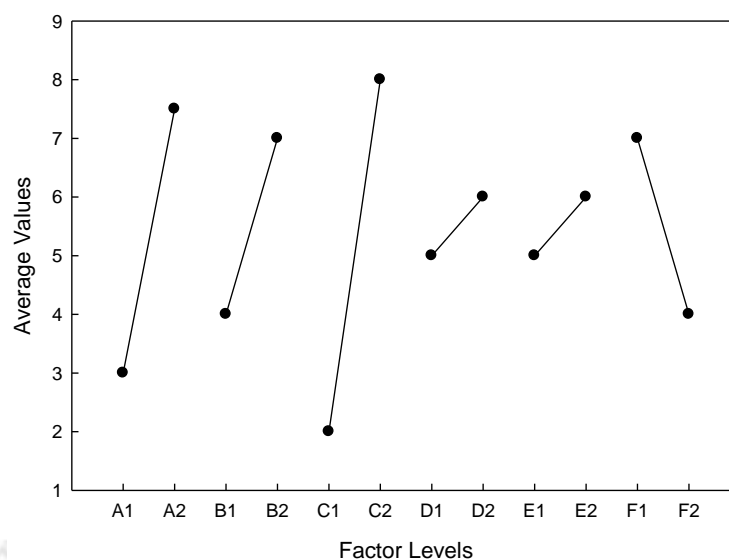


Figure 5.1 The mean of main effects plot for each medium component at two levels (1 and 2)

In the present study, we have used immobilized actively growing cells of *C. pasteurianum*, and not immobilized spores; and hence, the cells did not have very specific requirement for calcium. Among the four significant factors (with 10% or higher contribution to main effect mean), the total solvent production was higher at level 2 for factors A, B and C, while factor F formed more solvents at lower level (Fig. 5.1).

ANOVA was done to quantify the variation in products formation caused due to each factor, and also to determine whether the lower or the higher value of a factor is essential for preferred result, i.e. higher products formation. ANOVA of only those factors was done, which had more than 10% contribution to the main effect (Oskuie et al., 2007; Venil and Lakshamanaperumalasangam, 2009). Thus, factors A, B, C and F were considered for further analysis. ANOVA of total solvent production had a model SS (sum of squares), MS (mean squares), and F value of 63.2970, 15.8243, and 1663.895, respectively (Table 5.4).

Table 5.4 ANOVA table for the significant factors obtained from Taguchi analysis

Factors	DF	SS	MS	F ratio	<i>p</i> value	Confidence percentage
Model	4	63.2970	15.8243	1663.895	<i>p</i> < 0.001	99.62
A	1	11.9032	11.9032	714.77	<i>p</i> < 0.001	99.44
B	1	5.91332	5.91332	1907.93	<i>p</i> < 0.001	99.79
C	1	35.0683	35.0683	3388.59	<i>p</i> < 0.001	99.88
F	1	10.4122	10.4122	644.29	<i>p</i> < 0.001	99.38

DF = Degree of Freedom, SS = Sum of Squares, MS = Mean of Squares

The model obtained from ANOVA had R^2 (multiple regression coefficient) of 0.9962, which means that the model can explain 99.62% variation in the response. R^2 value closer to 1.0 indicates the robustness of the model, whereas the value greater than 0.75 implies the fitness of the model. ANOVA of factors clearly demonstrated that all factors considered had significant effect (as indicated by $p < 0.001$) on total alcohols production. The numerical values of the factors, which provided the highest total concentration of alcohols are KH_2PO_4 – K_2HPO_4 2 g/L, yeast extract 5 g/L, $\text{MgSO}_4 \cdot 2\text{H}_2\text{O}$ 0.1 g/L, and $(\text{NH}_4)_2\text{SO}_4$ 0.1 g/L. The values of first three factors correspond to higher level of factor, while the value of last factor, i.e. $(\text{NH}_4)_2\text{SO}_4$ corresponds to the lower level. Higher products concentration at lower concentration of $(\text{NH}_4)_2\text{SO}_4$ is probably a consequence of presence of other nitrogen (yeast extract) and sulfur source ($\text{MgSO}_4 \cdot 2\text{H}_2\text{O}$).

5.3.2 Result prediction and confirmatory experiments in shake flasks and scale-up to bioreactor level

The following equation estimates or predicts the total concentration of solvent sformed under optimized conditions (Sirisansaneeyakul et al., 2007; Sanjari et al., 2009) during the bioconversion of glycerol:

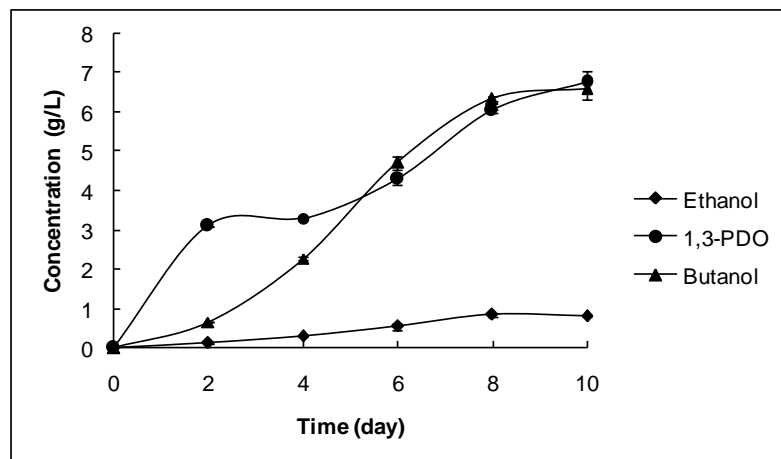
$$Y_{opt} = T_i + \sum (F_{i,avg} - T_{i,avg}) \quad (5.1)$$

Various notations are Y_{opt} = process output, T = average of all trial results/average of performance, i = significant factors, F_i – average effect of significant factors at each level. For the present study, in which we have four factors with each having two levels, the above equation can be rewritten as:

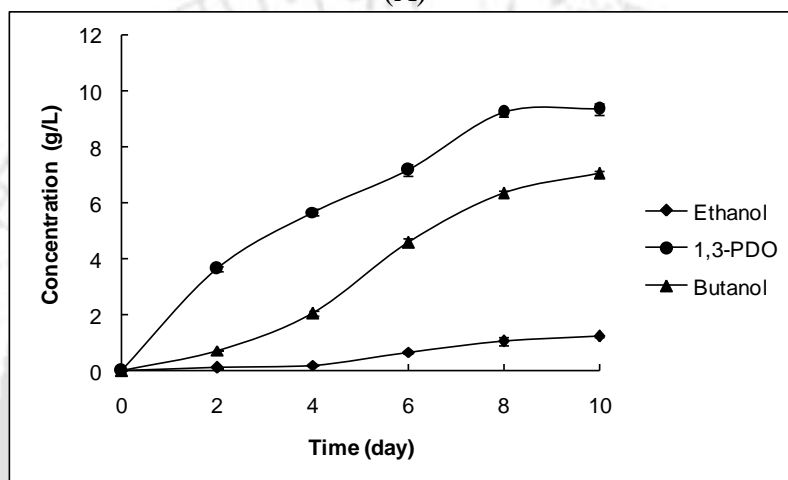
$$Y_{opt} = T + |A_1 - T| + |A_2 - T| + |B_1 - T| + |B_2 - T| + |C_1 - T| + |C_2 - T| + |F_1 - T| + |F_2 - T| \quad (5.2)$$

As per equation 5.2, the predicted value of total alcohols concentration under optimized condition was 17.51 g/L. In order to confirm the prediction, fermentation was carried out in shake flasks with medium of optimum composition. The trends in the production of 1,3-PDO, ethanol and butanol in shake flask experiments are depicted in Fig. 5.2A. The results presented are the mean of the two experimental sets. The final concentrations (in g/L) of ethanol, 1,3-PDO and butanol were calculated as 0.81 (0.03 g/g), 6.77 (0.28 g/g) and 6.59 (0.26 g/g), respectively. The total solvent concentration resulting from shake flask fermentation in optimized medium was 14.17 g/L, which was lower than the predicted value of 17.51 g/L. But, the value obtained after optimization of medium components in shake flask was higher than the value obtained in trial 5 (9.90 g/L). Thus, the effect of medium optimization is evident from these results. A lower product concentration than estimated value may be attributed to the reduced control of temperature and shaking speed in a shaker incubator. In order to obviate these limitations and to have a better control over fermentation conditions, the experiment was performed in a bioreactor under same conditions.

Fig. 5.2B depicts the trends of production of the three fermentation products, viz. ethanol, butanol and 1,3-PDO in a bioreactor in optimized medium. The total concentration of products formed after 10 days of fermentation was 17.67 g/L. The individual concentrations (g/L) of ethanol, butanol and 1,3-PDO were 1.25 (0.06 g/g), 7.06 (0.29 g/g) and 9.36 (0.37 g/g), respectively.



(A)



(B)

Figure 5.2 (A) Production of ethanol, butanol and 1,3-PDO in shake flasks containing optimized media. The total product concentration after completion of fermentation was 14.17 g/L, and (B) product formation profiles in stirred tank bioreactor with optimized media components. The final concentration of products achieved was 17.67 g/L which was higher than the predicted value

The result obtained is higher than the predicted value of 17.51 g/L, which not only demonstrates the robustness of the statistical analysis, but also validates the significance of the medium components, as indicated by the analysis. As can be seen from Figs. 5.2A and 5.2B, almost similar yields of all three products were obtained after 8 and 10 days of fermentation. Thus, the optimization of medium components also reduced the total glycerol fermentation time.

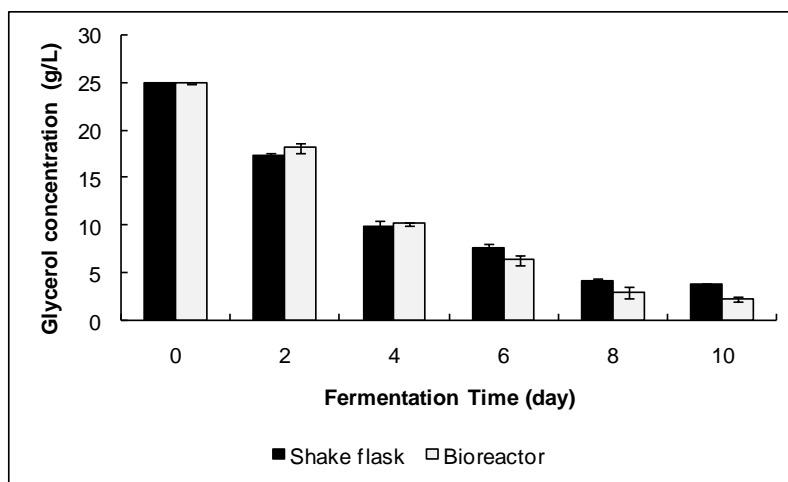


Figure 5.3 Trends in concentration of glycerol left unutilized in the fermentation broth during the course of fermentation. The final concentration of glycerol utilized by *C. pasteurianum* was higher in bioreactor than in shake flask

Fig. 5.3 depicts the concentration of glycerol left unutilized in fermentation broth during the course of fermentation in shake flask and bioreactor. The cells in bioreactor study were found to utilize a higher concentration of glycerol (91%) than the cells in shake flask (86%), which may be the reason behind higher production of solvents in bioreactor. The trends in ethanol, 1,3-PDO and butanol formation in both shake flask and bioreactor were similar as reported in a study by Dabrock et al. (1992). This paper describes that for glycerol concentration upto 8% w/v, equal quantities of the three products formed; however, for higher concentrations of glycerol more 1,3-PDO is produced with a concurrent decrease in ethanol production (Dabrock et al., 1992). In agreement with this result for 25 g/L glycerol in our study, which is relatively high concentration, 1,3-PDO was the major product. The yield of the two major products, viz. butanol and 1,3-PDO, obtained after optimization of medium components was higher than their yields reported by other groups (Dabrock et al., 1992; Biebl, 2001; Heyndrickx et al., 1991). Only the yields reported by Taconi et al. (2009) are higher than that obtained in the present study. We would like to mention an important point

that the yields reported in the present case are with immobilized *C. pasteurianum* cells, while previous researchers have used free cells of *C. pasteurianum*. A further increase in products yield is expected on optimizing fermentation parameters such as temperature, pH, agitation rate, etc.

5.3.3 Comparative evaluation with optimized media for free cells

The results obtained in present study match with the results of Moon et al. (2011) to some extent in that we have also found $(\text{NH}_4)_2\text{SO}_4$ and yeast extract to be the important factors influencing total products concentration. However, in addition to these, our study also establishes $\text{MgSO}_4 \cdot 7\text{H}_2\text{O}$ and $\text{K}_2\text{HPO}_4\text{--KH}_2\text{PO}_4$ as important components for alcohols production by immobilized *C. pasteurianum* cells. But, the total products concentration obtained with immobilized cells with optimized medium for butanol production by free cells was quite low. Ethanol was the major product (0.35 g/L) with no formation of butanol and 1,3-PDO. Similarly, the medium optimized for 1,3-PDO production by free cells also gave a very low total products concentration with formation of traces of ethanol (0.23 g/L), 1,3-PDO (0.87 g/L) and no butanol. This discrepancy in results points out that the medium requirement for free and immobilized cells are different.

5.4 CONCLUSIONS

In this chapter, we addressed a crucially important facet of the process for bioconversion of glycerol, i.e. optimization of the medium. The results presented in this chapter clearly reveal that production of bioalcohols through fermentation of glycerol by immobilized *C. pasteurianum* is a strong function of composition of the medium. We have adopted a statistical approach for medium optimization. Glycerol was metabolized faster by immobilized *C. pasteurianum* cells in an optimized medium. The optimization of medium components by Taguchi design helped in identifying key factors responsible for enhanced

production of alcohols. Further work in the process development must aim at optimizing the fermentation parameters such as temperature, pH, agitation rate, etc to obtain higher products yield.





PROCESS OPTIMIZATION FOR GLYCEROL BIOCONVERSION

6.1 INTRODUCTION

In any bioprocess, parameters such as temperature, medium pH, agitation rate etc. directly influence the metabolism of micro-organisms, which in turn is manifested in terms of yield and selectivity of different products formed by the micro-organism (Dabrock et al., 1992). Given the distinct advantages of immobilized cells as mentioned above, if the process of glycerol conversion with immobilized cells is also optimized in terms of operational parameters, it would further increase the efficacy and economy of the process that would add to potential of the process for large-scale implementation. It is in this spirit that in this chapter, we have addressed the issue of optimization of the process of bioconversion of glycerol with immobilized cells of *Clostridium pasteurianum*, for both crude as well as pure glycerol as fermentation substrate. The fermentation parameters have been optimized by well known statistical method given by Taguchi (Dasu et al., 2003; Chang et al., 2006;

Sirisansaneeyakul et al., 2007; Davarey and Pakshirajan, 2010). In addition to the statistical analysis of the results, we have also tried to get a physiological insight into the influence of different process parameters on glycerol bioconversion, and have tried to identify the interactions between them. The reusability of the biocatalyst (i.e. the microbial cells immobilized on a support) in successive fermentation cycles has also been studied.

6.2 MATERIALS AND METHODS

6.2.1 Materials

Column chromatography grade 80–120 mesh size silica gel was used as an immobilization support, and was purchased from Merck, India. The anaerobic tray system was purchased from Himedia, India. Pure glycerol was procured from Merck, India, while crude glycerol was manufactured in the laboratory by homogenous alkali catalyzed methanolysis of soybean oil. All chromatography grade standards were purchased either from Sigma Aldrich, Germany or Merck, Germany. All other chemicals used were of analytical grade and were purchased from Himedia, India and Merck, Germany.

6.2.2 Micro-organism, culture revival and maintenance

Clostridium pasteurianum (MTCC 6013) was procured from Institute of Microbial Technology (Chandigarh, India). The cells were revived on Cooked Meat Media (CMM) agar plates and in Reinforced Clostridial Media (RCM) broth. The revived cells were maintained on CMM agar slants and stored at 4°C to be used as stock for further experiments.

6.2.3 Fermentation conditions

C. pasteurianum was immobilized on column chromatography grade silica (Merck, India) according to the protocol described in previous chapters. For the optimization of fermentation, we have considered four process parameters, viz. agitation rate, initial glycerol

concentration, temperature and initial pH of the fermentation broth. The optimization studies were carried out in custom fabricated 250 mL anaerobic Erlenmeyer flasks. Each flask contained 3% w/v support (optimized previously as in chapter 3) with immobilized cells in 100 mL fermentation medium. The fermentation medium optimized in Chapter 5 was used in present study. Glycerol was added to the medium in different concentrations as determined by Taguchi experimental design. The flasks were sparged with nitrogen gas at the start of fermentation, and thereafter, every 24 h to maintain anaerobic conditions inside the flask. The samples were withdrawn after every 2 days upto a period of 8 days. All experiments were carried out in triplicate, and the results presented are the mean of three trials. For testing the reusability of immobilized biocatalyst, the same biocatalyst was used for 5 successive fermentation cycles (after separation by centrifugation, washing and drying at the end of each fermentation cycle) in both pure and crude glycerol containing media.

6.2.4 Taguchi's orthogonal array

A standard L18 orthogonal array was used to study the effect of each of 4 process parameters (listed earlier) on mixed alcohols (i.e. mixture consisting of 1,3-PDO, butanol and ethanol) production by immobilized *C. pasteurianum*, and to optimize fermentation process with either pure or crude glycerol for maximum solvent production. The first factor (agitation rate) was analyzed at 2 levels denoted by 1 and 2, and the rest of the factors were analyzed at 3 levels each, denoted by 1, 2 and 3 (Table 6.1). The experimental design matrix with permutation-combination of different values or levels of process parameters according to the Taguchi statistical design, constituting 18 sets of experiments is described in Table 6.2. Each of the 18 experiments was carried out for pure as well as crude glycerol as a carbon source. The evaluation of optimal product formation with respect to the each of the process parameter (or factor) was done by determining average S/N ratios for the factor at each level.

Table 6.1 The factors and their corresponding levels used in Taguchi statistical design for optimal mixed alcohols production by immobilized *C. pasteurianum*

Factors	Level 1	Level 2	Level 3	Units
Agitation Speed (A)	150	200	–	rpm
Glycerol Concentration (B)	5	10	25	g/L
pH (C)	3	5	7	–
Temperature (D)	30	37	45	°C

Table 6.2 Taguchi design matrix and corresponding total mixed alcohols production (g/L) by immobilized *C. pasteurianum* (MTCC 6013) with pure and crude glycerol as substrates in shake flask

Exp No	Agitation Rate	Glycerol Concentration	pH	Temperature	Average (g/L, pure glycerol)	Average (g/L, crude glycerol)
1	1	1	1	1	0.371	0.039
2	1	1	2	2	0.063	0.044
3	1	1	3	3	0.238	0.016
4	1	2	1	1	0.130	0.101
5	1	2	2	2	0.181	0.077
6	1	2	3	3	0.187	0.112
7	1	3	1	2	0.175	0.102
8	1	3	2	3	0.144	0.327
9	1	3	3	1	13.103	10.977
10	2	1	1	3	0.179	0.201
11	2	1	2	1	0.045	0.002
12	2	1	3	2	3.756	3.805
13	2	2	1	2	0.175	0.099
14	2	2	2	3	1.180	1.136
15	2	2	3	1	9.587	4.819
16	2	3	1	3	0.152	0.102
17	2	3	2	1	3.746	3.409
18	2	3	3	2	17.960	11.838

The total mixed alcohols production by immobilized *C. pasteurianum* was considered as a desired variable, and thus, larger the better S/N ratio was used for analysis of output.

Analysis of variance (ANOVA) was performed to determine the statistical significance of each factor. The Taguchi analysis and ANOVA were carried out using Minitab 15 software (trial version).

6.2.5 Confirmatory experiments

The confirmatory experiments were carried out in duplicate at both shake flask and bioreactor level. Glycerol fermentation (for both pure and crude version) at optimized process parameters was initially assessed in 250 mL anaerobic flasks. Next, the fermentation experiment at same conditions (or optimized levels of process parameters) was performed in a 2 L bioreactor (Zenith, India) with working volume of 1 L. Similar to previous experiments, the anaerobic conditions in the fermentation broth were maintained by sparging of 99.98% pure nitrogen at the commencement of fermentation, and thereafter every 24 h. The concentration of immobilized support (3% w/v), and the composition of the fermentation medium were the same as used for earlier experiments (Taguchi design) at shake flask level. The samples were withdrawn for analysis after every 48 h upto a period of 8 days.

6.2.6 Analysis

The concentration of 1,3-PDO, butanol and ethanol in the samples withdrawn from fermentation broth was determined using a gas chromatograph (Varian, Model: 3200) with the help of standard calibration plots. A CP Wax 52CB (250 mm × 0.25 mm × 0.39 mm) capillary column (Varian) was employed with a flame ionization detector. The oven temperature was programmed from 45°C to 100°C with an increment of 3°C/min and after 100°C, an increment of 5°C/min upto 200°C. The injector and detector temperatures were 230°C and 250°C, respectively. The utilization of both pure and crude glycerol was determined by HPLC analysis (Perkin Elmer, Model: Series 200) employing HiPlex-H column (Varian, 300 mm × 5 µm × 4.6 mm), and a refractive index detector. The HPLC grade water (Milli Q) was used as the mobile phase at a flow rate of 0.5 mL/min. The HPLC

analyses were carried out at $37 \pm 2^\circ\text{C}$.

6.3 RESULTS AND DISCUSSION

Before presenting the results, we would like to briefly reproduce the metabolism of glycerol in *C. pasteurianum* as a preamble (details have been given in Chapter 2). *C. pasteurianum* carries out anaerobic fermentation of glycerol simultaneously to 1,3-PDO, butanol and ethanol. The pathway for production of 1,3-PDO is independent of the pathway followed for ethanol and butanol production. 1,3-PDO formation follows the reductive branch of glycerol fermentation, and proceeds by dehydration of glycerol to an intermediate 3-hydroxypropionaldehyde, which is reduced in presence of 1,3-PDO dehydrogenase to 1,3-PDO. On the other hand, production of ethanol and butanol occurs by channeling of glycerol to EMP pathway via substrate level phosphorylation, for formation of an important intermediate pyruvate. Pyruvate so formed converts into acetyl CoA in presence of pyruvate dehydrogenase complex, which is anaerobically converted into ethanol via acetaldehyde formation in presence of ethanol dehydrogenase. Alternatively, acetyl CoA molecule may associate with another molecule of acetyl CoA, thus forming acetoacetyl CoA, which after further transformations eventually forms butanol catalyzed by butanol dehydrogenase. Glycerol is known to be an unconventional substrate for the dehydrogenases described above. The metabolic pathway for production of the three compounds involves a number of enzymes, the activity of which depends on the reaction parameters such as temperature, pH, substrate concentration, etc. Some of these enzymes (especially dehydrogenases) involved in metabolic pathway leading to butanol and 1,3-PDO are susceptible to substrate inhibition. Thus, the study of effect of these parameters on products formation and determination of optimum set of reaction conditions is crucial for efficient design and scale-up of glycerol fermentation process.

Table 6.3A Taguchi analysis of factors affecting total alcohols production by immobilized *C. pasteurianum* with pure glycerol as a carbon source

Level	A	B	C	D
1	– 11.4907	–12.7002	–14.9139	–0.2348
2	–0.4929	–7.0240	–11.6451	–5.4313
3	–	–1.7488	8.5837	–12.3093
Delta S/N (main effect)	10.9978	14.4490	23.4976	12.0745
Percentage Contribution	18.02	23.68	38.51	19.79
Rank	4	2	1	3

Table 6.3B Taguchi analysis of factors affecting total alcohols production by immobilized *C. pasteurianum* with crude glycerol as a carbon source

Level	A	B	C	D
1	–17.9734	–24.7303	–20.3853	–9.5188
2	–5.5427	–11.1207	–16.9299	–9.3903
3	–	0.5769	2.0412	–16.3649
Delta S/N (main effect)	12.4307	25.3072	22.4265	6.9746
Percentage Contribution	18.51	37.69	33.40	10.39
Rank	3	1	2	4

6.3.1 Taguchi analysis

The final concentration of total alcohols formed with different combinations of process parameters in presence of both pure and crude glycerol is depicted in Table 6.3A&B. Significant variation in solvents production with different magnitudes of process parameters indicates the influence of these parameters on bio-alcohols production. The highest concentration of total alcohols was obtained in run 18 for both pure and crude glycerol as substrate. As expected, pure glycerol formed higher concentration of products (17.96 g/L) than crude glycerol (11.84 g/L). This may be attributed to the inhibitory effect of impurities

present in crude glycerol: for example, methanol, soaps, alkali and unconverted oil (Taconi et al., 2009; Khanna et al., 2011). The percentage contribution of each factor on bio-alcohols production from pure and crude glycerol by immobilized *C. pasteurianum* is depicted in Table 6.3A&B, respectively. In order to assess the relative contribution and influence of each parameter on total alcohols production, the parameters were ranked on the basis of delta S/N value. Delta S/N value is the difference between the highest and lowest S/N value for a given factor or parameter. S/N ratio is an important quantity for identifying significant process variables. A high delta S/N ratio for a factor indicates its higher significance over other factors. Taguchi analysis of all four factors showed that all factors have a significant effect (contribution greater than 10%) on fermentation of both pure and crude glycerol by immobilized *C. pasteurianum* cells. The order of significance of parameters on total solvents (or mixed alcohols) production for medium containing pure glycerol was: pH > initial glycerol concentration > temperature > agitation rate. On the other hand, the order of significance for crude glycerol containing medium was: initial glycerol concentration > pH > agitation rate > temperature.

6.3.2 ANOVA results

After identification of significant factors for both pure and crude glycerol fermentation, ANOVA of the experimental results was done to validate these findings, and to quantify the variation in product formation induced by each factor. Tables 6.4A & B depict the ANOVA data for fermentation of pure and crude glycerol, respectively. ANOVA analysis shows that pH and initial glycerol concentration had the most significant effect on total bio-alcohols production for crude glycerol fermentation, while for pure glycerol fermentation, pH was the only significant parameter (indicated by p value < 0.05). Thus, the findings of ANOVA were in concurrence with results of Taguchi analysis.

Table 6.4A ANOVA table for all four significant factors and interaction of factor A and B for pure glycerol fermentation by immobilized *C. pasteurianum* cells

Factors	DF	SS	Adjusted SS	Adjusted MS	F-ratio	p value
A	1	27.347	27.347	27.347	2.20	0.177
B	2	86.248	86.248	43.124	3.46	0.082
C	2	193.383	193.383	96.691	7.77	0.013
D	2	58.406	58.406	29.203	2.35	0.158
A*B	2	4.515	4.515	2.257	0.18	0.838
Residual Error	8	99.605	99.605	12.451		
Total	17	469.503				

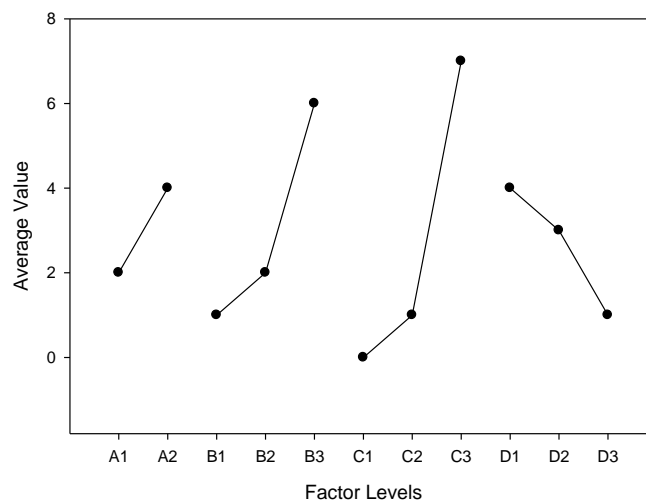
Table 6.4B ANOVA table for the significant factors for crude glycerol fermentation by immobilized *C. pasteurianum* cells

Factors	DF	SS	Adjusted SS	Adjusted MS	F ratio	p value
A	1	10.756	10.756	10.756	1.75	0.183
B	2	53.355	53.355	26.677	4.33	0.029
C	2	92.241	92.241	46.120	7.49	0.005
D	2	27.528	27.528	13.764	2.23	0.106
A*B	8	0.326	0.326	0.163	0.03	0.974
Residual Error	8	49.269	49.269	6.159		
Total	17	233.475				

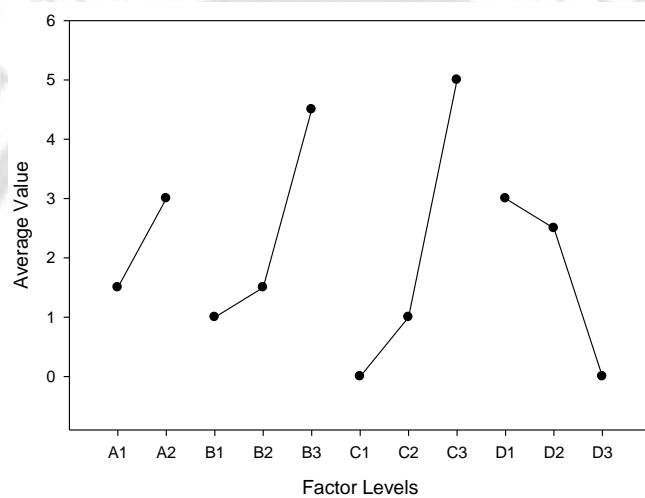
DF = Degree of Freedom, SS = Sum of Squares, MS = Mean of Squares

6.3.3 Selection of optimum levels of factors for enhancing bio-alcohols production

The effect of process parameters (in terms of main effect means) on total alcohols production with pure and crude glycerol is depicted in Fig. 6.1A and B, respectively. It can be perceived from results depicted in Fig. 6.1A & B that products formation is a function of the level of the parameter and shows significant variation with the level of that parameter.



(A)



(B)

Figure 6.1 Main effect mean plots of process variables with: (A) pure glycerol and, (B) crude glycerol

The total alcohols production from pure glycerol was more at level 1 for factor D (temperature), while for factors A (agitation speed), B (glycerol concentration) and C (pH), higher product formation was observed at the highest level (level 3). Quite interestingly, this trend was consistent for fermentation media containing both pure and crude glycerol as the substrate. This is a very interesting result from viewpoint of design and scale up of the process, as it demonstrates that the physics and physiology of the glycerol fermentation is

relatively independent of the type of glycerol used. The optimized sets of values of parameters for products formation for both pure and crude glycerol are: (1) pH = 7.0, (2) initial glycerol concentration = 25 g/L, (3) temperature = 30°C and (4) agitation rate = 200 rpm. These sets of optimized fermentation parameters were further investigated in confirmatory experiments as described below.

6.3.4 Confirmatory experiments

The confirmatory experiments were carried out at both shake flask and bioreactor levels for both pure and crude glycerol containing media. The total concentration of solvents or mixed alcohols formed under optimized fermentation conditions was predicted using following equation (Sirisansaneeyakul et al., 2007):

$$Y_{opt} = T_i + \sum (F_{i,avg} - T_{i,avg}) \quad (6.1)$$

where, T = average of all trial results/ average of performance, i = significant factors, F_i = average effect of significant factors at each level. The calculations were done separately for pure and crude glycerol fermentation for all 4 factors that were found to be significant (as per the S/N ratio in Taguchi analysis). Thus, equation 1 can be rewritten in the context of present study as:

$$Y_{opt} = T + |A_1 - T| + |A_2 - T| + |B_1 - T| + |B_2 - T| + |B_3 - T| + |C_1 - T| + |C_2 - T| + |C_3 - T| + |D_1 - T| + |D_2 - T| + |D_3 - T| \quad (6.2)$$

The predicted values of total bio-alcohols concentration formed from pure and crude glycerol under optimized fermentation conditions were 20.52 and 18.26 g/L, respectively. The trends in production of 1,3-PDO, ethanol and butanol in shake flask experiments under optimized fermentation conditions with pure glycerol is depicted in Fig. 6.2A. The final concentrations of ethanol, 1,3-PDO and butanol formed from pure glycerol fermentation in shake flask were 1.94, 9.23 and 7.73 g/L, respectively. The total concentration of products was 18.90 g/L, which was close to the predicted value of 20.50 g/L.

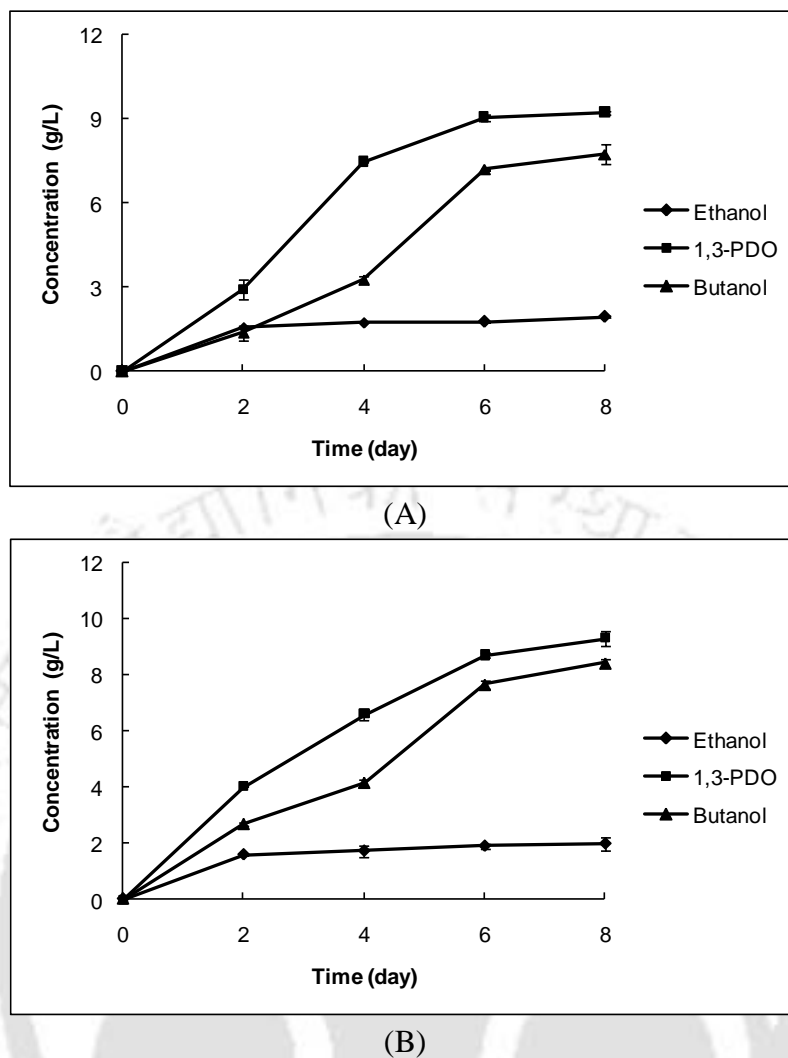
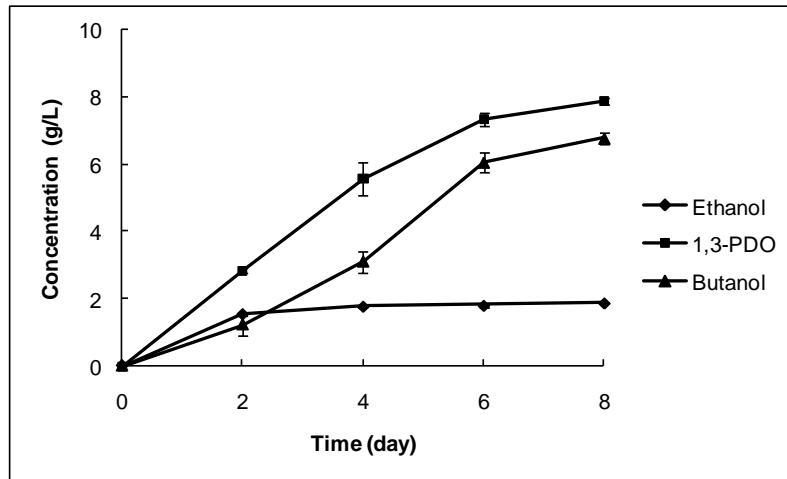
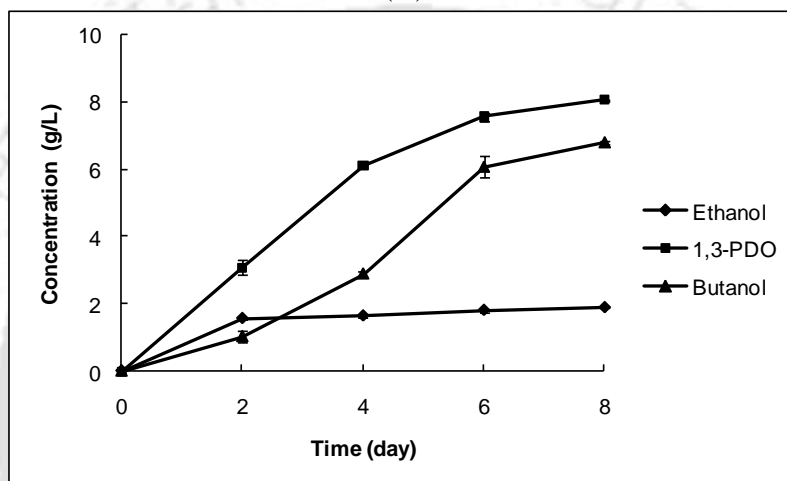


Figure 6.2 Trends in production of ethanol, butanol and 1,3-PDO under optimized fermentation conditions with pure glycerol as substrate in (A) anaerobic shake flask, and (B) bioreactor. The total product concentration after completion of fermentation in shake flask and in bioreactor was 18.9 and 19.7 g/L, respectively

Fig. 6.2B depicts the trends in production of the three fermentation products, in a bioreactor under optimized fermentation conditions. The final concentrations of ethanol, butanol and 1,3-PDO in a bioreactor were calculated as 1.98, 9.30 and 8.42 g/L, respectively. The total concentration of products formed after 10 days of fermentation was 19.70 g/L, which was higher than the concentration formed in shake flask, and close to the value predicted by the model.



(A)



(B)

Figure 6.3 Trends in production of ethanol, butanol and 1,3-PDO under optimized fermentation conditions with crude glycerol as substrate in (A) anaerobic shake flask, and (B) bioreactor. The final total product concentration in shake flask and in bioreactor was 16.54 and 16.75 g/L, respectively

Fig. 6.3A illustrates the trends in production of the three products with crude glycerol as a substrate in shake flasks. Fig. 6.3B depicts the production profile of the three solvents with crude glycerol as a substrate in a bioreactor. The individual concentrations of ethanol, 1,3-PDO and butanol formed in shake flask were 1.87, 7.89 and 6.78 g/L respectively, while those in bioreactor were 1.89, 8.06 and 6.80 g/L, respectively.

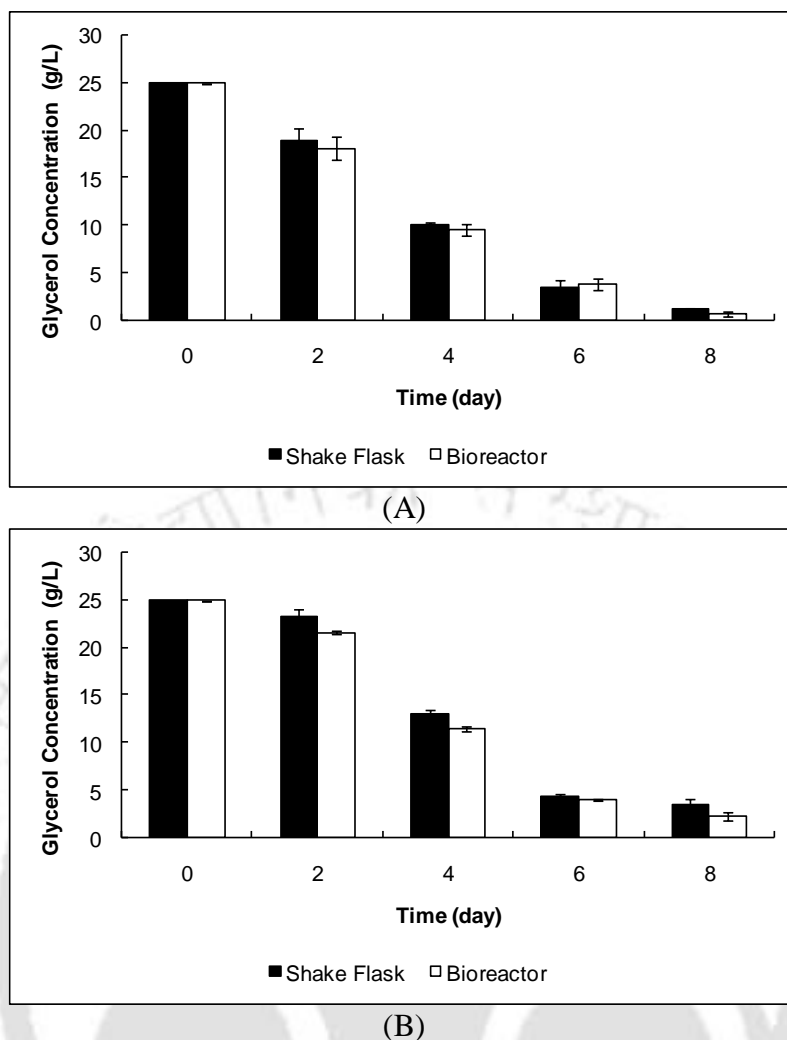


Figure 6.4 Comparison of uptake of glycerol in shake flask and in a bioreactor under optimized fermentation conditions with (A) pure glycerol as a substrate, and (B) crude glycerol as a substrate

The total concentration of products formed was similar in shake flasks (16.54 g/L) and in bioreactor (16.75 g/L), both of which were close to the predicted value (18.26 g/L). The proximity of the experimental results obtained under optimized fermentation conditions with the predicted value (as per equation 6.2) indicates the fitness of Taguchi model for the analysis of process of glycerol bioconversion. Figs. 6.4A and B depict pure and crude glycerol uptake with time in shake flasks and bioreactor under optimized set of fermentation parameters, respectively. As is evident from these figures, a higher concentration of pure

glycerol was taken up than crude glycerol in both shake flask and bioreactor level experiments. This may be attributed to the impurities present in crude glycerol particularly methanol, which alters the membrane permeability, thereby decreasing the uptake of glycerol by the cells. However, the uptake of glycerol (whether crude or pure) was almost same in shake flask and bioreactor. This result is in concurrence to our previous result on total product formation in shake flask and bioreactor. This indicates that under optimum process conditions, the substrate consumption as well as product formation is independent of the scale of operation. This result is also very crucial from viewpoint of scale up of the process.

The reusability of immobilized biocatalyst in pure and crude glycerol containing medium is shown in Fig. 6.5A and B, respectively. A consistent decrease in concentration of all three products was observed with an increase in number of fermentation cycles for both pure and crude glycerol fermentation. In case of crude glycerol, the bio-catalytic activity decreased to around 50% after 4 cycles, while for pure glycerol the immobilized biocatalyst retained its catalytic potential (greater than 50%) even after 5 fermentation cycles. This result indicates the adverse effect of impurities present in crude glycerol on cellular metabolism.

An analysis of the results vis-à-vis the metabolic pathway of glycerol conversion gives interesting insight into the links between the physics and physiology of the process. The process parameters used for optimization of glycerol (either pure or crude) fermentation have significant influence on the growth of microbial cultures as well as metabolism of the substrate, and this influence is essentially manifested in terms of extent of product formation for a given set of fermentation conditions. We have briefly described the specific effect of each process parameter on the fermentation process. The temperature of fermentation influences the growth and glycerol metabolism of *C. pasteurianum*, as the enzymes involved in metabolic cycle are known to have an optimum temperature for maximum activity.

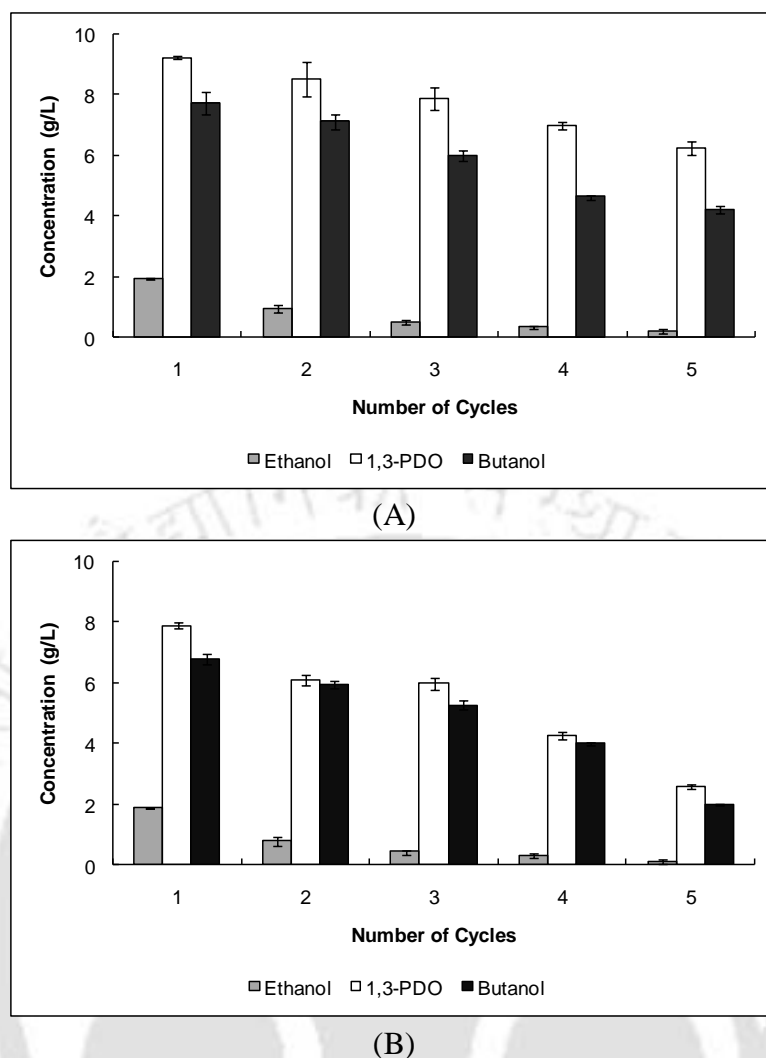


Figure 6.5 Recyclability study of immobilized biocatalyst in presence of (A) pure glycerol, and (B) crude glycerol. Immobilized biocatalyst retained its catalytic potential for more number of fermentation cycles in pure glycerol containing medium than crude glycerol containing medium

At low temperature, the enzymes remain active, while high temperatures denature the enzyme. The concentration of glycerol is an important factor, as our earlier studies have revealed that high concentrations of glycerol (typically above 25 g/L) prohibit the formation of products due to substrate inhibition of dehydrogenases involved in metabolic pathway. Agitation rate is known to affect the mass transfer in chemical and biological systems. In the present study, agitation rate is expected to increase the rate of diffusion of glycerol into the

cells, and rate of diffusion of products out of the cell. Finally, pH plays crucial role in regulation of metabolism of glycerol (Dabrock et al., 1992). The effect of pH is attributed to life cycle of solvent producing Clostridia, which consists of two phases, viz. acidogenic phase and solventogenic phase. These phases are tightly regulated by the pH of the fermentation broth. Acidogenic phase usually occurs during the log phase of the growth, wherein the bacteria produces acids such as acetate, butyrate, lactate, which decreases the pH of the fermentation broth. The pH drop so obtained affects the permeability of cell membrane for accumulated acids, and thus, the acids start diffusing inside the bacterial cell. During the stationary growth phase, solventogenesis occurs wherein, the cells utilize the accumulated acids to form solvents like ethanol and butanol that leads to increase in the pH of the fermentation broth. A decrease in external pH acts as a trigger for solventogenesis (Maddox et al., 2000). The macroscopic manifestation of influence of pH on the growth and metabolism of the cells is the variation in yield and selectivity of the products of fermentation. The well-known ABE fermentation with *Clostridium acetobutylicum* in batch mode at constant medium pH of 7.0 is inhibited by high concentrations of acids formed during fermentation (Maddox et al., 2000). A similar effect is also seen in glycerol fermentation by *C. pasteurianum*. Thus, batch fermentation without pH control (with fermentation broth at initial neutral pH) allows the cells to follow their normal acidogenic–solventogenic cycle, which is the desired mode of operation for high solvents yield. High initial pH of fermentation broth is favorable for solvent production, as it decreases the lag time of the culture, while low initial pH increases the lag time, and hence, causes delay in acidogenic to solventogenic phase shift of fermentation, as shown in study of Khanal et al. (2004).

6.3.5 Analysis of results and comparison with previous literature

The results of this study, i.e. the optimum values of all 4 process parameters, are very

much in consistence with the contemplations presented above. Among the three temperatures used in this study, the optimum yield was obtained at fermentation temperature of 30°C, which as per the database of microbial culture bank is, the optimum temperature for growth of the microbial culture. The optimum initial pH of the medium is 7.0, which is neutral. The highest agitation rate of 200 rpm (which eliminated the mass transfer limitations), and the highest glycerol concentration (prior to induction of substrate inhibition of dehydrogenases) of 25 g/L were the optimum values of these parameters.

For fermentation of pure glycerol, pH was the most significant process parameter. On the other hand, for crude glycerol fermentation, the initial concentration of glycerol was also a significant factor in addition to pH. High concentration of crude glycerol will also increase the concentration of impurities in the medium, which also have inhibitory effect (even at low concentrations) on the fermentation process (Khanna et al., 2011). As for the pure glycerol, the only possible inhibition is the substrate inhibition, which occurs at relatively high values of glycerol concentration (> 25 g/L) than used in this study, and hence, the effect of concentration is not as marked as in case of crude glycerol. Comparison of results obtained in present study with earlier published literature on bioconversion of glycerol with free cells, depicted in Table 6.5, reveals interesting aspects of dependence of glycerol fermentation on process parameters. We would like to specifically mention that there is no previously published study on glycerol bioconversion with immobilized cells, and a direct quantitative comparison of our results with previous literature is not possible. The highest total solvent yield (0.91 mol/mol) during fermentation of pure glycerol by free cells is reported by Taconi et al. (2009). The yield obtained in present study (0.82 mol/mol) after process optimization was lower, and we attribute this result to use of immobilized cells. However, for crude glycerol fermentation, an opposite trend is seen.

Table 6.5 Comparison of the maximum yields and selectivity of products obtained in the current work with published literature

References	Process Parameters (pH, rpm, temperature, initial glycerol concentration)	Pure Glycerol				Crude Glycerol			
		Ethanol	Butanol	1,3-PDO	Total Yield	Ethanol	Butanol	1,3-PDO	Total Yield
Heyndrickx et al. (1991)	10 g/L	0.01 (0.02)	0.11 (0.23)	0.36 (0.75)	0.48	–	–	–	–
Dabrock et al. (1992) (under Fe limitation)	pH 7.0, 160 rpm, 40 g/L	0.04 (0.08)	0.12 (0.24)	0.34 (0.68)	0.50	–	–	–	–
Biebl (2001)	pH 7.0, 30°C, 50 g/L	0.14 (0.25)	0.20 (0.36)	0.21 (0.38)	0.55	–	–	–	–
Taconi et al. (2009)	pH 7.0, 35°C, 25 g/L	0.05 (0.05)	0.39 (0.43)	0.47 (0.52)	0.91	0.13 (0.22)	0.37 (0.64)	0.08 (0.14)	0.58
Free cells (Chapter 3)	pH 7.0, 37°C, 5 g/L, 200 rpm	0.06 (0.06)	0.19 (0.30)	0.38 (0.64)	0.63	0.04 (0.07)	0.08 (0.21)	0.25 (0.72)	0.37
Silica immobilized cells after preliminary optimization (Chapter 3)	pH 7.0, 37°C, 25 g/L, 200 rpm	0.09 (0.10)	0.11 (0.20)	0.37 (0.70)	0.57	0.06 (0.09)	0.07 (0.16)	0.31 (0.75)	0.44
Medium optimization (Chapter 5)	pH 7.0, 37°C, 25 g/L, 200 rpm	0.12 (0.10)	0.18 (0.25)	0.45 (0.65)	0.75	–	–	–	–
Process optimization (This chapter)	pH 7.0, 30°C, 25 g/L, 200 rpm	0.16 (0.13)	0.21 (0.27)	0.45 (0.60)	0.82	0.15 (0.14)	0.17 (0.26)	0.39 (0.60)	0.71

All yields are in mole of product formed per mole glycerol added (or initial concentration), while selectivity is on the basis of glycerol converted

In this case, our total solvent yield (0.71 mol/mol) is higher than that reported by Taconi et al. (2009) for free cells (0.58 mol/mol). This result indicates higher tolerance of immobilized cells (as compared to free cells) towards inhibitors present in crude glycerol. As far as results of other published studies are concerned, these are with pure glycerol only, and the yields of our experiment are higher than the previously reported values.

6.4 CONCLUSIONS

In this chapter, we have presented our results on optimization of the fermentation process for production of mixed alcohols (1,3-PDO, ethanol and butanol) from pure and crude glycerol. The results indicate significant rise in the solvent production after optimization of the process in terms of 4 parameters, viz. pH, agitation rate, temperature and initial glycerol concentration. Analysis of the optimization results vis-à-vis the metabolic pathway of glycerol bioconversion reveals important links between the physics and physiology of the system. We believe that results of this study will give important input for the design and optimization of a large scale process for glycerol fermentation to value-added products.

ULTRASOUND ENHANCED BIOCONVERSION OF GLYCEROL BY FREE CELLS: MECHANISTIC ISSUES

7.1 INTRODUCTION

As stated in Chapter 2, there are two principal routes for conversion of glycerol into value added products, viz. catalytic conversion and biochemical conversion. For greater details on catalytic conversion of glycerol we refer the reader to the review by Zheng et al. (2008), while chapter 2 of this thesis gives the details of literature published in the area of bioconversion of glycerol to diverse products. Comparing among the two routes for glycerol conversion, the biochemical route shows better potential over the catalytic route, due to the latter's harsh operating conditions of temperature and pressure, lower selectivity and use of expensive catalyst. Microbial conversion of glycerol has merits such as requirement of cheaper biological catalysts, which operate at ambient conditions and higher selectivity, which makes this route more economical and environmental friendly than catalytic route. The principal

demerit of bioconversion of glycerol (like all other fermentation processes) is, however, slow kinetics. Enhancement of the kinetics of the biochemical processes is key to effective scale-up of these processes, and is thus, an important aspect of the process development for microbial glycerol conversion. In this chapter, we have addressed this important issue of the process development chain.

A possible remedy for enhancement of biochemical processes is application of ultrasound. Numerous authors have used ultrasound to enhance kinetics and yield of variety of biochemical processes (Bar, 1988; Zabaneh and Bar, 1991; Chuanyun et al., 2003; Chisti, 2003; Sulaiman et al., 2011). An excellent review of ultrasound-assisted biochemical processes is given by Gogate and Kabadi (2009).

Most of the biochemical processes (especially those employing immobilized cultures) are mass transfer limited operations, and the yield as well as kinetics of these processes increases with the level of convection or turbulence in the system. Ultrasound and its secondary effect, cavitation, which is nucleation, growth and implosive collapse of tiny gas bubbles (induced by bulk pressure variation during passage of ultrasound wave) can induce high intensity convection in the medium through various mechanisms such as micro-streaming, micro-convection, acoustic (or shock) waves and microjets developed during asymmetric collapse of bubbles. Although the overall convection generated in the medium is a resultant of all of these mechanisms, the physical nature of these mechanisms is different. Micro-streaming (oscillatory motion of fluid elements induced by ultrasound) and micro-convection (motion of liquid in vicinity of gas-liquid interface or bubble wall induced radial motion of bubble) are essentially continuous phenomena, while shock waves (waves generated due to reflection of converging liquid at bubble wall during collapse) and micro-jets (high velocity liquid jet generated due to uneven pressure gradient around bubble in the vicinity of an interphase boundary) are discrete in nature. In the previous studies published from our group

(Moholkar et al., 2004; Midathana and Moholkar, 2009; Chakma and Moholkar, 2011), it was revealed that ultrasound and cavitation do not alter the equilibrium characteristics of the system, but only intensify mass transfer rates in the direction of concentration gradient, which is a sort of catalytic action. It is due to the differences in the nature of these convection mechanisms that not all of them render beneficial influence on the process, as also revealed in our previous studies (Midathana and Moholkar, 2009; Chakma and Moholkar, 2011; Patidar et al., 2012). In the context of present study, shock waves and microjets can cause disruption of microbial cells or denaturing of enzyme, which adversely affects the process (Doulah, 1977; Chisti and Moo-Young, 1986; Save et al., 1994; Jyoti and Pandit, 2001; Patidar et al., 2012). However, with moderation in the operating conditions like raising the static pressure in the medium, these adverse effects can be avoided (Patidar et al., 2012), as discussed in detail in subsequent sections.

In this chapter, we have presented our results on investigation of ultrasonic enhancement of glycerol bioconversion from mechanistic viewpoint. To simplify the overall problem, in this initial study (which essentially is an assessment of option of ultrasound for enhancing bioconversion kinetics), we have used the free cells of *Clostridium pasteurianum* (instead of immobilized cells). Our aim in this study is two-fold; first, to assess the extent of enhancement of yield, selectivity and kinetics of glycerol bioconversion with ultrasound, and secondly, to get a physical insight into the exact mechanism of this enhancement. In view of this, we have taken approach of coupling experimental results with simulations of cavitation bubble dynamics (using a mathematical model), and the results of enzyme kinetic analysis. As revealed in subsequent sections of this chapter, our analysis has brought forth several interesting mechanistic aspects of ultrasound enhanced glycerol bioconversion.

7.2 MATERIALS, METHODS & SIMULATIONS

7.2.1 Micro-organism, growth and maintenance

Clostridium pasteurianum MTCC 116 (ATCC 6013) was procured from Microbial Type Culture Collection, Chandigarh, India. The lyophilized cells were revived in Cooked Meat Media (CMM) agar slants, which were kept in an anaerobic tray system (Himedia, India) at 37°C for 24 h in an incubator. The revived cells on CMM agar slants were kept at 4°C and were sub-cultured every month. This stock culture was used throughout for inoculum preparation. Agar plates were prepared from CMM agar slants. 250 mL specially fabricated Erlenmeyer flask was filled with sterilized 100 mL Reinforced Clostridial Media (RCM) containing yeast extract (3 g/L), beef extract (10 g/L), peptone (10 g/L), NaCl (5 g/L), CH₃COONa (3 g/L), glucose (5 g/L), cysteine hydrochloride (0.5 g/L), soluble starch (1 g/L) and agar (0.5 g/L) and was inoculated with single colony from the agar plate. The initial pH of the media was adjusted to 6.8 ± 0.2. Agar was added to the broth to enhance the thickness of the media so that less of oxygen diffuses in it. The flask was kept at 120 rpm and 37°C in an orbital shaker incubator for 24 h. The broth was sparged with nitrogen gas before incubation to ensure anaerobic conditions inside the flask. 10% v/v of this broth was used as an inoculum for carrying out fermentation of glycerol. Fermentation of glycerol was carried out in fermentation media containing KH₂PO₄ (0.5 g/L), K₂HPO₄ (0.5 g/L), CaCO₃ (2 g/L), MgSO₄·7H₂O (0.2 g/L), CaCl₂·2H₂O (0.02 g/L), FeSO₄·7H₂O (0.005 g/L), (NH₄)₂SO₄ (3 g/L), yeast extract (1 g/L), and SL₇ trace element solution (2 mL/L). The composition of SL₇ trace element solution is as follows: MnCl₂·4H₂O (0.1 g/L), ZnCl₂ (0.07 g/L), H₃BO₃ (0.06 g/L), NaMoO₄·2H₂O (0.04 g/L), CoCl₂·2H₂O (0.02 g/L), CuCl₂·2H₂O (0.02 g/L), NiCl₂·2H₂O (0.02 g/L), 25% HCl (1 mL/L). Glycerol was autoclaved separately. 5, 10 and 25 g/L of glycerol concentration were added to the fermentation medium. All chemicals used were of analytical grade and were purchased from Merck, Germany, Himedia, India and Sigma Aldrich, USA.

7.2.2 Apparatus and reaction setup

Ultrasonic irradiation of the glycerol fermentation mixture was carried out in a sonic bath (Make: Elma, Germany; Model: Transonic T-460, 2L) operating at a frequency of 35 kHz and rated power input of 35 W. A schematic diagram of the experimental set up is shown in Fig. 7.1. The total working volume of the bath (dimensions: 25 × 15 × 10 cm) was 2 L with transducers attached to the bottom of the bath. During sonication, the bath was filled with water, which formed the medium for the transmission of ultrasound waves to the reaction mixture. Experiments were carried out in a 15 mL test tube made of borosilicate glass, fitted with cork. The test tube containing fermentation broth was placed at a specific location in the central region of the ultrasound bath, and the test tube was immersed to about 75% of its length in water. The temperature of the water in the bath was maintained at 37°C. The pressure in the test tube was maintained at 2 bar with the help of 99.98% pure nitrogen gas (same gas was used for sparging the flasks). The rationale underlying raising of static pressure of the fermentation mixture will be explained in the subsequent section. An added merit of having high pressure nitrogen atmosphere on the fermentation mixture was that it helped in maintaining perfectly anaerobic conditions inside the test tube conducive for *C. pasteurianum* cells. The control experiments were carried out in test tube of similar dimension and volume as used in case of experiments with ultrasound irradiation, except that the pressure inside the test tube was atmospheric (1 bar). The tube was kept in an incubator shaker (Make: Scigenics, India, Model: Orbitek) at 37°C and 150 rpm. Aliquots of fermentation broth in both test and control experiments were withdrawn after every 6 h upto a total period of 24 h. In case of ultrasound assisted experiments, high pressure in the test tube was released during withdrawal of the sample, and was restored when the test tube was placed back in the ultrasound bath.

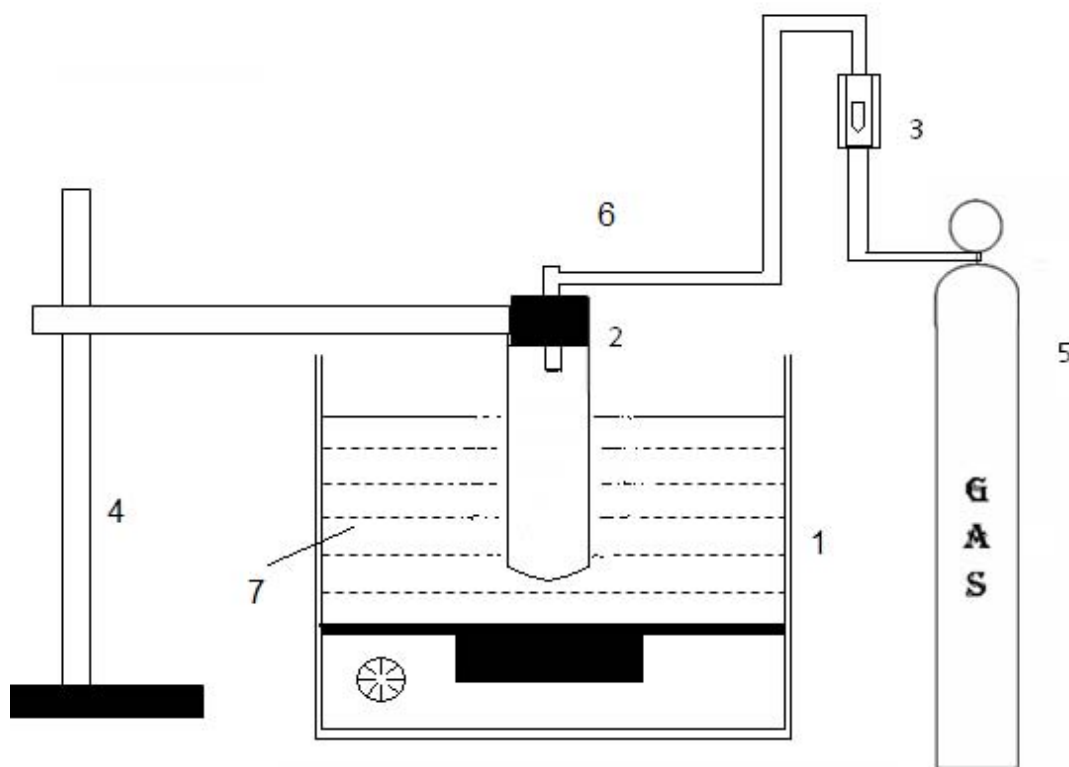


Figure 7.1 Schematic diagram of the experimental setup (Legends: (1) Ultrasound bath; (2) Test tube containing glycerol fermentation mixture; (3) Rotameter for control of gas flow; (4) Burette stand and test tube holder; (5) Nitrogen cylinder; (6) Connection of the gas to the rubber cork covering test tube)

All experiments were carried out in triplicate and the results presented are the means of three data sets with the error bars depicting standard deviations. The analysis of variance (ANOVA) of both 1,3-PDO and ethanol production in test and control experiments was carried out using Minitab 15 statistical software (Trial Version).

7.2.3 Analytical methods

The analytical standards for gas chromatographic analysis and HPLC analysis were purchased from Sigma Aldrich, USA and Merck, Germany. The fermentation products and their quantities were determined using Gas Chromatograph (Varian, CP 3800). 1 μ L of supernatant from centrifuged fermentation broth was injected in a CP Wax 52 CB capillary column (250 mm \times 0.25 mm \times 0.39 mm, Varian). The oven temperature was programmed

from 45 to 100°C with an increment of 3°C/min and after 100°C, an increment of 5°C/min upto 200°C. The injector and detector temperatures were 230 and 250°C, respectively. Nitrogen gas was used as a carrier at a flow rate of 2 mL/min. The utilization of glycerol by *C. pasteurianum* cells was determined by HPLC analysis. The HPLC apparatus comprised of a pump (Series 200, Perkin Elmer), a refractive index detector (Series 200, Perkin Elmer), a vacuum degasser (Series 200, Perkin Elmer) and a HiPlex-H column (300 mm × 5 µm × 4.6 mm, Varian). HPLC grade water (Milli Q) was used as the mobile phase at a flow rate of 0.5 mL/min. The HPLC analyses were carried out at 37±2°C. Samples were filtered through a 0.2 µm membrane filter, and diluted appropriately prior to analysis. Standard calibration plots were used for all calculations.

Morphological changes of *C. pasteurianum* cells in both control (without sonication) and test samples (with sonication) were investigated by Flow cytometry (BD FACS caliber). Flow cytometric analysis of both control and sonicated cells was done using 488 nm laser and 530 nm emission filter. FSC (Forward Scatter) and SSC (Side Scatter) were used to evaluate the morphological changes in the cells. The morphology of the cells (stained by Grams' method) before and after sonication was also observed under a Nikon light microscope (Model: Eclipse E200, Japan) equipped with a CCD Camera (Model: DS Fi 1).

7.2.4 Simulations of cavitation bubble dynamics

Ultrasound, which essentially is the acoustic wave with frequency higher than the upper limit of human audible range (16 kHz), is well-known as a tool for enhancement of diverse physical, chemical and biological processes (Suslick, 1988; Mason and Lorimer, 1989, Shah et al., 1999). Most of the physical and chemical effects of ultrasound are attributed to phenomenon of cavitation, which is nucleation, growth and implosive transient collapse of gas bubbles under the influence of variation in the static (or bulk) pressure in the medium induced by propagation of the ultrasound wave, which is essentially a longitudinal wave comprising of

alternate compression / rarefaction cycles.

Theoretically, cavitation phenomenon involves creation of voids in the liquid. With progression of sound wave in the medium, the molecules of the liquid oscillate about mean position. In the compression phase, the distance between the molecules decreases, while during rarefaction the molecules are pulled apart and the distance between them increases. If the amplitude of the acoustic wave is large enough, the distance between molecules may exceed the critical distance to hold the liquid intact (also known as van der Waal's distance), resulting in creation of voids. Typically, this pressure amplitude required for this phenomenon is $2\sigma/R$, where σ is the surface tension and R is the van der Waal's distance. For water, the values are $\sigma = 0.072$ N/m and $R = 4 \times 10^{-10}$ m. Thus, the theoretical pressure amplitude required for creation of void is ~ 1500 atm. However, actual cavitation phenomenon occurs at far lower pressure amplitude. This is attributed to the phenomenon of nucleation. Nucleation occurs due to presence of solid particles, or tiny free-floating bubbles present in the liquid that act as weak spots. Another source of nucleation is the gas pockets trapped in the crevices of the solid boundaries in the medium. These solid boundaries could be walls of the reactor or tip of the ultrasound horn.

With bulk pressure variation induced by ultrasound, these nuclei or gas pockets expand to form cavitation bubbles, as the local pressure in the liquid medium falls below ambient pressure in the rarefaction half cycle of ultrasound. In the subsequent compression half cycle of ultrasound, the bubble undergoes compression. These volume oscillations of the bubbles are in phase with bulk pressure variation, if the pressure amplitude of the ultrasound (or acoustic) waves is low (i.e. below the transient cavitation threshold, which typically equal to the static pressure imposed on the system). For higher acoustic pressure amplitude (above the transient cavitation threshold), the inertial forces dominate the volume oscillations (or radial motion) of the bubbles. In this case, the bubble keeps on expanding even after the rarefaction cycle is

completed. Moreover, the expansion is more than twice the original size. In the subsequent compression cycle, rapid spherical convergence of fluid elements imparts high kinetic energy to the bubble. The velocity of the bubble wall (or gas–liquid interface) can reach or even exceed the sonic speed in liquid medium. The compression of the bubble is adiabatic, and temperatures and pressures in the bubble reach extreme (~ 5000 K, ~ 500 bar) (Brenner et al., 2002). The radial motion of the bubble also gives rise to strong convection in the medium through two principal physical effects, viz. microturbulence and acoustic (or shock) waves. A direct measurement of the magnitude of these effects is beyond the capabilities of the instrumentation used in this study, and hence, we rely on numerical simulations of radial motion of the cavitation bubbles to estimate magnitude of these phenomena under different experimental conditions. In the context of the present study, shockwaves of high amplitude emitted by transient cavitation bubbles are detrimental for bioconversion of glycerol, as these can cause disruption of microbial culture.

A solution to this problem is to raise the static or ambient pressure in the medium above the pressure amplitude of the ultrasound wave (Moholkar et al., 2004; Patidar et al., 2012), due to which the transient motion of the cavitation bubbles is transformed into a stable oscillatory motion. The cavitation bubble still emits shock waves in stable oscillatory motion, but the amplitude of these waves is far reduced, so as not to cause any damage to the microbial culture. It is for this reason that we have raised static pressure in the experimental test tube to 2 bar. For our analysis, we have chosen the following bubble dynamics equation (Leighton, 1994; Lofstedt et al., 1995; Hilgenfeldt et al., 1996; Barber et al., 1997) which is essentially a modified form of the original Rayleigh–Plesset equation (Plesset, 1949) with inclusion of the compressibility effect (Keller and Miksis, 1980; Prosperetti and Lezzi, 1986).

$$R \frac{d^2 R}{dt^2} + \frac{3}{2} \left(\frac{dR}{dt} \right)^2 = \frac{1}{\rho} (p(R,t) - P_0 - P(t)) + \frac{R}{\rho c} \frac{d}{dt} [p(R,t) - P(t)] - \frac{4\mu}{\rho R} \frac{dR}{dt} - \frac{2\sigma}{\rho R} \quad (7.1)$$

Notations are as follows: R = radius of the bubble; dR/dt = velocity of bubble wall; P_0 = ambient or static pressure in liquid; ρ = density of liquid; c = sonic speed in liquid; μ = viscosity of the liquid; σ = surface tension of liquid. $p(R,t)$ and $P(t)$ denote pressures inside the cavitation bubble and the time variant pressure of the acoustic wave, respectively; and are written as:

$$p(R,t) = \left(P_0 + \frac{2\sigma}{R_0} - P_v \right) \left(\frac{R_0^3 - h^3}{R^3 - h^3} \right)^v + P_v \quad (7.2)$$

$$P(t) = P_A \cos(2\pi ft) = P_A \cos(\omega t) \quad (7.3)$$

Various notations are as follows: R_0 = initial or equilibrium radius of the bubble; P_0 = vapor pressure of bulk liquid; h = van der Waal's hard core radius; r = polytropic constant of bubble content; P_A = pressure amplitude of ultrasound wave; f = frequency of ultrasound wave; ω = angular frequency of ultrasound waves. With substitution as $dR/dt = s$, equation 7.1 can be split into two simultaneous ordinary differential equations. The numerical solution of these equations (basically time series of R and dR/dt) could be obtained using Runge–Kutta adaptive step size method (Press et al., 1992). Magnitude of velocity of the microturbulence $u(r,t)$ and pressure amplitude of the shock waves $P_s(r,t)$ can be calculated using the solution of equation 1 as follows (Young, 1989; Grossmann et al., 1997):

$$u(r,t) = \frac{R^2}{r^2} \left(\frac{dR}{dt} \right) \quad (7.4)$$

$$P_s(r,t) = \rho \frac{R}{r} \left[2 \left(\frac{dR}{dt} \right)^2 + R \frac{d^2 R}{dt^2} \right] \quad (7.5)$$

where r is the distance from bubble centre.

Simulation parameters: Various physical parameters and physical properties of the

fermentation mixture are required for numerical solution of the bubble dynamics model. Values of these parameters / properties have been either taken from literature or measured experimentally. For three parameters, viz. vapor pressure, density of fermentation mixture and sonic velocity through fermentation mixture, we have used values for pure water, as the concentration of glycerol in the fermentation mixture is relatively low to cause any major change in these parameters. The numerical values of all parameters are listed below:

Frequency of the ultrasound waves (f) = 35 kHz (same as the frequency of the sonic bath); P_A = 1.5 bar (estimated using calorimetric techniques (Sivasankar et al., 2007)); R_0 = 5 μm (taken as representative value (Metin et al., 1997)); γ = 1/3 (polytropic constant of air); h (van der Waal's hard core radius) = $R_0/8.86$; r = 100 μm (taken as representative value); c = 1481 m/s (for water); σ = 58.6 mN/m (for 5 g/L glycerol), 61.5 (for 10 g/L glycerol) and 66.8 mN/m (for 25 g/L glycerol); ρ = 1000 kg/m³ (for water); T = 310 K (or 37°C); μ = 7.4×10^{-4} Pa-s (5 g/L glycerol), 8.26×10^{-4} Pa-s (10 g/L glycerol) and 12.65×10^{-4} Pa-s (25 g/L glycerol). The vapor pressure (P_v) of water has been calculated using Antoine type correlation (NIST Data Gateway, 2011).

7.2.5 Enzyme extraction and kinetic study

The enzymes ethanol dehydrogenase and 1,3-PDO dehydrogenase were extracted from *C. pasteurianum* cells immobilized on silica gel. The activities of both the enzymes in test (with ultrasound) and in control experiments were determined. The protocol followed for this is as follows: The cells immobilized on silica support were centrifuged at 6000 rpm for 15 min. The immobilized cells were suspended in 50 mM phosphate buffer (pH 7.5) and sonicated in ice bath for 6 cycles (30 s on / 10 s off). The supernatant so obtained was separated from the support and cell lysate by centrifugation at 6000 rpm for 10 min. This supernatant was tested for 1,3-PDO dehydrogenase and ethanol dehydrogenase activity. The activity of 1,3-PDO dehydrogenase in the supernatant was determined by monitoring the increase in NADH

concentration at 340 nm using a UV–Vis spectrophotometer (Make: Perkin Elmer, Model: Lambda 3). The assay mixture (1 mL final volume) for 1,3–PDO dehydrogenase had following constitution: 100 mM glycerol, 2 mM NAD⁺, 30 mM ammonium sulfate and 10 mM potassium carbonate buffer (pH 9.7) (Malaoui and Marczak, 2000). Similar to 1,3–PDO dehydrogenase activity determination, the activity of ethanol dehydrogenase was also calculated by monitoring the absorbance at 340 nm, indicative of conversion of NAD⁺ to NADH. The assay was carried out according to the protocol given by Kato et al. (1984). The assay mixture consisted of 10 mM NAD⁺, 20 mM glycerol and 10 mM glycine–NaOH buffer (pH 9.0).

The nature of influence of ultrasound on fermentation process was assessed using enzyme kinetics models. A simple metabolic pathway for bioconversion of glycerol to 1,3–PDO and ethanol is given in Figs. 7.2A and 7.3A, respectively, along with names of enzymes involved in the process. It could be seen that from these schemes that metabolic pathway for 1,3–PDO involves only one intermediate, while ethanol pathway has multiple intermediates. The major difference among the two pathways is that 1,3–PDO production is inhibited by substrate (glycerol) as well as 3–hydroxypropionaldehyde (3–HPA), which is an intermediate of 1,3–PDO production pathway, while no such effect is seen in metabolic pathway for Ethanol (Barbirato et al., 1996; Reed et al., 2010). We, therefore, adopt Michaelis–Menten reaction scheme (depicted in Fig. 7.2B) for bioconversion of ethanol, while the substrate inhibition reaction scheme (depicted in Fig. 7.3B) is adopted for bioconversion of 1,3 PDO (Haldane, 1930). Kinetic expression for Michaelis–Menten reaction scheme is:

$$V = \frac{k_2 E_o [S]}{K_m + [S]} = \frac{V_{\max} [S]}{K_m + [S]} \quad (7.6)$$

Notation: k_1 , k_{-1} , k_2 – kinetic constants, K_m – Michaelis constant.

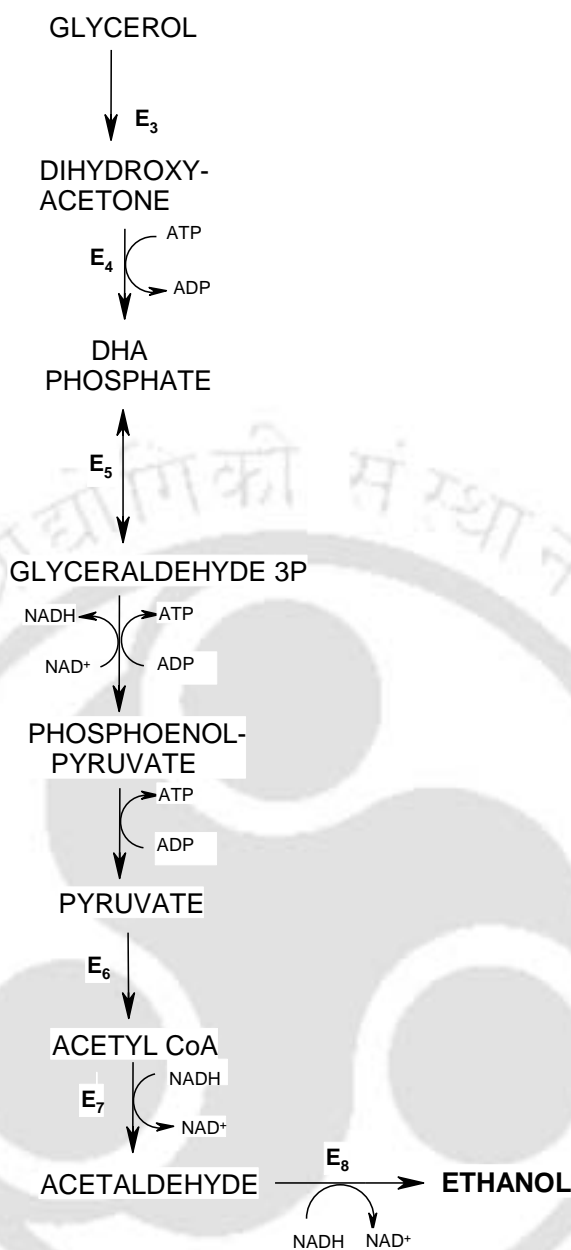


Figure 7.2(A) Metabolic pathway for glycerol bioconversion to ethanol (Enzymes: E_3 = Glycerol dehydrogenase Type I; E_4 = Dihydroxyacetone kinase; E_5 = Triose phosphate isomerase; E_6 = Pyruvate dehydrogenase complex; E_7 = Acetaldehyde dehydrogenase; E_8 = Alcohol dehydrogenase)

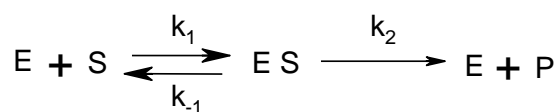


Figure 7.2(B) Michaelis–Menten reaction scheme

(1930) derived following kinetic expression for substrate inhibited reaction scheme:

$$V = \frac{k_2 E_o [S]}{K_m + [S] + \frac{[S]^2}{K_I}} = \frac{V_{\max} [S]}{K_m + [S] + \frac{[S]^2}{K_I}} \quad (7.7)$$

where K_I is the dissociation equilibrium ($1/K_N$) for the reaction $S \cdot E \cdot S \longleftrightarrow S + E \cdot S$. From this expression, one can perceive that reaction velocity goes to zero as the substrate concentration $[S]$, becomes large, due to significant amount of enzyme being engaged in non-productive complex. The constants in the kinetic expressions have physical significance. Lower values of K_m indicates greater affinity of enzyme towards substrate, while higher value of K_I indicates lower tendency of enzyme towards substrate binding to non-catalytic site that leads to inhibition. High value of V_{\max} indicates greater tendency of E·S complex to split into the products. Comparative evaluation of these constants for the control and test experiments gives a mechanistic account of the influence of ultrasound on bioconversion process. The kinetic data of glycerol conversion into the two products with different initial substrate concentrations was fitted to equations 7.6 and 7.7 to get the enzyme kinetics parameters.

7.3 RESULTS AND DISCUSSION

Fig. 7.4 depicts the time history of production of 1,3-PDO and ethanol with mechanical shaking (control experiments) and with ultrasound irradiation (test experiments), respectively. Also shown in these figures is the time history of glycerol concentration in the fermentation mixture. Difference in initial glycerol concentration in the fermentation mixture, and the concentration at any time would be equal to the glycerol diffused into the microbial cells. The rate of glycerol consumption is determined by the kinetics of various enzymatic reactions in the metabolic pathway of glycerol bioconversion. The amount of glycerol consumed in the cells can be estimated by measurement of the products' concentration.

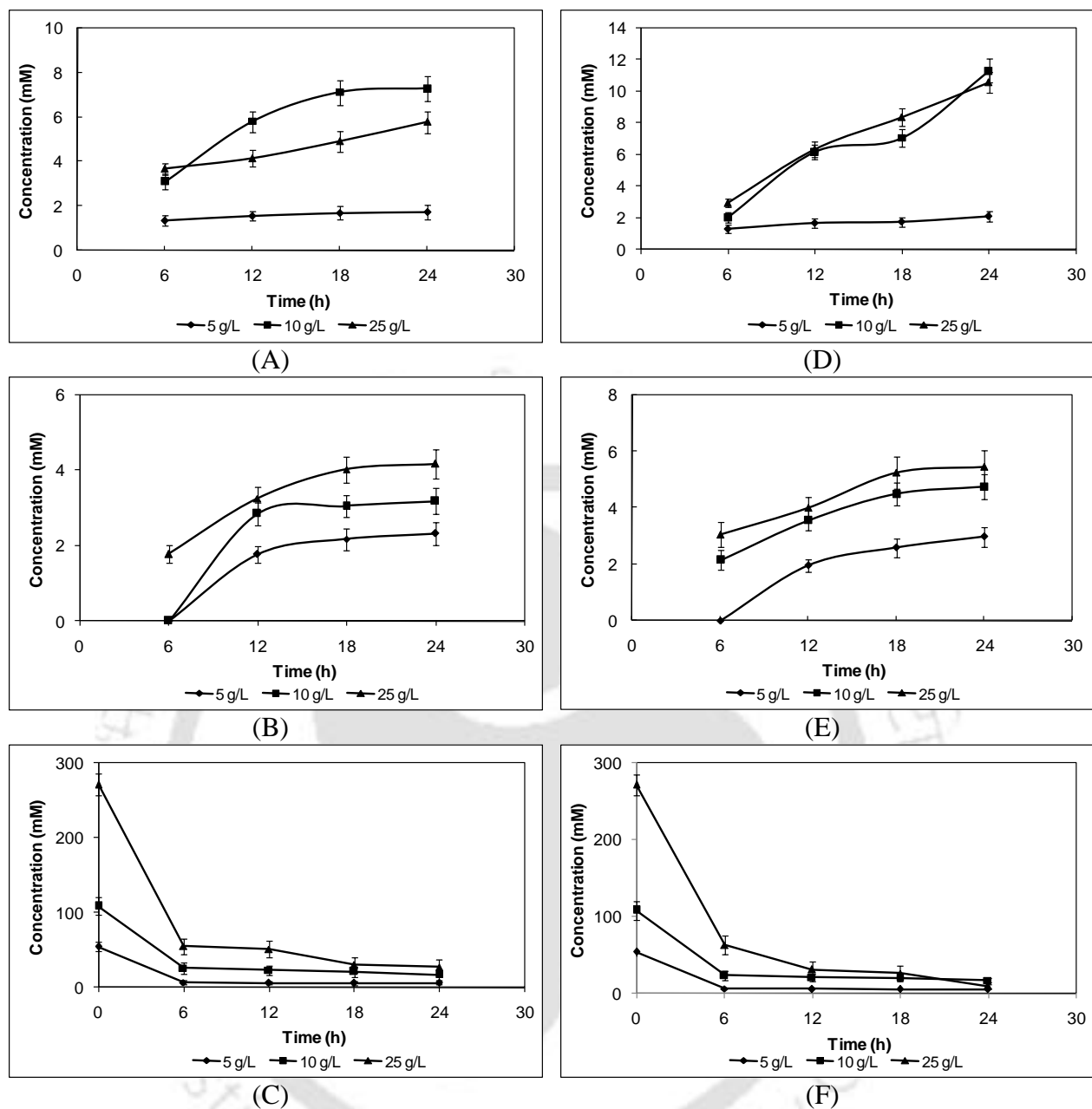


Figure 7.4 Trends in bioconversion of glycerol at different initial concentrations (5, 10 and 25 g/L) with mechanical shaking (control experiments), (A) time variation of ethanol production, (B) time variation of 1,3-PDO production, (C) time variation of glycerol concentration in fermentation broth. Trends in bioconversion of glycerol at different initial concentrations (5, 10 and 25 g/L) with ultrasound irradiation (test experiments), (D) time variation of ethanol production, (E) time variation of 1,3-PDO production, (F) time variation of glycerol concentration in fermentation broth

Table 7.1 Material balance for glycerol bioconversion

Final Concentrations (mM)	Initial Glycerol Concentration					
	5 g/L (54.4 mM)		10 g/L (108.7 mM)		25 g/L (271.7 mM)	
	Ultrasound	Without Ultrasound	Ultrasound	Without Ultrasound	Ultrasound	Without Ultrasound
Ethanol	2.12 ± 0.13	1.74 ± 0.07	11.33 ± 0.22	7.29 ± 0.19	10.58 ± 0.32	5.78 ± 0.05
1,3 Propanediol	2.98 ± 0.01	2.33 ± 0.18	4.76 ± 0.15	3.19 ± 0.10	5.47 ± 0.26	4.18 ± 0.10
Glycerol Uptake*	48.6	48.4	91	91.5	262	244
Glycerol Consumption* (Stoichiometric)	5.1	4.07	16.09	10.48	16.05	9.96
Unaccounted Glycerol*	43.5	44.33	74.91	81.02	245.95	234.04
Percentage enhancement in glycerol consumption with ultrasound*	25.3	N.A.	53.5	N.A.	61.1	N.A.
Percentage Glycerol utilized*	10.5	8.4	17.7	11.5	6.1	4.1
Percentage Glycerol remained unutilized*	89.5	91.6	82.3	88.5	93.9	95.9

N.A. Not Applicable

* Calculated using mean values of ethanol and 1,3-PDO production

If the rate of glycerol diffusion and rate of glycerol conversion are unequal, large amount of glycerol remains unconverted inside the cells, although bulk measurement of glycerol in fermentation mixture shows depletion of this amount. The entire summary of results in the form of material balance for glycerol is given in Table 7.1, while the yield and selectivity for the two products of bioconversion, viz. 1,3-PDO and ethanol, are depicted in Tables 7.2 and 7.3, respectively. We would like to specifically mention that yield of a product is calculated on the basis of initial quantity (or concentration) of glycerol added to the fermentation mixture, while selectivity of the product is determined on the basis of moles of glycerol consumed in the process, which, as stated earlier, are calculated from the moles of products formed and stoichiometry of conversion. The values of enzyme kinetics parameters in equations 7.6 and 7.7 are listed in Table 7.4.

Table 7.2 Yields for products of glycerol bioconversion and enhancement effect of ultrasound

Initial Glycerol Concentration	Yield (mole / mole initial glycerol)					
	Ethanol			1,3 Propanediol		
	Ultrasound	Without Ultrasound	η (%)	Ultrasound	Without Ultrasound	η (%)
5 g/L (54.4 mM)	0.039	0.032	21.87	0.055	0.043	27.9
10 g/L (108.7 mM)	0.104	0.067	55.22	0.044	0.029	51.72
25g/L (271.7 mM)	0.039	0.021	85.71	0.02	0.015	33.33

η - percentage enhancement in yield with ultrasound

Table 7.3 Selectivity for products of glycerol bioconversion

Initial Glycerol Concentration	Ethanol		1,3-Propanediol	
	Ultrasound	Without Ultrasound	Ultrasound	Without Ultrasound
5 g/L (54.4 mM)	0.416	0.428	0.584	0.572
10 g/L (108.7 mM)	0.704	0.696	0.296	0.304
25g/L (271.7 mM)	0.659	0.58	0.341	0.42

Table 7.4 Enzyme kinetics parameters

Kinetic Parameter	Ethanol dehydrogenase		1,3-PDO dehydrogenase	
	Ultrasound	Without Ultrasound	Ultrasound	Without Ultrasound
V_{\max} (mM/min)	0.01	0.03	0.61	0.02
K_m (mM)	124.7	331.1	10100	327.7
K_I (mM ⁻¹)	N.A.	N.A.	8.1	187.7

N.A. = Not Applicable

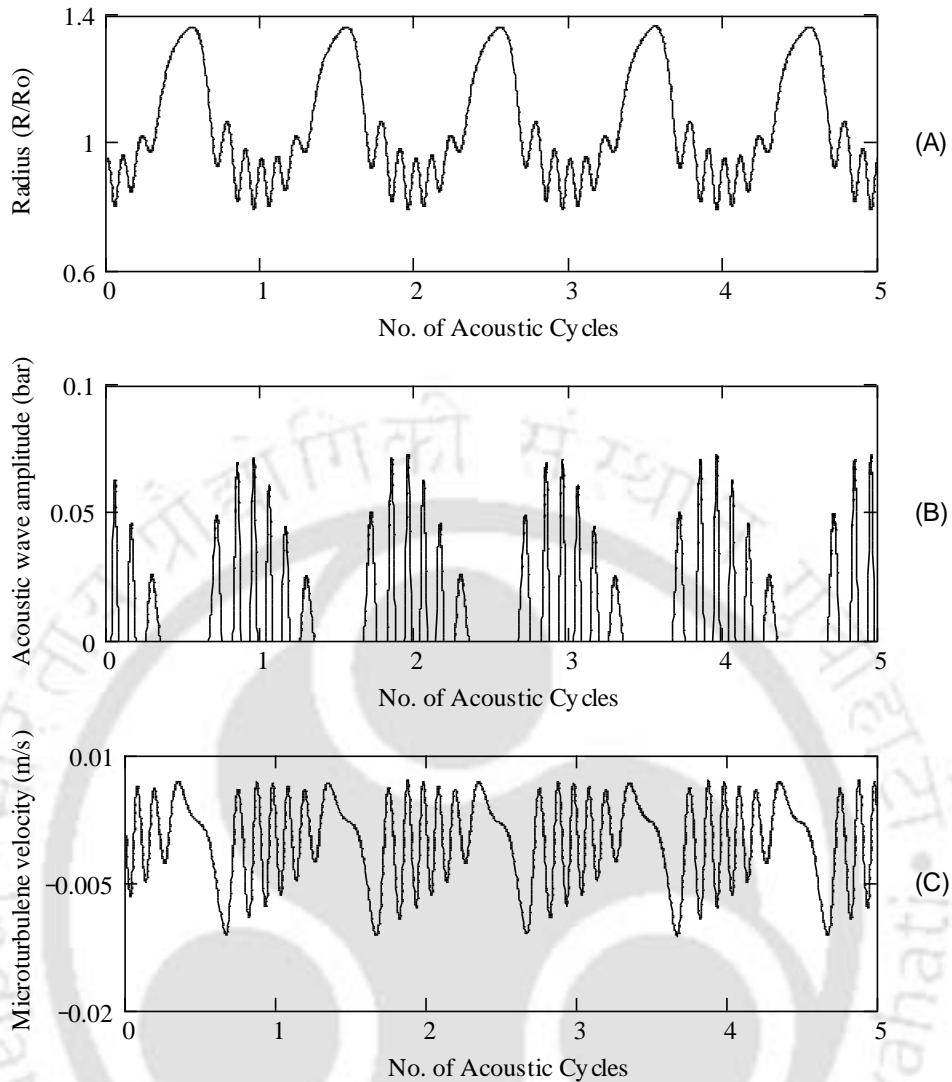


Figure 7.5 Simulation results for the radial dynamics of 5 micron air bubble and the convection generated thereby in the fermentation medium with 10 g/L glycerol concentration. (Positive velocity indicates liquid motion away from bubble center, while negative velocity indicates motion towards bubble center)

The statistical analysis of the results in the form of ANOVA is shown in Table 7.5A and 7.5B. Fig. 7.3 shows representative simulation results for cavitation bubble dynamics for a 5 micron air bubble in fermentation mixture with 10 g/L glycerol concentration. It could be perceived from Fig. 7.5 that radial motion of cavitation bubble (with expansion up to 40% of original radius) generates convection with two components, viz. oscillatory microturbulence

velocity of magnitude ~ 1 cm/s, and mild shock waves of magnitude 10 kPa (or 0.1 bar). We would like to specifically mention that convection generated by cavitation bubbles adds to the oscillatory liquid motion induced due to propagation of ultrasound wave. Simulations for cavitation bubble of same size for fermentation mixtures with 5 and 25 g/L glycerol gave similar results (not shown here).

7.3.1 Determination of cell morphology and growth

SSC-H is a measure of cell surface topology i.e. when cell is under stress condition, its surface becomes rough and SSC-H increases. FSC parameter indicates the size of the cell i.e. greater the FSC, more will be the cell size. As per results shown in Fig. 7.6, we did not find any significant change in FSC and SSC upon sonication as most of the cells are in the lower left quadrant in control cells (96.78%) as well as in sonicated cells (94.28%). Also, histogram plots showed similar pattern in both control and sonicated cells as M1 of both is almost same (91.72% and 87.98%). Therefore, there is no morphological change in *C. pasteurianum* cells after sonication. Thus, sonication at high static pressure had no adverse effect on cell morphology. The retention of morphology of *C. pasteurianum* cells after sonication was also confirmed by light microscopy. *C. pasteurianum* cells are gram positive but can be stained negative depending on the age of the culture. The cells before and after sonication exhibited similar morphology as depicted in Figs. 7.7 A and B, which confirmed that sonication at high static pressure had no adverse effect on cell morphology. This observation is in concurrence with that of Sulaiman et al. (2011) who did not detect change in morphology of cultures of *K. marxianus* during production of Ethanol from lactose. The typical cell cycle of *C. pasteurianum* is of 48 h (Khanna et al., 2011). The cells remain in lag phase of growth for around 24 h (Khanna et al., 2011). Hence, the 24 h of fermentation time was not sufficient enough for the new cells in the fermentation mixture in the lag phase to grow to the log and stationary phase, where solvents production starts.

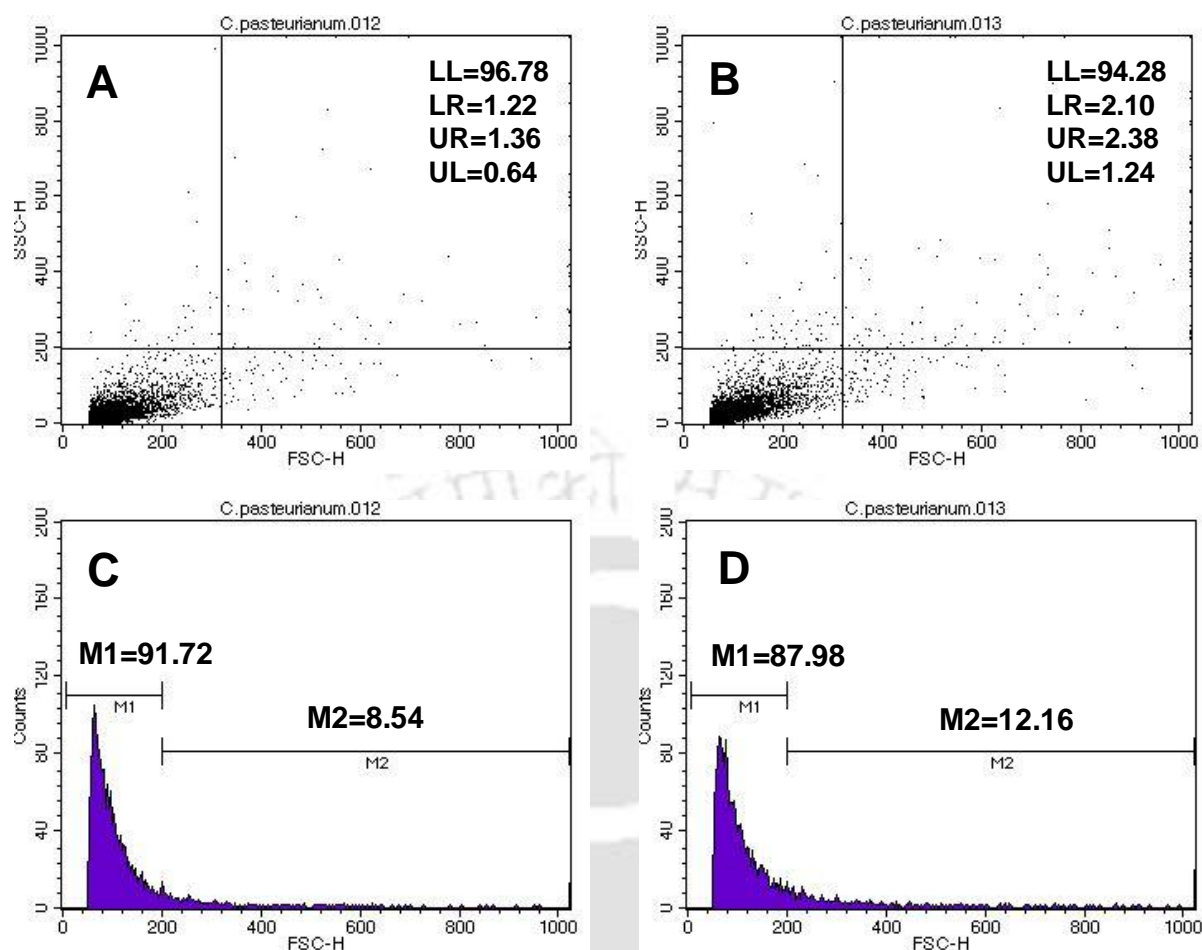


Figure 7.6 Flow Cytometric analysis for estimation of morphological changes (A) and (B) Acquisition dot plots (FSC vs SSC) of *C. pasteurianum* cells in control and test samples, respectively. (C) and (D) Histogram plots (Counts vs FSC) of *C. pasteurianum* in control and test samples cells, respectively. As there is no significant change in FSC after sonication as shown by both plots, therefore morphology of cells remains same

This means the solvent production during glycerol fermentation was due to the cells in the inoculum. The population density of these cells in the fermentation mixture was quite low, due to 10% v/v inoculum with optical density of 1.63 added to fermentation mixture, and this was reflected in low yields of solvents during fermentation. Moreover, to ensure that the yield enhancement is not a result of increase in microbial cell population, the optical density of both control and ultrasound treated samples was checked before and after fermentation and was found to be similar after 24 h of fermentation (OD = 0.2–0.3 at 660 nm).

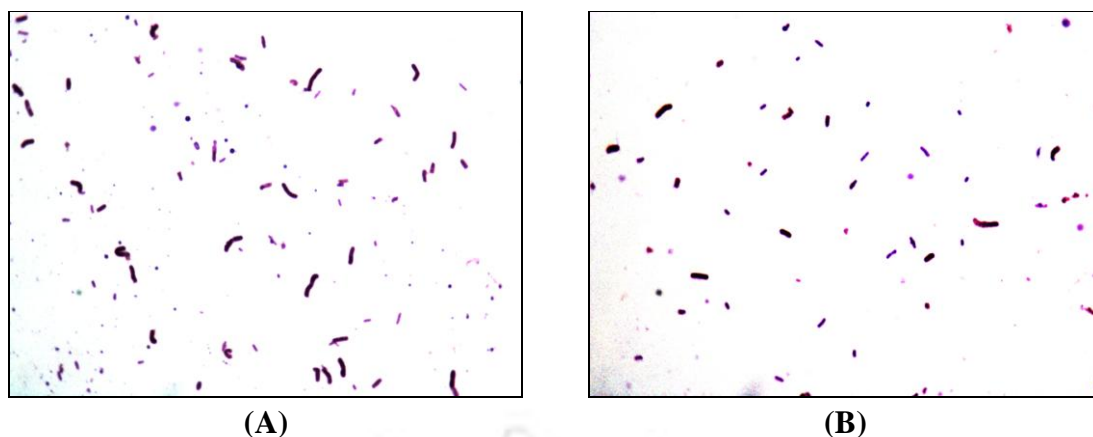


Figure 7.7 Morphology of cells of *C. pasteurianum* (A) before sonication, and (B) after sonication

Table 7.5A ANOVA of ethanol concentrations formed in absence and in presence of ultrasound at different concentrations of glycerol

Substrate Concentration (g/L)	DF	SS	MS	F ratio	p value	R ²
5	1	0.22	0.22	20.68	0.010	83.79
10	1	24.47	24.47	568.66	0.000	99.30
25	1	34.56	34.56	662.68	0.000	99.40

DF = Degree of Freedom, SS = Sum of Squares, MS = Mean of Squares

Table 7.5B ANOVA of 1,3-PDO concentrations formed in absence and in presence of ultrasound at different concentrations of glycerol

Substrate Concentration (g/L)	DF	SS	MS	F ratio	p value	R ²
5	1	0.62	0.62	39.91	0.003	90.89
10	1	3.68	3.68	224.29	0.000	98.25
25	1	2.49	2.49	65.22	0.001	94.22

7.3.2 Analysis of variance (ANOVA)

Table 7.5A and B depict the statistical analysis of the results obtained in absence and in presence of ultrasound at all substrate concentrations studied. As can be seen from the p values (< 0.5) in Table 7.5A and B, both ethanol and 1,3-PDO production is significantly enhanced by the application of ultrasound in the medium at all three glycerol concentrations studied.

7.3.3 Analysis of results

From data given in Tables 7.1 and 7.2, some peculiarities of influence of ultrasound irradiation on glycerol fermentation system can be identified as follows:

1. Glycerol uptake by the microbial cells remains practically constant or unaltered when mechanical shaking is replaced by ultrasound irradiation. However, rate of glycerol utilization (and hence product formation) shows significant rise under ultrasound irradiation.
2. Quite interestingly, percentage utilization of glycerol quantified as (mol glycerol converted/mol glycerol added), by the microbial cells shows a maxima with initial glycerol concentration, in that the highest consumption of glycerol is seen for fermentation mixture with 10 g/L concentration. Amount of unutilized glycerol in the cells is the highest for 25 g/L glycerol concentration, due to the substrate inhibition caused by glycerol for enzymes in the metabolic pathway of 1,3-PDO formation.
3. Production of both 1,3-PDO and ethanol increases with ultrasound. The percentage enhancement of yield of ethanol with ultrasound irradiation shows a monotonous increase with initial glycerol concentration, while enhancement of yield of 1,3-PDO shows a maxima in that the highest enhancement is seen for 10 g/L concentration. The absolute yield (mole/mole glycerol added) for both products is the lowest for 25 g/L glycerol concentration, due to large quantities of glycerol remaining unutilized, as noted earlier.
4. At low concentration of glycerol (5 g/L), higher selectivity is seen towards 1,3-PDO, while at higher glycerol concentration, the selectivity shifts towards ethanol. The difference in

selectivity towards the two products widens with application of ultrasound, in that selectivity for Ethanol is higher, while selectivity towards 1,3-PDO is lower in test experiments than control experiments.

Values of enzyme kinetic parameters help us in perceiving the above trends in experimental results. The intrinsic rate of diffusion of glycerol into the cells is quite fast, and hence, does not show any enhancement with ultrasound. The rate of utilization of the diffused glycerol, however, shows an enhancement with ultrasound. Mild shock waves emitted by cavitation bubbles cause rapid movement of microbial cells in the fermentation broth with inter-collisions and/or collisions with the walls of the test tube. These phenomena can help accelerate the enzymatic reactions inside the cells. In addition, the high velocity micro-streaming generated by ultrasound causes desorption of the CO_2 produced in the metabolic pathway and thus help higher conversion of glycerol. Comparative evaluation of the enzyme kinetic parameters for the two products in test and control experiments, and their manifestation on yield and selectivity is given below. It must be mentioned that due to faster diffusivity of glycerol into the microbial cells, the overall enzymatic reaction system or metabolic pathway is always expected to be substrate saturated, with enzyme being the limiting reactant.

(1) For ethanol formation, the Michaelis constant reduces with ultrasound irradiation, which indicates rise in formation of the E·S complex. However, reduced value of V_{max} indicates that rate of splitting of the E·S complex into the product decreases. Even with this limitation, higher concentration of the E·S complex results in increase in net yield of ethanol.

(2) For 1,3-PDO formation, interesting variations are seen in Michaelis constant, inhibition constant and velocity of reaction in control and test experiments. Under ultrasound irradiation, K_m increases, which is indicative of reduced formation of E·S complex. This is counteracted by reduction in K_i in test experiments, which is indicative of greater tendency of binding of E·S complex to non-catalytic site, and formation of the non-productive S·E·S complex. On the

contrary, the reaction velocity in test experiments also increases, signifying higher rate of splitting of the E·S complex into the products. Despite counterproductive influences of these kinetic parameters on the overall rate of production of 1,3-PDO, we have observed an enhancement in the yield in test experiments as compared to control experiments. We attribute this result to saturation of cells with substrate (i.e. glycerol), due to its faster intrinsic diffusivity into the cells, as mentioned earlier. Nonetheless, the effect of reduction in K_I (i.e. higher substrate inhibition) under ultrasound is reflected into lesser enhancement in yield, as compared to the other product, ethanol, where the enzymes are not inhibited by the substrate. This discrepancy is even more pronounced at higher substrate concentration (25 g/L) where yield enhancement with ultrasound irradiation is lesser than that for 10 g/L concentration. It is for the same reasons that we got higher selectivity towards 1,3-PDO at low glycerol concentration (5 g/L), while higher selectivity towards ethanol for initial glycerol concentration of 10 and 25 g/L.

All of these results point out that convection generated by ultrasound and cavitation enhances the rates of enzymatic reactions in pathway of glycerol bioconversion: either the formation of E·S complex as in case of conversion to ethanol, or splitting of E·S complex into products, in addition to binding of substrate to E·S complex at non-catalytic site as in case of conversion to 1,3-PDO. However, ultrasound does not affect the biochemistry of metabolic pathway of glycerol conversion, as evident from exactly same product profiles (in terms of absolute rate of production and yield) in test and control experiments. Thus, the role of ultrasound irradiation in enhancement of bioconversion of glycerol is found to be of physical nature.

7.4 CONCLUSIONS

In this chapter, we have evaluated the option of ultrasound irradiation for enhancing the kinetics of glycerol bioconversion. The results have given mechanistic insight into the ultrasonic enhancement of glycerol bioconversion into two value added products, viz. 1,3-PDO and Ethanol. Ultrasound irradiation of the fermentation mixture was found to enhance the yield of both products of glycerol bioconversion with interesting trends with respect to the initial concentration of glycerol. The nature of convection generated by ultrasound irradiation at raised static or ambient pressure in the medium has dual character in that there is oscillatory motion of liquid, accompanied by medium amplitude jerks by the acoustic or shock waves emitted by the bubbles, which could contribute towards enhancement of the enzymatic reactions in metabolic pathway. The role of ultrasound is found to be merely of physical nature, with no influence on the basic biochemistry of glycerol conversion. Due to substrate inhibition, the enhancement effect of ultrasound was less marked for 1,3-PDO than ethanol. With the mechanistic insight gained in this study by coupling cavitation physics and enzyme kinetics, we shall extend the theme of process intensification with ultrasound for glycerol bioconversion with immobilized cells in the next chapter.

ULTRASOUND ENHANCED BIOCONVERSION OF GLYCEROL WITH IMMOBILIZED CELLS

8.1 INTRODUCTION

In Chapter 7, we have reported ultrasonic enhancement of bioconversion of glycerol with free cells of *Clostridium pasteurianum*. Due to several merits of immobilized microbial cultures for large scale processes, we have furthered our study of ultrasound enhanced glycerol bioconversion using immobilized cells of *C. pasteurianum* over silica support. This chapter reports the results and analysis of this study. We have assessed the extent of enhancement of yield, selectivity and kinetics of glycerol bioconversion with ultrasound. Secondly, we have attempted to give a physical insight into the observed enhancement by coupling the experimental results to enzyme kinetic model, and simulations of cavitation bubble dynamics. Our study has revealed several interesting mechanistic aspects of the ultrasonic enhancement of bioconversion of glycerol with immobilized microbial cells, which

have been described in subsequent sections.

8.2 MATERIALS, METHODS & SIMULATIONS

8.2.1 Materials

Clostridium pasteurianum MTCC 116 (ATCC 6013 type strain) was procured from Microbial Type Culture Collection (MTCC), Chandigarh, India. Anaerobic tray system for maintenance of anaerobic conditions for the agar slants was procured from Himedia (India). 60–120 mesh size column chromatography grade silica gel (Merck, India) was used as an immobilization support. All chemicals used for standardization of gas and liquid chromatographs were procured from Sigma Aldrich and Merck (Germany). All other chemicals and media components used were of analytical grade and were purchased from either Merck (Germany) or Himedia (India).

8.2.2 Micro-organism growth and maintenance

C. pasteurianum cells were revived on Cooked Meat Media (CMM) agar slants and incubated at 37°C for 24 h. The agar slants were kept in an anaerobic tray system during incubation. The revived cells on slant so obtained were further stored at 4°C to be used as stock and were sub-cultured every month.

8.2.3 Immobilization of *C. pasteurianum* and glycerol fermentation

C. pasteurianum cells were immobilized on 60–120 mesh size column chromatography grade silica gel. The immobilization procedure followed was same as described in Chapter 3. Fermentation of glycerol was carried out in medium optimized in Chapter 5. The composition of the medium was as follows: KH_2PO_4 (1.0 g/L), K_2HPO_4 (1.0 g/L), $\text{MgSO}_4 \cdot 7\text{H}_2\text{O}$ (0.1 g/L), $(\text{NH}_4)_2\text{SO}_4$ (0.1 g/L) and yeast extract (5 g/L). The amount of support (with immobilized cells) to be added to the fermentation broth was also pre-optimized. 3% w/v support with immobilized cells (as found in chapter 3) was used as biocatalyst in present study. 5, 10 and 25 g/L glycerol was added to the fermentation medium.

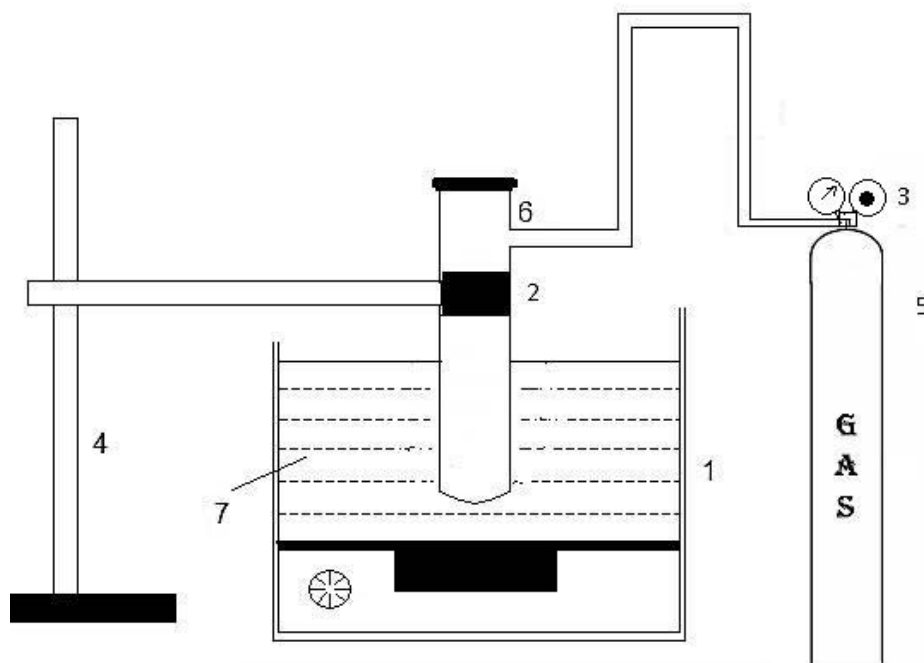


Figure 8.1 Schematic of experimental set-up. Legends: 1 – ultrasound bath, 2 – test tube containing fermentation broth and immobilized cells, 3 – pressure gauge and gas flow control valve, 4 – burette stand for holding test tube, 5 – gas cylinder, 6 – silicon tubing

8.2.4 Apparatus and reaction setup

A sonic bath was used for ultrasonic irradiation of the glycerol fermentation mixture (Make: Elma, Germany; Model: Transonic T-460, Vol 2 L, Frequency 35 kHz, Power input 35 W). Fig. 8.1 shows the picture of the experimental set up used in this study. The dimensions of the bath were $25 \times 15 \times 10$ cm with transducers attached to the bottom of the bath. The bath was filled with water during sonication, which formed the medium for ultrasound transmission. Experiments were carried out in custom-fabricated 15 mL screw capped test tube made of borosilicate glass. This test tube also had a neck at the top, which could be connected to a nitrogen cylinder (99.98% pure) for raising the static pressure of the fermentation mixture to 2 bar. The rationale underlying increasing of static pressure of the fermentation mixture has already been explained in Chapter 7. Maintaining nitrogen atmosphere over the fermentation mixture also helps in achieving anaerobic conditions as

required by *C. pasteurianum*. Since the spatial distribution of cavitation intensity in the bath shows significant variation, the position of the test tube in the central region of the ultrasound bath was maintained exactly the same in all experiments. The test tube was immersed to about 75% of its length in water during sonication. The temperature of the water in the bath was maintained at a pre-determined temperature of 37°C conducive for solvent production by *C. pasteurianum*.

The control experiments were carried out in test tube of exactly same dimensions and volume as used in experiments with ultrasound irradiation. The static pressure inside the test tube was atmospheric (1 bar) in this case. The tube was kept in an incubator shaker (Make: Scigenics, India, Model: Orbitek) at a temperature of 37°C and agitation rate of 150 rpm. Samples of the fermentation broth were withdrawn every 6 h (upto 24 h) in both test and control experiments. In case of ultrasound assisted experiments, sonication was stopped and high pressure in the test tube was released during withdrawal of the sample, and was restored thereafter with resumption of sonication. The results presented are the means of three experimental runs for each set of experiment with the error bars depicting standard deviations. The analysis of variance (ANOVA) of 1,3-PDO concentrations formed in test and control experiments was carried out using Minitab 15 statistical software (Trial Version).

8.2.5 Analysis

The procedure for analysis of product formation and substrate consumption was similar to the procedure described in previous chapter for free cells. The quantities of ethanol and 1,3-PDO formed during fermentation were determined by Gas Chromatograph (Varian, CP 3800). CP Wax 52 CB capillary column (250 mm × 0.25 mm × 0.39 mm, Varian) was used for gas chromatographic analysis. The oven temperature was programmed from 45°C to 100°C with an increment of 3°C/min and after 100°C, an increment of 5°C/min upto 200°C. The injector and detector temperatures were 230°C and 250°C, respectively. Nitrogen gas at a

flow rate of 2 mL/min was used as a carrier.

The utilization of substrate (glycerol) during the course of fermentation by *C. pasteurianum* cells was determined using HiPlex-H HPLC column (300 mm × 5 μm × 4.6 mm, Varian). The HPLC apparatus comprised of a pump (Series 200, Perkin Elmer), a refractive index detector (Series 200, Perkin Elmer), and a vacuum degasser (Series 200, Perkin Elmer). HPLC grade water (Milli Q) was used as the mobile phase at a flow rate of 0.5 mL/min. The HPLC analyses were carried out at 37±2°C. Standard calibration plots were used for all calculations.

8.2.6 Simulations of cavitation bubble dynamics

Simulations of cavitation bubble dynamics were carried out using the same model (with same physical and process parameters) as in the study with free cell (described in Chapter 7).

8.2.7 Enzymes extraction and kinetic parameters determination

The procedure followed for enzymes extraction was similar as for the free cells (described in last chapter), however, for the convenience of the reader we reproduce it here. The enzymes ethanol dehydrogenase and 1,3-PDO dehydrogenase were extracted from *C. pasteurianum* cells immobilized on silica gel. The activities of both the enzymes in test (with ultrasound) and control experiments (mechanical agitation) were determined. The protocol followed for this is as follows: The cells immobilized on silica support were centrifuged at 6000 rpm for 15 min. The immobilized cells were suspended in 50 mM phosphate buffer (pH 7.5) and sonicated in ice bath for 6 cycles (30 s on / 10 s off). The supernatant so obtained was separated from the support and cell lysate by centrifugation at 6000 rpm for 10 min. This supernatant was tested for 1,3-PDO dehydrogenase and ethanol dehydrogenase activity. The activity of 1,3-PDO dehydrogenase in the supernatant was determined by monitoring the increase in NADH concentration at 340 nm using a UV-Vis spectrophotometer (Make:

Perkin Elmer, Model: Lambda 3). The assay mixture (1 mL final volume) for 1,3-PDO dehydrogenase had following constitution: 100 mM glycerol, 2 mM NAD^+ , 30 mM ammonium sulfate and 10 mM potassium carbonate buffer (pH 9.7) (Malaoui and Marczak, 2000). Similar to 1,3-PDO dehydrogenase activity determination, the activity of ethanol dehydrogenase was also calculated by monitoring the absorbance at 340 nm, indicative of conversion of NAD^+ to NADH. The assay was carried out according to the protocol given by Kato et al. (1984). The assay mixture consisted of 10 mM NAD^+ , 20 mM glycerol and 10 mM glycine–NaOH buffer (pH 9.0).

As described in last chapter, the enzyme kinetic parameters were calculated by fitting experimental data (i.e. nonlinear regression) to Michaelis–Menten kinetics (for no inhibition) and Haldane kinetics (for substrate inhibition) (Haldane, 1930) using PolyMath 5.0. The apparent K_m , V_{\max} and K_I were determined by fixing the concentration of co-enzyme and varying the concentration of non conventional substrate glycerol. The metabolic pathways for bioconversion of glycerol to 1,3-PDO and ethanol are given in Chapter 1 and also in Chapter 7. The pathway for 1,3-PDO formation is inhibited by glycerol (a non conventional substrate for 1,3-PDO dehydrogenase) and an intermediate from glycerol to 1,3-PDO conversion, 3-hydroxypropionaldehyde (Haldane, 1930; Barbirato et al. 1996; Reed, 2010). No such effect is observed in metabolic pathway of formation of ethanol from glycerol. Therefore, Michaelis–Menten kinetics is adopted for ethanol dehydrogenase, while Haldane kinetics for substrate inhibited enzymatic systems is used for 1,3-PDO dehydrogenase. The mechanisms and mathematical expressions of the enzyme kinetics for these systems are given in previous chapter.

8.3 RESULTS AND DISCUSSION

The results of the experiments (test as well as control) are depicted in Fig. 8.2. The material balance for glycerol is given in Table 8.1. Also shown in Table 8.1 are the results of our earlier study with free cells for comparison. Table 8.2A depicts the yields of two major products of fermentation (viz. ethanol and 1,3-PDO) along with individual percentage enhancement for these products observed with ultrasound irradiation for different initial glycerol concentrations. Table 8.2B gives the analysis of selectivity among these products in the test and control experiments. In both of these tables, we have given results of our previous study (for each parameter) with free cells in parentheses for comparison. The major trends in glycerol consumption, product formation and yield & selectivity of individual products that could be seen from results given in Tables 8.1 and 8.2 and Figs. 8.2 and 8.3 can be summarized as follows:

(1) The time history of glycerol concentration in bulk medium shows that large amount of glycerol diffuses into the microbial cells. The rate of this diffusion is already quite fast, and shows only negligible enhancement with either immobilization or ultrasound irradiation or both. This result is consistent for all three concentrations of glycerol. The amount of glycerol uptake increases proportionately with initial glycerol concentration in the fermentation medium. However, the rate of glycerol consumption does not show a consistent rise. This essentially means that metabolic pathway of glycerol conversion is kinetically controlled, and large glycerol uptake does not lead to large conversion.

(2) The rate of consumption of glycerol shows significant variation with immobilization and ultrasound irradiation or both. The data given in Table 8.1 helps identify individual contribution of these two techniques on observed enhancement. Comparing the results of control experiments (i.e. mechanical shaking) for free and immobilized cells reveals significant rise in the glycerol consumption with immobilization. However, the extent of this

rise is a function of initial glycerol concentration. For low concentration of 5 g/L glycerol, the rise in glycerol consumption is 5-fold, while for 10 g/L this rise is 2-fold. Quite interestingly, at high glycerol concentration of 25 g/L, no enhancement is seen in glycerol consumption with immobilization. Comparison of results of test and control experiments for immobilized cells reveals the additive effect of ultrasound irradiation on glycerol bioconversion. For low concentration of glycerol of 5 g/L, the rise in glycerol consumption with ultrasound irradiation is only marginal (~ 27%). For 10 g/L glycerol concentration, the enhancement in glycerol consumption rises to 31%, which is rather trivial. However, for 25 g/L, there is drastic rise (~ 175%) in glycerol consumption of immobilized cells with ultrasound.

(3) As expected, in case of free as well as immobilized cells, no formation of butanol was seen in test as well as control experiments in 24 h as the butanol production starts in stationary phase of the cell growth cycle, which commences after 24 h (Khanna et al., 2011). Thus, the products of glycerol bioconversion are ethanol and 1,3-PDO. In case of free cells, the selectivity towards ethanol was higher than 1,3-PDO. Interestingly, the selectivity among these products shows a sweeping change towards 1,3-PDO with immobilization of cells in both test and control experiments. This is evident from the data presented in Table 8.1 and 8.2. Practically no ethanol forms in control experiments. With ultrasound irradiation of immobilized cells in test experiments, very small formation of ethanol is seen, which shows a gradual increase with initial glycerol concentration.

(4) The kinetic parameters (V_{\max} – maximum rate of reaction, K_m – Michaelis constant or substrate concentration at $V_{\max}/2$) for the enzymes ethanol dehydrogenase and 1,3-PDO dehydrogenase are shown in Table 8.3. For ethanol dehydrogenase, ultrasound did not show any effect as evident from same values of the kinetic parameters for test and control experiments.

Table 8.1 Material balance for glycerol bioconversion by immobilized *C. pasteurianum* in presence and in absence of ultrasound

Final Concentrations (mM)	Initial Glycerol Concentration					
	5 g/L		10 g/L		25 g/L	
	Test	Control	Test	Control	Test	Control
Ethanol	1.28 ± 0.03 (2.12 ± 0.13) [#]	0 (1.74 ± 0.07) [#]	1.70 ± 0.08 (11.33 ± 0.22) [#]	0 (7.29 ± 0.19) [#]	3.83 ± 0.27 (10.58 ± 0.32) [#]	0 (5.78 ± 0.05) [#]
1,3-PDO	25.51 ± 0.09 (2.98 ± 0.01) [#]	20.44 ± 0.03 (2.33 ± 0.18) [#]	30.41 ± 0.80 (4.76 ± 0.15) [#]	23.97 ± 2.84 (3.19 ± 0.1) [#]	24.84 ± 0.67 (5.47 ± 0.26) [#]	9.78 ± 0.00 (4.18 ± 0.1)
Glycerol uptake	42.98 (48.6) [#]	40.00 (48.4) [#]	91.73 (91.0) [#]	86.78 (91.5) [#]	236.95 (262.0) [#]	231.10 (244.0)
Glycerol consumption	26.79 (5.1) [#]	20.44 (4.07) [#]	32.41 (16.09) [#]	23.97 (10.48) [#]	28.67 (16.05) [#]	9.78 (9.96)
Unaccounted Glycerol	16.19 (43.5) [#]	19.56 (44.33) [#]	59.32 (74.91) [#]	62.81 (81.02) [#]	208.28 (245.95) [#]	221.32 (234.04)
% Glycerol utilized	62.33 (10.5) [#]	51.1 (8.4) [#]	35.33 (17.7) [#]	27.62 (11.5) [#]	12.09 (6.1) [#]	4.23 (4.1)
% Glycerol remained unutilized	37.67 (89.5) [#]	48.9 (91.6) [#]	64.67 (82.3) [#]	72.38 (88.5) [#]	87.91 (93.9) [#]	95.77 (95.9)
% Enhancement in glycerol consumption with ultrasound	27.39 (25.3) [#]	N.A	31.27 (53.5) [#]	N.A	175.67 (61.1) [#]	N.A

Test = With Ultrasound; Control = Without Ultrasound

[#] Results of experiments with free cells (Khanna et al., 2012a) are given in parentheses for comparison

Table 8.2A Yields for products of glycerol bioconversion and percentage enhancement by ultrasonic treatment

Initial Glycerol Concentration	Yield (mole / mole)					
	Ethanol			1,3 Propanediol		
	Test	Control	η (%)	Test	Control	η (%)
5 g/L (54.35 mM)	0.024 (0.044) [#]	Nil (0.036) [#]	N.A. (22.78) [#]	0.468 (0.061) [#]	0.377 (0.048) [#]	24.14 (28.14) [#]
10 g/L (108.70 mM)	0.016 (0.124) [#]	Nil (0.079) [#]	N.A. (55.52) [#]	0.275 (0.052) [#]	0.202 (0.035) [#]	36.14 (49.17) [#]
25 g/L (271.74 mM)	0.013 (0.04) [#]	Nil (0.024) [#]	N.A. (83) [#]	0.093 (0.021) [#]	0.038 (0.017) [#]	14.47 (30.89) [#]

η – Percentage enhancement

[#] Results of experiments with free cells (Khanna et al., 2012a) are given in parentheses for comparison

Table 8.2B Selectivity for ethanol and 1,3–PDO production from bioconversion of glycerol

Initial glycerol concentration	Ethanol		1,3–Propanediol	
	Test	Control	Test	Control
5 g/L (54.35 mM)	0.048 (0.416) [#]	0.00 (0.428) [#]	0.952 (0.584) [#]	1.0 (0.572) [#]
10 g/L (108.70 mM)	0.052 (0.704) [#]	0.00 (0.696) [#]	0.938 (0.296) [#]	1.0 (0.304) [#]
25 g/L (271.74 mM)	0.134 (0.659) [#]	0.00 (0.58) [#]	0.866 (0.341) [#]	1.0 (0.42) [#]

[#] Results of experiments with free cells (Khanna et al., 2012a) are given in parentheses for comparison

Table 8.3 Enzyme kinetics parameters for ethanol dehydrogenase and 1,3–PDO dehydrogenase

Kinetic Parameters	Ethanol dehydrogenase		1,3–PDO dehydrogenase	
	Test	Control	Test	Control
V_{max} (mM/min)	0.016	0.016	0.023	1.699
K_m (mM)	1.1	1.1	16.56	3691.90
K_i (mM ⁻¹)	N.A	N.A	1036.14	1.61

Table 8.4 Analysis of Variance (ANOVA) of 1,3-PDO concentrations formed in test and in control experiments at different concentrations of glycerol

Substrate Concentration (g/L)	DF	SS	MS	F ratio	p value	R ²
5	1	25.63	25.63	5751.40	0.000	99.97
10	1	41.37	41.37	9.53	0.091	82.66
25	1	226.97	226.97	495.06	0.002	99.60

DF = Degree of Freedom, SS = Sum of Squares, MS = Mean of Squares

For 1,3-PDO dehydrogenase, however, ultrasound irradiation shows remarkable effects in that K_m decreases significantly with concurrent increase in K_1 . On the other hand, the value of V_{max} decreases with ultrasound. Nonetheless, the net effect of these reverse variations is rise in rate of 1,3-PDO formation on absolute basis, as seen in Table 8.1. The reduction in V_{max} is manifested through decreasing yield of the 1,3-PDO with respect to initial glycerol concentration as latter rises from 5 to 25 g/L. The physical interpretations for these findings can be given as follows: Glycerol is a non-conventional substrate for 1,3-PDO dehydrogenase, which leads to lower affinity of this enzyme towards glycerol and higher affinity towards conventional substrate such as 1,3-PDO, 3-hydroxypropionaldehyde. The same is indicated by low K_m value for 1,3-PDO dehydrogenase with glycerol as a substrate in control experiments. Application of ultrasound at elevated pressure increases the affinity of 1,3-PDO dehydrogenase towards glycerol leading to higher 1,3-PDO formation as depicted by drastic reduction in K_m and enhancement in K_1 value. Thus, the conversion of glycerol to 1,3-PDO predominantly becomes a one step reaction although, some conversion may also occur via 3-hydroxypropionaldehyde formation.

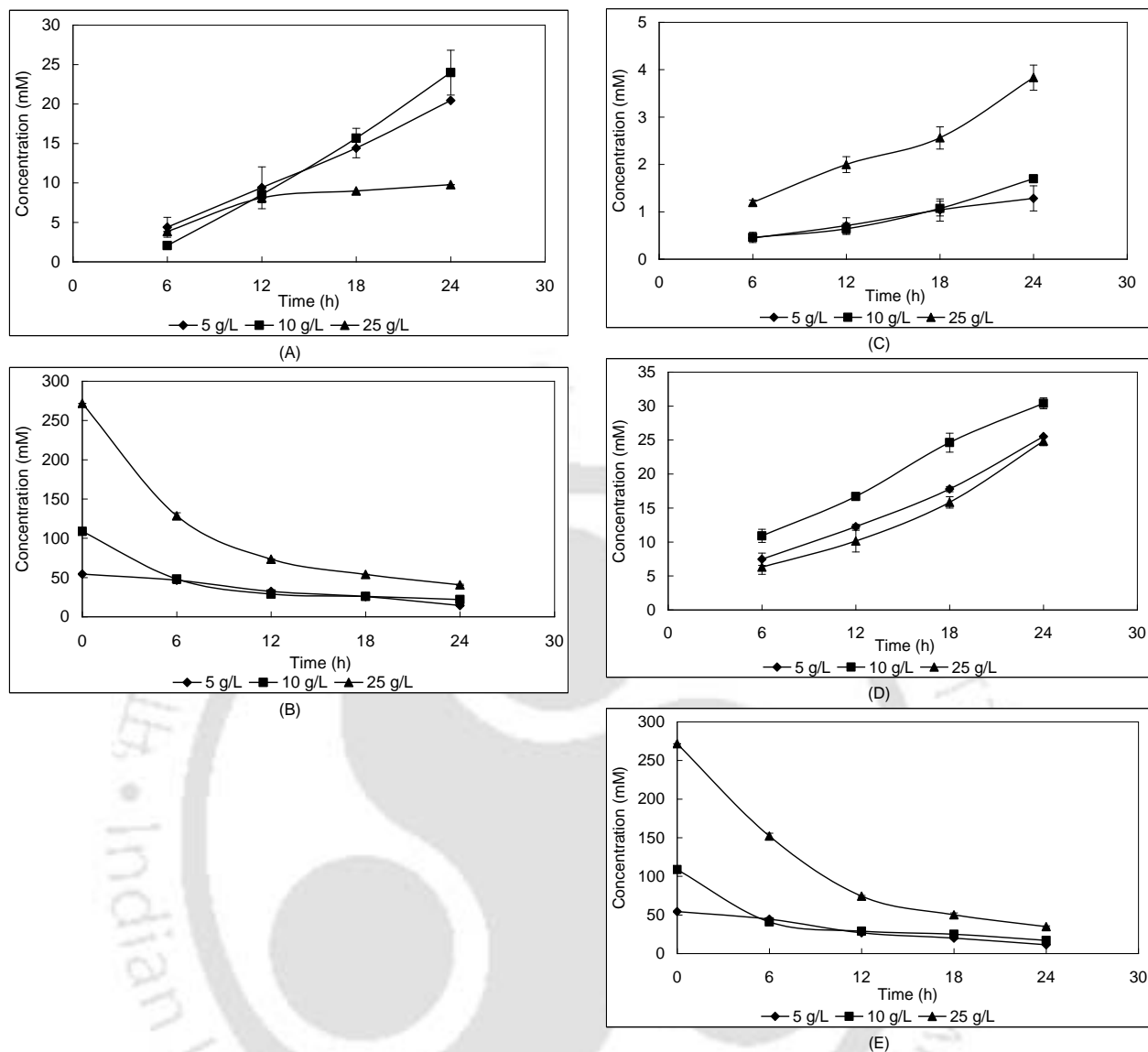


Figure 8.2 (A) Trends in bioconversion of glycerol to 1,3-PDO by immobilized *C. pasteurianum* with mechanical shaking at different initial glycerol concentrations, (B) time variation of different initial glycerol concentrations with mechanical shaking. Trends in bioconversion of different initial glycerol concentrations to (C) ethanol, (D) 1,3-PDO in presence of ultrasound at elevated pressure. (E) Time variation of different initial glycerol concentrations in the fermentation broth subjected to ultrasound treatment at elevated pressure

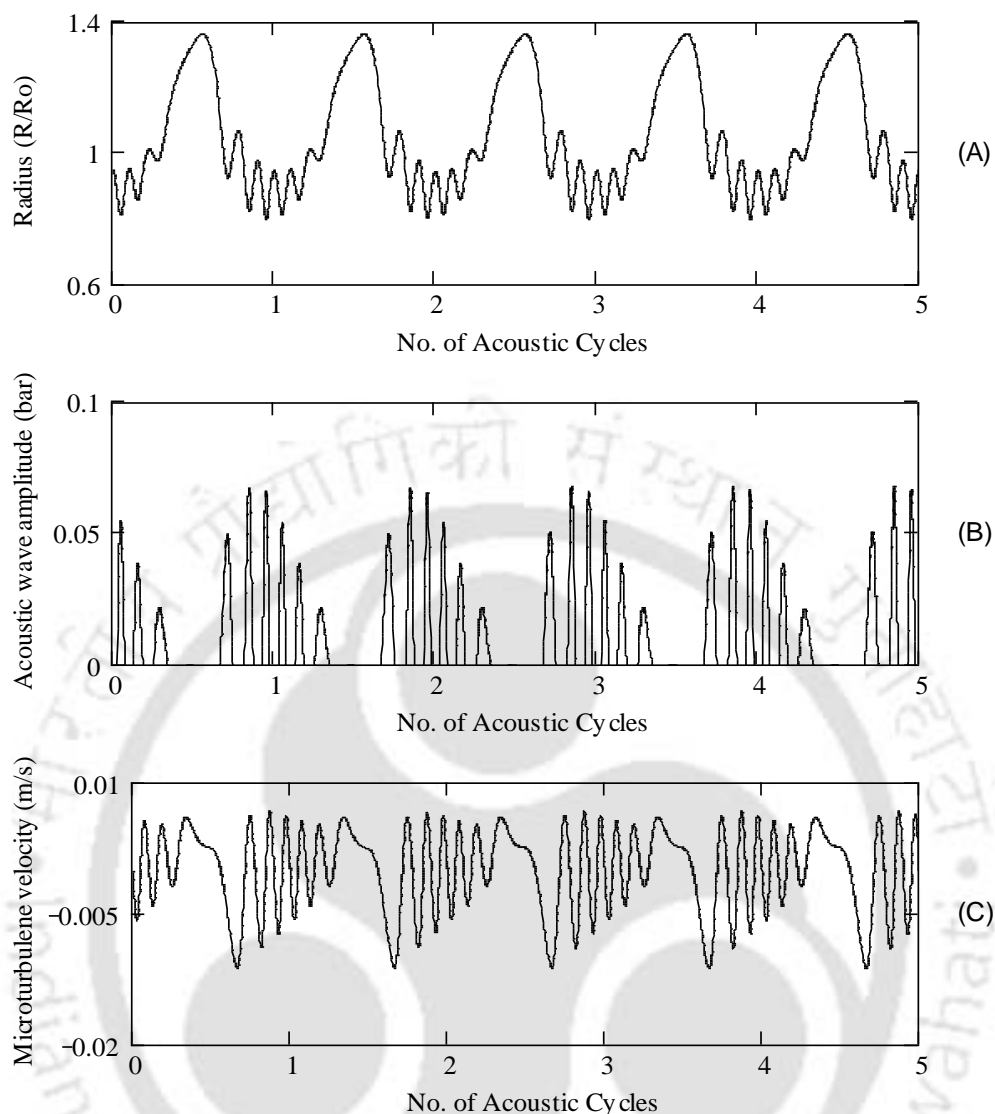


Figure 8.3 Simulation results for the radial dynamics of 5 micron air bubble and the convection generated thereby in the fermentation medium with 25 g/L glycerol concentration

(5) ANOVA of 1,3-PDO formation presented in Table 8.4 shows that effect of ultrasound is insignificant at 10 g/L glycerol concentration indicated by p value of 0.09.

(6) Figure 8.3 shows representative simulations of the radial motion of cavitation bubble in fermentation broth with initial concentration of glycerol as 25 g/L. It could be perceived that convection generated by ultrasound and cavitation has dual characteristics, viz. an oscillatory

fluid motion with velocities upto 1 cm/s, and mild shock waves of magnitude ~ 10 kPa. The microbial cells get drifted in the rapid fluid motion and can undergo inter-collisions or collision with the walls of the test tube used for fermentation.

8.3.1 Analysis

(1) The major enzyme of metabolic pathway of 1,3-PDO, i.e. 1,3-PDO dehydrogenase is substrate inhibited, and its kinetics is described by Haldane kinetic scheme. The metabolic pathway for ethanol does not have any such limitation. The experiments with free cells formed ethanol as the major product, while the immobilized cells formed 1,3-PDO as the dominant product. This is clearly an effect of change in kinetic parameters of 1,3-PDO dehydrogenase in immobilized cells, wherein, there was an increase in K_I and a decrease in K_m (as compared to the free cells) leading to higher 1,3-PDO formation. Also, the concentrations of total products formed were higher with immobilized cells, which may be attributed to the greater tolerance of immobilized cells towards substrate inhibition. Ultrasound was found to enhance the bioconversion of glycerol in both free and immobilized cells, however, the enhancement effect was more pronounced in case of free cells, which suffered greater substrate inhibition. In case of immobilized cells, the immobilization itself counteracts the inhibition, and hence, the additional contribution by ultrasound is less marked.

(2) Ultrasound has enhancement effect on glycerol consumption. However, this effect is marked for higher glycerol concentration. The major mechanism of the ultrasonic enhancement of glycerol consumption at high glycerol concentration is found to be reduction in substrate inhibition and increase in substrate-enzyme affinity favoring metabolic pathway of glycerol transformation to 1,3-PDO. Ultrasound is also seen to increase ethanol production, but enhancement is insignificant as revealed by same K_m and V_{max} values of ethanol dehydrogenase for both test and control experiments.

(3) The overall effect of immobilization and ultrasound is enhanced and selective production of 1,3-PDO through glycerol bioconversion.

8.4 CONCLUSIONS

In this chapter, we have explored a solution for enhancement of slow kinetics of the bioconversion of glycerol to ethanol and 1,3-propanediol (1,3-PDO) by immobilized *C. pasteurianum* cells on silica support in terms of ultrasound irradiation of the fermentation mixture. Concomitant analysis of the experimental results with simulations of cavitation bubble dynamics and enzyme kinetics have revealed interesting physical features of influence of ultrasound on bioconversion of glycerol with immobilized cells. In the first place, glycerol uptake by cells was not affected by either immobilization or ultrasound. However, both immobilization and ultrasonication are found to have positive effect on glycerol consumption. The enhancement effect of ultrasound on glycerol consumption is found to be a function of initial glycerol concentration, and was most marked at the highest glycerol concentration of 25 g/L. The immobilization of cells shifted the metabolic pathway almost completely towards 1,3-PDO. Analysis of enzyme kinetics parameters reveals that ultrasonication of the fermentation mixture leads to increased substrate–enzyme affinity and decreased substrate inhibition for 1,3-PDO dehydrogenase that is manifested in terms of preferential conversion of glycerol into 1,3-PDO. The results of this chapter could form useful guidelines for design of large scale process for ultrasound–enhanced glycerol bioconversion.



OVERVIEW AND SCOPE FOR FUTURE WORK

9.1 OVERVIEW

With biodiesel industry growing at an unprecedented rate; very large quantities of crude glycerol are bound to enter international market, creating a crisis situation for glycerol industry. The glycerol coming from the biodiesel industry is rather crude, and thus is not useful for conventional applications as in cosmetic or food industry. The current installed capacity of glycerol refinery is not able to handle these large quantities of crude glycerol. The prices of refined glycerol have also fallen sharply in the past one decade making additional investment for enlargement of refining capacity uneconomical. The current fate of crude glycerin is only as a fuel substitute for furnaces and reboilers, where it is burnt. Glycerol, according to the conventional inorganic chemistry, is a basic building block for many value added products through catalytic conversion. However, the reaction conditions as well as catalyst cost is prohibitive for design of a large scale process for glycerol conversion.

Biochemical conversion of crude glycerol, which is an excellent carbon source for fermentation, is a viable option that biodiesel industry can explore for forward integration of the industry. The literature reports conversion of glycerol to large number of products through fermentation using different microbial species. These processes are much less cost intensive (both in terms of capital and operational cost) than the catalytic route, and thus, are economically viable. Forward integration of the biodiesel industry can boost the economy of biodiesel as well. It is in this spirit that the current research work was undertaken. We have taken a step-by-step approach for development, optimization and intensification of the glycerol bioconversion process to two value added products, as described in previous chapters. We summarize herewith the major findings of our study addressing different facets of the glycerol bioconversion process. These results, when viewed all at a glance, give a coherent and interesting picture of the glycerol bioconversion process.

In Chapter 2, we presented a comprehensive review of the literature on conversion of glycerol to as many as 23 products. We also described the basic biochemistry and metabolic pathway of glycerol conversion to different products including the target products of present study viz. 1,3-propanediol and butanol.

In Chapter 3, we have presented the preliminary or initial steps of process development such as selection of suitable micro-organism for the process, and the immobilization supports. The immobilized cells have been selected for process development, as they have several distinct merits (as compared to free cells) such as easy control over cell density, ease of separation and recycle and greater inhibition resistance. We have screened several possible supports for immobilization, techniques of immobilization, and the quantity of cell loaded support added to the broth containing both pure and crude glycerol. A comparison of free and immobilized cells revealed higher catalytic potential of immobilized cells for handling crude glycerol at relatively higher concentrations.

In Chapter 4, we proceeded with the kinetic studies for determining rate as well as activation energy for glycerol bioconversion process. A factorial design comprising of three levels of initial glycerol concentrations (5, 10 and 25 g/L) and temperature (30, 37, 45°C) was used for optimization. The time data of glycerol fermentation was fitted to first order kinetics, and the activation energy was determined as -57.6 kcal/mol.

In Chapter 5, we addressed the issue of optimization of glycerol based fermentation medium for enhanced conversion using a statistical design of experiments (DOE) approach. Total 10 media constituents were attempted initially, using one component at a time approach. Out of these 10 components, 6 components showed significant effect on glycerol conversion. A Taguchi DOE method was adopted further to deduce the significance level of each of these components. Four components, viz. $\text{MgSO}_4 \cdot 7\text{H}_2\text{O}$, $(\text{NH}_4)_2\text{SO}_4$, yeast extract and $\text{KH}_2\text{PO}_4\text{--K}_2\text{HPO}_4$ showed significant effect on glycerol conversion. With these results, we obtained the optimum composition of the medium, which was further tested on a bioreactor scale. The actual solvent production on bioreactor level matched well with the predicted result from Taguchi analysis. Therefore, the optimum medium composition for immobilized cells was found to be significantly different than the free cells.

The next step in the process development of glycerol bioconversion was optimization of the physical and process parameters, which has been addressed in Chapter 6. The factors which were considered for optimization were agitation rate, temperature, pH and initial glycerol concentration in the medium. Taguchi analysis showed that all of these factors have significant effect on fermentation of both pure and crude glycerol. Moreover, quite interestingly, the optimum values of these parameters were same for both pure and crude glycerol. At optimized conditions of processes and physical parameters, as well as at optimized medium composition, the total concentration of solvent production at 25 g/L glycerol concentration differed only slightly for pure as well as crude version of glycerol. In

addition, the concentration of products was almost similar at both shake–flask and bioreactor level. This essentially meant that the process was very much conducive for scale–up at optimized conditions. The recyclability of the immobilized biocatalyst was also assessed, and it was found that the immobilized biocatalyst retained its activity for a larger number of cycles for both pure and crude glycerol.

After development and optimization of the process, we have also attempted to intensify the process with application of ultrasound. In Chapter 7, we have assessed the feasibility as well as mechanistic issues of ultrasound–assisted enhancement of the glycerol bioconversion kinetics. A dual approach of coupling experimental results to simulations of cavitation bubble dynamics as well as enzyme kinetics model (Michaelis–Menten and Haldane kinetics) was adopted. The nature of convection generated by ultrasound irradiation at static pressure has dual character of oscillatory motion with mild shock waves superimposed over it, which contributes towards enhancement of enzymatic reactions in metabolic pathway of glycerol bioconversion. Yield of both 1,3–PDO and ethanol enhances with ultrasound, but lesser enhancement is seen for 1,3–PDO than ethanol. The morphology of the cells was not found to change under ultrasound irradiation. The role of ultrasound in enhancement of glycerol was found to be of physical nature, without any influence on biochemistry of glycerol assimilation.

With the results on ultrasonic enhancement of glycerol conversion with free cells, we extended the theme for immobilized cells in Chapter 8. In addition to coupling experimental results with simulations of bubble dynamics and enzyme kinetics, we have also done statistical analysis of the results. The glycerol uptake by the cells was not affected by either immobilization or with sonication; yet, both immobilization and sonication were found to enhance the glycerol consumption rate. The enhancement effect of ultrasound on glycerol consumption was most marked (175%) at the highest glycerol concentration of 25 g/L. The

immobilization of cells shifted the metabolic pathway almost completely towards 1,3-PDO, which is the most value-added product among all three possible products. Ultrasound irradiation of the fermentation mixture at raise static pressure of just 2 bar is, thus, established to be an effective means of enhancement of glycerol bioconversion.

9.2 SCOPE FOR FUTURE WORK

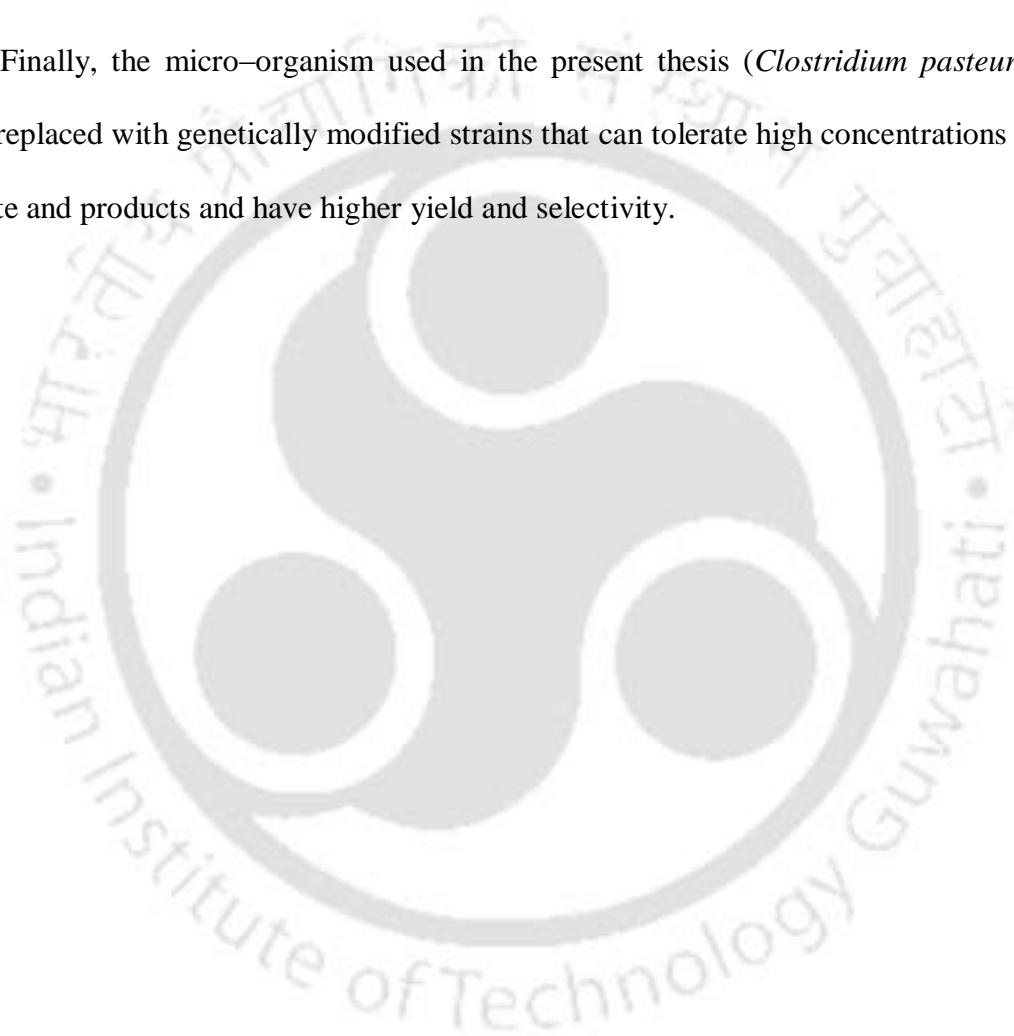
The present thesis has established glycerol bioconversion process with immobilized *Clostridium pasteurianum* cells on laboratory as well as bioreactor level. The results of this thesis can form further guidelines for further research in developing a large-scale process. Some suggestions for future work can be given as follows:

1. The mode of fermentation in the present thesis is batch mode. This could be replaced with either fed-batch or continuous mode. These modes of operations are more suitable for large-scale processes.
2. Use of different reactor configurations: The process can be designed with other reactor configurations like fixed bed or fluidized bed. These modes can increase the throughput of the process for enhanced production level.
3. In-situ removal of fermentation products to counteract product inhibition using technique such as gas stripping.
4. The ultrasound enhanced processes need further optimization with higher frequencies. The ultrasound power input (which determines the acoustic pressure amplitude) was kept constant in present thesis. This factor is crucial, as it directly affects the operating cost of the process, and thus, needs to be optimized with systematic approach.
5. The anaerobic condition may be monitored by noting the variation in electrostatic potential (E_h) of this anaerobic glycerol fermentation process using a redox sensitive dye such as Resazurin. Resazurin is colorless at 110 mV and remains pink at redox potential above 51

mV. Many anaerobes will only grow when the E_h is below 110 mV. The variation in E_h can change the operation of metabolic pathways, and hence it is important to ensure that the medium E_h is known.

6. Study on suitability of use of different compounds such as oxyrase, sodium thioglycollate, cysteine, sulphides, dithionite for creating and maintaining anaerobiosis can be done.

7. Finally, the micro-organism used in the present thesis (*Clostridium pasteurianum*) can be replaced with genetically modified strains that can tolerate high concentrations of both substrate and products and have higher yield and selectivity.



REFERENCES

- Abbad–Andaloussi S, Manginot–Dürr C, Amine J, Petidemange E, Petidemange H. (1995). Isolation and characterization of *Clostridium butyricum* DSM 5431 mutants with increased resistance to 1,3–Propanediol and altered production of acids. *Appl Env Microbiol*, 61(12), 4413–4417.
- Adachi O, Ano Y, Shinagawa E, Matsushita K. (2008). Purification and properties of two different dihydroxyacetone reductases in *Gluconobacter suboxydans* grown on glycerol. *Biosci Biotechnol Biochem*, 72, 2124–2132.
- Adhikari S, Fernando SD, Haryanto A. (2008). Hydrogen production from glycerin by steam reforming over Nickel catalysts. *Renew Energy*, 33, 1097–1100.
- Adlercreutz P, Holst O, Mattiasson B. (1985). Characterization of *Gluconobacter oxydans* immobilized in calcium alginate. *Appl Microbiol Biotechnol*, 22, 1–7.
- Alves VD, Freitas F, Costa N, Carvalheira M, Oliveira R, Gonçalves MP, Reis MAM. (2010). Effect of temperature on the dynamic and steady shear rheology of a new microbial extracellular polysaccharide produced from glycerol byproduct. *Carbohydrate Polymers*, 79, 981–988.
- Amaral PFF, Ferreira TF, Fontes GC, Coelho MAZ. (2009). Glycerol valorization: New biotechnological routes. *Food Bioprod Process*, 87, 179–186.

REFERENCES

- Anastassiadis S, Rehm HJ. (2006). Citric acid production from glucose by yeast *Candida oleophila* ATCC 20177 under batch, continuous and repeated batch cultivation. *Electronic J Biotechnol*, 9(1), 26–39.
- Andrade JC, Vasconcelos I. (2003). Continuous cultures of *Clostridium acetobutylicum*: culture stability and low-grade glycerol utilization. *Biotechnol Lett*, 25, 121–125.
- André A, Diamantopoulou P, Philippoussis A, Sarris D, Komaitis M, Papanikolaou S. (2010). Biotechnological conversions of biodiesel derived waste glycerol into added-value compounds by higher fungi: production of biomass, single cell oil and oxalic acid. *Ind Crops Prod*, 31, 407–416.
- Asawanonda P, Oberlender S, Taylor C. (1999). The use of dihydroxyacetone for photo protection in variegata porphyria. *Int J Dermatol*, 38(12), 916–918.
- Ashby RD, Nuñez A, Solaiman DKY, Foglia TA. (2005a). Sophorolipid biosynthesis from a biodiesel Co-product stream. *J Am Oil Chem Sec*, 82(9), 625–630.
- Ashby RD, Solaiman DKY, Foglia TA. (2004). Bacterial Poly(hydroxyalkanoate) polymer production from the biodiesel co-product stream. *J Polym Environ*, 12(3), 105–112.
- Ashby RD, Solaiman DKY, Foglia TA. (2005b). Synthesis of short-/medium-chain-length Poly(hydroxyalkanoate) blends by mixed culture fermentation of glycerol. *Biomacromolecules*, 6, 2106–2112.
- Ashby RD, Solaiman DKY, Foglia TA. (2006). The use of fatty acid esters to enhance free acid sophorolipid synthesis. *Biotechnol Lett*, 28, 253–260.
- Asmer HJ, Lang S, Wagner F, Wray V. (1998). Microbial production, structure elucidation and bioconversion of sophorose lipids. *J Am Oil Chem Sec*, 65, 1460–1466.
- Athalye SK, Garcia RA, Wen Z. (2009). Use of biodiesel derived crude glycerol for producing Eicosapentaenoic Acid (EPA) by the fungus *Pythium irregular*. *J Agric Food Chem*, 57, 2739–2744.

- Bahrami A, Shojaosadati SA, Khalilzadeh R, Farahani EV. (2008). Two stage glycerol feeding for enhancement of recombinant hG-CSF production in a fed-batch culture of *Pichia pastoris*. *Biotechnol Lett*, 30, 1081–1085.
- Bar R. (1988). Ultrasound enhanced bioprocesses: cholesterol oxidation by *Rhodococcus erythropolis*. *Biotechnol Bioeng* 32, 655–663.
- Barber BP, Hiller RA, Lofstedt R, Putterman SJ, Weninger KR. (1997). Defining the unknowns of sonoluminescence. *Phys Rep*, 281, 65–143.
- Barbirato F, Bories A. (1997). Relationship between the physiology of *Enterobacter agglomerans* CNCM 1210 grown anaerobically on glycerol and the culture conditions. *Res Microbiol*, 148, 475–484.
- Barbirato F, Chedaille D, Bories A. (1997). Propionic acid fermentation from glycerol: a comparison with conventional substrate. *Appl Microbiol Biotechnol*, 47, 441–46.
- Barbirato F, Grivet JP, Soucaille P, Bories A. (1996). 3-Hydroxypropionaldehyde, an inhibitory metabolite of glycerol fermentation to 1,3-Propanediol by Enterobacterial species. *Appl Env Microbiol*, 62(4), 1448–1451.
- Barbirato F, Himmi EH, Conte T, Bories A. (1998). 1,3-propanediol production by fermentation: An interesting way to valorize glycerin from the ester and ethanol industries. *Ind Crops Prod*, 7, 281–289.
- Batzing BL, Claus GW. (1971). Biphasic growth of *Acetobacter suboxydans* on a glycerol-limiting medium. *J Bacteriol*, 108, 592–595.
- Bauer R, du Toit M, Kossmann J. (2010). Influence of environmental parameters on production of the acrolein precursor 3-hydroxypropionaldehyde by *Lactobacillus reuteri* DSMZ 20016 and its accumulation by wine lactobacilli. *Int J Food Microbiol*, 137, 28–31.

REFERENCES

- Bell JB, Silver L, Arthur V. (1959). Method for preparing glycerin carbonate. US Patent, 2, 915, 529.
- Bertrand G. (1898). Recherches sur la production biochimique du sorbose. Ann Inst Pasteur (Paris), 12, 385–399.
- Biebl H, Hanisch HS, Spröer C, Lundsorf H. (2000). *Propionispora vibroides*, nov .gen., nov. sp., a new gram negative, spore forming anaerobe that ferments sugar alcohol. Arch Microbiol, 174, 239–247.
- Biebl H. (2001). Fermentation of glycerol by *Clostridium pasteurianum*– batch and continuous culture studies. J Ind Microbiol Biotechnol, 27, 18–26.
- Biodiesel 2020, a global market survey, 2nd edition. Available at <http://www.emerging-markets.com/biodiesel/swf>.
- Biswas PK, Pohit S. (2013). What ails India's biodiesel programme? Energ Policy, 789–796.
- Boenigk R, Bowien S, Gottschalk G. (1993). Fermentation of glycerol to 1,3–propanediol in continuous cultures of *Citrobacter freundii*. Appl Microbiol Biotechnol, 38, 453–457.
- Bormann EJ, Roth M. (1999). The production of polyhydroxybutyrate by *Methylobacterium rhodesianum* and *Ralstonia eutropha* in media containing glycerol and casein hydrolysates. Biotechnol Lett, 21, 1059–1063.
- Braunegg G, Genser K, Bona R, Haage G. (1999). Production of PHAs from agricultural waste materials. Macromol Symp, 144, 375–383.
- Brenner M, Hilgenfeldt S, Lohse D. (2002). Single bubble sonoluminescence. Rev Mod Phys, 74, 425–484.
- Byrd AJ, Pant KK, Gupta RB. (2008). Hydrogen production from glycerol by reforming in supercritical water over Ru/ Al₂O₃ catalyst. Fuel, 87, 2956–2960.

- Carrettin S, Mc Morn P, Johnston P, Griffin K, Hutchings GJ. (2002). Selective oxidation of glycerol to glyceric acid using a gold catalyst in aqueous sodium hydroxide. *Chem Commun*, 696.
- Cavalheiro JMBT, de Almeida MCMD, Grandfils C, da Fonseca MMR. (2009). Poly(3-hydroxybutyrate) production by *Cupriavidus necator* using waste glycerol. *Process Biochem*, 44, 509–515.
- Çelik E, Ozbay N, Oktar N, Çalik P. (2008). Use of biodiesel byproduct crude glycerol as the carbon source for fermentation processes by recombinant *Pichia pastoris*. *Ind Eng Chem Res*, 47, 2985–2990.
- Cerón Garcia MC, Sánchez Mirón A, Fernández Sevilla JM, Molina Grima E, García Camacho F. (2005). Mixotrophic growth of the microalga *Phaeodactylum tricorutum* Influence of different nitrogen and organic carbon sources on productivity and biomass composition. *Process Biochem*, 40, 297–305.
- Chakma S, Moholkar VS. (2011). Mechanistic features of ultrasonic desorption of aromatic pollutants. *Chem Eng J*, 175, 356–367.
- Chaminand J, Djakovitch LA, Gallezot P, Marion P, Pinel C, Rosier C. (2004). Glycerol hydrolysis on heterogeneous catalysts. *Green Chem*, 6, 359.
- Chang MY, Tsai GJ, Houg JY. (2006). Optimization of the medium composition for the submerged culture of *Ganoderma lucidum* by Taguchi array design and steepest ascent method. *Enzyme Microb Tech*, 38, 407–414.
- Che TM. (1987). Catalytic conversion of glycerol and synthesis gas to propanediols. US Patent 4, 642, 394.
- Chen KC, Lin YH, Tsai CM, Hsieh CH, Houg JY. (2002). Optimization of glycerol feeding for clavulanic acid production by *Streptomyces clavuligerus* with glycerol feeding. *Biotechnol Lett*, 24, 455–458.

REFERENCES

- Cheng KK, Liu HJ, Liu DH. (2005). Multiple growth inhibition of *Klebsiella pneumoniae* in 1,3-propanediol fermentation. *Biotechnol Lett*, 27, 19–22.
- Cheng KK, Zhang JA, Liu DH, Sun Y, Liu HJ, Yang MD, Xu JM. (2007). Pilot scale production of 1,3-propanediol using *Klebsiella pneumoniae*. *Process Biochem*, 42, 740–744.
- Cheng KK, Zhang JA, Liu DH, Sun Y, Yang MD, Xu JM. (2006). Production of 1,3-propanediol by *Klebsiella pneumoniae* from glycerol broth. *Biotechnol Lett*, 28, 1817–1821.
- Chi Z, Pyle D, Wen Z, Frear C, Chen S. (2007). A laboratory study of producing docosahexaenoic acid from biodiesel-waste glycerol by microalgal fermentation. *Process Biochem*, 42, 1537–1545.
- Chiruvolu V, Eskridge K, Cregg J, Meagher M. (1998). Effects of glycerol concentration and pH on growth of recombinant *Pichia pastoris* yeast. *Appl Biochem Biotechnol*, 75, 163–173.
- Chisti Y, Moo-Young M. (1986). Disruption of microbial cells for intracellular products. *Enzyme Microb Technol*, 8, 194–204.
- Chisti Y. (2003). Sonobioreactors: using ultrasound for enhanced microbial productivity. *Trends Biotechnol*, 21, 89–93.
- Chuanyun D, Bochu W, Chuanren D, Sakanishi A. (2003). Low ultrasonic stimulates fermentation of riboflavin producing strain *Ecemothecium ashbyii*. *Colloid Surface B*, 30, 37–41.
- Ciapina, EMP, Melo WC, Santa Anna LM, Santos AS, Freire DMG, Periere NJr. (2006). Biosurfactant production by *Rhodococcus erythropolis* grown on glycerol, as sole carbon source. *Appl Biochem Biotechnol*, 129–132, 880–886.

- Ciriminna R, Palmisano G, Ia Pina C, Rossi M, Pagliaro M. (2006). One pot electrocatalytic oxidation of glycerol to DHA. *Tetrahedron Lett*, 2006, 47, 6993–6995.
- Claret C, Bories A, Soucaille P. (1992). Glycerol inhibition of growth and dihydroxyacetone production by *Gluconobacter oxydans*. *Curr Microbiol*, 25, 149–155.
- Claus GW, Batzing BL, Baker CA, Goebel EM. (1975). Intracytoplasmic membrane formation and increased oxidation of glycerol growth of *Gluconobacter oxydans*. *J Bacteriol*, 123, 1169–1183.
- Colin T, Bories A, Lavinge C, Moulin G. (2001). Effects of acetate and butyrate during glycerol fermentation by *Clostridium butyricum*. *Curr Microbiol*, 43, 238–243.
- Colin T, Bories A, Moulin G. (2000). Inhibition of *Clostridium butyricum* by 1, 3 Propanediol and diols during glycerol fermentation. *Appl Microbiol Biotechnol*, 54, 210–205.
- Coral J, Karp SG, de Souza Vandenberghe LP, Parada JL, Pandey A, Soccol CR. (2008). Batch fermentation model of propionic acid production by *Propionibacterium acidipropionici* in different carbon sources. *Appl Biochem Biotechnol*, 151, 333–341.
- da Silva GP, Mack M, Contiero J. (2009). Glycerol: A promising and abundant carbon source for industrial microbiology. *Biotechnol Adv*, 27, 30–39.
- Dabrock B, Bahl H, Gottschalk G. (1992). Parameters affecting solvent production by *Clostridium pasteurianum*. *Appl Env Microbiol*, 58(4), 1233–1239.
- Dasu VV, Panda T, Chidambaram M. (2003). Determination of significant parameters for improved griseofulvin production in a batch bioreactor by Taguchi's method. *Process Biochem*, 38, 877–880.
- Datta R, Glassner Da, Jain MK, Vick Roy JR. (1992). Fermentation and purification process for succinic acid. US Patent 5, 168, 055.
- Davarey A, Pakshirajan K. (2010). Kinetics of growth and enhanced sophorolipids

REFERENCES

- production by *Candida bombicola* using a low-cost fermentative medium. *Appl Biochem Biotechnol*, 160, 2090–2101.
- de Almeida A, Nickel PI, Giordano AM, Pettinari MJ. (2007). Effects of granule-associated protein PhaP on glycerol-dependent growth and polymer production in poly(3-hydroxybutyrate)-producing *Escherichia coli*. *Appl Environ Microbiol*, 73, 7912–7916.
- de Gelder J, Scheledeman P, Leus K, Heyndrickx M, Vandenabeele P, Moens L, de Vos P. (2007). Raman spectroscopic study of bacterial endospores. *Analyt Bioanalyt Chem*, 389, 2143–2151.
- Deckwer W-D. (1995). Microbial conversion of glycerol to 1,3-propanediol. *FEMS Microbiol Rev*, 16, 143–149.
- Demirel S, Lehvert K, Lucas M, Claus P. (2007). Use of renewable for the production of chemicals: Glycerol oxidation over carbon supported gold catalysts. *Appl Catal B*, 70, 637.
- Deppenmeier U, Hoffmeister M, Prust C. (2002). Biochemistry and biotechnological applications of *Gluconobacter* strains. *Appl Microbiol Biotechnol*, 60, 233–242.
- Douhah MS. (1977). Mechanism of disintegration of biological cells in ultrasonic cavitation. *Biotechnol Bioeng*, 19, 649–660.
- Dürre P, Kuhn A, Gottwald M, Gottschalk G. (1987). Enzymatic investigations on butanol dehydrogenase and butyraldehyde dehydrogenase in extracts of *Clostridium acetobutylicum*. *Appl Microbiol Biotechnol*, 26, 268–272.
- El-Ziney MG, Arneborg N, Uyttendaele M, Debevere J, Jakobsen M. (1998). Characterization of growth and metabolite production of *Lactobacillus reuteri* during glucose/glycerol cofermentation in batch and continuous cultures. *Biotechnol Lett*, 20, 913–916.

- Escapa A, Manuel MF, Morán A, Gómez X, Guiot SR, Tartakovsky B. (2009). Hydrogen production from glycerol in a membraneless microbial electrolysis cell. *Energ Fuels*, 23, 4612–4618.
- Fakas S, Papanikolaou S, Batsos A, Galiotou–Panayotou M, Mallouchos A, Aggelis G. (2008). Evaluating renewable carbon sources as substrates for single cell oil production by *Cunninghamella echinulata* and *Mortierella isabellina*. *Biomass Bioenerg*, 33, 573–580.
- Fesq H, Brockow K, Strom K, Mempel K, Ring J, Abeck D. (2001). Dihydroxyacetone in a new formulation– A powerful therapeutic option in vitiligo. *Dermatol*, 203, 241–243.
- Fickers P, Benetti P–H, Wache Y, Marty A, Mauersberger S, Smit MS, Nicaud J–M. (2005). Hydrophobic substrate utilization by the yeast *Yarrowia lipolytica*, and its potential applications. *FEMS Yeast Res*, 5, 527–543.
- Files D, Ogawa M, Scaman CH, Baldwin SA. 2001. A *Pichia pastoris* fermentation process for producing high– levels of recombinant human cystatin–C. *Enzyme Microb Technol*, 29, 335–340.
- Fountoulakis MS, Manios T. (2009). Enhanced methane and hydrogen production from municipal solid waste and agro–industrial by–products co–digested with crude glycerol. *Bioresour Technol*, 100, 3043–3047.
- Freitas F, Alves VD, Carvalheira M, Costa N, Oliveira R, Reis MAM. (2009a). Emulsifying behavior and rheological properties of the extracellular polysaccharide produced by *Pseudomonas oleovorans* grown on glycerol byproduct. *Carbohydrate Polymers*, 78, 549–556.
- Freitas F, Alves VD, Pais J, Costa N, Oliveira C, Mafra L, Hilliou L, Oliveira R, Reis MA. (2009b). Characterization of an extracellular polysaccharide produced by a *Pseudomonas* strain grown on glycerol. *Bioresour Technol*, 100, 859–865.

REFERENCES

- Garai–Ibabe G, Ibarburu I, Berregi I, Claisse O, Lonvaud–Funel A, Irastorza A, Duenas MT. (2008). Glycerol metabolism and bitterness producing lactic acid bacteria in cidermaking. *Int J Food Microbiol*, 121, 253–261.
- Garcia R, Besson M, Gallezot P. (1995). Chemoselective catalytic oxidation of glycerol with air on Platinum metals. *Appl Catal A*, 127, 165.
- Gätgens C, Degner U, Bringer–Meyer S, Herrmann U. (2007). Biotransformation of glycerol to dihydroxyacetone by recombinant *Gluconobacter oxydans* DSM 2343. *Appl Microbiol Biotechnol*, 76, 553–559.
- Glassner DA, Datta R. (1992). Process for the production and purification of succinic acid. US Patent 5, 143, 834.
- Glycerin Market Analysis. U.S. Soybean Export Council Inc. Accessed from http://biodiesel@ucsd.edu/media_gallery (dated 20 July 2012).
- Gogate PR, Kabadi AM. (2009). A review of applications of cavitation in biochemical engineering / biotechnology. *Biochem Eng J*, 44, 60–72.
- Gonzalez R, Campbell P, Wong M. (2010). Production of ethanol from thin stillage by metabolically engineered *Escherichia coli*. *Biotechnol Lett*, 32, 405–411.
- González–Pajuelo M, Andrade JC, Vasconcelos I. (2004). Production of 1,3–Propanediol by *Clostridium butyricum* VPI 3266 using a synthetic medium and raw glycerol. *J Ind Microbiol Biotechnol*, 31, 442–446.
- González–Pajuelo M, Andrade JC, Vasconcelos I. (2005a). Production of 1,3–propanediol by *Clostridium butyricum* VPI 3266 in continuous cultures with high yield and productivity. *J Ind Microbiol Biotechnol*, 32, 391–396.
- González–Pajuelo M, Meynial–Salles I, Mendes F, Andrade JC, Vasconcelos I, Soucaille P. (2005b). Metabolic engineering of *Clostridium acetobutylicum* for the industrial production of 1,3–propanediol from glycerol. *Metab Eng*, 7, 329–336.

- Grossmann S, Hilgenfeldt S, Zomack M, Lohse D. (1997). Sound radiation of 3 MHz driven gas bubbles. *J Acoust Soc Am*, 102, 1223–1227.
- Günzel B, Yonsel S, Deckwer W–H. (1991). Fermentative production of 1,3–propanediol from glycerol by *Clostridium butyricum* up to a scale of 2m³. *Appl Microbiol Biotechnol*, 36, 289–294.
- Guo–liang Z, Yue–ting W, Xin–ping Q, Qin M. (2005). Biodegradation of crude oil by *Pseudomonas aeruginosa* in the presence of rhamnolipids. *J Zhejiang Univ Sci*, 8, 725–730.
- Gupta A, Singh VK, Qazi GN, Kumar A. (2001). *Gluconobacter oxydans*: Its Biotechnological Applications. *J Mol Microbiol Biotechnol*, 3(3), 445–456.
- Habe H, Fukuoka T, Kitamoto D, Sakaki K. (2009b). Biotransformation of glycerol to D–glyceric acid by *Acetobacter tropicalis*. *Appl Microbiol Biotechnol*, 81, 1033–1039.
- Habe H, Fukuoka T, Kitamoto D, Sakaki K. (2009d). Biotechnological production of D–glyceric acid and its application. *Appl Microbiol Biotechnol*, 84, 445–452.
- Habe H, Fukuoka T, Kitamoto D. (2009c). Biotechnological production of D–glyceric acid and its application. *Appl Microbiol Biotechnol*, 84, 445–452.
- Habe H, Shimada Y, Fukuoka T, Kitamoto D, Itagaki M, Watanabe K, Yanagishita H, Sakaki K. (2009a). Production of glyceric acid by *Gluconobacter sp.* NBRC3259 using raw glycerol. *Biosci Biotechnol Biochem*, 73(8), 1799–1805.
- Haldane J. (1930). *Enzymes*. Longmans Green and Co, New York.
- Hekmat D, Bauer R, Fricke J. (2003). Optimization of the microbial synthesis of dihydroxyacetone from glycerol with *Gluconobacter oxydans*. *Bioprocess Biosyst Eng*, 26, 109–116.

REFERENCES

- Heyndrickx M, Vos PD, Vancanneyt M, Ley JD. (1991). The fermentation of glycerol by *Clostridium butyricum* LMG 1212t₂ and 1213t₁ and *C. pasteurianum* LMG 3285. *Appl Microbiol Biotechnol*, 34, 637–642.
- Hilgenfeldt S, Lohse D, Brenner MP. (1996). Phase diagrams for sonoluminescing bubbles. *Phys Fluids*, 8, 2808–2826.
- Himmi EH, Bories A, Barbirato F. (1999). Nutrient requirements for glycerol conversion to 1,3–propanediol by *Clostridium butyricum*. *Bioresour Technol*, 67, 123–128.
- Himmi EH, Bories A, Boussaid A, Hasani L. (2000). Propionic acid fermentation of glycerol and glucose by *Propionibacterium acidipropionici* and *Propionibacterium freundenreichii* ssp. *shermanii*. *Appl Microbiol Biotechnol*, 53, 435–440.
- Hou CT. (2008). Production of arachidonic acid and dihomo- γ -linolenic acid from glycerol by oil-producing filamentous fungi, *Mortierella* in the ARS culture collection. *J Ind Microbiol Biotechnol*, 35, 501–506.
- Huh YS, Hong YK, Hong WH, Chang HN. (2004). Selective extraction of acetic acid from the fermentation broth produced by *Mannheimia succiniciproducens*. *Biotechnol Lett*, 26, 1581–1584.
- Indian Petroleum and Natural Gas statistics. Government of India, Ministry of Petroleum and Natural Gas, 2010–11.
- Ito T, Nakasimada Y, Senba K, Matsui T, Nishio N. (2005). Hydrogen and Ethanol production from glycerol-containing wastes discharged after biodiesel manufacturing process. *J Biosci Bioeng*, 100(3), 260–265.
- Ji XJ, Huang H, Zhu JG, Hu N, Li S. (2009). Efficient 1,3–propanediol production by fed–batch culture of *Klebsiella pneumoniae*: The role of pH fluctuation. *Appl Biochem Biotechnol*, 159, 605–613.
- Jyoti KK, Pandit AB. (2001). Water disinfection by acoustic and hydrodynamic cavitation.

- Biochem Eng J, 7, 201–212.
- Kato S, Ishii H, Kano S, Hagihara S, Todoroki T, Nagata S, Takahashi H, Nagasaka M, Sato J, Tsuchiya M. (1984). Improved assay for alcohol dehydrogenase activity in serum by centrifugal analysis. *Clin Chem*, 30, 1817–1820.
- Kawata Y, Aiba S. (2010). Poly(3–hydroxybutyrate) production by isolated *Halomonas* sp. KM–1 using waste glycerol. *Biosci Biotechnol Biochem*, 74(1), 175–177.
- Keller JB, Miksis MJ. (1980). Bubble oscillations of large amplitude. *J Acoust Soc Am*, 68, 628–633.
- Khamduang M, Packdibamrung K, Chutmanop J, Chisti Y, Srinophakun P. (2009). Production of L–phenylalanine from glycerol by a recombinant *Escherichia coli*. *J Ind Microbiol Biotechnol*, 36, 1267–1274.
- Khan A, Bhide A, Gadre R. (2009). Mannitol production from glycerol by resting cells of *Candida magnoliae*. *Bioresour Technol*, 100, 4911–4913.
- Khanal SK, Chen WH, Li L, Sung SW. (2004). Biological hydrogen production: effects of pH and intermediate products. *Int J Hydrog Energ*, 29, 1123–1131.
- Khanna S, Goyal A, Moholkar VS. (2011). Production of n–butanol from biodiesel derived crude glycerol using *Clostridium pasteurianum* immobilized on amberlite. *Fuel*, doi:10.1016/j.fuel.2011.10.071.
- Khanna S, Jaiswal S, Goyal A, Moholkar VS. (2012a). Ultrasound enhanced bioconversion of glycerol by *Clostridium pasteurianum*: A mechanistic investigation. *Chem Eng J*, 200–202, 416–425.
- Kim BS, Hong YK, Hong WH. (2004). Effect of salts on the extraction characteristics of succinic acid by pre–dispersed solvent extraction. *Biotechnol Bioprocess Eng*, 9, 207–211.

REFERENCES

- Kim JW, Park TJ, Ryu DD, Kim JY. (2000). High cell density culture of *Yarrowia lipolytica* using a one-step feeding process. *Biotechnol Prog*, 16, 657–660.
- Klepacova K, Mravec D, Bajus M. (2005). Tertiary butylation of glycerol catalyzed by ion-exchange resins. *Appl Catal A*, 294, 141–147.
- Koh ES, Lee TH, Lee DY, Kim HJ, Ryu YW, Seo JH. (2003). Scale up of erythritol production by an osmophilic mutant of *Candida magnoliae*. *Biotechnol Lett*, 25, 2103–2105.
- Koller M, Bona R, Braunegg G, Hermann C, Horvat P, Kroutil M. (2005). Production of polyhydroxyalkanoates from agricultural wastes and surplus material. *Biomacromolecules*, 6, 561–565.
- Kumar S, Chaube A, Jain SK. (2012). Critical review of Jatropha biodiesel promotion policies in India. *Energy Policy*, 41, 775–781.
- Lee SY, Hong SH, Lee SH, Park SJ. (2004). Fermentative production of chemicals that can be used for polymer synthesis. *Macromol Biosci*, 4, 157–164.
- Leighton TG. (1994). *The acoustic bubble*. Academic Press, San Diego.
- Levinson WE, Kurtzman CP, Kuo TM. (2007). Characterization of *Yarrowia lipolytica* and related species for citric acid production from glycerol. *Enzyme Microb Technol*, 41, 292–295.
- Liu HJ, Zhang DJ, Xu YH, Mu Y, Sun YQ, Xiu ZL. (2007). Microbial production of 1,3-propanediol from glycerol by *Klebsiella pneumoniae* under micro-aerobic conditions up to a pilot scale. *Biotechnol Lett*, 29, 1281–1285.
- Lofstedt R, Weninger K, Puttermann SJ, Barber BP. (1995). Sonoluminescing bubbles and mass diffusion. *Phys Rev E*, 51, 4400–4410.

- Ma BB, Xu XL, Zhang GL, Wang LW, Wu M., Li C. (2009). Microbial production of 1,3-Propanediol by *Klebsiella pneumoniae* XJPD–Li under different aeration strategies. *Appl Biochem Biotechnol*, 152, 127–134.
- Maddox IS, Steiner E, Hirsch S, Wessner S, Gutierrez NA, Gapes JR, Schuster KC. (2000). The cause of “acid crash” and “acidogenic fermentations” during the batch acetone–butanol–ethanol (ABE–) fermentation process. *J Mol Microbiol Biotechnol*, 2, 95–100.
- Malaoui H, Marczak R. (2000). Purification and characterization of the 1,3-PDO dehydrogenase of *Clostridium butyricum* E5. *Enzym Microb Technol*, 27, 399–405.
- Mantzouridou F, Naziri E, Tsimidou MZ. (2008). Industrial glycerol as a supplementary carbon source in the production of beta–carotene by *Blakeslea trispora*. *J Agric Food Chem*, 56, 2668–2675.
- Mason TJ, Lorimer JP. (1989). *Sonochemistry: Theory, application and uses of ultrasound in chemistry*. Ellis Horwood, New York.
- Menzel K, Zeng AP, Deckwer WD. (1997). High concentration and productivity of 1,3–propanediol from continuous fermentation of glycerol by *Klebsiella pneumoniae*. *Enzyme Microb Technol*, 20, 82–86.
- Metsoviti M, Paramithiotis S, Drosinos EH, Galiotou–Panayotou M, Nychas GJE, Zeng AP, Papanikolaou S. (2012). Screening of bacterial strains capable of converting biodiesel–derived raw glycerol into 1,3–propanediol, 2,3–butanediol and ethanol. *Eng Life Sci*, 12, 57–68.
- Mettin R, Akhatov I, Parlitz U, Ohl CD, Lauterborn W. (1997). Bjerknes forces between small cavitation bubbles in a strong acoustic field. *Phys Rev E*, 56, 2924–2931.
- Midathana VR, Moholkar VS. (2009). Mechanistic studies in ultrasound–assisted adsorption for removal of aromatic pollutants. *Ind Eng Chem Res*, 48, 7368–7377.

REFERENCES

- Moholkar VS, Warmoeskerken MMCG, Ohl CD, Prosperetti A. (2004). Mechanism of mass-transfer enhancement in textiles by ultrasound. *AIChE J*, 50, 58–64.
- Moon C, Lee CH, Sang BI, Um Y. (2011). Optimization of medium compositions favoring butanol and 1,3-propanediol production from glycerol by *Clostridium pasteurianum*. *Bioresource Technol*, 102, 10561–10568.
- Morita T, Konishi M, Fukuoka T, Imura T, Kitamoto D. (2007). Microbial conversion of glycerol into glycolipid biosurfactants, Mannosylerythritol lipids, by a Basidiomycete yeast, *Pseudozyma antarctica* JCM 10317^T. *J Biosci Bioeng*, 104(1), 78–81.
- Mu Y, Teng H, Zhang DJ, Wang W, Xiu ZL. (2006). Microbial production of 1,3-propanediol by *Klebsiella pneumoniae* using crude glycerol from biodiesel preparations. *Biotechnol Lett*, 28, 1755–1759.
- Nabe K, Izuo N, Yamada S, Chibata I. (1979). Conversion of glycerol to dihydroxyacetone by immobilized whole cells of *Acetobacter xylinum*. *Appl Env Microbiol*, 38(6), 1056–1060.
- Nikel PI, Pettinari MJ, Galvagno MA, Méndez BS. (2008). Poly(3-hydroxybutyrate) synthesis from glycerol by a recombinant *Escherichia coli* arcA mutant in fed-batch microaerobic cultures. *Appl Microbiol Biotechnol*, 77, 1337–1343.
- NIST Data Gateway (Chemistry Webbook) Home Page. <http://webbook.nist.gov/chemistry> (accessed August 2011).
- Nuñez A, Ashby R, Foglia TA, Solaiman DY. (2001). Analysis and characterization of sphorolipids by liquid chromatography with atmospheric pressure using chemical ionization. *Chromatographia*, 53, 673–677.
- Ohrem HL, Voß H. (1995). Kinetics of polyol oxidation with *Gluconobacter oxydans*. *Biotechnol Lett*, 17, 1195–1200.
- Oskouie SFG, Tabandeh F, Yakhchali B, Eftekhar F. (2007). Enhancement of alkaline

- protease production by *Bacillus clausii* using Taguchi experimental design. *Afr J Biotechnol*, 6, 2559–2564.
- Ott L, Bicker M, Vogel H. (2006). Catalytic degradation of glycerol in sub and supercritical water: a new chemical process for acrolein. *Green Chem*, 8, 214–220.
- Papanikolaou S, Aggelis G. (2002a). Lipid production by *Yarrowia lipolytica* growing on industrial glycerol in a single–stage continuous culture. *Bioresour Technol*, 82, 43–49.
- Papanikolaou S, Fakas S, Fick M, Chevalot I, Panayotou M–G, Komaitis M, Marc I, Aggelis G. (2008). Biotechnological valorization of raw glycerol discharged after biodiesel (fatty acid methyl esters) manufacturing process: production of 1,3–propanediol, citric acid and single cell oil. *Biomass Bioenerg*, 32, 60–71.
- Papanikolaou S, Muniglia L, Chevalot I, Aggelis G, Marc I. (2002b). *Yarrowia lipolytica* as a potential producer of citric acid from raw glycerol. *J Appl Microbiol*, 92, 737–744.
- Papanikolaou S, Ruiz–Sanchez P, Pariset B, Blanchard F, Fick M. (2000). High production of 1,3–propanediol from industrial glycerol by a newly isolated *Clostridium butyricum* strain. *J Biotechnol*, 77, 191–208.
- Park JB, Seo BC, Kim JR, Park YK. (1998). Production of erythritol in fed–batch cultures of *Trichosporon sp.* *J Ferment Bioeng*, 86, 577–580.
- Pasteris SE, Strasser de Saad AM. (2005). Aerobic glycerol catabolism by *Pediococcus pentosaceus* isolated from wine. *Food Microbiol*, 22, 399–407.
- Patidar R, Khanna S, Moholkar VS. (2012). Physical features of ultrasound assisted enzymatic degradation of recalcitrant organic pollutants. *Ultrason Sonochem*, 19, 104–118.
- Petitdemange E, Dürr C, Abbad–Andaloussi S, Raval G. (1995). Fermentation of raw glycerol to 1,3–Propanediol by new strains of *Clostridium butyricum*. *J Ind Microbiol*, 15, 498–502.

REFERENCES

- Petrova K, Petrova P. (2009). High production of 2,3–butanediol from glycerol by *Klebsiella pneumoniae* G31. *Appl Microbiol Biotechnol*, 84, 659–665.
- Pflugmacher U, Gottschalk G. (1994). Development of an immobilized cell reactor for the production of 1,3–propanediol by *Citrobacter freundii*. *Appl Microbiol Biotechnol*, 41, 313–316.
- Planning Commission (2003). Report of the committee on development of biofuels, Government of India. (http://planningcommission.nic.in/reports/genrep/cmtt_bio.pdf).
- Plesset M. (1949). The dynamics of cavitation bubbles. *J Appl Mech (Trans ASME)*, 16, 277–282.
- Porta F. (2004). Selective oxidation of glycerol to sodium glycerate with gold on carbon catalyst: an insight into reaction stability. *J Catal*, 224, 397.
- Portilla–Rivera OM, Téllez–Luis SJ, de León JAR, Vázquez M. (2009). Production of microbial transglutaminase on media made from sugarcane molasses and glycerol. *Food Technol Biotechnol*, 47, 19–26.
- Press WH, Teukolsky SA, Flannery BP, Vetterling WT. (1992). *Numerical recipes*, second ed. Cambridge University Press, New York.
- Prosperetti A, Lezzi A. (1986). Bubble dynamics in a compressible liquid. part 1. first order theory. *J Fluid Mech*, 168, 457–477.
- Pyle DJ, Garcia RA, Wen Z. (2008). Producing Docosahexaenoic acid (DHA)–rich algae from biodiesel–derived crude glycerol: Effects of impurities on DHA production and algal biomass composition. *J Agric Food Chem*, 56, 3933–3939.
- Qatibi AI, Bennisse R, Jana M, Garcia JL. (1998). Anaerobic degradation of glycerol by *Desulfovibrio fructosovorans* and *D. carbinolicus* and evidence for glycerol dependent utilization of 1,2–propanediol. *Curr Microbiol*, 36, 283–290.

- Raj SM, Rathnasingh C, Jo JE, Park S. (2008). Production of 3-hydroxypropionic acid from glycerol by a novel recombinant *Escherichia coli* BL21 strain. *Process Biochemistry*, 43, 1440–1446.
- Ramayya S, Brittain A, De Almeida C, Mok W, Antal J. (1987). Acid catalyzed dehydration of alcohols in supercritical water. *Fuel*, 66, 1364–1371.
- Rashedi H, Jamshidi E, Mazaheri Assadi M, Bonakdarpour B. (2005). Isolation and production of biosurfactant from *Pseudomonas aeruginosa* isolated from Iranian southern wells oil. *Int J Environ Sci Tech*, 2(2), 121–127.
- Reed MC, Lieb A, Nijhout HF. (2010). The biological significance of substrate inhibition: a mechanism with diverse functions. *Bioessays*, 32, 422–429.
- Reimann A, Biebl H. (1996). Production of 1,3 Propanediol by *Clostridium butyricum* DSM 5431 and product tolerant mutants in fed batch culture: feeding strategy for glycerol and ammonium. *Biotechnol Lett*, 18(7), 827–832.
- Roehr M, Kubicek CP, Kominek J. (1996). Citric acid. In: Roehr M, ed. *Biotechnology: Products of primary metabolism*. 2nd ed. Weinheim (Germany): VCH Verlagsgesellschaft mBH, 307–345.
- Rosseto R, Tcacenco CM, Ranganathan R, Hajdu J. (2008). Synthesis of phosphatidylcholine analogues derived from glyceric acid: a new class of biologically active phospholipid compounds. *Tetrahedron Lett*, 49, 3500–3503.
- Rymowicz W, Rywińska A, Gładkowski W. (2008). Simultaneous production of citric acid and erythritol from crude glycerol by *Yarrowia lipolytica* Wratlavia K1. *Chem Pap*, 62(3), 239–246.
- Rymowicz W, Rywińska A, Marcinkiewicz M. (2009). High yield production of erythritol from raw glycerol in fed batch cultures of *Yarrowia lipolytica*. *Biotechnol Lett*, 31, 377–380.

REFERENCES

- Rymowicz W, Rywińska A, Żarowska B, Juszczyk P. (2006). Citric Acid production from raw glycerol by acetate mutants of *Yarrowia lipolytica*. Chem Pap, 60(5), 391–394.
- Ryu HW, Kang KH, Yun JS. (1999). Bioconversion of fumarate to succinate using glycerol as a carbon source. Appl Biochem Biotechnol, 77–79, 511–520.
- Rywińska A, Rymowicz W, Zarowska B, Wojtatowicz M. (2009). Biosynthesis of Citric Acid from glycerol by acetate mutants of *Yarrowia lipolytica* in fed–batch fermentation. Food Technol Biotechnol, 47, 1–6.
- Sabourin–Provost G, Hallenbeck PC. (2009). High yield conversion of a crude glycerol fraction from biodiesel production to hydrogen by photofermentation. Bioresour Technol, 100, 3513–3517.
- Sabourin–Provost G, Hallenbeck PC. (2009). High yield conversion of a crude glycerol fraction from biodiesel production to hydrogen by photofermentation. Bioresour Technol, 100, 3513–3517.
- Saint–Amans S, Perlot P, Goma G, Soucaille P. (1994). High production of 1,3–propanediol from glycerol by *Clostridium butyricum* VPI 3266 in a simply controlled fed–batch system. Biotechnol Lett, 16(8), 831–836.
- Sanchez DLR. (2009). Butanol production from glycerol by *Clostridium pasteurianum* in defined culture media–A phenotypic approach. M.Sc Thesis, University of Maryland, USA.
- Sanjari M, Karimi Taheri A, Movahedi MR. (2009). An optimization method for radial forging process using ANN and Taguchi method. Int J Adv Manuf Technol, 40, 776–784.
- Santa Anna LM, Sebastian GV, Periera NJr, Alves, TLM, Menezes EP, Freire DMG. (2001). Production of biosurfactant from a new and promising strain of *Pseudomonas aeruginosa* PA1. Appl Biochem Biotechnol, 91–93, 459–467.

- Santos AS, Sempio APW, Vasquez GS, Santa Anna LM, Periere NJr, Freire DMG. (2002). Evaluation of different carbon and nitrogen sources in production of Rhamnolipids by a strain of *Pseudomonas aeruginosa*. *Appl Biochem Biotechnol*, 98–100, 1025–1035.
- Sauvageot N, Gouffi K, Laplace J–M, Auffray Y. (2000). Glycerol metabolism in *Lactobacillus collinoides*: production of 3–hydroxypropionaldehyde, a precursor of acrolein. *Int J Food Microbiol*, 55, 167–170.
- Save SS, Pandit AB, Joshi JB. (1994). Microbial cell disruption: role of cavitation. *Chem Eng J Biochem Eng J*, 55, B67–B72.
- Saxena RK, Anand P, Saran S, Isar J. (2009). Microbial production of 1,3–Propanediol : Recent developments and emerging opportunities. *Biotechnol Adv*, 27, 895–913.
- Scholten E, Dägele D. (2008). Succinic acid production by a newly isolated bacterium. *Biotechnol Lett*, 30, 2143–2146.
- Scholten E, Renz T, Thomas J. (2009). Continuous cultivation approach for fermentative succinic acid production from crude glycerol by *Basfia succiniciproducens* DD1. *Biotechnol Lett*, 31, 1947–1951.
- Seifert K, Waligorska M, Wojtowski M, Laniecki M. (2009). Hydrogen generation from glycerol in batch fermentation process. *Int J Hydrogen Energy*, 34, 3671–3678.
- Selembo PA, Perez JM, Lloyd WA, Logan BE. (2009). High hydrogen production from glycerol or glucose by electrohydrogenesis using microbial electrolysis cells. *Int J Hydrogen Energy*, 34, 5373–5381.
- Seyfried M, Lyon D, Rainey FA, Wiegel J. (2002). *Caloramator viterbensis* sp. nov., a novel thermophilic, glycerol–fermenting bacterium isolated from a hot spring in Italy. *Int J Syst Evol Microbiol*, 52, 1177–1184
- Shah YT, Pandit, AB, Moholkar VS. (1999). Cavitation reaction engineering. Plenum Press, New York.

REFERENCES

- Simopolous AP. (1999). Essential fatty acids in health and chronic disease. *Am J Clin Nutr*, 70, 560S–569S.
- Sirisansaneeyakul S, Luangpipat T, Vanichsiratana W, Srinophakum T, Chen HH–H, Chisti Y. (2007). Optimization of lactic acid production by immobilized *Lactococcus lactis* IO–1. *J Ind Microbiol Biotechnol*, 34, 381–391.
- Sivasankar T, Paunekar AW, Moholkar VS. (2007). Mechanistic approach to enhancement of the yield of a sonochemical reaction. *AIChE J*, 53, 1132–1143.
- Sobeřon–Chávez G, Lépine F, Déziel E. (2005). Production of rhamnolipids by *Pseudomonas aeruginosa*. *Appl Microbiol Biotechnol*, 68, 718–725.
- Sobolov M, Smiley KL. (1960). Metabolism of glycerol by an acrolein forming *Lactobacillus*. *J Bacteriol*, 79, 261–266.
- Socol CR, Vandenberghe LPS, Rodrigues C, Pandey A. (2006). New perspectives for Citric Acid production and application. *Food Technol Biotechnol*, 44(2), 141–149.
- Solaiman DKY, Ashby RD, Foglia TA, Marmer WN. (2006). Conversion of agricultural feedstock and coproducts into poly(hydroxyalkanoates). *Appl Microbiol Biotechnol*, 712, 783–789.
- Song H, Lee SY. (2006). Production of succinic acid by bacterial fermentation. *Enzyme Microb Technol*, 39, 352–361.
- Sulaiman AZ, Ajit A, Yunus RM, Chisti Y. (2011). Ultrasound–assisted fermentation enhances bioethanol productivity. *Biochem Eng J*, 54, 141–150.
- Suslick KS. (1988). *Ultrasound: Its physical, chemical and biological effects*. VCH, New York.
- Švitel J, Šturdik E. (1994). Product yield and by–product formation in glycerol conversion to dihydroxyacetone by *Gluconobacter oxydans*. *J Ferment Bioeng*, 78, 351–355.

- Syu MJ. (2001). Biological production of 2,3-butanediol. *Appl Microbiol Biotechnol*, 55, 10–18.
- Taconi KA, Venkataramanan KP, Johnson DT. (2009). Growth and solvent production by *Clostridium pasteurianum* ATCC® 6013™ utilizing biodiesel-derived crude glycerol as the sole carbon source. *AIChE Environ Prog Sust Energy*, 28(1), 100–110.
- Tanaka O, Komatsu T, Oshibe A, Cai Y, Miyazaki S, Nakanishi K. (2009). Production of 3-hydroxypropionaldehyde in silage inoculated with *Lactobacillus coryniformis* plus glycerol. *Biosci Biotechnol Biochem*, 73, 1494–1499.
- Tang S, Boehme L, Lam H, Zhang Z. (2009). *Pichia pastoris* fermentation for phytase production using crude glycerol from biodiesel production as the sole carbon source. *Biochem Eng J*, 43, 157–162.
- Teodoro JC, Baptista-Neto A, Cruz-Hernández IL, Hokka CO, Badino AC. (2006). Influence of feeding conditions on clavulanic acid production in fed-batch cultivation with medium containing glycerol. *Appl Microbiol Biotechnol*, 72, 450–455.
- Tou CT. (2008). Production of arachidonic acid and dihomo- γ -linolenic acid from glycerol by oil-producing filamentous fungi, *Mortierella* in the ARS culture collection. *J Ind Microbiol Biotechnol*, 35, 501–506.
- Tran N, Illukpitiya P, Yanagida JF, Ogoshi R. (2011). Optimizing biofuel production; An economic analysis for selected biofuel feedstock production in Hawaii. *Biomass Bioenerg*, 35, 1756–1764.
- Trchounian K, Trchounian A. (2009). Hydrogenase 2 is most and hydrogenase 1 is less responsible for H₂ production by *Escherichia coli* under glycerol fermentation at neutral and slightly alkaline pH. *Int J Hydrogen Energy*, 34, 8839–8845.
- Tsukuda E, Sato S, Takahashi R, Sodesowa T. (2007). Production of acrolein from glycerol over Silica supported heteropoly acids. *Catal Commun*, 8, 1349–1353.

REFERENCES

- Van Ede CJ. (1994). Bioconversions catalyzed by growing immobilized bacteria, analytical models describing diffusion and reaction in substrate or product inhibited biofilms. Dissertation, University of Groningen.
- Van Gerpen J. (1999). Biodiesel processing and production. *Fuel Processing Technol*, 86, 1097–1107.
- Venil CK, Lakshmanaperumalsamy P. (2009). Taguchi experimental design for medium optimization for enhanced production by *Bacillus subtilis* HB04. *eJST*, 4, 1–10.
- Verhoef S, Ruijssenaars HJ, de Bont JAM, Wery J. (2007). Bioproduction of p-hydroxybenzoate from renewable feedstock by solvent tolerant *Pseudomonas putida* S12. *J Biotechnol*, 132, 49–56.
- Wang ZX, Zhuge J, Fang H, Prior BA. (2001). Glycerol production by microbial fermentation: a review. *Biotechnol Adv*, 19, 201–223.
- Wei YH, Cheng CL, Chien CC, Wan HM. (2008). Enhanced di-rhamnolipid production with an indigenous isolate *Pseudomonas aeruginosa* J16. *Process Biochem*, 43, 769–774.
- Wei Y-H, Chou CL, Chang JS. (2005). Rhamnolipid production by indigenous *Pseudomonas aeruginosa* J4 originating from petrochemical wastewater. *Biochem Eng J*, 27, 146–154.
- Werpy T, Frye J, Zacher A, Miller D. (2002). Hydrogenolysis of 6-Carbon sugars and other organic compounds using multimetallic catalysts. World Organisation Patent 03, 035, 582.
- Wikipedia, Mannitol. (2011a). Available at <http://en.wikipedia.org/wiki/Mannitol>.
- Wikipedia, Oxalic acid. (2011b). Available at http://en.wikipedia.org/wiki/Oxalic_acid.
- Wittlich P, Thermann A, Vorlop KD. (2001). Conversion of glycerol to 1,3-propanediol by a newly isolated thermophilic strain. *Biotechnol Lett*, 23, 463–466.

- Wu JY, Yeh KL, Lu WB, Lin CL, Chang JS. (2008a). Rhamnolipid production with indigenous *Pseudomonas aeruginosa* EM1 isolated from oil-contaminated site. *Bioresour Technol*, 99, 1157–1164.
- Wu KJ, Saratale GD, Lo YC, Chen W, Tseng ZJ, Chang MC, Tsai BC, Su A, Chang JS. (2008b). Simultaneous production of 2,3-butanediol, ethanol and hydrogen with a *Klebsiella* sp. Strain isolated from sewage sludge. *Bioresour Technol*, 99, 7966–7970.
- Wu Q, Xu H, Liang J, Yao J. (2010). Contribution of glycerol on production of poly(γ -Glutamic Acid) in *Bacillus subtilis* NX-2. *Appl Biochem Biotechnol* 160: 386–392.
- Yamada, Shimizu S, Shinmen Y. (1987). Production of arachidonic acid by *Mortierella elongata* 1S-5. *Agric Biol Chem*, 51, 785–790.
- Yang Y, Tsukahara K, Sawayama S. (2008). Biodegradation and methane production from glycerol containing synthetic wastes with fixed bed bioreactor under mesophilic and thermophilic anaerobic conditions. *Process Biochem*, 43, 362–367.
- Yazdani SS, Gonzalez R. (2007). Anaerobic fermentation of glycerol: a path to economic viability for the biofuels industry. *Curr Opin Biotechnol*, 18, 213–219.
- Young FR. (1989). *Cavitation*. McGraw Hill, London.
- Zabaneh M, Bar R. (1991). Ultrasound-enhanced bioprocess II. dehydrogenation of hydrocortisone by *Arthrobacter simplex*. *Biotechnol Bioeng*, 37, 998–1003.
- Zhang A, Yang ST. (2009). Propionic acid production from glycerol by metabolically engineered *Propionibacterium acidipropionici*. *Process Biochem*, 44, 1346–1351.
- Zhang B, Tang X, Li Y, Xu Y, Shew W. (2007a). Hydrogen production from steam reforming of ethanol and glycerol over ceria support. *Int J Hydrogen Energy*, 32, 2367–2373.
- Zhang GL, Ma BB, Xu XL, Li C, Wang L. (2007b). Fast conversion of glycerol to 1,3-propanediol by a new strain of *Klebsiella pneumoniae*. *Biochem Eng J*, 37, 256–260.

REFERENCES

- Zhang W, Hywood Potter KJ, Plantz BA, Schlegel VL, Smith LA, Meagher MM. (2003). *Pichia pastoris* fermentation with mixed feeds of glycerol and methanol: growth kinetics and production improvement. *J Ind Microbiol Biotechnol*, 30, 210–215.
- Zhao YN, Chen G, Yao SJ. (2006). Microbial production of 1,3–propanediol from glycerol by encapsulated *Klebsiella pneumoniae*. *Biochem Eng J*, 32, 93–99.
- Zheng Y, Chen X, Shen Y. (2008). Commodity chemicals derived from glycerol, an important biorefinery feedstock. *Chem Rev*, 108, 5253–5277.



ACKNOWLEDGMENTS

I owe my deepest gratitude to all those who made this thesis possible. The first and foremost appreciation goes to my supervisors Prof. V. S. Moholkar and Prof. A. Goyal for their valuable guidance throughout the research work. Their continuous encouragement, patience towards research and support gave me lot of spirit in regard to research. I would like to thank them for spending their precious time for discussion by which I have gained immense skills of knowledge in terms of research. I am fortunate to have them as my mentors.

I would like to extend my sincere gratitude to my doctoral committee members, Prof. P. Goswami, Dr. K. Pakshirajan and Dr. K. Mohanty for their insightful advices and suggestions throughout the research.

My sincere thanks go to the Center for Energy and also to the faculty members associated with Center for their constant support. The kind and constant help of the staff member of Center for Energy and Department of Chemical Engineering is also duly acknowledged. I am also thankful to the Indian Institute of Technology Guwahati for providing me with the infrastructure and facilities for advanced research. I also acknowledge Ministry of Human Resources Development, New Delhi for providing me fellowship for pursuing Ph. D.

I am thankful to my friends Anasuya, Sumitra, Namita, Bharati for all the love and support rendered to me during the course of my stay in IIT Guwahati. I am grateful to my senior Mrs. Amrita Ranjan, her husband Mr. Kumar Pallav and their daughter Anvesha for making me feel at home away from home. I also extend my thanks to my colleagues and friends, Hanif, Sankar, Jaykumar, Buljit, Ritesh Malani, Ritesh Patidar, Partho, Peeush Kumar for their constant help and enthusiastic company.

I am also thankful to my Aunts Mrs. Sunita Shukla, Mrs. Soma Ganguly, Mrs. Dimple Mehrotra, and, Uncles Mr. Avadhesh Shukla, Dr. K.L. Ganguly, Mr. Sanjay Mehrotra,

ACKNOWLEDGEMENTS

brothers Virendra, Kumar Kanti, Shubham, Mrigank, Kunal Kanti, and sisters Ruby, Manju and Renu for their love and concern for me.

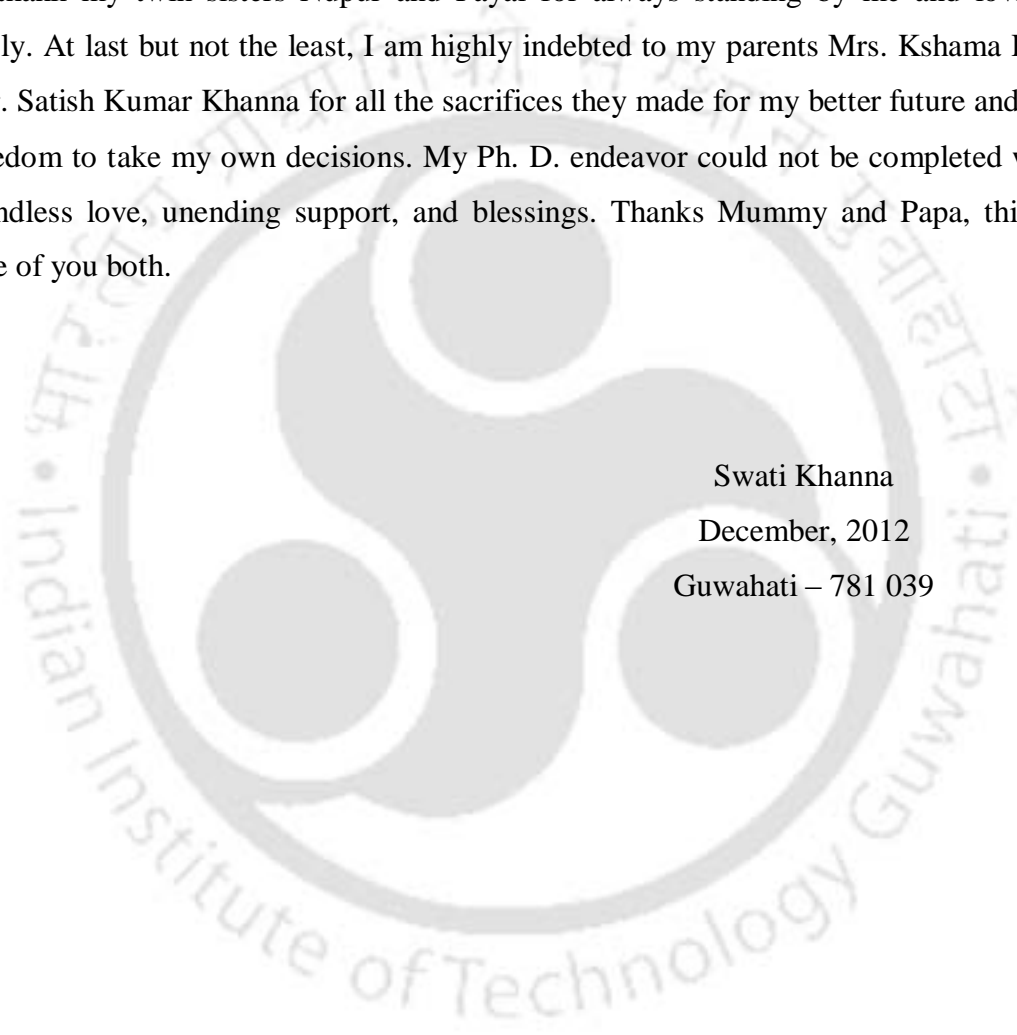
I need to specially thank Dr. Anil Kumar Shukla, my friend and former colleague during my post-graduation and Ph. D days for his constant suggestions, constructive criticism and for being my philosopher, strength, motivation and support. This would not have been possible without him.

I also thank my twin sisters Nupur and Payal for always standing by me and loving me selflessly. At last but not the least, I am highly indebted to my parents Mrs. Kshama Khanna and Mr. Satish Kumar Khanna for all the sacrifices they made for my better future and giving me freedom to take my own decisions. My Ph. D. endeavor could not be completed without their endless love, unending support, and blessings. Thanks Mummy and Papa, this is all because of you both.

Swati Khanna

December, 2012

Guwahati – 781 039



RESEARCH OUTPUT OF THE THESIS

PUBLISHED/ ACCEPTED IN PEER REVIEWED INTERNATIONAL JOURNALS

- Khanna S, Goyal A, Moholkar VS. (2013). Mechanistic investigations on ultrasound enhanced bioconversion of glycerol by immobilized *Clostridium pasteurianum* on silica support. *Biotechnology and Bioengineering*, doi: 10.1002/bit.24839.
- Khanna S, Jaiswal S, Goyal A, Moholkar VS. (2012). Ultrasound enhanced bioconversion of glycerol by *Clostridium pasteurianum*: A mechanistic investigation. *Chem Eng J*, 200–202, 416–425.
- Khanna S, Ranjan A, Goyal A, Moholkar VS. (2013). Selection and optimization of medium components for mixed alcohols production by glycerol utilizing immobilized *Clostridium pasteurianum* MTCC 116. *Chemical and Biochemical Engineering Quarterly* (Accepted).
- Khanna S, Goyal A, Moholkar VS. (2013). Effect of fermentation parameters on bio-alcohols production from glycerol using immobilized *Clostridium pasteurianum*: An optimization study. *Preparative Biochemistry and Biotechnology* (Accepted).
- Khanna S, Goyal A, Moholkar VS. (2012). Microbial conversion of glycerol: Present status and future prospects. *Crit Rev Biotechnol*, 32(3), 235–262.

- Khanna S, Goyal A, Moholkar VS. (2012). Bioconversion of biodiesel derived crude glycerol by immobilized *Clostridium pasteurianum*: Effect of temperature. (2012). Int J Chem Biolog Eng, 6, 301–304.
- Khanna S, Goyal A, Moholkar VS. (2011). Production of n-butanol from biodiesel derived crude glycerol using *Clostridium pasteurianum* immobilized on Amberlite. Fuel, doi:10.1016/j.fuel.2011.10.071.

COMMUNICATED IN PEER REVIEWED INTERNATIONAL JOURNALS

- Khanna S, Shukla AK, Goyal A, Moholkar VS. Alcoholic biofuels production from biodiesel derived glycerol by *Clostridium pasteurianum* whole cells immobilized on silica.

CONFERENCE PRESENTATIONS

- Khanna S, Goyal A, Moholkar VS. Bioconversion of biodiesel derived crude glycerol by immobilized *Clostridium pasteurianum*: Effect of temperature. International Conference on Agricultural Biology, Biotechnology and Biosystems Engineering–2012. Venice, Italy. April 2012.
- Khanna S, Goyal A, Moholkar VS. Comparative assessment of Amberlite, polyurethane foam and silica as immobilization supports for glycerol utilizing *Clostridium pasteurianum* cells. SECONE–2012. Oil India Limited, Guwahati. April 2012.
- Khanna S, Goyal A, Moholkar VS. Effect of pH on solvent production by immobilized whole cells of *Clostridium pasteurianum* utilizing biodiesel glycerol as a carbon source. Post ISCBC–2012. IASST, Guwahati. January 2012.
- Khanna S, Goyal A, Moholkar VS. Effect of varying concentration of crude glycerol

- on solvent production by silica immobilized *Clostridium pasteurianum*. International Conference on Environmental Research–2011. SVNIT, Surat, India. December 2011.
- Khanna S, Goyal A, Moholkar VS. Production of n–butanol from biodiesel derived crude glycerol using *Clostridium pasteurianum* immobilized on amberlite. International Conference on Renewable Energy. Rajasthan University, Jaipur, India. January 2011.
 - Khanna S, Goyal A, Moholkar VS. n–Butanol production by immobilized *Clostridium pasteurianum* utilizing biodiesel derived crude glycerol as a sole carbon source. CHEMCON–2010. Anna Malai University, Chidambaram, India. December 2010.
 - Khanna S, Moholkar VS. A conceptual integrated whole cell biocatalytic process for biodiesel production and up gradation of glycerol to value added products. CHEMCON–2009. Andhra University, Vishakhapatnam, India. December 2009.
 - Khanna S, Moholkar VS. Conceptual process for up gradation of biodiesel derived crude glycerol to value added products. 78th Annual Meeting of Society of Biological Chemists. National Center for Cell Scientists, Pune, India. October 2009.



CORRECTION APPENDIX

CHAPTER 3



Figure A1 Picture of a custom fabricated Erlenmeyer flasks for anaerobic fermentation

Normal 250 mL Erlenmeyer flasks manufactured by JSGW, India were custom fabricated. The flask had a screw capped top and an extended tubular bottom at one end meant for connecting silicon tubing for sparging nitrogen and sealing the flask. After sparging, the silicon tubing attached to the tubular opening is sealed/ closed using a stainless steel pinchcock.

CHAPTER 4

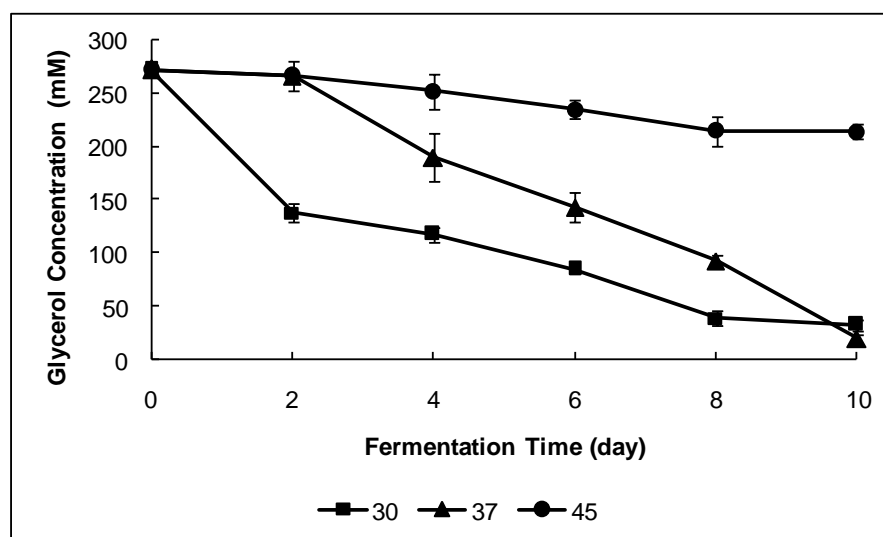


Figure A2 Trends in consumption of glycerol during the course of fermentation at three different fermentation temperatures